Cover image :

The Great Wave off Kanagawa, by Katsushika Hokusai (Japanese, Tokyo (Edo) 1760–1849 Tokyo (Edo))
From Thirty-six Views of Mount Fuji (c. 1830-1832)
Collection of the Metropolitan Museum of Art (New-York, NY, USA)
Public Domain

FACULTÉ DE MÉDECINE

INSTITUT DE RECHERCHE EXPÉRIMENTALE ET CLINIQUE

PÔLE NEURO MUSCULO SQUELETTIQUE

IN-VITRO AND IN-VIVO STUDY OF BIOFILM DISRUPTION STRATEGIES FOR THE TREATMENT OF PROSTHETIC JOINT INFECTIONS

Hervé POILVACHE

Thesis submitted in fulfillment of the requirements for the degree of
"Docteur en Sciences Biomédicales et Pharmaceutiques"

Supervisors: Professors Olivier CORNU and Françoise VAN BAMBEKE

September 2021

Remerciements

Alors que la rédaction de ce manuscrit de thèse de doctorat touche à sa fin, marquant la fin d'une aventure de quatre années, il m'apparait nécessaire de souligner les contributions de celles et ceux qui auront rendu cette aventure possible et plaisante. Cet exercice est délicat, les remerciements d'une thèse étant souvent le chapitre le plus attendu, lu, et commenté d'un manuscrit. C'est donc avec un réel plaisir, mêlé du souci de n'oublier aucune contribution ou rencontre, que je souhaite faire part de ma gratitude et de mes remerciements les plus sincères à toutes celles et à tous ceux qui auront rendu cette thèse possible.

Mes premiers remerciements s'adressent à mes promoteurs, les Professeurs Olivier Cornu et Françoise Van Bambeke qui m'ont accompagné et fait confiance tout au long des quatre années de cette thèse. Dans des rôles distincts mais complémentaires, ils auront rendu cette thèse possible et agréable, et ce malgré de nombreuses difficultés. Je leur suis extrêmement reconnaissant de m'avoir donné l'opportunité de réaliser ce projet.

Le Professeur Olivier Cornu, connaissant mon intérêt pour la recherche, et après avoir patiemment écouté certaines de mes idées de projets de thèse un peu farfelus – dont l'étude de l'ostéonécrose de la tête fémorale et de son traitement par cellules souches chez les émeus… - a eu l'heureuse intuition de me proposer d'entamer un projet de recherche ayant pour thème le traitement des infections d'implants orthopédiques, et en particulier l'étude de nouveaux traitements interférant avec le biofilm bactérien nouvellement décrits dans le laboratoire du Professeur Van Bambeke. Une fois le projet lancé, il a fait preuve d'un soutien indéfectible et d'une grande disponibilité malgré des charges cliniques et administratives lourdes et parfois écrasantes, tout en veillant à faciliter le déroulement de mes expériences.

Le Professeur Françoise Van Bambeke, malgré une première rencontre un peu décousue alors que j'amenais le brouillon de mon projet FNRS l'avant-veille de la date limite, m'a accueilli dans son grand laboratoire – 16 doctorants et post-doctorants de toutes origines ! - où j'ai rapidement commencé à me former aux techniques de microbiologie et d'étude des biofilms et de leurs réponses aux traitements. Le Professeur Van Bambeke m'a ensuite permis de mener mon projet avec une grande liberté, en favorisant le développement d'un modèle *in-vitro* inédit au laboratoire FACM, en mettant une énergie incroyable pour permettre l'éclosion du projet *in-vivo*

malgré les résistances de membres de l'IREC, en coordonnant notre consortium Win²Wal, en m'entraînant de manière intensive au concours du FRIA, et j'en passe ! Tout au long de cette thèse, j'ai également pu compter sur sa très grande disponibilité, que ce soit pour corriger mes manuscrits, abstracts et présentations, ou pour venir discuter à l'improviste de problèmes scientifiques, de projets de carrière, de problèmes du quotidien ou encore de voyages islandais.

J'adresse mes plus sincères remerciements aux membres de mon jury de thèse qui, malgré des emplois du temps chargés, ont eu à cœur d'encadrer ce projet, offrant des conseils précieux tout au long des quatre dernières années.
Le Professeur Alain Poncelet a présidé pendant quatre ans les réunions de mon comité d'accompagnement et ensuite du jury de thèse avec professionnalisme, rigueur, et bienveillance.
Le Professeur Christine Dupont m'a fait prendre conscience de l'utilité de l'impression 3D lors d'une visite chez Materialise, et m'a donné l'opportunité de découvrir le domaine des coatings d'implants en favorisant une collaboration avec un de ses doctorants, Cédric Vranckx.
Le Professeur Thomas Schubert m'a fait découvrir la recherche alors que j'étais son étudiant chercheur au sein du laboratoire de Chirurgie Expérimentale il y a maintenant plus de dix ans, contribuant à l'éclosion de ma vocation de chercheur et m'a ensuite fait bénéficier de ses conseils au cours de cette thèse.
Le Professeur Jean-Cyr Yombi m'a fait prendre conscience au cours de ma première année d'assistanat à Saint-Luc de l'importance des complications infectieuses en Chirurgie Orthopédique et s'est assuré de la pertinence clinique de ce projet.
Le Professeur Hector Rodriguez-Villalobos m'a fait bénéficier de son expertise, de souches cliniques ayant favorisé la pertinence de mes expériences, et m'a permis l'utilisation de matériel de son laboratoire, rendant ainsi possible la réalisation de points majeurs de cette thèse.
Professors Olivier Borens and Andrej Trampuz who made me the immense honor to take part in the evaluation and discussion of my work, inspiring me to deliver what I hope is a quality manuscript.

J'adresse également mes plus sincères remerciements aux autres responsables des pôles NMSK et FACM qui m'ont accueilli au cours de cette thèse.
Le Professeur Christine Detrembleur, responsable du pôle NMSK, a eu à cœur de veiller à mon bien-être au sein du laboratoire, que ce soit en veillant à un approvisionnement régulier en biscuits et sucreries diverses, ou en me

prêtant une oreille attentive lors de nos discussions impromptues où je pouvais librement exprimer mes frustrations ou difficultés liées à mon projet de recherche ou à mes perspectives de carrière.
Le Professeur Philippe Mahaudens que j'étais heureux de croiser afin de discuter alors que le laboratoire NMSK était si vide lorsque les restrictions liées au Covid battaient leur plein.
Le Professeur Marie-Paule Mingeot, responsable du pôle FACM, dont la bonne humeur, les conseils avisés, et les questions parfois complexes ont jalonné ma thèse.
Le Professeur Paul Tulkens dont l'expérience et les connaissances ne cessent de m'impressionner et dont l'exigence et la disponibilité lors de ma préparation au concours du FRIA ne sont certainement pas étrangères à ma réussite.

L'agrément d'un parcours de thèse repose également sur les rencontres avec des collègues formidables. Je les remercie d'avoir été présents, de m'avoir poussé à me frotter à des réalités différentes, et de m'avoir enrichi de leur amitié.
Je remercie mes collègues du laboratoire NMSK : **Julien Lebleu**, dont le cerveau toujours en ébullition a mené à une publication commune, **Anh Phong Nguyen**, dont l'hyperactivité, la joie de vivre, et les bons goûts culinaires m'ont accompagné au cours de cette thèse, **Alexis Lheureux**, qui nous a malheureusement quitté trop tôt, et avec qui nous avons découvert les joies de la réalité virtuelle, **Elise Piraux**, dont la bonne humeur quasi constante a été communicative et à qui j'ai pu faire don des caramels immangeables offerts par l'épicier du campus, **Stéphanie Dehem**, doyenne du laboratoire, et organisatrice en chef, **Timothée Cayrol**, dont les discussions parfois philosophiques ont manqué suite au Covid, **Clara Selves**, avec qui j'ai pu de nombreuses fois discuter des difficultés inhérentes à l'exercice de la médecine dans un cadre universitaire, **Virginie Cordemans**, qui est plusieurs fois revenue mettre de l'ambiance au laboratoire, **Maxime Valet**, avec qui j'ai partagé mon bureau pendant plusieurs années et qui m'aura fait découvrir l'utilité d'Auvio, **Nicolas Lambricht**, qui aura réussi à me faire découvrir le labo de marche après 4 ans de thèse, **Loïc Fonkoué**, dont la rigueur et l'exigence m'ont inspiré, **Eric Kouassi**, dont la volonté de rendre accessible une médecine de qualité est inspirante, **Robin Evrard**, dont les discussions autour de ses bouillons de fémurs de porc m'ont permis de me sentir moins seul au labo au cours de la rédaction de ce manuscrit, **Gauthier Everard**, dont la productivité m'abasourdi, ainsi que **Ioannis Doumas**,

Virginie Otlet, **Alexandre Luc**, **Julie Manon**, **Alexandre Englebert**, **Kevin Wendo**, **Frank Assogba**, **Laura Wallard**.
Je remercie également mes collègues du laboratoire FACM : **Yvan Diaz Iglesias**, qui m'aura non seulement appris le B.A.-BA des biofilms, mais également à voir Pokémon Go sous un autre œil, **Frédéric Peyrusson**, qui a toujours accepté les victoires et les défaites de l'équipe de France avec dignité et qui nous aura fait rêver de Mars, **Alix Mangin**, pour son aide inestimable lors des expériences in-vivo et sans qui cette partie du projet aurait été impossible, **Albert Ruiz-Sorribas**, who was always ready to discuss results as well as some of my less realistic hypotheses, **Ambre Freyberg**, que j'ai eu le plaisir d'encadrer lors d'un stage et qui a permis à mon projet de continuer à avancer alors que j'écrivais ce manuscrit, **Vasileios Yfantis**, pour les conseils techniques et les parties de Civilization, **Hélène Thirot**, pour sa bonne humeur communicative ses talents d'organisatrice, **Sandrine Verstraeten**, pour avoir inauguré la série de bustes, **Audrey Comein**, pour son dynamisme, sa gentillesse et ses masques chats, **Aline Lardinois**, pour sa bonne humeur et ses pâtisseries succulentes, **Gang Wang**, whose work ethic astonished all of us, **Mandeep Kaur**, whose wits and travel advice were welcomed, **Steven De Soir**, wie heeft nieuwe projecten en bacteriophages in onze lab gebracht, **Perrin Ngougni**, qui m'a accueilli avec cordialité et m'a donné une leçon de courage, **Tiep Nguyen**, qui nous aura répété qu'on travaillait trop, tout en en faisant deux fois plus que nous, **Hussein Chalhoub**, pour ses discussions au sujet de mon projet de recherche ou du Liban, **Negar Mozaheb**, for her insightful discussion over Iran, and restaurant recommendations**, Virginie Mohymont**, pour m'avoir formé à certaines techniques et son aide lors des tests de cytotoxicité, **Romain Tricot**, pour son aide technique, **Murielle Callier**, pour son extraordinaire disponibilité et sa flexibilité malgré mes commandes souvent hors clous, ainsi que **Jitendriya Swain**, **Valo Varik**, **Tamara Milosevic**, **Jules Bayiha**, **Gert-Jan Wijnant**.

Au-delà des pôles NMSK et FACM, ma thèse m'a amené à côtoyer et à bénéficier de l'aide de membres d'autres laboratoire que je souhaiterais remercier.
Je souhaite remercier tout particulièrement le **Professeur Jean-Paul Dehoux**, responsable de l'animalerie facultaire, qui a soutenu mon projet de recherche in-vivo et nous a permis de le réaliser dans de bonne condition, tout en me prodiguant des conseils utiles afin de prendre soin des animaux qui m'étaient confiés. Il est important de souligner également la contribution du laboratoire MIRO et en particulier de ses responsables, le **Professeur John Lee** et le

Docteur Ann Bol, qui ont accepté d'accueillir nos animaux dans leur animalerie. Je remercie également le pôle CHEX de m'avoir mis à disposition des instruments chirurgicaux, ainsi que **Martial Vergauwen** pour m'avoir permis de réaliser des clichés de radioscopie.
Je remercie également l'équipe de la plateforme d'imagerie de l'IREC (2IP), et tout particulièrement le **Docteur Caroline Bouzin**, dont les conseils et l'aide ont été décisifs pour l'acquisition des images à l'aide de l'ApoTome ainsi qu'en histologie, **Marc de Bournonville**, pour ses conseils de préparation de prélèvements osseux, ainsi que **Michèle de Beukelaer**, sans qui l'analyse histologique de mes prélèvements n'aurait pas été possible.
Certaines analyses sanguines n'ont été rendues possibles que part des collaborations d'autres laboratoire. Je remercie le **Professeur Pierre Wallemacq** pour m'avoir autorisé à faire réaliser les dosages de vancomycine sérique dans son laboratoire. J'ai également pu bénéficier de l'aide de **Sébastien Druart** du laboratoire de néphrologie pour les dosages de créatinine sérique ainsi que pour les dosages initiaux de CRP.
Je remercie également **Cédric Vranckx** du pôle Bio and Soft Matter pour m'avoir fait découvrir le monde des coatings et avec qui j'ai fortement apprécié travailler, ainsi que sa mémorante **Alix Mertens** à qui nous avons enseigné certaines techniques de microbiologie.
Le Professeur Anne des Rieux m'a donné un cours accéléré sur l'utilisation de gels comme carriers de principes actifs, permettant ainsi de donner un nouveau souffle à mon projet.

Dans le cadre de ce projet, nous avons monté un consortium de recherche. Je souhaite en remercier les membres, au premier rang desquels la société **OneLife** qui a soutenu mon projet en mettant à disposition les enzymes utilisées dans ces études. Je remercie également **Thomas Vanzieleghem** et **Laetitia Fontaine** pour leurs conseils. Je souhaite également remercier les **Professeurs Loic Quinton** et **Edwin de Pauw**, ainsi que **Mathieu Tiquet** de l'ULg pour leur collaboration au sein de ce consortium.

Un tel projet est évidemment impossible sans financements. Je suis extrêmement reconnaissant à la **Fondation Saint-Luc** et au **FNRS** de m'avoir fait bénéficier de leurs bourses, ainsi qu'à la **région Wallonne** et à la **Société Royale Belge de Chirurgie Orthopédique et de Traumatologie** d'avoir soutenu mes expériences.

Je remercie également tous ceux qui m'auront transmis leurs connaissances, insufflé un désir de savoir et de découverte, et poussé à faire preuve de rigueur

tout au long de mes formations scolaires au **collège Saint-Michel**, universitaires à **l'Université catholique de Louvain**, et en cours de spécialisation en Chirurgie Orthopédique dans les services de **Saint-Luc**, **Tournai**, et **Ottignies**.

Je souhaite également remercier mes amis et mes proches pour leur soutien tout au long de cette thèse, mais aussi des longues années de formation qui y ont mené. **Mes parents** m'ont transmis le goût du savoir et de l'expérimentation et m'ont offert un cadre familial et matériel stable qui m'ont permis de mener ce projet à bien. Je remercie également **mon frère et ma sœur** pour leurs encouragements tout au long de cette thèse. Enfin, je voudrais avoir une pensée pour **mes grands-parents** qui n'auront pas eu la possibilité de voir aboutir mes études, mais qui, j'en suis certain, auraient été fiers du résultat.

Table of contents

Remerciements 5
Jury 15
Summary 17
Résumé 18
List of Abbreviations 19
Chapter I: Introduction - Prosthetic Joint Infections 23
1 Foreword 23
2 Epidemiology 25
3 Diagnosis 30
4 Pathogens 40
5 Treatment strategies 46
Chapter II: Introduction - Biofilms 53
1 Definition and historical perspective 53
2 Biofilm formation and regulation 54
3 Matrix composition 57
4 Consequences of biofilm formation 60
5 Experimental Models 64
6 Experimental therapeutics 80
Aims of the thesis 93
Chapter III: *in-vitro* study of pulsed-lavage 97

1 Introduction 99
2 Materials and Methods 101
3 Results 107
4 Discussion 115
5 Conclusion 118
6 Author Contributions 118
7 Funding 118
8 Conflict of Interest 119
9 Acknowledgments 119
10 Supplementary material 120
Chapter IV: *in-vitro* study of enzymatic debridement 125
1 Introduction 127
2 Materials and Methods 129
3 Results 137
4 Discussion 151
5 Authors Contributions 155
6 Funding 155
7 Conflicts of Interest 155
8 Acknowledgments 155
9 Supplementary material 156
Chapter V: *in-vivo* study of the association of DAIR and enzymes 169
1 Introduction 172

2 Methods 174
3 Results 184
4 Discussion 192
5 Conclusion 198
6 Data Availability Statement 199
7 Authors Contributions 199
8 Funding 199
9 Conflicts of Interest 199
10 Acknowledgments 199
11 Supplementary material 201
Chapter VI: General discussion 205
1 Main achievements of the thesis 205
2 Limitations of this work 208
3 Perspectives 213
4 Conclusion 216
References 217

Jury

Chair

Professor Alain Poncelet
Cardiovascular Research Unit, Institut de Recherche Expérimentale et Clinique, Université catholique de Louvain, Belgium

Supervisors

Professor Olivier Cornu
Neuro Musculo Skeletal Laboratory, Institut de Recherche Expérimentale et Clinique, Université catholique de Louvain, Belgium

Professor Françoise Van Bambeke
Cellular and Molecular Pharmacology Laboratory, Louvain Drug Research Institute, Université catholique de Louvain, Belgium

Committee

Professor Olivier Borens
Orthopedic Trauma Unit and Septic Surgery Unit, Centre Hospitalier Universitaire Vaudois, Université de Lausanne, Switzerland

Professor Andrej Trampuž
Infectious Diseases Research Laboratory, Charité - Universitätsmedizin Berlin, Germany

Professor Christine Dupont
Bio and Soft Matter Division, Institute of Condensed Matter and Nanosciences, Université catholique de Louvain, Belgium

Professor Hector Rodriguez-Villalobos
Department of Microbiology, Cliniques Universitaires Saint-Luc, Belgium

Professor Thomas Schubert
Experimental Surgery and Transplant Laboratory, Institut de Recherche Expérimentale et Clinique, Université catholique de Louvain, Belgium

Professor Jean-Cyr Yombi
Department of Internal Medicine and Infectious Diseases, Cliniques Universitaires Saint-Luc, Belgium

Summary

Prosthetic joint infection (PJI) is a devastating complication of joint replacement surgeries, affecting 0.5 to 2% of patients following a hip or a knee arthroplasty. Its treatment is complicated by the rapid formation of bacterial biofilms on the implants' surfaces. Biofilms are bacterial communities enveloped in a complex self-produced matrix that isolates bacteria from their environment, leading to an increased tolerance to antimicrobials. Therefore, new therapeutic options targeting biofilms are in development to improve the outcome of PJI.

The objectives of this work were to investigate biofilm disruption using a standard irrigation technique (pulsed-lavage) or an enzyme combination targeting the matrix of the biofilms, and its impact on the susceptibility of bacteria to antibiotics. Pulsed-lavage and the enzymatic combination were studied in two successive *in-vitro* studies, using a model of biofilms grown on titanium alloy substrates. Our experiments showed that the successive application of biofilm disrupting treatments and antibiotics, used at clinically relevant concentrations, was synergistic. Considering these encouraging results, an *in-vivo* model of PJI was developed to study the use of the enzymatic combination as an adjuvant to a treatment with debridement, systemic antibiotics, and implant retention. Regrettably, the addition of the enzymatic combination did not appear to improve the outcome of the treatment. However, these experiments open new perspectives to optimize the use of enzymes in this setting, and the tools developed for this work could prove useful to investigate the application of other strategies for the treatment of PJI.

Résumé

La survenue d'une infection périprothétique est une complication sévère des arthroplasties, touchant 0,5 à 2% des patients dans le décours d'une arthroplastie de la hanche ou du genou. Le traitement de ces infections est rendu complexe par la formation rapide d'un biofilm bactérien. Les biofilms sont des communautés bactériennes complexes, entourées d'une matrice auto-produite, isolant les bactéries de leur environnement et menant au développement de tolérances aux agents antimicrobiens. Dans ce contexte, de nouvelles approches thérapeutiques ciblant les biofilms sont à l'étude afin d'améliorer le pronostic des infections périprothétiques.

Les objectifs de ce travail étaient d'étudier la dispersion des biofilms en utilisant une méthode standard (lavage pulsé) ou une combinaison d'enzymes spécifiques de la matrice des biofilms, et son impact sur la sensibilité aux antibiotiques des bactéries. Nous avons étudié ces traitements dans deux études *in-vitro* successives en utilisant un modèle de biofilms cultivés sur des substrats en alliage de titane. Nos expériences ont montré que l'application successive de traitements dispersant les biofilms et d'antibiotiques à des concentrations pertinentes était synergiques. Dès lors, nous avons développé un modèle *in-vivo* afin d'étudier l'effet de l'utilisation du traitement enzymatique comme traitement adjuvant à un traitement par débridement et antibiothérapie. Malheureusement, les résultats n'ont pas permis de conclure à un impact favorable des enzymes sur le traitement. Néanmoins, ces expériences ont ouvert de nouvelles perspectives d'optimisation du traitement enzymatique, et les modèles développés dans ce cadre pourraient s'avérer utiles pour l'étude d'autres stratégies de traitement de ces infections.

List of Abbreviations

AIP: Auto-Inducing Peptide

AMP: Anti-Microbial Peptide

ANOVA: ANalysis Of VAriance

ASTM: American Society for Testing and Materials

ATCC: American Type Culture Collection

CA-MHB: Cation Adjusted MHB

CBD: Calgary Biofilm Device

CBR: CDC Biofilm Reactor

CDC: Center for Diseases Control

CFU: Colony Forming Unit

CoNS: Coagulase-Negative Staphylococci

CRP: C-Reactive Protein

DAIR: Debridement, Antibiotics, and Implant Retention

DFR: Drip Flow Reactor

DNA: DeoxyriboNucleic Acid

DNAse I: Type I Deoxyribonuclease

DspB: Dispersin B

DTT: DiThioThreitol

EBJIS: European Bone and Joint Infection Society

eDNA: Extra-cellular DNA

EPA: Environmental Protection Agency

EPS: Extra-cellular Polymeric Substance

ESR: Erythrocyte Sedimentation Rate

EUCAST: European Committee on Antimicrobial Susceptibility Testing

FRIA: Fonds pour la Recherche dans l'Industrie et l'Agriculture

FRS – FNRS: Fonds de la Recherche Scientifique

HPF: High-Power Field (400x magnification)

ICG: International Consensus Group

ICM: International Consensus Meeting

IDSA: Infection Disease Society of America

K-wire: Kirschner's wire

LDH: Lactate DeHydrogenase

MBEC: Minimal Biofilm Eradication Concentration

MHB: Mueller Hinton Broth

MIC: Minimal Inhibitory Concentration

MIP: Maximum Intensity Projection

MRSA: Methicillin-Resistant *Staphylococcus aureus*

MRSE: Methicillin-Resistant *Staphylococcus epidermidis*

MSCRAMM: Microbial Surface Components Recognizing Adhesive Matrix Molecules

MSIS: MusculoSkeletal Infection Society

NZW: New-Zealand White

PBS: Phosphate Buffer Saline

PCR: Polymerase Chain Reaction

PIA: Polysaccharide Intercellular Adhesin

PK/PD: PharmacoKinetics/PharmacoDynamics

PL: Pulsed-Lavage

PMMA: PolyMethylMethAcrylate

PMN: PolyMorphoNuclear

PNAG: Poly-*N*-AcetylGlucosamine

OECD: Organisation for Economic Co-operation and Development

PJI: Prosthetic Joint Infection

RNA: RiboNucleic Acid

SEM: Standard Error of the Mean

SOSSID: Swiss Orthopaedics and the Swiss Society of Infectious Diseases

TEC: Tri-Enzymatic Cocktail

TGN: TSB supplemented with 1% NaCl and 2% Glucose

THA: Total Hip Arthroplasty

ThC: Therapeutic Concentration

TKA: Total Knee Arthroplasty

TSB: Tryptic Soy Broth

Tukey HSD: Tukey's Honestly Significant Difference

WBC: White Blood Cells

Chapter I: Introduction - Prosthetic Joint Infections

1 Foreword

Prosthetic Joint Infection (PJI), defined as an infection involving a joint replacement implant and its surrounding tissues (5), is among the most feared and catastrophic complications of joint replacement surgeries.



Figure I.1. Infected TKA.

Despite a relatively low incidence of 0.4% to 2.18% after total hip arthroplasties (THA) and total knee arthroplasties (TKA), PJI represents a significant burden because of the high numbers of joint replacement surgeries performed in western countries (6).

PJI and its treatments have severe consequences for patients and are associated with a high complication rate (7, 8), pain (9), loss of joint function (10), psychological distress (11), and mortality (12). The treatment of PJI is particularly complex and challenging, involving a combination of medical and surgical strategies (13). One of the factors driving the complexity of PJI care is the formation of biofilms on the implants (14), microbial communities adhering to a substrate and embedded in a self-produced extra-cellular matrix (15). Biofilm formation limits our ability to identify the causative pathogens (16), leads to irreversible adherence of bacteria to the colonized surfaces (17), facilitates bacterial evasion from the immune system (18), and leads to the

emergence of antimicrobial tolerance (19). An introduction to biofilm biology, the mechanisms of antibiotic tolerance and host immune system evasion, and the models and experimental therapeutics targeting biofilms are presented in the second section of the introduction.

PJI is associated with high costs arising from the treatments and the impact on patients' health (20, 21). Combined with a growing incidence of osteoarthritis and joint replacement surgeries, PJI is poised to represent significant medical, societal, and economic burdens over the coming years (22, 23).

The importance of the issues raised by PJI is increasingly recognized, and over the last decade, PJI has become one of the leading research areas in orthopedic surgery. This is illustrated by the steady increase in published works referenced on PubMed on the topic (Figure I.2).

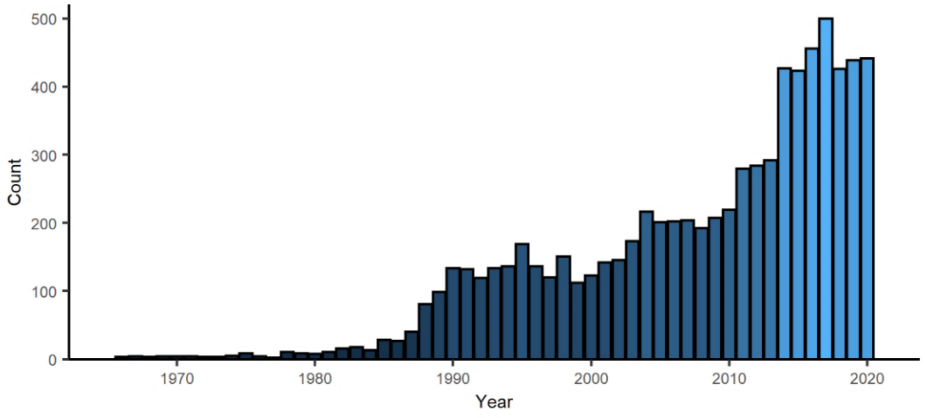


Figure I.2. PubMed publication count for "prosthetic OR periprosthetic joint infection".

2 Epidemiology

The epidemiology of PJI is closely linked to that of joint replacement procedures. THA and TKA are extremely common surgical procedures. In 2017, 182 TKA/100.000 inhabitants and 135 THA/100.000 inhabitants were performed in the OECD countries. The incidences were even higher in western European countries, reaching 274 THA/100.000 inhabitants and 210 TKA/100.000 inhabitants in Belgium (6). These procedures have a favorable impact on patients' quality of life (24, 25) and have low revision rates (26, 27). Among the reasons for THA and TKA revisions, PJI is pre-eminent, representing the most common mode of failure following TKA (28) and the fourth most common following THA (29) in the international literature. In Belgium in 2018, infection was the second most common indication for TKA revision and the third for THA revision (30).

The estimates of PJI incidence are variable and depend on the characteristics of the initial surgery, the definitions of PJI used in the studies, and the origins of the data. For THA, the incidence of PJI is estimated between 0.43% and 2.18% following a primary arthroplasty and between 5.6% and 8.11% following a revision procedure (23, 31-33), while for TKA, the incidence is estimated between 0.53% and 2.18% following a primary arthroplasty and between 5.52% and 8.42% following revision surgery (23, 31, 34, 35). PJI incidence following primary shoulder arthroplasty is relatively low (0.40% to 0.7%) but has been reported to reach 9.8% with certain implants (36, 37). It is more common following ankle arthroplasty, affecting 2.4% to 3.2% of patients in recent cohorts (38, 39).PJI places a significant burden on patients and the healthcare systems.

Patients suffering from PJI endure significant disability, morbidity, and mortality. The negative impact of PJI on the joint function and the quality of life of patients has been well described by multiple authors. In a 2020 study, Mur et al. showed that patients suffering from an infected hip or knee arthroplasty were significantly more susceptible to require an assistive device to ambulate or to be unable to ambulate when compared to a matched cohort of non-infected patients (10). A 2021 study of 442 patients with an infected THA by Wildeman et al. confirmed these observations, concluding to a 3.1 odds ratio of patients suffering from PJI to require ambulatory aids in comparison to non-infected patients, and were more at risk of requiring assisted living. In the same study, the authors have also showed that patients treated for PJI had poorer patients reported outcome measures (EQ-5D-5L score 0.83 vs 0.94, higher scores are better) and Oxford Hip Scores (36 vs 44, higher scores are better) (40). The impact of PJI on joint function may be influenced by the therapeutic strategy used to treat the infection, with less invasive debridement surgeries being associated with better Oxford Hip Scores than staged implant exchanges (41). In addition, the treatment of PJI is associated with a high prevalence of complications. In a retrospective cohort study of 134 patients treated for an infected TKA with a staged revision, Hartzler et al. described a 27% rate of medical complications (e.g.: venous thromboembolism, kidney failure, cardiopulmonary complication) and a 41 % rate of surgical complications (e.g.: septic and aseptic reoperations, wound complications, recurrences of infections), underlining the dreadful morbidity associated with PJI (7). Furthermore, multiple studies have established that the mortality rate in patients suffering from PJI considerably increased. In a 2013 study, Zmistowski et al. showed that the

one- and five-years mortality rates of patients suffering from PJI were significantly increased in comparison to patients requiring arthroplasty revision for aseptic loosening, with mortality rates estimates of 10.6% at one year and 25.9% at five years following treatments, which compares unfavorably to that of some of the most common cancers such as prostate cancer, breast cancer or melanoma (42). A 2018 meta-analysis by Lum et al., compiling the results of 14 studies reporting the mortality of patients benefiting from staged implant exchange for a knee PJI, confirmed these estimates, with a total five years mortality rate of 21.64% (43).

The complex treatments required for the care of patients suffering from PJI as well as the significant morbidity and disability associated with this pathology make PJI a significant financial burden for healthcare systems. In 2005, Bozic and Ries estimated the direct cost of a revision arthroplasty at $96,166 (44). Cost estimates in European countries are lower because of differences in healthcare systems. Nevertheless, the cost of an implant revision for PJI is estimated at 3.6 to 5 times the price of a revision for other causes (20, 45).

Despite a better knowledge of the risk factors of PJI and the implementation of more stringent aseptic techniques, the risk of PJI appears to remain stable or even slightly increase over the years. A longitudinal cohort study performed in Olmsted County, MN, USA over four decades did not reveal any significant decrease in the incidence of PJI over time (9). Similarly, a study of the incidence of PJI following THA and TKA reported in a national database led Kurtz et al. to describe a moderate increase between 2001 and 2009 from 1.99% to 2.18% in THA, and 2.05% to 2.18% in TKA (23).

At the same time, the incidences of THA and TKA have been increasing steadily since 2000 in OECD countries (6) and are projected to increase significantly over the following decade in high-income countries (46-50). These increases are explained by a growing incidence of osteoarthritis in these countries (51) due to an aging population (52, 53) and a rising incidence of obesity (54, 55).

The association of a rising number of arthroplasties performed each year and a stagnant incidence of PJI leads to a projected increase of total PJI (Figure I.3.A). This increase is particularly worrying and is expected to increase the financial burden on healthcare systems over the coming decades (Figure I.3.B) (22, 23).

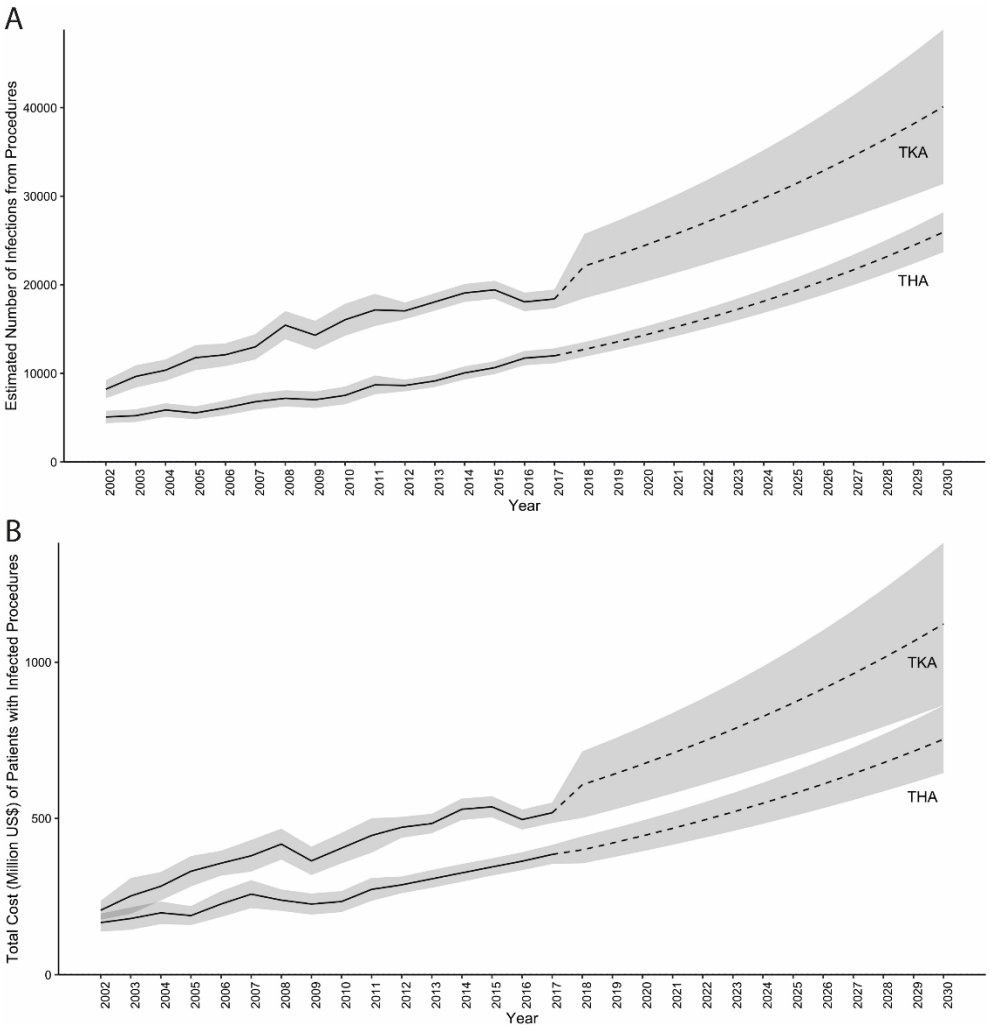


Figure I.3. Projected PJI numbers following THA and TKA in the USA.

A: number of patients; B: cost. Reproduced from Premkumar et al. 2021 (56).

3 Diagnosis

3.1 Clinical definitions of PJI

The clinical definition of PJI used to establish the diagnosis is controversial. It is based on a combination of clinical signs, laboratory tests, histology, and microbiological cultures. Multiple definitions of PJI have been proposed over the years, each based on a different set of criteria, according varying levels of importance to each criterion, and indicating varying levels of likelihood of infection. The MSIS (57), the SOSSID (58), the IDSA (59), the ICM (60) definitions are the most commonly used in the literature. A new EBJIS definition has recently been published, taking into account additional diagnostic modalities (61). As these definitions differ in sensitivity and specificity, knowing the definition used in a study is important to contextualize the reported outcomes.

The MSIS proposed the earliest definition of PJI in 2011 (updated in 2014 by the ICG), using a combination of major and minor criteria, with different thresholds for acute and chronic infections (Table I.1). This definition is the only one not considering purulence as a diagnostic criterion, does not assign a weight to minor criteria, and does not address ambiguous situations.

Table I.1. MSIS PJI definition.

	Acute (< 90 days)	Chronic (> 90 days)
1 Major Criteria	Two cultures of periprosthetic tissues with phenotypically identical organisms	
	Sinus tract communicating with the joint	
OR		
≥3 Minor Criteria	CRP ≥ 10 mg/dL	CRP ≥ 1 mg/dL AND ESR ≥ 30 mm/h
	Synovial fluid WBC ≥ 10,000 OR ++ leukocyte esterase test strip	Synovial fluid WBC ≥ 3,000 OR ++ leukocyte esterase test strip
	Synovial PMN % ≥ 90%	Synovial PMN % ≥ 80%
	≥ 5 PMN per high power field in 5 high power field (400x)	
	1 positive culture	

(57). The authors note that PJI may be present without meeting those criteria, especially when less virulent organisms such as *Cutibacterium acnes* are involved. Adapted from Parvizi et al. 2014

The Swiss Orthopaedics and the Swiss Society of Infectious Diseases (SOSSID) proposed a definition of PJI in 2012 (58). This definition of PJI is based on the presence of highly specific criteria presented in Table I.2. The presence of one positive criterion is sufficient to establish the diagnosis of PJI following this definition.

Table I.2. SOSSID/EBJIS definition of PJI.

Criteria		Sensitivity	Specificity
Sinus tract communicating with the joint		20-30%	100%
Positive histology [a]		95-98%	98-99%
Synovial fluid leukocyte count and differential [b]	Knee: ≥1.7*10^6/mL, ≥65% neutrophils	96%	98%
	Hip: ≥4.2*10^6/mL, ≥80% neutrophils	95%	98%
Purulence around prosthesis		20-30%	100%
Microbial growth	Synovial fluid	60-80%	97%
	Periprosthetic tissue [c]	70-85%	92%
	Sonication fluid (≥50 CFU/mL)	85-95%	95%

[a]: ≥1 to ≥10 neutrophils/high-power field; [b]: excluding the early post-operative period and rheumatoid diseases; [c]: growth of the same organism in ≥2 tissue samples required. Adapted from Corvec et al. 2012 (58).

The IDSA definition, published in 2013, is particularly open to interpretation by the attending physician. The presence of (a) a sinus tract communicating with the joint, (b) the presence of purulence surrounding the prosthesis (with no other possible etiology), (c) two or more intraoperative cultures or a combination of aspiration and intraoperative cultures yielding the same organism or one culture yielding a virulent organism (e.g., *S. aureus*) are considered definitive evidence of PJI. Histological signs of acute infection are considered highly suggestive. A single tissue culture or aspiration culture yielding a common contaminant is not considered definitive evidence of PJI

and has to be interpreted in the clinical context. The ISDA adds that PJI is still a possibility if these criteria are not met and that the definitive diagnosis should be left to the clinician's appreciation (59).

The variable inclusion and interpretation of diagnostic criteria in these earlier definitions lead to discrepancies in the diagnosis of PJI, as illustrated by Renz et al. in 2018 (62). This raised the issue of the sensitivity of these definitions and led to the development of newer definitions from the ICM and the EBJIS.

The ICM proposed a new definition of PJI in 2018 (60). This definition considers major and minor criteria, with a scoring system applied to minor criteria that address ambiguous cases (Table I.3). The scores associated with minor criteria were determined by analyzing 1504 cases of septic and aseptic revisions cases.

Table I.3. ICM definition of PJI.

Major criteria (at least one)			Decision
Two positive cultures of the same organism			Infected
Sinus tract communicating with the joint			
Minor criteria (scored)			
Preoperative diagnosis		Score	Decision
Serum	CRP > 1mg/dL OR D-Dimer > 860 ng/mL	2	≥ 6: Infected 2-5: Possibly infected 0-1: Not infected
	ESR > 30mm/h	1	
Synovial fluid	Synovial WBC count > 3,000/mL OR Leukocyte esterase ++	3	
	Positive alpha-defensin	3	
	Synovial PMN% >80%	2	
	Synovial CRP > 6.9mg/L	1	
Intra-operative diagnosis (if inconclusive pre-op score or dry-tap)		Score	Decision
Preoperative score		-	≥ 6: Infected 4-5: Inconclusive ≤3: Not infected
Positive histology		3	
Positive purulence		3	
Single positive culture		2	

Adapted from Parvizi et al. 2018 (60).

This definition was compared to the initial and updated versions of the MSIS classification using a cohort of 222 septic and 200 aseptic revisions. The new definition achieved a significantly higher sensitivity of 97.7% and a 99.5% specificity similar to previous definitions.

The new EBJIS definition, published in 2020, integrates a broader spectrum of diagnostic modalities than other definitions while adding nuance in ambiguous cases (Table I.4). In contrast to the ICM, the EBJIS based the definition on a literature review and its sensitivity and specificity were not assayed (61).

These definitions share some common criteria. The presence of a sinus tract communicating with the joint is consistently recognized as a clear sign of PJI, as well as the culture of identical microorganisms from at least two intraoperative samples. The importance of other criteria is more controversial and may lead to discrepancies in the identification of PJI cases. This consideration is important when trying to compare published results and should be considered when evaluating diagnostic and therapeutic modalities applied to PJI.

Table I.4. New EBJIS definition of PJI.

	Unlikely (all negative)	Likely (two positive findings) [a]	Confirmed (any positive finding)
Clinical and blood work-up			
Clinical features	Clear alternative reason for implant dysfunction	Implant loosening within five years Wound healing problem Fever or bacteremia Purulence around the implant	Sinus tract communicating with the joint
CRP		> 1 mg/dL	
Synovial fluid analysis			
Leukocyte count (cell/µL)	≤1,500	>1,500	>3,000
PMN%	≤ 65%	> 65%	> 80%
Alpha defensin			Positive
Microbiology			
Aspiration fluid		Positive	
Intraoperative	All negative	1 positive	≥ 2 positives
Sonication (CFU/mL)	No growth	> 1	> 50
Histology			
High-power field	Negative	≥5 neutrophils in one HPF	≥5 neutrophils in ≥5 HPF Visible microorganisms
Others			
Nuclear imaging	Negative three phase bone scan	Positive WBC scintigraphy	

[a] Likely only if a clinical feature is present or CRP is raised together with another test. Adapted from McNally et al. 2020 (61).

3.2 Classification of PJI

PJIs are commonly classified according to the time between the index surgery and the onset of symptoms, their duration, and the presumed origin of the infection. These parameters are of particular interest as they are often related to the type of pathogen causing the infection as well as the formation and maturity of biofilm, providing important guidance to the choice of therapeutic strategy. The classification proposed by Tsukayama in 1996 is commonly used for this purpose (63). The infections are divided into four categories:

- Positive intra-operative cultures: fortuitous identification of a microorganism during a revision for aseptic loosening. These cases are ambiguous and may result from contamination of samples. This is illustrated by the low prevalence of histological signs of inflammation in the original publication describing this classification (63).
- Early postoperative infections: infections occurring less than four weeks after the initial surgery. These infections are usually considered as resulting from peri-operative contamination and are associated with more virulent pathogens.
- Late chronic infections: infections occurring over four weeks after the initial surgery. These infections are also believed to be caused by the peri-operative contamination of the joint and are associated with less virulent pathogens.
- Acute hematogenous infections: acute infection following an episode of bacteremia resulting in bacterial seeding of the joint.

The proportion of each presentation is variable. Based on a recent multicentric study, late chronic infections are the most common (46.1%), closely followed

by early postoperative infections (36.8%), while acute hematogenous infections and positive intra-operative cultures are less common (respectively 11.6% and 5.5%) (64).

Broadly speaking, early post-operative infections and acute hematogenous infections are often amenable to a debridement procedure, whereas a revision is favored in chronic infections (65).

Further refinements on Tsukayama classification have been proposed by McPherson for PJI following TKA and THA, integrating the comorbidities of the patients and the state of the affected limbs (66, 67). The added benefit of the McPherson classification is the identification of patients that could be considered for single-stage revisions (68) as well as those at risk of reinfection following revision arthroplasty (69).

3.3 Pathogens identification

The identification of the causative pathogens is crucial to the diagnosis and the care of patients suffering from PJI. All definitions of PJI consider the isolation of a microorganism from at least two samples to be a major criterion confirming the PJI diagnosis. Also, identifying the pathogen and its antibiotic susceptibility is necessary for selecting an appropriate antibiotic therapy, and is associated with the prognosis of some treatment strategies.

Classically, pathogen identification is made by culturing periprosthetic tissues or synovial fluid. After collection, liquid samples should be inoculated in non-specific solid and liquid media, as well as in BACTEC blood culture systems, while solid samples are usually homogenized and inoculated on solid media (70). While this approach is relatively simple and accessible to

most microbiology departments, it suffers from a low sensitivity resulting from multiple factors such as the pre-operative use of antibiotics, delayed handling of samples, inadequate medium or culture times, fastidious organisms, and biofilm formation (71). Consequently, culture-negative PJI – defined as cases where a diagnosis of PJI has been established but no micro-organism was identified (68) - is a common occurrence with standard techniques and represents 5% to 45% of cases (71).

New methods have been introduced to improve the sensitivity of cultures by detaching the bacteria from the implants or from bone. Implant sonication is used to detach bacteria from explanted implants by immersing the samples in Ringer's solution and submitting them to 30 seconds of vortexing, 5 minutes of sonication in an ultrasound bath, and 30 seconds of vortexing, detaching the bacteria through alternating cycles of bubbles formation and collapse. The solution is then plated for bacterial enumeration and identification. This technique has been shown to have a sensitivity of 78.5% compared to 60.8% for tissue culture (72). Sonication fluid was also shown to be superior to tissue samples for the detection of bacteria using molecular methods such as PCR (73). The use of dithiothreitol (DTT) has been proposed in the last decade to break up biofilms and facilitate the recuperation of bacteria. DTT is a reducing agent known to break up disulfide bonds of proteins while presenting no toxicity against bacteria. For this technique, the implants are immersed in a 0.1% DTT solution and stirred for 15 minutes. The solution is then centrifugated and resuspended before plating. The promoters of the technique report a significantly higher sensitivity (85.7%) compared to standard culture techniques (71.4%) and the sonication method (71.4%) while presenting a specificity similar (94.1%) to sonication (94.1%) but higher than

standard cultures (76.5%) (74). A later independent study confirmed the interest of this technique for the diagnosis of PJI over standard tissue cultures but did not demonstrate superiority over sonication (75), and the position of DTT in the diagnosis of PJI remains controversial (76).

While these techniques improve the sensitivity of cultures over standard culture techniques, the risk of culture-negative cases remains high (77). Molecular techniques have been proposed to improve the identification of the causative agents. Polymerase chain reaction (PCR) amplification of the 16S ribosomal RNA from sonication fluid samples has been shown to improve the identification of bacteria in multiple studies when used in combination with culture-based techniques (78, 79). However, this technique is unable to assess antimicrobial susceptibility or to detect fungi, and next-generation sequencing techniques have been proposed to improve on these aspects but are not yet in broad usage (80).

4 Pathogens

The microbial etiology of PJIs is varied and is influenced by the affected joint (5), the temporality and mode of infection (64), and national differences (81). Overall, *Staphylococcus aureus* and coagulase-negative staphylococci (CoNS) are the most frequently isolated pathogens, followed by aerobic Gram-negative bacilli, streptococci, enterococci, and *Cutibacterium acnes*. Polymicrobial infections are observed in up to 27.4% of cases (64). A multitude of other species are infrequently encountered - including Gram-positive bacilli, *Mycobacterium* sp., and fungi – and will not be discussed.

4.1 Staphylococcus aureus

Staphylococcus aureus is non-motile Gram-positive spherical bacteria measuring 0.5 to 1.5 µm forming grape-like structures, with a facultative anaerobe metabolism (82). *S. aureus* is a common commensal bacterium found in the anterior nares of up to 30% of healthy individuals (83). It is also an important pathogen involved in skin infections, pneumonia, and osteomyelitis. *S. aureus* is the second most common pathogen in nosocomial infections and the most common in surgical site infections (84). While initially susceptible to antibiotics, *S. aureus* has developed resistance mechanisms to most antibiotics, mainly through target modifications and acquisition of enzymes degrading the antibiotics by horizontal genes transfer (85). Methicillin-Resistant *S. aureus* (MRSA) strains are of particular concern because of their prevalence in nosocomial infections and their association with resistance to other antibiotics (86).

In PJI, *S. aureus* is the first to second most common species isolated (81, 87). It is particularly common in early post-operative and acute hematogenous infections, representing respectively 35.6% and 39.2% of cases in a large multicentric study (64). This distribution of cases is indicative of the high virulence of *S. aureus* and of a dual origin, with contaminations occurring during surgeries or through bacteremia (88). The prevalence of MRSA among *S. aureus* isolated in PJI is variable, reflecting national differences in MRSA prevalence (86), making up 48.1% of cases in the USA but only 12.8% of cases in Germany (81).

In addition to being highly prevalent in PJI, infection with *S. aureus* has been shown to be an important risk factor for failure following treatment with

surgical debridement, antibiotics, and implant retention (DAIR) (89, 90). The impact of methicillin resistance on these failures is uncertain but has been associated with additional failure risks in some studies (91, 92), while a large multicentric study focusing on *S. aureus* infections did not show significant differences in failures between MRSA and MSSA (93).

Multiple factors may explain failures following infections with S. aureus treated with DAIR. Besides the high prevalence of antibiotic resistance, *S. aureus* is known to readily form biofilms on abiotic surfaces, sheltering the bacteria from antibiotics and the immune system (94). Moreover, *S. aureus* is able to isolate itself further through the infection of osteoblasts and the invasion of bone canaliculi which may become reservoirs of bacteria (95, 96). These persistence mechanisms limit our ability to eradicate the infections in cases where debridement is imperfect and may explain the more favorable outcomes observed with implant removal instead of DAIR (97).

4.2 Coagulase-negative staphylococci

Coagulase-negative staphylococci (CoNS) are a vast group of non-motile Gram-positive spherical bacteria measuring 0.5 to 1.5 µm forming grape-like structures, with a facultative anaerobe metabolism (82). CoNS are common skin commensal bacteria and are usually regarded as less virulent than *S. aureus* (98, 99). The main virulence factor of CoNS is their strong ability to form biofilms on abiotic surfaces, explaining their common occurrence in medical device infections (100). As is the case with *S. aureus*, CoNS frequently exhibit resistance mechanisms to antibiotics and antiseptics acquired through mutations and horizontal gene transfers. Methicillin-

resistant CoNS are particularly common in PJIs, representing 45.0% to 51.9% of the strains isolated in an international study (81).

CoNS share the position of first to second most commonly isolated pathogens in PJI with *S. aureus* (81, 87). They are usually isolated in late chronic infections and positive intra-operative culture cases, making up respectively 54.5% and 57.1% of cases (64), which may be explained by the low virulence of CoNS, resulting in indolent or late presentation of symptoms.

Contrarily to *S. aureus*, CoNS have not been associated with more frequent failures despite forming strong biofilms. Indeed, the late presentation of CoNS infections leads to the use of surgical strategies involving implant revision, which facilitates the mechanical removal and disruption of biofilms. Moreover, contrarily to *S. aureus*, CoNS present a low affinity for osteoblasts infection, limiting their potential niches following debridement (101).

4.3 Aerobic Gram-negative bacilli

When defining the pathogens responsible for PJIs, the term aerobic Gram-negative bacilli is often used to encompass a broad range of bacteria belonging to the families *Enterobacteriaceae*, *Pseudomonadaceae*, and *Moraxellaceae* (64, 81). In earlier studies, aerobic Gram-negative bacilli were thought to represent only a limited portion of the pathogens involved in PJIs, but recent series have observed their presence in up to 47.1% of early postoperative infections (64, 81). The most common bacteria from this group found in PJI cases are *Escherichia coli* and *Pseudomonas aeruginosa*, which are involved in respectively 15.4% and 15.3% of early postoperative infections (64). *E. coli* is also isolated in 12.5% of acute hematogenous infections. Infections with these pathogens are particularly concerning as they

are associated with more common failures following treatment that may be explained by a high prevalence of antibiotic resistance, virulence mechanisms, and biofilm formation (102, 103).

4.4 Streptococci

Streptococcus sp. belong to a large group of Gram-positive cocci commensal to the oral environment and responsible for various pathologies in humans (104). *Streptococcus agalactiae* and streptococci of the *viridans* group are the most prevalent in PJI and are usually associated with acute hematogenous infections, making up 10.9% and 4.5% of cases, respectively. The outcome of infections caused by streptococci is relatively poor, with failures following DAIR observed in 42.1% of patients in a large multi-centric study (105), which could be explained by the propensity of these species to form biofilms (106).

4.5 Enterococci

Enterococcus sp. are a family of Gram-positive cocci commensal to the digestive tract of humans. Two species (*E. faecium* and *E. faecalis*) are common human pathogens and present intrinsic and acquired resistance to antibiotics. Acquired resistances are particularly common in enterococci because of their susceptibility to horizontal gene transfer and a particular tendency for mutations in pathogenic strains (107). *E. faecalis* is the most prevalent in PJIs and is identified in 11.3% of early postoperative infections and is frequently associated with polymicrobial infections (64). These infections were classically considered to be challenging to treat. However, recent series have shown good results, especially in acute cases treated with DAIR (108, 109).

4.6 Cutibacterium acnes

Cutibacterium acnes is an anaerobic Gram-positive bacillus commensal of the sebaceous glands of the skin (110). *C. acnes* is an opportunistic pathogen whose association with medical device infections is increasingly recognized thanks to advances in diagnostic modalities. Recent studies show that overall, *C. acnes* is present in up to 6.1% of late chronic infections and 15.1% of positive intra-operative cultures (64). The prevalence of *C. acnes* is even higher in revision shoulder arthroplasties. A retrospective study of 193 should arthroplasties revisions revealed positive cultures for *C. acnes* in 39% of cases (111). Resistance is not a significant issue with *C. acnes*, and successful treatments are reported in most cases (112-114).

4.7 Polymicrobial infections

The identification of more than one pathogen in PJI cases is frequent. It has been reported to occur in 27.4% of early postoperative infections and 13.1% of late chronic infections (64). An important variety of germs have been identified in this setting. While the proportion of *S. aureus*, Gram-negative bacilli, and streptococci is similar to what is observed in mono-microbial infections, *S. epidermidis* and enterococci appear more frequently (115). Polymicrobial PJIs are associated with more frequent treatment failures, but the variety of pathogens involved limits the investigation of the impact of specific associations in clinical series (116). A better understanding of the dynamic of pathogens combinations appears particularly important as in-vitro studies have shown that some combinations resulted in a more pronounced tolerance to antibiotics (117, 118).

5 Treatment strategies

5.1 Overview

The treatment of PJIs is multidisciplinary and involves in most cases the combination of surgical and medical therapies. Antibiotic therapy alone is insufficient to cure a patient of a PJI and should be reserved for patients unfit for surgery and candidates to lifelong suppressive treatments (119). In patients treated with the intent of eradicating the infection, antibiotic therapy is preceded by the surgical excision of infected and necrotic tissues, biofilm disruption by irrigation of the implant, or removal by explantation of the implant, and coverage of the joint in cases of wound defects (13). The choice of surgical technique is of paramount importance regarding the outcome of the infection and is usually guided by characteristics of the infection, the patient, and the implant.

5.2 Surgical strategies

5.2.1 Debridement surgery, antibiotic therapy with implant retention

Implant retention through the use of the debridement surgery, antibiotic therapy, with implant retention (DAIR) strategy is usually attempted in early post-operative infections and acute hematogenous infections. The correct application of this strategy requires the following criteria to be met (59):

- Infection occurring within 30 days of the index surgery or less than 3 weeks of symptoms after a bacteremia
- Well-fixed, functioning implant
- No sinus tract

- Pre-operative identification of a pathogen susceptible to oral antibiotics

The procedure consists in a thorough open debridement of grossly infected and necrotized joint tissues, exchange of mobile parts of the implant (e.g., the tibial polyethylene articular surface of a TKA), and irrigation of the implant and the joint using a pulsed-lavage device with 6 to 9 L of saline with or without an antiseptic (120). It is then followed by six to twelve weeks of antibiotic therapy (121).

This approach presents significant advantages over those relying on implant revision with regards to the functional outcome (41), preservation of bone stock, acceptable medium-term mortality (89), and costs (122) without precluding further treatments (123).

However, DAIR is characterized by a highly variable occurrence of treatment failures, ranging from 12 % (8) to 82% (92), with most studies reporting failure rates around 40% (89, 124, 125). These failures are related to multiple factors, including patient-related factors (co-morbidities, age, sex), implant characteristics, initial presentation, time from the beginning of symptoms, and PJI caused by *S. aureus* or enterococci (121). The importance of the elapsed time and the causative organisms point towards an implication of maturing biofilms in for the risk of treatment failure.

5.2.2 Implant revision

The removal of the infected implants, associated with joint space debridement and wound coverage in case of defects, is recommended in late chronic

infections, in patients for whom DAIR is contra-indicated, or following DAIR failure (13).

This procedure is classically carried out in two steps – debridement, explantation, and temporary reconstruction with a cement spacer containing antibiotics, followed by the implantation of a new implant – separated by up to eight weeks. In well-selected patients, implant revision may be performed in a one-stage procedure. The ICM recommends this procedure for non-immunocompromised patients, without systemic sepsis, presenting adequate bone stock and soft tissues, and with a preoperatively identified micro-organism with known sensitivities to antibiotics (126).

Antibiotic treatment is administered after the initial surgery and is continued for a total of three to six months (59, 127).

Implant revision, whether executed in one or two steps, is generally considered to result in better infection control than DAIR, with failures occurring in 5 to 25% of cases (128, 129).

However, this approach also presents some drawbacks, explaining why DAIR remains an accepted procedure in acute cases. Implant revision is associated with a high rate of complications (12), diminished functional results in comparison to DAIR or aseptic revisions (10, 130), significant 5-year mortality (131), and extremely high costs (45).

5.2.3 Resection arthroplasty and amputations

In case of treatment failure with implant revision, salvage procedures such as resection arthroplasty (removal of the implant without reimplantation, e.g., Girdlestone procedure), arthrodesis (fusion of the joint), or amputation of the

limb are proposed. Indeed, the chances of success of a second revision are reported at 36.4% to 61.6% (132, 133) and are usually regarded as minimal by experts following a third or fourth revision (134).

These procedures are performed in frail patients and are associated with significant morbidity, high mortality, and high complication rate (135-137).

An alternative to these procedures is the administration of a lifelong suppressive antibiotic treatment following a minimal surgical debridement, performed to evacuated abscedated collections, to control the symptoms of infection through a limitation of bacterial proliferation instead of their eradication. This treatment is only applicable in patients infected with an identified pathogen susceptible to a potentially well-tolerated antibiotic such as tetracyclines and should be considered palliative (138).

5.3 Antibiotic therapy

Antibiotic therapy is an essential element of PJI treatment, relying on the identification of the causative pathogens and the determination of their susceptibilities (13). Ideally, the selected antibiotics should present a good activity against biofilms, good penetration in bone, and be well tolerated.

Antibiotics should ideally be introduced after surgical sampling and be withheld for two weeks prior to the revision surgery (139). The duration of the antibiotic treatment is still the object of discussion. The IDSA guidelines differentiate the treatment duration on the basis of the surgical procedure, the causative pathogen, as well as the affected joint.

Following DAIR for staphylococcal PJIs, the IDSA guidelines suggest 2 to 6 weeks of IV antibiotics in combination with oral rifampin, followed by an

oral antibiotic therapy with rifampin and a companion antibiotic for a total duration of 3 months of treatment for THA and 6 months of treatment for TKA. A 4 to 6 weeks treatment using a pathogen-specific IV or highly bioavailable oral antibiotic is recommended in cases of PJI caused by non-staphylococcal micro-organisms treated with DAIR.

Following one stage revisions for staphylococcal PJIs, patients should be treated 2 to 6 weeks with IV antibiotics in combination with rifampin, followed by an oral antibiotic therapy with rifampin and a companion antibiotic for a total duration of 3 months of treatment.

Following a two stages implant revision or DAIR for other pathogens, the IDSA recommends the administration of antibiotics for 4 to 6 weeks following implant resection, using either IV antibiotics or highly bioavailable oral antibiotics. No consensus exists concerning the administration of antibiotics following the implantation of a new prosthesis.

These guidelines were mostly the result of experts' opinions and consensus, or based mainly on moderate quality evidence (59). In particular, the duration of antibiotic treatment is not well established. However, recent evidence from a non-inferiority randomized controlled trial comparing 6 weeks with 12 weeks antibiotic treatments for patients treated for PJI, irrespectively of the causative micro-organism or surgical strategy, found shorter treatments to be associated with more failures, while no differences in adverse events were found between the two groups. Although the authors note that further randomized trials should investigate the duration of treatments in regard to the type of surgery, the results of this study should point towards the application of longer treatments (140).

The antibiotic regimens recommended by the IDSA are described in Table I.5. Recommended oral companions antibiotics are quinolones, or, if necessary because of allergies, intolerance or non-susceptible micro-organism, co-trimoxazole, a tetracycline, a first-generation cephalosporin, or an anti-staphylococcal penicillin. The IDSA recommendations suggest using either ciprofloxacin or levofloxacin, but other molecules, such as moxifloxacin, appear to have excellent results and have been proposed as alternatives (141).

Table I.5. Recommended antibiotics for the treatment of PJI.

Organism	Preferred antibiotics	Alternative antibiotics	Suppressive antibiotics
Methicillin susceptible staphylococci [a]	Nafcillin, Cefazolin, Ceftriaxone	Vancomycin, Daptomycin, Linezolid	Cefalexin, Cefadroxil, Dicloxacillin, Clindamycin, Amoxicillin-clavulanate
Methicillin-resistant staphylococci [a]	Vancomycin	Daptomycin, Linezolid	Cotrimoxazole, Minocycline, Doxycycline
Penicillin susceptible enterococci	Penicillin G, Ampicillin	Vancomycin, Daptomycin, Linezolid	Penicillin V, Amoxicillin
Penicillin resistant enterococci	Vancomycin	Linezolid, Daptomycin	
Pseudomonas aeruginosa	Cefepime, Meropenem	Ciprofloxacin, Ceftazidime	Ciprofloxacin
Enterobacter sp	Cefepime, Ertapenem	Ciprofloxacin	
Enterobacteriaceae	β-lactam, Ciprofloxacin		Co-trimoxazole, β-lactam
Streptococcus sp.	Penicillin G, Ceftriaxone	Vancomycin	Penicillin V, Amoxicillin, Cefalexin
C. acnes	Penicillin G, Ceftriaxone	Clindamycin, Vancomycin	

[a]: in association with oral rifampin in non-suppressive treatments. Adapted from Osmon et al. 2013 (59)

Chapter II: Introduction - Biofilms

1 Definition and historical perspective

Donlan and Costerton defined biofilms as "*a microbially derived sessile community characterized by cells that are irreversibly attached to a substratum or interface or to each other, are embedded in a matrix of extra-cellular polymeric substances that they have produced, and exhibit an altered phenotype with respect to growth rate and gene transcription*" (142).

Bacteria organized in what we would now describe as biofilms were among the first specimen observed and described by Antoni Van Leeuwenhoek in 1693, following the observation of numerous "animalcules" living in his own oral plaque (143). However, the study of this mode of bacterial life was overshadowed by that of planktonic bacteria until the 1980s, when the importance of slime producing *S. epidermidis* and *S. aureus* to medical device infections began to be recognized thanks to advances in scanning electron microscopy (144, 145).

Nowadays, the importance of biofilm formation to the development of recalcitrant infections, such as medical device infections and chronic wound infections, is well recognized and is the subject of intense research (Figure II.1). The presence and impact of bacterial biofilms have been established in the orthopedic field at the turn of the century (14, 146-148) and have since become a major consideration in the diagnosis and treatment of patients suffering from PJI (13, 149).

The recognition of the implication of biofilms in PJI and orthopedic devices related infections has further led to active research efforts from multiple groups aiming at preventing biofilm formation on implants, improving the isolation of bacteria embedded in biofilms, and facilitating biofilm eradication through the use of specific therapeutics.

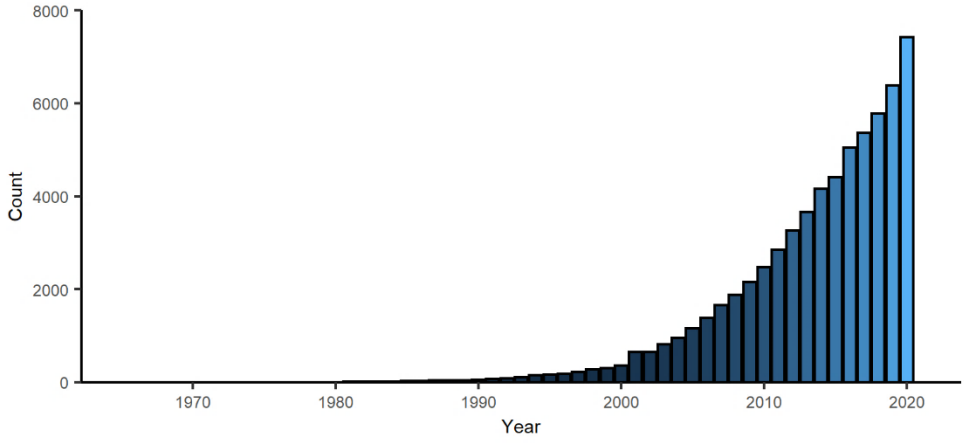


Figure II.1. PubMed publication count for "biofilm".

2 Biofilm formation and regulation

Biofilm formation and maturation are complex processes, forming a continuum from bacterial adhesion to a substratum to the dispersion of parts of the biofilm and seeding of bacterial cells to new locations. This process is typically described as occurring in four main steps (Figure II.2): bacterial adhesion to a substratum, bacterial multiplication and formation of an extra-cellular matrix, maturation of the biofilm, and finally, a self-regulated dispersal of the biofilm and seeding to a new location (150).

After reaching a substratum through passive – Brownian motion, gravitational forces – or active motion – active motility of flagellated bacteria – the bacteria interact with the surface through aspecific and specific mechanisms. The initial adhesion of bacteria to abiotic surfaces results from general physicochemical mechanisms such as Van der Waals interactions, electrostatic forces, and hydrogen bonds, as well as species-specific mechanisms, such as staphylococcal autolysin-associated attachment to polystyrene (151). These mechanisms are influenced by the surface properties, such as topography, charge, and hydrophobicity (152), and by bacterial characteristics, such as bacterial wall composition and cell shape (153), resulting in the variable affinities for materials exhibited by some species (154-156).

Following contact with biological fluids, artificial surfaces rapidly adsorb host proteins (157), forming a conditioning film of proteins. These proteins are the target of bacterial surface-bound or secreted proteins that allow the bacteria to adhere to the surfaces. In staphylococci, the main proteins involved in this process belong to the MSCRAMMs family of adhesins (158). MSCRAMMs adhesins are part of a family of over 20 proteins found in staphylococci that are covalently bound to the cell wall peptidoglycan and specifically bind to host proteins such as fibronectin, fibrinogen, or collagen (159). Different adhesins have been described in other species. For example, the main adhesins involved in *E. coli* adhesion are the pili adhesins and the curli fibers (160).

The adhesion of bacteria to the substrate induces the expression of genes associated with the production of the extra-cellular polymeric substance

(EPS) components like the *icaABCD* – involved in the synthesis of poly-*N*-acetylglucosamine (PNAG) - and *cidAB* – involved in bacterial lysis and release of extra-cellular DNA (eDNA) - operons in staphylococci (161), leading to the irreversible adhesion of bacteria to the substratum and the formation of biofilm.

Following these initial steps, biofilm maturation continues through cell division, production of EPS, and remodeling. The maturation is influenced by the biofilm environment and the stresses to which it is confronted. For example, the exposition of biofilms to sub-inhibitory concentrations of antibiotics is a known factor promoting biofilm development (162). Mechanical challenges such as shear stress at the biofilm interface and medium or the application of pressure on the biofilm are also factors known to influence the production of EPS (163).

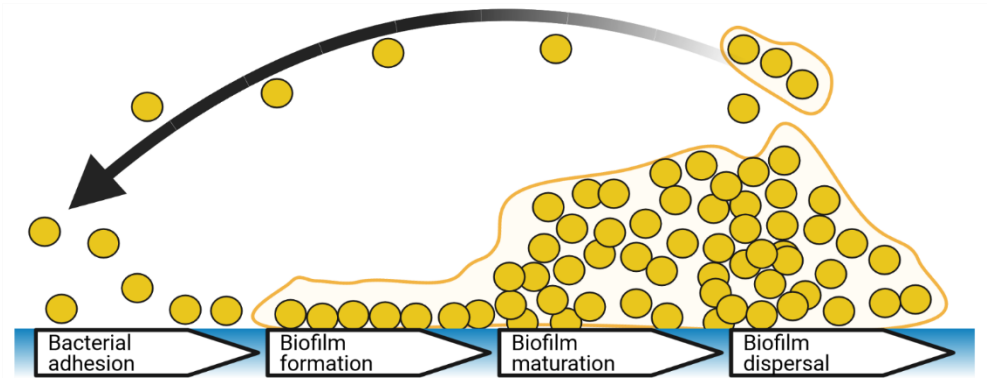


Figure II.2. Stages of biofilm formation and development. Adapted from Arciola et al. 2018 (17).

Another mechanism at play during biofilm maturation is the expression of signaling molecules involved in the quorum-sensing system that regulates the

density of biofilms and promotes their dispersal. These small molecules are produced during bacterial growth, and their concentration serves as an indicator of bacterial density. For example, in staphylococci, the best-known quorum-sensing mechanism is the *agrABCD* system, which is under the control of the auto-inducing peptide (AIP). The AIP is a small cyclical peptide originating from the cleaving of agrD by agrB and subsequently secreted (164). Through the increase in AIP extra-cellular concentration, the *agr* locus transcription is activated, upregulating the production of serine proteases, phenol-soluble modulins – small peptides acting as surfactants disrupting the EPS - and exotoxins, while inhibiting the expression of adhesins leading to biofilm rearrangement and dispersal (165, 166).

3 Matrix composition

The production of the EPS by the bacteria following their attachment to the substratum is an essential process in the development of the biofilm, leading to the establishment of complex structures, isolating the bacteria from their surrounding environment, protecting them from the immune system and antibiotics, and leading to the emergence of distinct phenotypes (17, 167). The composition of the EPS is complex and is influenced by multiple

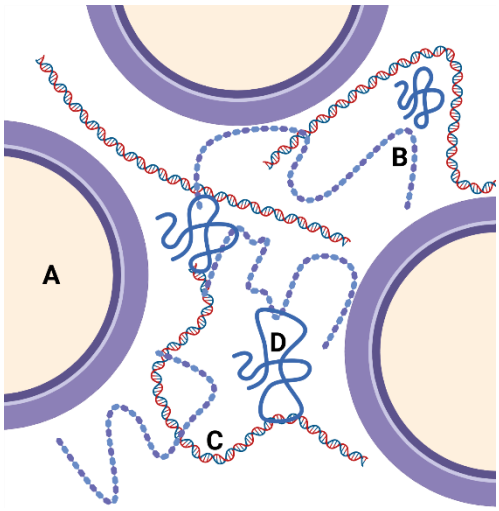


Figure II.3. Schematic representation of EPS composition. A: Bacterial cell, B: Polysaccharide, C: eDNA, D: Protein. Adapted from Flemming et al. 2010 (1).

parameters, including the bacterial species and strain, their environment, and the stresses to which the bacterial communities are exposed. The main constituents identified in most species are polysaccharides, extra-cellular DNA, and proteins (17).

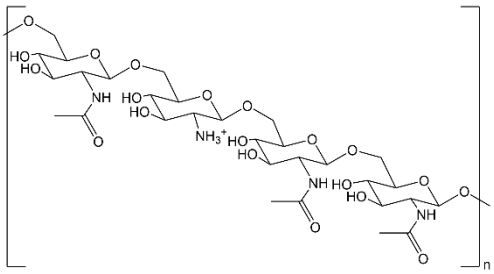


Figure II.4. Poly-*N*-acetylglucosamine (Structure drawn in ChemDraw by A. Ruiz-Sorribas).

The most common polysaccharide in biofilms of species relevant to PJIs is poly-*N*-acetylglucosamine (PNAG), also referenced to as polysaccharide intercellular adhesin (PIA). It constitutes the main component of biofilms formed by *S. epidermidis* (168), *E. coli* (169), and by *S. aureus* strains expressing the *icaABCD* operon (170). PNAG is actively synthesized by proteins encoded by the *icaABCD* operon in staphylococci (170) and by the *pgaABCD* operon in *E. coli* (169). It is implicated in the adhesion of bacteria to the substratum, and its production is crucial for biofilm development and virulence in most *S. epidermidis* strains (171). The regulation of the expression of the *icaABCD* operon is complex and involves multiple signaling pathways, reflecting the function of PNAG (172). Of note, *icaABCD* expression is modulated by adhesion forces, with stronger adhesion resulting in a lower expression (161), and is upregulated by the exposure of bacteria to environmental stresses such as anaerobic conditions (173), NaCl, ethanol (174), glucose (175), shear stress (163), and subinhibitory antibiotic concentrations (176). *PgaABCD* expression in *E. coli* was also found to be upregulated when the bacteria were exposed to similar environmental stresses (177). The biofilms of some species

contain other polysaccharides in significant proportions that are important to mention. Cellulose is a major component of the EPS of *Enterobacteriaceae* (178, 179). It is produced by the proteins encoded by the *bcsABZC* operon, and mutations in these genes lead to the formation of weaker biofilms (179). The EPS of mucoid strains of *P. aeruginosa* biofilms are characterized by the presence of alginate, which has been shown to protect the bacteria from phagocytosis by macrophages in patients with cystic fibrosis (180).

Extra-cellular DNA (eDNA) is another important element of EPS. The presence of eDNA is required for the adhesion of *P. aeruginosa* (181) and multiple Gram-positive bacteria (182) to their substratum and is required for biofilm formation. It is present in the EPS of staphylococci and appears to predominate PNAG in *S. aureus* biofilms (168). In biofilms, eDNA binds to other polysaccharides and proteins of the matrix, thus stabilizing the matrix (183). Furthermore, eDNA appears to be involved in horizontal gene transfers, facilitating the acquisition of resistances (184). The origins of eDNA are multiple. *In-vitro* observations point towards regulated autolysis, under the control of quorum-sensing systems, in most Gram-positive and Gram-negative species (184). Some species possess alternative mechanisms of eDNA production. For example, *Neisseria gonorrhoea* uses a type IV secretion system to secrete eDNA without inducing cell death (185), whereas in *E. faecalis* biofilms, a subset of the population is preyed upon by the rest of the population by the secretion of the GelE protease (186). It should however be noted that these mechanisms were described in *in-vitro* models. Evidence of the origin of eDNA in *in-vivo* models are scarce but point towards the use by bacteria of DNA derived from the host (187).

Extra-cellular proteins constitute a major component of the EPS, fulfilling structural and functional roles in the biofilms (1, 188). Enzymes represent a significant portion of these proteins. They are retained by the EPS leading to their accumulation and their protection from proteolytic enzymes (189). The production of these enzymes is regulated by the bacteria. These enzymes serve multiple functions in the biofilm, including nutrients metabolism, resistance to stresses, host tissues degradation, and antibiotic degradation (190-192). Other proteins secreted by the bacteria are involved in the remodeling of the biofilm or its dispersal. Examples of this are the phenol soluble modulins, whose production is under the control of the agr quorum-sensing system, that are involved in the structuration of staphylococci biofilms (193), or the hexosaminidase dispersin B, involved in the dispersal of the *Aggregatibacter actinomycetemcomitans* biofilms (194).

Multiple proteins also play an important role in the adhesion and cohesion of biofilms, particularly in *icaABCD* deficient staphylococci (195). Examples of proteins involved in *S. aureus* biofilm are the fibronectin binding proteins (196), clumping factor B (197), SdrC (198), SasC (199), SasG (200), and Protein A (201). Phenol-soluble modulins also present a structural role, besides their maturation effect, by forming amyloid fibrils within the biofilm (202).

4 Consequences of biofilm formation

The formation of biofilms has significant impacts on the evolution and treatment of implant-related infections. Indeed, biofilm formation is

associated with a tolerance of bacteria to antimicrobials and a reduced susceptibility to the host's immune defenses (17).

Antimicrobial tolerance, defined as the ability of bacteria to survive a transient exposure to antibiotic concentrations exceeding the MIC (203), is a well-documented phenomenon in biofilms (19). The tolerance of biofilms may be appreciated by determining the Minimal Biofilm Eradication Concentration (MBEC), the minimal concentration of antimicrobial necessary to kill all bacteria in a biofilm, which has been shown to exceed 1000x the MIC of planktonic cultures (204). Multiple mechanisms have been proposed to explain the tolerance of biofilms to antimicrobials.

A decreased penetration of antimicrobials in the biofilms was initially thought to be the primary mechanism driving antimicrobial tolerance (205). This hypothesis was supported by early observations of hindered penetration of antiseptics and antibiotics in the biofilms that were attributed to either limited diffusion (206), sorption by the matrix (207), or reaction within the matrix (208). This effect appears particularly strong for positively-charged antibiotics such as aminoglycosides, whereas fluoroquinolones are able to diffuse within the biofilm (209). However, it was later observed that even with antibiotics that readily diffuse through biofilms, such as rifampin, bacterial killing did not occur at rates equivalent to planktonic cultures, suggesting that other mechanisms are at play (210).

Biofilm formation leads to the establishment of gradients of nutrients concentration, oxygen concentration, metabolic by-products, and pH, that in turn lead to the development of physiologically heterogeneous bacterial populations, with bacteria in the center of the biofilm being less metabolically

active and growing slowly (167, 211, 212). These harsh conditions and slow metabolism have been associated with reduced susceptibility of cells in biofilms to β-lactams and aminoglycosides (213, 214). Still, these metabolic modifications and environment do not account for the tolerance observed to all antibiotic classes. For example, fluoroquinolones are known to exert a bactericidal effect on non-growing cells but to have a reduced activity on biofilms (213, 214).

Biofilms are also characterized by modifications in genes expression and transfer between bacteria when compared to planktonic cultures. These modifications are well studied in *P. aeruginosa* and *E. coli*, for which it has been shown that the expression of genes coding for efflux pumps were upregulated in biofilms, which was associated with a reduced susceptibility to antimicrobials (215-217).

Biofilms are also known to harbor a specific bacterial subpopulation, representing less than 1% of the total bacterial population of a biofilm, of cells that are not killed by antibiotics while presenting no genetic difference from the rest of the population, called persisters. These cells are non-dividing in the presence of antibiotics but resume their growth once the antibiotics are removed, which may lead to infection relapse (218).

Horizontal gene transfer is also known to be more common in biofilms of Gram-negative and of Gram-positive species (219), facilitating biofilm formation (220) and leading to the acquisition of new resistance genes (221), which may be further selected by the exposure to sub-inhibitory antibiotic concentrations favored by the biofilm environment (222, 223).

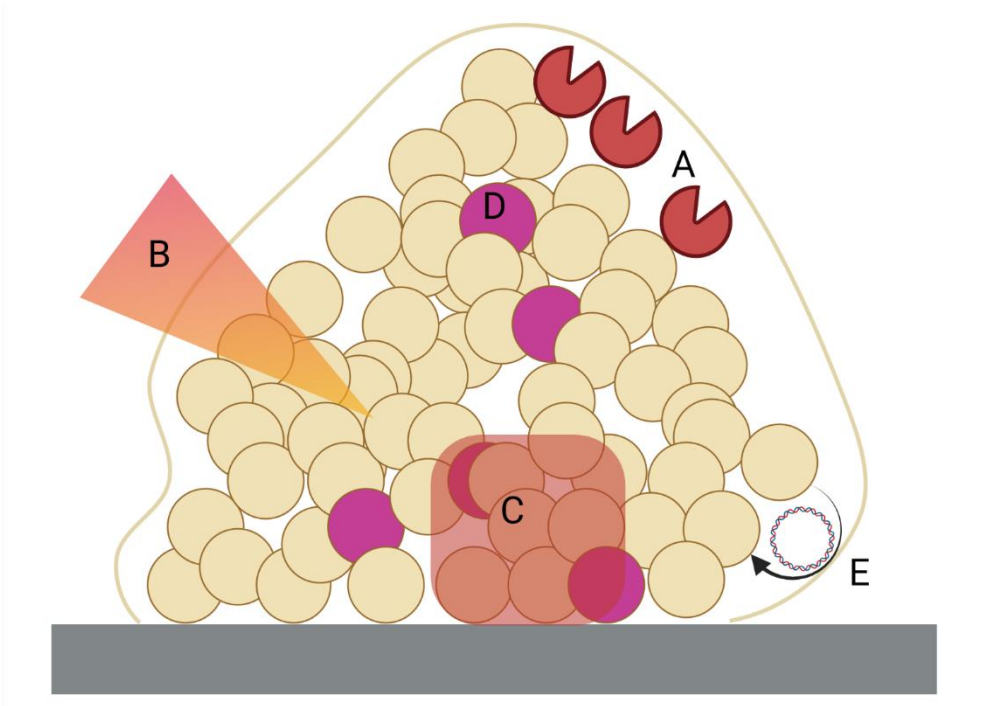


Figure II.5. Schematic representation of the mechanisms of antibiotic tolerance in biofilms. A: accumulation of enzymes in the EPS, B: penetration gradient of antibiotics, C: slow growing population, D: persister cells, E: horizontal gene transfers. Adapted from Lebeaux et al. (223).

Bacteria in biofilms also present a capacity to evade the host immune system through various mechanisms (224). Biofilm formation appears to limit the phagocytosis of staphylococci biofilms by polymorphonuclears as the biofilm matures (225) and impedes the phagocytosis by macrophages while inducing their death (226). This phenomenon may be explained by the adsorption of immunoglobulins and complement factors by EPS (227) and the size of biofilm particles that could lead to frustrated phagocytosis. Staphylococcal biofilms are also able to interfere with the inflammatory pathways of their

hosts, attenuating the production of proinflammatory mediators and leading to a fibrotic reaction to the biofilms (228, 229). Other species-specific mechanisms of resistance to the host immune system exist, such as the production of toxins by *S. aureus* that cause the dysfunction or death of leukocytes (230, 231).

5 Experimental Models

An extraordinary variety of models have been proposed over the years to study biofilm-related infections (232). These models range in complexity from simple generalists *in-vitro* models to complex *in-vivo* models reproducing specific conditions, including prosthetic joint infections.

5.1 *In-vitro* models

A broad range of in-vitro models has been used over the years to study biofilm formation and physiology, to study the effect of antibiotics on biofilms, and to initiate the study of biofilm-specific treatments. These models have been classified by Lebeaux et al. into two main categories (232):

- Closed models: Models where the biofilms are grown or exposed to substances in batch-mode (no flow of medium), for example, microtiter plate models. These models are usually high throughput allowing the assay of varied conditions.
- Open models: Models where the medium is continuously replaced, allowing better control of the biofilm environment, for example, the drip-flow bioreactor. These models are substantially more complex to set up than closed models and present a lower throughput.

The models relevant to the study of biofilms in PJI are described below.

5.1.1 Closed models

The most common model used to study biofilms is the microtiter plate biofilm model. Biofilms form on the surface of the wells or, for some species such as *P. aeruginosa*, at the interface between air and medium, following the addition of a bacteria suspended in growth medium to the plates (233, 234). This model presents the advantage of being cheap and simple, allowing the realization of high-throughput experiments. Multiple parameters are easily analyzed, such as biomass estimates through staining with crystal violet or safranin, CFU counts, or metabolic assays (ex: MTT, resazurin). The microtiter plate biofilm assay can easily be modified to refine their results further or take into account specific parameters of the situation they aim to reproduce.

One such modification is the Calgary biofilm device (CBD). It consists of a special lid for 96 wells plates fitted with pegs made of polystyrene or coated with hydroxyapatite or titanium dioxide. The lid is placed over a standard 96 wells plate, allowing the biofilm formation on the pegs. Besides the use of specific materials, this model has the advantage of avoiding the sedimentation of bacteria that occurs in standard microtiter plate assays and to limit operator-induced variations, producing reproducible results (204). The CBD is mainly used to study the effect of antimicrobials on mature biofilms, allowing the determination of the Minimal



Figure II.6. Calgary Biofilm Device

Biofilm Eradication Concentration, and is the object of a standardized method published by the ASTM (235). Other uses of this model include the study of the 3D structure of biofilm through microscopy (236), the influence of shear stresses on the development of biofilms (237), or the effect of quorum-sensing (238).

Another variation of the microtiter plate assays consists in the use of coupons of materials of interest as the substratum of biofilms. Typically, disks of specific materials are places at the bottom of 6, 12, or 24 wells plates and are incubated with a bacterial suspension with or without agitation. The biofilms are then recovered to analyze biofilm development or to be submitted to treatments. This model presents the advantage of offering a more relevant substratum for the development of biofilms and allowing for more advanced analysis techniques such as scanning electron microscopy or confocal microscopy (Figure 8). It has been used to study the impact of substratum on the development of biofilms (161, 239), the use of coated surfaces to prevent biofilm formation (240, 241), to develop new bacterial isolation techniques such as the use of DTT (242), or the use of antimicrobials and antiseptics (243). This model is also well suited for the evaluation of treatment combinations involving non-pharmaceutical interventions such as the combination of pulsed-lavage and antiseptics (244).

These models present several limitations. By design, the medium is not continuously replaced, leading to important variations in nutrient concentrations and accumulation of signaling molecules (245). The biofilms in microtiter plates and the CBD develop on surfaces of little or no clinical relevance, which may influence their composition (161). While the

introduction of shear stress in these models is possible by placing the plates on rotating platforms, the resulting shear stresses are non-measurable and empirically determined. Usually, experiments run in plates are limited in duration as the risk of contamination increases with the number of manipulations required to maintain a nutrient-rich medium. Also, the batch nature of these models limits our ability to reproduce the pharmacokinetics of the drugs studied, further limiting the relevance of the results obtained.

The advantages and limitations of these models make them well-suited for initial research steps, where numerous variables are studied, and for screening experiments where the need for a high throughput method outweighs considerations for the relevance of the model.

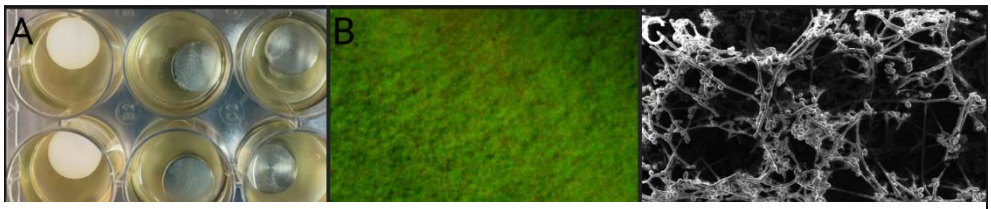


Figure II.7. Biofilms grown on coupons. Panel A: *S. aureus* biofilms grown on (left to right) UHMWPE, 316L stainless steel, Ti-6Al-4V coupons; B: Confocal image of *S. aureus* biofilm grown on a Ti-6Al-4V coupon following live/dead staining (10x); C: Scanning electron microscopy image of a *S. aureus*; *E. coli*; *C. albicans* biofilm grown on a Ti-6Al-4V coupon (650x; courtesy of A. Ruiz-Sorribas; FACM; LDRI; UCLouvain).

5.1.2 Open models

Some of the limitations of closed models may be overcome by using more advanced *in-vitro* models in which the biofilms are developed in bioreactors where the medium is continuously exchanged, and a controlled shear stress may be applied.

The CDC biofilm reactor (CBR) model is the best example of this category. In this model, biofilms are grown on standardized coupons of specific materials held by polypropylene rods in a glass vessel with ports allowing for a controlled flow of the medium, stirred by a magnetic bar, inducing a relatively high shear stress. The tight control on the culture conditions that the CBR allows for result in reproducible results (246, 247), and standard operating procedures for the culture of *S. aureus* and *P. aeruginosa* biofilms have been produced by the US EPA and the ASTM (248, 249). This reproducibility makes this model well suited for the evaluation of anti-biofilm coatings (250) or the evaluation of antibacterial compounds on mature biofilms after removal from the bioreactor (251). The controlled



Figure II.8. CDC biofilm reactor.

flow of medium also allows for the reproduction of antimicrobials pharmacokinetic profiles (252, 253).

The drip flow reactor (DFR) is another bioreactor used to grow biofilms in more controlled conditions. In this model, biofilms are grown on slides over which small volumes of medium are continuously poured, inducing a low shear stress. Like the CBR, this model produces reproducible biofilms, and the ASTM developed a standard operating procedure for the culture of *P. aeruginosa* biofilms (254) and has been used to study the effect of coatings on the development of biofilms (255). This model presents the advantage of using relatively limited volumes compared to the CBR, which facilitates the study of the exposure of biofilms to antimicrobial substances (256).

While these models present interesting characteristics, only a few studies investigating treatments evaluated with the aim of treating PJI have been reported. A PubMed research using the terms "prosthetic joint infection reactor" yielded only five results. This limited literature may be explained by the high costs, relative complexity, and low throughput of these models. Moreover, while shear stress is known to impact biofilm formation on the surface of implant materials, there is no data concerning its *in-vivo* values (257). Thus, no consensus exists concerning this parameter, limiting the benefits of such complex models for the study of PJI.

5.2 *In-vivo* models

While *in-vitro* models are efficient tools to screen for potential new therapies, their simplicity limits the clinical relevance of the results. *In-vivo* models, adequately designed to reproduce the pathology or some aspects of it, are

required to assess the validity of the hypotheses and, eventually, move over to clinical studies.

Multiple models have been proposed to study PJI *in-vivo*, ranging from infected foreign body models to models of infected joint replacement using custom implants. These models present pros and cons, and the model choice depends on the specific hypothesis tested.

One of the most commonly used *in-vivo* models for the study of biofilm formation, host response to a foreign body infection, and the effect of antibacterial agents on biofilms is the tissue cage model developed by W. Zimmerli in the 1980s (258). This model consists in the subcutaneous implantation of a perforated Teflon cylinder, in some cases filled with samples of materials of interest (259), in rats or guinea pigs. Infection is caused by the percutaneous injection of a bacterial suspension in the cages after wound healing. A major advantage of this model resides in the possibility to obtain fluid samples from the exudate without explanting the cages. Tissue cage fluid recovery allows to study parameters such as drugs pharmacokinetics (260), the evolution in bacterial titers (259), or bacterial gene expression (261) over the course of the experiment. This model has been central to the study of antimicrobial combinations using rifampin to treat *S. aureus* and *S. epidermidis* infections, as was recently summarized by Renz et al. (262). However, the tissue cage model is not a model of PJI. The homogeneous subcutaneous tissue where the tissue cages reside does not reflect the complex organization of the joint, which impacts the penetration of antimicrobials (263, 264), limiting the interpretation of the results. For the

same reason, studies investigating the pathogenesis, local reactions to PJI, or surgical strategies are impossible using the tissue cage model.

Several models have been described over the years that attempt to more closely reproduce PJI in mammals. These models differ by the animal species used, the type of implant and its position in the joint, the mode of infection chosen, the analyzed parameters, and, when applicable, the type of therapeutic intervention assayed. These parameters are extremely important considerations driving the choice of model, as they directly influence the clinical relevancy of the experiments (265).

The most common model found in the literature consists of the intra-medullar implantation of Kirschner wires (k-wires) in either the femur or the tibia of mice, rats, or rabbits. Infection is induced either by growing bacteria on the k-wires before implantation or by intra-medullar canal injection during surgery. This model has been used to study biofilm and implant-associated osteomyelitis development (266, 267), as well as the effect of therapeutic interventions such as antibiotic combinations (268), implant coatings (269), and staged revision procedures (270). The k-wire model has multiple advantages. The combination of relatively simple surgical procedures and cheap and easily housed small rodents facilitates the replication of the model. Also, the small size of mice allows the use of innovative techniques to evaluate the bacterial burden and inflammation through the use of bioluminescent bacterial strains and genetically modified mice expressing fluorescent markers (269). However, it can be argued that this model poorly emulates PJI. Indeed, the implants are buried in the medullar canal and thus are not exposed to the joint, do not bear weight, and have little stability. As

some of the promotors of this model argue, it should be reserved for the initial screening of select strategies (269).

An alternative to this model has been proposed by Craig et al. in 2005, using a cemented stainless-steel screw and a polyethylene washer implanted in the lateral metaphysis of rabbits infected by the intra-articular injection of a *S. aureus* suspension (271). While this initial study was performed with no therapeutic intents, two more teams used the model to investigate the effect of a copper coating (267) and washing solutions during debridement surgeries (272). The main critic of this model is the lack of mechanical constraints applied to the implant as it is placed in a non-weight bearing position and does not penetrate the medullar space (265).

More complex models attempting to reproduce more precisely a joint arthroplasty by using small implants have been described. The earliest example is an infected knee arthroplasty model using a Silastic implant, designed for metatarsophalangeal joint replacement in humans, implanted in rabbit knees was developed in the 90s (273). While this implant reproduces the function of a knee arthroplasty implant, the material used is not relevant to most PJIs, as silastic is a flexible silicone-elastomer, presenting a moderately hydrophobic surface (274), whereas most implanted materials in orthopedics present a hydrophilic surface (275, 276). Several authors considered this factor to be a significant limitation to the relevancy of this model (265, 271).

Over the last decade, innovative models using custom-made implants have been described that attempt to reproduce more precisely joint arthroplasty in small animals. They are characterized by the use of load-bearing knee

replacement implants made of clinically relevant materials such as stainless steel, titanium alloy, and polyethylene. Soe et al. developed an infected total knee replacement model in Sprague-Dawley rats using machined implants made of stainless steel (femur) and polyethylene (tibia) infected with reference and clinical *S. aureus* strains (277). While this model appeared promising, the authors observed a normalization of the inflammation parameters after 2 weeks, in the absence of any treatment, that was attributed to a strong response of the rats' immune system. The authors considered this spontaneous healing to be a substantial limitation to the use of their model for the study of PJI treatment. To our knowledge, this model has not been used in any subsequent studies.

Increased accessibility of metal 3D printing with laser sintering techniques now facilitates the development of custom metallic implants for PJI models. The first use of this technology was reported by A. Carli et al. in 2016 (265). The authors designed a Ti-6Al-4V tibial replacement implant adapted to mice knees and infected by the intra-articular injection of *S. aureus* (278). This model was recently used to study the application of an adjuvant treatment using bacteriophage lysins after a surgical debridement followed by a vancomycin treatment (279). To us, the main limitations of this model are the limited possibilities of repeated blood sampling in mice, preventing the study of the pharmacokinetics as well as the monitoring of the antibiotic treatment, and the impossibility to perform histological and microbiological analysis in the same animal.

Improving on these aspects, López-Torres et al. described in 2019 a new model of rabbit tibial arthroplasty using 3D printed implants, whose design

was based on 3D reconstructions of CT scans of the cranial part of rabbit tibias (280). This model was used to study the development of PJI following intra-articular inoculation with *S. aureus* (281). However, to our knowledge, this promising model has yet to be used to study PJI treatments.

As the complexity of our models increases, the animals are subjected to increasingly invasive procedures, and while it is now possible to get as close as possible to an actual PJI *in-vivo* model, the ethical implications become more evident. Following the trends observed in other fields, alternative models are now investigated for the study of PJI. A particularly interesting model is the implantation of steel wires in greater wax moth – *Galleria mellonella* - larvae (282). While this model does not reproduce the joint environment and presents an entirely different immune system than humans, it may provide an alternative to models based on the introduction of k-wires in small rodents for the early evaluation of coatings or systemic antimicrobials.

5.3 **Common methods for the evaluation of the effects of treatments on biofilms**

The study of the effects of therapeutic agents against biofilms in experimental model relies on a variety of techniques investigating different aspects of the biofilms. These techniques may be grouped in the following categories:

- Bacterial viability assays
- Bacterial metabolic assays
- Biofilm biomass assays
- *In-situ* morphological analyses

5.3.1 **Bacterial viability assays.**

These assays aim to estimate the number of viable bacterial cells in a sample. The classical way to determine the amount of viable bacterial cells in a sample is the realization of cultures on solid media which was first introduced by Robert Koch in 1881 (283). In the setting of biofilm study, the bacteria are usually first detached from their substrate and disaggregated in a buffer solution using mechanical means such as scrapping, sonication in an ultrasound bath, or centrifugation. Following this initial step, the bacterial suspension is serially diluted, plated on solid agar medium, and incubated for a variable duration dependent on the bacterial species and culture conditions. Colonies are then enumerated. Standard round Petri dishes containing 25 to 250 colonies are usually considered for quantitative analysis, while the lower limit of detection is 1 colony (284). A limit of this method is the possibility for undercounting the bacteria present in the sample as a subpopulation of viable but non-culturable bacteria may be present or that would remain attached to the substrate (285, 286). Other methods of identification of viable cells have been developed to overcome this limitation, especially for *in-vitro* experiments. An example is the use of fluorescent dyes that discriminate bacteria with intact or disrupted membranes (i.e. live or dead bacteria). Biofilms are either stained *in-situ* and imaged using fluorescence microscopy, allowing the realization of qualitative or semi-quantitative analyses such as live/dead ratios (287), or stained following mechanical disruption allowing for a quantitative analysis with flow cytometry (288). The main drawbacks of fluorescence microscopy is the reliance on arbitrarily selected regions of the samples for the analysis which may introduce biases, the use of complex image analysis programs which function as black box, impeding the

verification of the process by the researchers (287), and the lack of standardization of the analysis procedures (289).

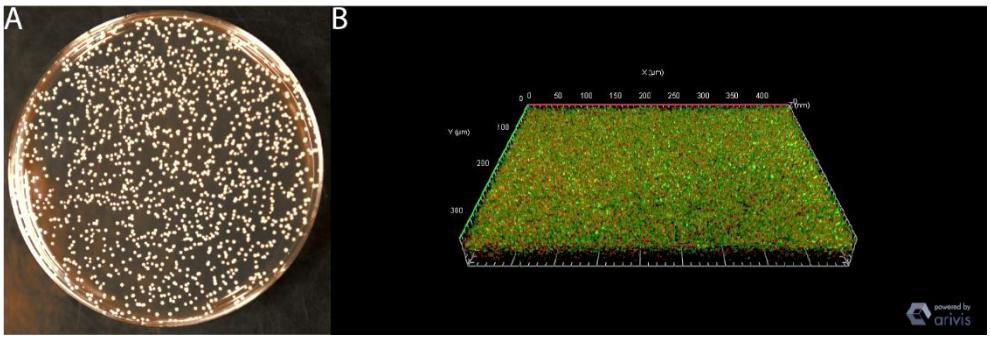


Figure II.9. Examples of plated colonies for CFU counts and of Live/Dead stained biofilm. A: *S. aureus* colonies plated on Tryptic Soy Agar for enumeration; B: 3D view of a *S. aureus* biofilm stained with Syto 9 (Live bacteria, green signal) and propidium iodide (Dead bacteria, red signal).

5.3.2 **Bacterial metabolic assays.**

Metabolic assays are frequently used to investigate the development of biofilms as well as their response to antimicrobial treatments, mainly in microtiter plates models. These assays are typically based on the reduction reaction of either tetrazolium salts to formazan (XTT and MTT (290) assays), the abundance of which can be determined by measuring the absorbance of the supernatant using a spectrophotometer, or of the non-fluorescent dye resazurin into the pink fluorescent resorufin, the abundance of which is determined by measuring the fluorescence of the supernatant using a spectrophotometer (291, 292). These assays are reproducible and are less time-consuming than CFU counts. However, they are limited by narrow linear

ranges (from 5 to 8 $\log_{10}$ CFU/well for either XTT and resazurin assays) (293), which reduce their utility when a large treatment effect is expected. An alternative to these assays is the use of isothermal microcalorimetry, which measures the heat generated by the metabolic activity of the bacteria. This technique is non-destructive and permits the real-time analysis of the effect of an antimicrobial on a bacterial population (294). While this technique appears promising, its usage is relatively limited, owing to the complexity of the analysis of the data produced as well as the cost of the equipment (294, 295). Moreover, the detection limit of the technique remains high, with bacterial populations of 4 to 5 $\log_{10}$ CFU being required to generate a detectable amount of heat (294). A general limitation of metabolic assays is the possible underestimation of persisters cells following treatment as these bacteria present a reduced metabolic activity (296).



Figure II.10. Examples of a resazurin metabolic assay. In presence of biofilm containing living cells, the blue dye resazurin is reduced to the pink fluorescent resorufin (center wells) while it remains unchanged in empty wells (left wells). Image courtesy of Yvan Diaz-Iglesias (FACM, LDRI, UCLouvain).

5.3.3 **Bacterial biomass assays.**

The quantification of the total amount of biological materials of biofilms, which includes the matrix components as well as live and dead bacteria, is important to estimate the formation and development of biofilms (297), as well as their dispersal following treatments (298). The most common method used for this purpose is the staining of heat or methanol fixed samples with crystal violet, a cationic dye which binds to anionic molecules that is used in the first step of Gram staining, followed by its re-solubilization in ethanol or acetic acid. The concentration of crystal violet in the supernatant is then determined by absorbance measurements using a spectrophotometer (297). Safranin may be used as a non-toxic alternative to crystal violet (299). This assay presents the advantages of allowing high throughput experiments, to stain any microorganisms or eukaryotic cells, and that it does not require the detachment of the biofilm. However, the results are highly variable as parts of the biofilms may be detached during the multiple washing steps, and that part of the measured biomass may correspond to planktonic cells sedimented on the biofilm. Moreover, this method is aspecific and does not discriminate live or dead bacteria, in the case of multi-species biofilms, the different species studied (300).

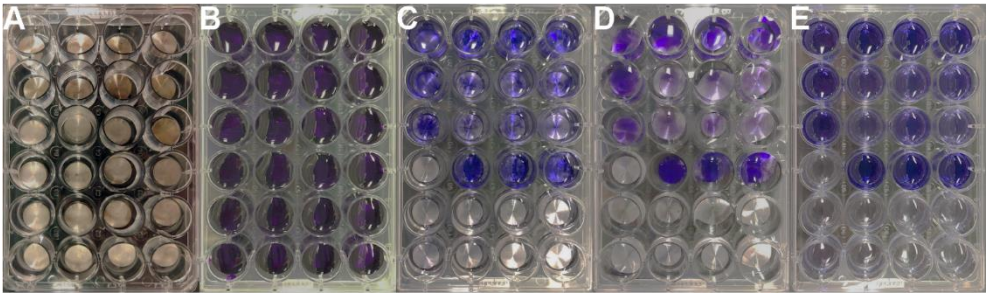


Figure II.11. Steps of crystal violet staining assay. Left to right: A: heat-fixed biofilms grown on coupons; B: staining with 1% crystal violet; C: rinsing in water; D: solubilization of the remaining dye in 66% acetic acid; E: resulting acetic acid solution containing crystal violet.

5.3.4 ***In-situ*** **biofilm morphological analysis.**

Different microscopy methods are used to study the morphology of biofilms. Confocal laser scanning microscopy is one of the preferred options because of the flexibility of applications granted by the use of specific fluorescent probes. This high-definition microscopy technique allows for the acquisition of images of planes at varying depths, while eliminating the background noise, that can then be combined to study the three-dimensional topography of biofilms. Confocal microscopy can be used to study the distribution of viable cells using live/dead dyes (287) or of specific species in polymicrobial biofilms using fluorescent *in-situ* hybridization techniques (301) . Scanning electron microscopy is also commonly used to study the structure of biofilms. This technique has a high-resolution, while allowing for the acquisition of images at varying magnifications. It is however a complex and time-

consuming method. In particular, the dehydration and coating steps of samples are known to produce artifacts (302).

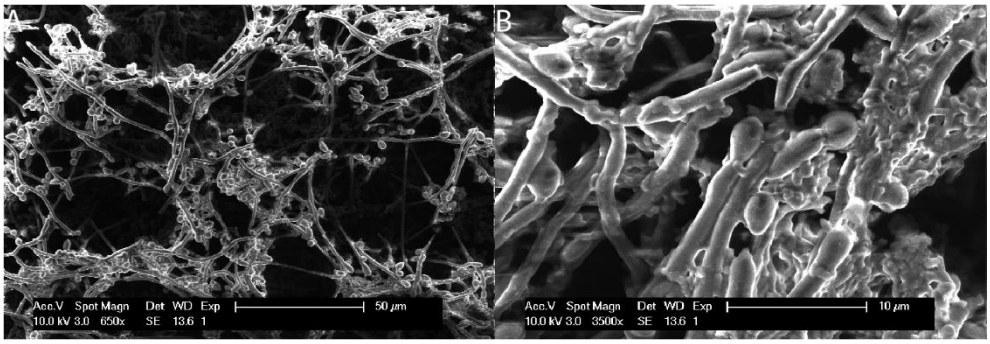


Figure II.12. Examples of Scanning Electron Microscopy images of multispecies biofilms of *S. aureus*, *E. coli*, and *C. albicans*. A: 50x magnification; B: 500x magnification. Images courtesy of Albert Ruiz-Sorribas (FACM, LDRI, UCLouvain).

6 Experimental therapeutics

The consequences of biofilm formation on antibiotic tolerance and immune response are particularly problematic for the treatment of PJI, especially in acute cases where the retention of the implants is attempted. The importance of this problem has led to sustained research efforts over the last two decades for new therapeutics targeting biofilms. These new therapeutics can be divided into three main categories:

- Preventive surface modifications
- Bactericidal treatments
- Biofilm disrupting treatments

6.1 Preventive surface modifications

Besides the general principles of infection prevention used in orthopedic surgery, such as the use of prophylactic antibiotics and aseptic techniques, numerous techniques based on implant surface modification have been proposed to limit the risk of infection. The number of proposed strategies is staggering - over 2.000 results for a PubMed research for “infection implant coating” – and a comprehensive description of all coatings would be out of the scope of this manuscript, and only a few promising examples will be discussed. Romano et al. proposed in 2015 a classification of these surface modifications based on the type of surface modifications (303):

Passive surface modifications: This category includes surface modifications that aim to reduce bacterial adhesion without the release of bactericidal substances. This is usually achieved by chemical or physical alterations of the surfaces of the implants. Examples of these modifications include surface nano-patterning (304), surface hydrophilicity alterations (305), or surfactants coatings (306). These surface modifications are challenging to design as they could interfere with the osseointegration of implants, and their efficacy is often limited (303). To our knowledge, there is currently no approved implant using this technology on the market.

Active surface modifications: This category covers the modification of surfaces by coating antimicrobial agents, active by elution or contact with the implant. This category is heterogeneous and includes metal-ion coatings, antibiotic coatings, and “smart” coatings that respond to specific stimuli, including the presence of bacteria. Among metal-ion coatings, the best-known example is the use of silver-coated implants. Co-Cr-Mo and Ti-6Al-

4v implants coated with silver by electroplating are currently in clinical use (for example, the products of ImplantCast GmbH, Buxtehude, Germany). These coatings release silver ions, which exert an anti-microbial effect by multiple mechanisms, including membrane damages and protein denaturation (307). These coatings have been found effective in preventing infection in animal models (308) and patients (309). However, some reserves persist as data about the kinetics of silver release and the potential for osteointegration of these implants remains unknown (310). Implant coatings with antibiotics have been proposed by multiple teams, relying on either covalently bound antibiotics (311) or coatings eluting antibiotics (312). These coatings have used multiple different antibiotics, including vancomycin (241, 311), gentamicin (312), and doxycycline (313). While the experimental results of these coatings are usually good, only gentamicin-based coatings are currently available in clinical practice (PROtect coating, DePuy-Synthes, Raynham, MA, USA). This coating consists of a resorbable poly(D,L-lactide) matrix containing gentamicin sulfate, applied to the surface of a tibial nail, releasing 80% of the antibiotic in 48h (314). While no significant adverse effect was observed with this system, none of the published studies included a control group, and no conclusion concerning the clinical benefits of this coating for infection prevention can be drawn (314-316). Limitations of coatings relying on antibiotics are the spectrum of the molecules used, which limits their effectiveness to some species, the possible selection of resistant bacteria, uncertain impacts on osteointegration, and the local and general toxicities of the substance used (303). Another class of antimicrobial agents considered for antibacterial coatings is antimicrobial peptides (AMP). These molecules are short peptides that are part of the innate immunity of most organisms,

from bacteria to humans, and present a staggering variety, with over 3,200 peptides referenced (as of May 2021) (317). These peptides' main mode of action is the permeabilization of bacterial lipid membranes through pore formation or lipids segregation, but some peptides appear to also have metabolic targets (318). Metallic surfaces can be coated with AMPs by covalent bonding to functionalized surfaces or adsorption (319). Some AMPs coatings of titanium surfaces have been shown in *in-vitro* and *in-vivo* models to reduce bacterial colonization (320-322). AMPs present significant advantages over antibiotics, including low toxicity, a broad-spectrum, and a relatively uncommon occurrence of resistances (318). More advanced coating options - called smart coatings – are under development. These coatings respond to the presence of bacteria, reacting to changes in pH or the secretion of bacterial enzymes, thus releasing antimicrobials in specific conditions (323, 324). These approaches are extremely interesting as they would increase the specificity of the coatings, limiting the toxicity to the host and an unwarranted release of antimicrobials.

Perioperatively applied antibiotic carriers: The last category of coatings described in this classification is the per-operative application of an antibiotic-laden carrier. The most common example of this is the polymethylmethacrylate (PMMA) cement used to fix cemented implants and cement spacers. Gentamicin is routinely added to PMMA cement in primary arthroplasty and is associated with a reduction of the risk of developing a PJI (325). In staged revisions, the antibiotic added to the cement spacer is selected on the basis of the antibiotic susceptibility profile of the microorganism (326). It allows the rapid (48-72h) release of high antibiotic concentrations in the joint (327). While the use of antibiotic-laden PMMA is widespread, it should

be noted that it may not always prevent biofilm development as was observed *in-vitro* (328) and could lead to the selection of resistant strains as the concentrations in the joint decrease over time (329). In non-cemented implants, where PMMA is not used, some authors propose using a resorbable hydrogel composed of hyaluronic acid and poly-D,L-lactide mixed with antibiotics (330). This material appears to not interfere with the osseointegration of implants (331) and to effectively prevent the development of PJI in high-risk revision surgeries (332).

The combination of different types of surface modifications has been proposed, for example, surface nano-patterning and silver coating (255), or passive and smart coatings (333), showing interesting *in-vitro* and *in-vivo* results.

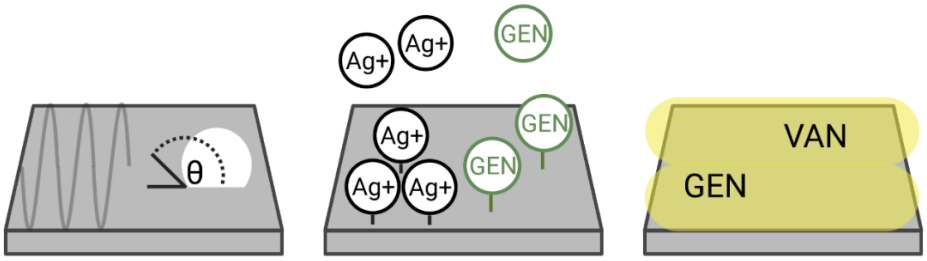


Figure II.13. Schematic representation of the some of the possible preventive surface modifications described. Left to right: surface nano-patterning, hydrophilicity modification, silver ions coating, gentamicin coating, application of an antibiotic carrier.

6.2 Bactericidal treatments

Because of the innate tolerance to antibiotics exhibited by biofilms, new bactericidal treatments relying on alternative mechanisms of action are currently investigated to treat PJI and other biofilm-associated infections.

The use of bacteriophages in this setting appears extremely promising. Bacteriophages are viruses specific to bacteria that, in some cases, can induce bacterial cell lysis as well as biofilm matrix destruction (334). Their clinical potential was recognized at the beginning of the 20th century (335), but they fell out of favor in Western countries following the introduction of antibiotics, while they continued to be studied and used in communist countries throughout (336). As bacterial resistance becomes a growing issue, the use of bacteriophages as therapeutic agents sees renewed interest (337). Bacteriophages present several advantages over antibiotics, including high specificity, safety for the host (338), a potential biofilm dispersal effect (339), and an effect against persistent bacteria (340). Bacteriophages, administered by systemic injection or coated on implants, and used in combination with local or systemic antibiotics, have been shown to be effective against *S. aureus* infections in preclinical models of PJI (240, 341). The use of bacteriophages, administered systemically or locally, for the treatment of patients suffering from PJI has been documented in a few case reports published over the last three years, hinting at a promising potential for this therapy (342-347). However, a more widespread use of phages for this indication is still impossible because of regulatory hurdles regarding the use of live viruses, limiting their utilization to compassionate and experimental uses (348).

An alternative to the use of live phages is the use of purified phage proteins. The most promising results are seen with lysins. These are hydrolytic enzymes encoded in phages' genome that degrade the peptidoglycan of the bacterial cell wall and induce bacterial lysis (349). The effect of bacteriophage lysins is limited to Gram-positive bacteria. Lysins are also usually species-specific (350), but some exhibit a broader spectrum and are promising drug candidates (351). One of these lysins, PlySs2, has recently been shown to work synergistically with vancomycin in *in-vitro* and *in-vivo* models of PJI (279), while the CF-301 lysin (exebacase) has recently been shown to be effective for the treatment of patients with endocarditis in a phase II study (352).

AMPs have also been proposed as therapeutic agents in PJI. Multiple AMPs have been shown to be effective against biofilms of multiple species *in-vitro* (251, 353, 354). The activity of some peptides has also been tested in *in-vivo* models of implant-related infections as therapeutic agents (355) with promising results.

6.3 Biofilm disrupting treatments

Another interesting approach to the treatment of biofilm-related infections is the dispersal of established biofilms, with the aim to release bacteria and to rescind their acquired tolerance mechanisms. Multiple methods have been proposed to achieve this result, including physical dispersal techniques, treatments interfering with the quorum sensing system, and the use of hydrolytic enzymes. As these treatments are usually not bactericidal, and as the dispersal of bacteria from biofilms is associated with bacteremia (356),

they are usually studied in combination with antibiotics or other antimicrobials.

The mechanical disruption of biofilms is already a tool in the arsenal of surgeons treating patients for PJI in the form of the pulse lavage systems that are commonly used during surgery (121). While the use of pulse lavage appears to improve the effect of antiseptics on biofilms (244, 357), some authors consider these systems to be insufficient to effectively remove biofilms from implants (358). New physical methods have been proposed over the last few years, aiming at either disrupting or killing bacteria in biofilms.

An interesting suggestion is the use of non-contact induction heating of metallic implants. By using induction coils, Pijls et al. have shown that heating *S. aureus* and *S. epidermidis* biofilms grown on Ti-6Al-4V substrates at 60°C for 3.5 minutes significantly reduced the biofilms' bacterial population. The exposure of heated biofilms to a combination of rifampin and vancomycin for 24h led to a complete eradication of the bacteria from the biofilms (359, 360). While these results are promising, they have not been confirmed in *in-vivo* models yet, and the potential effects of heating uncemented implants on osteointegration are unknown. Other techniques have been described, including the exposure of biofilms stained with methylene blue to a blue light laser, killing bacteria by inducing the formation of radicals (361), or the use of ultrasounds combined with microbubbles – micrometric particles consisting of a gas core and a shell - and antibiotics (362, 363). While these techniques appear promising *in-vitro*, the practical considerations of their use in the setting of PJI appear to be considerable hurdles.

An elegant proposition is the use of molecules interfering with quorum sensing or other regulatory mechanisms of biofilms to exploit the physiological dispersal mechanisms of biofilms (364). Various molecules have been described that interfere directly with the quorum sensing systems, for example, via inhibition of the receptor of signal molecules, degradation of signaling molecules, or their binding by monoclonal antibodies, blocking the transduction signal (365). An example of this strategy is the use of RNA III inhibiting peptide (RIP). RIP inhibits the activation of the *agr* system in *S. aureus* by blocking the phosphorylation of the membrane protein TRAP, leading to a decreased virulence (366). While RIP was found to act synergistically with teicoplanin in a wound model (367), evidence concerning its effects in models relevant to PJI is inconclusive (368, 369). Another example is the use of the nitric oxide donor sodium nitroprusside. This molecule was found to promote the dispersal of biofilms of multiple Gram-negative and Gram-positive bacteria, as well as *C. albicans*, and to act synergistically with hypochlorous acid and tetracycline (370). The effect of nitric oxide has been mainly studied in *P. aeruginosa* and was shown to activate phosphodiesterases and thus reduce c-di-GMP concentrations (371), leading to the expression of matrix-degrading enzymes (372). A proof of concept study of the effect of nitric oxide combined with tobramycin and ceftazidime was performed in patients with cystic fibrosis infected with *P. aeruginosa*, showing a reduction in biofilms in sputum, confirming *in-vitro* observations (373). However, to our knowledge, the effects of nitric oxide or of other drugs interfering with quorum sensing systems have never been assayed in PJI models.

An enticing approach to induce biofilm dispersal is the use of enzymes degrading specific constituents of the EPS. Several enzymes have been shown to disperse biofilms *in-vitro* and *in-vivo*. Most enzymes used in these studies belong to three classes: glycoside hydrolases, deoxyribonucleases, and proteases (374).

Among glycoside hydrolases, dispersin B (DspB) is the most extensively studied enzyme. DspB is a 42 kDa β-hexosaminidase specific to the β-1,6 glycosidic liaisons of PNAG, isolated from *Aggregatibacter actinomycetemcomitans* by Kaplan et al. in 2003 (375). *A. actinomycetemcomitans* biofilms contain PNAG and DspB was found to be necessary to induce biofilm dispersal. The enzyme was later found to disperse the biofilms of various PNAG producing species, including *S. epidermidis*, *E. coli* (376), and, to a lesser extent, *S. aureus* (168, 377). Multiple studies have shown that the dispersal of biofilms with DspB sensitizes biofilm bacteria to antibiotics and antiseptics. This effect has been shown *in-vitro* against *S. epidermidis*, *S. aureus*, and *E. coli* biofilms grown on catheters treated with DspB and triclosan (378), on *S. epidermidis* and *S. aureus* biofilms grown on polyurethane treated with DspB and cefamandole

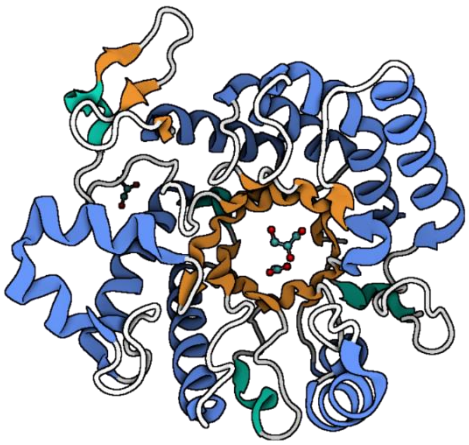


Figure II.14. Dispersin B (Ribbon diagram made in BioRender, structure from Ramasubbu et al. 2005 (3). Visible in the centre are one glycerol and one acetate molecules).

(379), and on *S. aureus* biofilms treated with DspB and either tobramycin (380) or a combination of rifampin and clindamycin (243). The effect of DspB on *S. epidermidis* and *S. aureus* biofilms was also explored in an *in-vivo* wound model, showing a synergistic effect with povidone-iodine alone (*S. epidermidis*) or in combination with the endonuclease DNAse I (*S. aureus*). *In-vitro* studies on *S. aureus* biofilms also showed that DspB was often less effective than DNAse I but did not suggest a synergy of the two enzymes (243, 380). Besides the effect on antimicrobials susceptibility, biofilm dispersal by DspB has also been shown to increase the susceptibility to the killing of *A. actinomycetemcomitans* by macrophages (381). Other glycoside hydrolases have been proposed to disperse biofilms, such as α-amylase (382) or cellulase (383). These enzymes cleave different polysaccharides and present thus a different spectrum of effect. In particular, cellulase appears particularly effective against the biofilms of Gram-negative bacilli such as *E. coli* and *P. aeruginosa* (383, 384).

The biofilm dispersal potential of multiple endonucleases has been investigated since the 2002 observation by Whitchurch et al. of the dispersal of *P. aeruginosa* biofilms by DNAse I (181). Since then, DNAse I, a pancreatic 35 kDa specific endonuclease that hydrolyses double-stranded DNA (385), has been shown to disperse the biofilms of multiple species, including *S. aureus* (380), *E. coli* (383), *S. pyogenes* (386), and *E. faecalis* (387). Similarly to DspB, the dispersal of biofilms by DNAse I has been shown to reduce the tolerance of biofilms to multiple antibiotics across a broad range of species in *in-vitro* models of biofilms (243, 380, 386). *In-vivo*

experiments carried on *Caenorhabditis elegans* infected with *S. aureus* have shown a synergistic effect of DNAse I and tobramycin on the survival of the nematodes (388). A potential limitation to the use of DNAse I as an agent of biofilm dispersal, besides a spectrum limited to species and strains dependent on eDNA for biofilm formation, is the reduction of its effect on more mature biofilms (over 3 days old) observed in the initial experiments of Whitchurch (181). Other endonucleases specific to DNA have been shown to disperse the biofilms of similar species (389, 390). There has been no comparative study of these enzymes, but no significant differences should be expected as their substrate is identical.



Figure II.15. DNAse I complexed with DNA (Ribbon diagram made in BioRender, structure from Lahm and Suck 1991 (4))

Multiple proteases of various origins have also been investigated for their potential to disperse biofilms, displaying promising effects against a broad range of microorganisms (374). Proteinase K, a 29 kDa aspecific endopeptidase isolated from the fungus *Engyodontium album* (391), has been particularly well studied for the dispersal of biofilms. It has been shown to disperse the biofilms of multiple bacterial species grown *in-vitro*, including those of *S. aureus* (392, 393), *E. coli* (383, 394), *S. pyogenes*, *agalactiae*, and

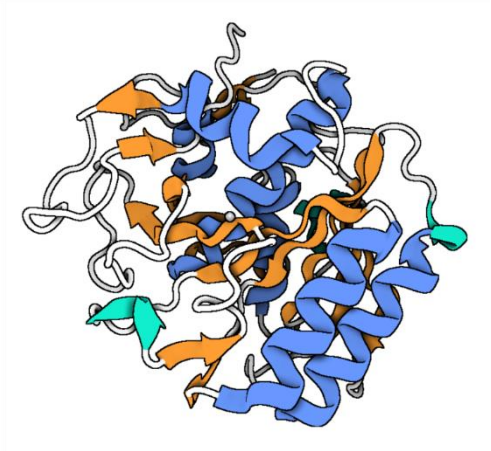


Figure II.16. Proteinase K (Ribbon diagram made in BioRender, structure from Pechkova et al. 2009 (2)).

oralis (395), and some CoNS (396-398). Similarly to other enzymes, the combination of proteinase K and antimicrobials has been shown to be synergistic in *in-vitro* models (392, 393, 395, 399), but, to our knowledge, this has not been demonstrated *in-vivo* yet.

A common limitation to enzymatically mediated biofilm dispersal methods is the relative specificity of each enzyme for some bacterial species or even strains, complicating their empirical application (397). For this reason, some authors advocate the use of enzymes sequentially or in the form of enzymatic cocktails, achieving varying degrees of success (380, 383, 397). The compatibility of enzymes combination may be problematic, for example, proteinase K is known to present a proteolytic effect on nucleases (400), and should be considered for their design.

Aims of the thesis

PJI is a devastating complication of joint replacement surgeries. It affects up to 2% of patients following a hip or knee replacement and presents major implications for the health of the patients and the finances of developed countries' healthcare systems. As the prevalence of osteoarthritis increases as a result of an aging population, the burden of PJI is set to grow substantially over the next decades. Current therapeutic options are often unsatisfactory. The gold standard of PJI treatment, staged revision, while successful in over 80% of cases, is associated with high costs, relatively poor functional outcomes, and a significant mid-term mortality. On the other hand, DAIR, the treatment of choice of most acute infections, is significantly less invasive and expensive, but has been associated with more frequent reinfections. These treatment failures are multifactorial but appear to be associated with the development of biofilms, which are complex bacterial communities embedded in a self-produced matrix, adhering to the surface of the implant. The organization of bacteria in biofilms leads to the acquisition of mechanisms of tolerance to antimicrobial treatments and of evasion from the host’s immune defenses. Multiple innovative therapeutic strategies have been studied over the last two decades to eradicate biofilm-associated infections. Among these, biofilm disruption using enzymes targeting matrix components appears promising and has been shown to restore the activity of antimicrobials against bacteria in biofilms. However, this strategy is inherently limited in its application to a clinical setting because of the relatively narrow spectrum of bacterial species dispersed by each enzyme stemming from differences in matrix composition. An enticing option to

overcome this limitation of matrix targeting enzymes is the development of combinations of enzymes with distinct activity spectra. Prior to the beginning of this thesis project, our laboratory, in collaboration with an industrial partner (OneLife SA, Louvain-la-Neuve), developed a broad-spectrum combination of three enzymes targeting components of the matrixes of the most commonly encountered bacterial species.

In this thesis, we explored the hypothesis that biofilm dispersal, using this enzymes combination or conventional irrigation techniques, would restore the susceptibility of bacteria in biofilms to antibiotics in an *in-vitro* model relevant to prosthetic joint infection, and that the use of enzymes combinations combined to a standard debridement and antibiotic therapy would prove superior to standard therapy alone in an *in-vivo* model of prosthetic joint infection. To that end, the project was organized in three main steps:

1. The design of a clinically relevant *in-vitro* model of *S. aureus* biofilm and the study of the combination of pulsed-lavage with clinically relevant antibiotics. Biofilms of either reference or clinical strains of MSSA or MRSA were grown on Ti-6Al-4V coupons under light shear stress in a closed model and were successively treated with pulsed-lavage and either flucloxacillin (MSSA strains) or vancomycin (MRSA strains). The results of this study are presented in the first article.

2. The *in-vitro* study of the combination of the aforementioned enzymatic cocktail and clinically relevant antibiotics against biofilms of *S. aureus*, *S. epidermidis*, and *E. coli*, and the study of the cytotoxicity of the

enzymatic cocktail. Biofilms of reference strains of these species were successively exposed to the enzymatic cocktail and antibiotics representative of the different classes recommended for the treatment of PJI at clinically relevant concentrations. The cytotoxicity of the cocktail was assayed against cell lines relevant to the joint environment. The results of this study are presented in the second article.

3. The design of a clinically relevant *in-vivo* model of acute PJI treated with DAIR and the study of the *in-vivo* effect of the enzymatic cocktail. An innovative model of unicompartmental tibial arthroplasty in New-Zealand White rabbits, using a Ti-6Al-4V 3D printed implant, infected with an MRSA reference strain and treated with intravenous vancomycin was developed. The pharmacokinetic of vancomycin in this model was studied in order to reach clinically relevant serum concentrations. Treatments with DAIR and DAIR combined with an intra-articular injection of enzymatic cocktail were compared. The results of this study are presented in the third article.

Chapter III: *in-vitro* study of pulsed-lavage

Synergistic effects of pulsed lavage and antimicrobial therapy against *Staphylococcus aureus* biofilms in an in-vitro model

Hervé Poilvache, MD[1,2,3*], Albert Ruiz-Sorribas, MSc[2], George Sakoulas, MD[4], Hector Rodriguez-Villalobos, MD, PhD[5], Olivier Cornu, MD, PhD[1,3], Françoise Van Bambeke, PharmD, PhD[2]

[1]Laboratoire de neuro-musculo-squelettique, Institut de Recherche Expérimentale et Clinique, Université catholique de Louvain, Brussels, Belgium

[2]Laboratoire de Pharmacologie Cellulaire et Moléculaire, Louvain Drug Research Institute, Université catholique de Louvain, Brussels, Belgium

[3]Orthopaedic surgery department, Cliniques Universitaires Saint-Luc, Brussels, Belgium

[4]School of Medicine, University of California, San Diego, CA, USA

[5]Clinical microbiology department, Cliniques Universitaires Saint-Luc, Brussels, Belgium

Published in *Frontiers in Medicine*, September 2020, 7(527): 527. DOI: https://doi.org/10.3389/fmed.2020.00527

Abstract

Background: Prosthetic joint infections (PJI) are difficult to treat complications of joint arthroplasty. Debridement with implant retention is a common treatment strategy and frequently involves the use of pulsed lavage (PL). However, PL effects on biofilms and antibiotic activity have been scarcely studied in-vitro. We report the effects of PL, vancomycin or flucloxacillin used independently or in combination against *Staphylococcus aureus* biofilms.

Methods: Biofilms of 3 methicillin-susceptible (MSSA) and of 3 methicillin-resistant (MRSA) *S. aureus* were grown on Ti6Al4V coupons in TGN (TSB + 1%glucose + 2%NaCl). After 24h, PL was applied to half the samples (50mL saline from 5cm). Samples were either reincubated for 24h in TGN or TGN + flucloxacillin or vancomycin. Analyses included CFUs counts, biomass assays or fluorescence microscopy.

Results: PL transiently reduced bacterial counts by 3-4 Log_{10} CFU/coupon, but bacterial regrowth to baseline levels was seen after 24h. At 20mg/L, flucloxacillin reduced both the CFU counts (3 Log_{10} CFU/coupon) and biomass (-70%) in one MSSA only, while vancomycin had no effects against MRSA. PL combined with a 24h reincubation with vancomycin or flucloxacillin at 20mg/L was synergistic (-5-6.5 Log_{10} CFU/coupon; 81-100% biomass reduction). Fluorescence microscopy confirmed that PL removed most of the biofilm and that subsequent antibiotic treatment partially killed bacteria.

Conclusions: While PL only transiently reduces the bacterial load and antibiotics at clinically relevant concentrations show no or limited activity on biofilms, their combination is synergistic against MRSA and MSSA biofilms. These results highlight the need for thorough PL before antibiotic administration in PJI.

Keywords: biofilm, MRSA, MSSA, pulsed lavage, vancomycin, flucloxacillin, prosthetic joint infection

1 Introduction

Prosthetic Joint Infections (PJI), defined as infections involving joint replacement implants and the surrounding articular tissues, are devastating complications, affecting 0.5 to 2% of patients benefiting from hip or knee replacement (23, 401) and are among the most common causes of arthroplasty failures (26, 402).

These infections result from either a peri-operative contamination of the joint, generating acute (less than four weeks from the index surgery) or late infections, or an hematogenous seeding of bacteria to the joint following a bacteremia (401). The prevalence of the causative micro-organisms varies depending on the origin and interval from the index surgery, with *Staphylococcus aureus* being the most frequently isolated in cases of acute PJI, whereas coagulase-negative staphylococci and *Streptococci* spp. predominate late infections and hematogenous infections, respectively (17, 87, 403, 404).

Infections by *S. aureus* are characterized by the rapid adhesion of bacterial cells to the implant surface, followed by the development of a self-produced extracellular matrix composed of poly-*N*-acetylglucosamine, extracellular DNA, proteins, and lipids, forming complex communities known as biofilms (17). The development of the biofilm induces phenotypic changes of the bacteria, which, combined with the isolating effects of the matrix, make bacteria tolerant to antibiotics at up to 1000x the minimal inhibitory concentration (MIC) observed in a planktonic state (405). This explains the limited success of antimicrobial therapy and the necessity for surgical strategies aiming to disrupt or remove the biofilm (401).

The Debridement, Antibiotics and Implant Retention (DAIR) strategy is often recommended for the treatment of acute PJI due to lower morbidity and costs than staged implant replacement. The surgical procedure consists in the open debridement of the infected joint, with the excision of necrotic tissues and a synovectomy, replacement of bearing surfaces if possible, followed by a thorough lavage of the joint space usually performed with a pulsed-lavage device which projects normal saline intermittently at pressures between 30 and 350 kPa (406, 407). However, DAIR presents a relatively high failure rate (16-57.4%), with a worse prognosis for patients infected with *S. aureus* (65, 89, 93, 125, 408). These failures may be partly explained by an inadequate removal of biofilms during the debridement surgery and their tolerance to antibiotics. However, only a few studies have looked into the effects of irrigation performed using standard pulsed lavage devices against *S. aureus* biofilms grown on metallic substrates, and none of these investigated the effects of its combination with antibiotics at clinically relevant dosages for systemic administration (244, 357, 358, 409). The purpose of this study was to describe the effects of pulsed lavage and clinically relevant antibiotics used at recommended concentrations for systemic use, (i) in combination or (ii) independently, on the amount of cultivable cells, the biomass, and the microscopic aspects of MRSA and methicillin-susceptible *S. aureus* (MSSA) biofilms on titanium alloy coupons.

2 Materials and Methods

2.1 **Bacterial strains**

The laboratory strains ATCC 25923 and ATCC 33591 were used as references for MSSA and MRSA biofilms, respectively. Two MSSA clinical isolates (strains 578 and 611) and two MRSA clinical isolates (strains 676 and 749), collected from orthopedic device-related infections cases were also studied.

2.2 **Antibiotics**

Oxacillin (powder potency: 81.5 %) was obtained as a microbiological standard from Sigma-Aldrich (Sigma-Aldrich Corp., Saint-Louis, MO, USA). Vancomycin (Vancomycin Mylan, powder potency: 97.5 %, Mylan Inc, Canonsburg, PA, USA) and flucloxacillin (Floxapen, powder potency: 91.9 %, Actavis Group, Hafnarfjördur, Iceland) were used as a powder for injection approved for human use in Belgium.

2.3 **Susceptibility testing**

MICs were determined by broth microdilution in cation-adjusted Mueller-Hinton broth (CA-MHB, Sigma-Aldrich Corp., Saint-Louis, MO, USA) as per the Clinical & Laboratory Standards Institute protocol (410), and in Tryptic soy broth (VWR Chemicals, Leuven, Belgium) supplemented with 1 % Glucose (Sigma-Aldrich Co., Saint-Louis, MO, USA) and 2 % NaCl (VWR Chemicals, Leuven, Belgium) (TGN) (Table 1).

2.4 **Biofilm culture**

Biofilms were grown on titanium alloy Ti6Al4V coupons (Biosurface Inc., Bozeman, MT, USA) in order to mimic implant surface characteristics. These coupons are unpolished cylinders measuring 12.7mm in diameter and 3.175mm in height. The initial inoculum was prepared from bacteria grown overnight on Tryptic Soy Agar (VWR, Leuven, Belgium) (TSA), suspended in Phosphate Buffer Saline (PBS), adjusted to an optical density at 620 nm of 0.5 (CECIL 2021 spectrophotometer, CECIL, United-Kingdom) and diluted 1:100 in TGN, reaching a bacterial density of approximately 6.5 $\log_{10}$ CFU/mL. Sterile coupons were incubated for 24h at 37°C in twelve wells plates containing 2mL of bacterial suspension in TGN per well, under a continuous orbital shaking of 50 rpm in order to induce shear stress. Biofilms reached maturity after 24h (i.e. no meaningful change in biomass or bacterial counts was observed when prolonging the incubation for 48h, supplementary data figure III.1) and used for testing the treatments.

2.5 **Biofilm treatments**

2.5.1 **Irrigation**

Half of the biofilm samples (referred to as irrigation samples) were irrigated with 50 mL of sterile saline (Baxter International Inc, Deerfield, IL, USA) from 5 cm, using Interpulse battery-powered irrigation devices (Stryker Co., Kalamazoo, MI, USA). The Interpulse were fitted with soft tissue tips, delivering the sterile saline at a flow rate of 700ml/min and a pressure of 68.95-82.74 kPa or 10-12 PSI (manufacturer's data). The samples were then rinsed twice in sterile PBS before allocation to one of the subgroups. The

other half of the samples (referred to as control samples) were rinsed twice in sterile PBS before being allocated to one of the subgroups.

2.5.2 **Antibiotic treatments**

Control and irrigation coupons were allocated to one of the subgroups: immediate analysis (T0); 24 h reincubation in TGN (T24h - TGN); 24 h reincubation in TGN containing antibiotic at MIC (T24h – MIC); 24 h reincubation in TGN containing therapeutic concentration of antibiotic (T24h – ThC) according to the flowchart shown in figure III.1. Reincubations were done at 37°C, under a continuous rotating movement at 50 rpm. As antibiotics, flucloxacillin was used for MSSA biofilms, considering as therapeutic concentration 20mg/L, an estimate of the serum concentration 3h after injection when administered 2g IV four times daily, as inferred from pharmacokinetic data (411). MRSA biofilms were reincubated with vancomycin at a therapeutic concentration of 20mg/L, corresponding to target trough serum concentration for bone and joint infections (412).

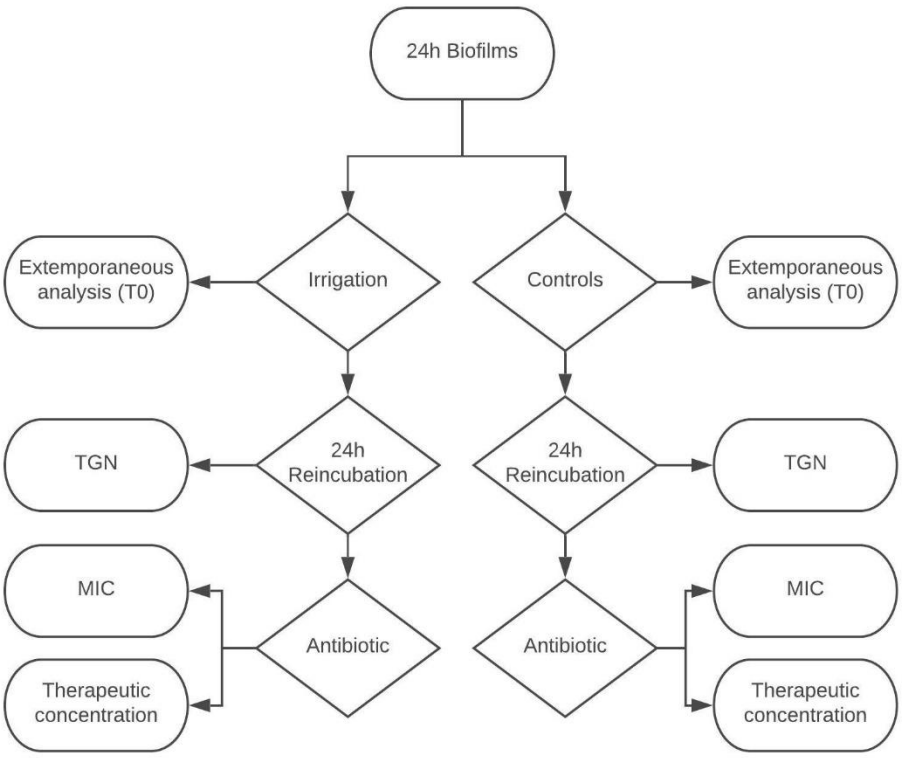


Figure III.1. Flowchart describing the experimental design.

2.6 **Biofilm analysis**

2.6.1 **CFU counts**

Coupons were individually placed in 15mL conical tubes (Greiner Bio-One International GmbH, Kremsmünster, Austria) containing 2mL of sterile PBS. The tubes were vortexed for 30s, sonicated for 5min (Branson 5510 Ultrasonic bath, Emerson Electric, Saint-Louis, MO, USA) and vortexed 30s again. Aliquots of the supernatant were serially diluted, plated on TSA and incubated for 24h at 37°C. CFU counts were performed using an automated

method (image acquisition using Gel Doc XR+ and image processing using Quantity One (BioRad, Hercules, CA, USA)).

2.6.2 **Biomass quantification**

After drying overnight at 60°C, coupons were stained with 1mL of 1% crystal violet (Sigma-Aldrich Corp., Saint-Louis, MO, USA). After eliminating the excess of dye by rinsing the samples with deionized water, biofilm-bound crystal violet was resolubilized in 1mL of a 66% acetic acid (Merck KGaA, Darmstadt, Germany). The coupons were then removed from the solution and the absorbance was read at 570nm using a Spectramax M3 spectrophotometer (Molecular Devices, San Jose, CA, USA).

2.6.3 **Fluorescence microscopy**

Samples were stained using the FilmTracer LIVE/DEAD biofilm viability kit (ThermoFisher, Waltham, MA, USA) following the manufacturer's instructions. DAKO fluorescence mounting medium (Agilent, Santa Clara, CA, USA) was added after staining and a coverslip was placed. Images were acquired as Z-stacks using an AxioImager.Z1 microscope fitted with an ApoTome1 attachment (Zeiss, Oberkochen, Germany) at a 20x magnification using the structured light illumination technique. Image post-processing was performed using FIJI (413, 414). Images were reconstructed using Maximum Intensity Projection (MIP) and were further post-processed by increasing the brightness of each channel separately to the maximum value.

2.7 **Statistical analysis**

CFU counts were transformed to logarithmic values before statistical analysis. Biomass values were normalized in the percentage of positive

controls after subtracting the average value of negative controls (coupons incubated in sterile TGN). Statistical analysis was performed using the mean of each repetition (n=4, with n=3 per replicate) using GraphPad 7.01 (GraphPad Software, San Diego, CA, USA). Means were compared using 2-way ANOVA, followed by Holm-Sidàk post-hoc test. Differences were considered statistically significant when $p<0.05$. Synergy was defined as a significant factor interaction (415).

3 Results

3.1 **Antimicrobial susceptibility.**

Minimal inhibitory concentrations (MIC) for the MSSA and MRSA strains are shown in Table III.1. MSSA strains exhibited low MICs to flucloxacillin in either media, with MICs in TGN one to two dilutions lower than in CA-MHB. MRSA strains were resistant to flucloxacillin in both media. All strains were susceptible to vancomycin in CA-MHB, but their MIC was 2 to 3 dilutions higher when tested in TGN.

Table III.1. MIC (mg/L) values for the tested strains[a]

	Strains	Oxacillin[b]	Flucloxacillin		Vancomycin	
		CA-MHB	CA-MHB	TGN	CA-MHB	TGN
MSSA	ATCC 25923	0.25	0.13	0.06	1	8
MSSA	578	0.25	0.25	0.13	2	8
MSSA	611	0.25	0.25	0.06	1	8
MRSA	ATCC 33591	>64	>64	>64	1	4
MRSA	749	>64	>64	>64	1	8
MRSA	676	>64	64	64	1	8

[a]CLSI breakpoints values (in CA-MHB; mg/L): Flucloxacillin: N/A; Oxacillin: S≤2, R≥4; Vancomycin: S≤2, R≥16.
[b] used to check the MRSA character of the strain, according to CLSI guidelines(410)

3.2 **Antimicrobial Activity in Biofilms.**

Bacterial counts (CFU) are shown in figure III.2.A for MRSA strains and in figure III.3.A for MSSA strains. The CFU counts of control coupons of all strains did not change between T0 and T24, indicating biofilm maturity at T0. Incubation of control MRSA coupons with vancomycin at either MIC or

20mg/L concentrations did not result in reductions in CFU counts when compared to the T0 control samples. A similar observation was made for MSSA biofilms exposed to flucloxacillin at MIC. However, exposure to flucloxacillin at 20mg/L resulted in a statistically significant decrease of the CFU counts in strains ATCC 25923 ($-2.98\log_{10}$) and 611 ($-1.49\log_{10}$). The results of biomass assays are shown in figure III.2.B for MRSA strains and figure III.3.B for MSSA strains. As we observed with CFU counts, no statistically significant differences in biomass were observed between controls at T0 and T24, except for strain 578 (+29.6%, $p<0.001$). 24h exposure to vancomycin at MIC did not reduce biomass in control coupons of all MRSA strains. Exposure to a concentration of 20mg/L did not affect the biomass, except for strain 676 (-27.5%, $p=0.03$). The biomass of control MSSA samples was not modified in a statistically significant manner after a 24h incubation with flucloxacillin at MIC. The diminutions of biomass of ATCC 25923 samples observed after a 24h exposure to flucloxacillin at MIC and 20mg/L did not reach statistical significance (-30.3%, $p=0.79$ and -69.9%, $p=0.05$ respectively). The incubation with a 20mg/L concentration of flucloxacillin caused a significant biomass reduction for biofilms of strain 611 (-24.1%, $p=0.04$). Fluorescence microscopy maximum intensity projection images of the Z-stacks at 20x magnification are shown in figure III.2.C for strain ATCC 33591 and in figure III.3.C for strain ATCC 25923. ATCC 33591 control biofilms uniformly covered the surface of the coupons. Live (green) cells were the most prevalent, but a small proportion of dead (red) cells was observed. Re-incubated controls were comparable without or with vancomycin. ATCC 25923 control biofilms appeared to have a looser aspect than those of ATCC 33591. The proportion of dead cells remained stable after

re-incubation without flucloxacillin but appeared to increase when the samples were reincubated with flucloxacillin at MIC or 20mg/L.

3.3 **Antimicrobial Effects of Pulsed Lavage with and without sequential antibiotics.**

The use of pulsed lavage significantly reduced the CFU counts in all MRSA and MSSA strains by 2.74 to 4.04 $\log_{10}$ when compared to T0 controls (figures III.2.A and III.3.A). The remaining bacterial load was found to be sufficient to promote the regrowth of bacteria within the biofilms to baseline (T0) levels after 24h. The addition of vancomycin at MIC inhibited the regrowth of the biofilms of strains ATCC 33591 and 749 and reduced the CFU counts of strain 676 (-1.29$\log_{10}$). Flucloxacillin at MIC inhibited the regrowth of strains 578 and 611 and reduced the CFU counts of strain ATCC 25923 (-2.11$\log_{10}$). Sequential treatment with pulsed lavage and then 24h exposure to either vancomycin (MRSA strains) or flucloxacillin (MSSA strains) at a 20mg/L concentration reduced the CFU counts in all strains by 1.90 to 2.54$\log_{10}$ when compared to coupons analyzed after pulsed lavage alone. The two-way ANOVA revealed a highly significant ($p<0.001$) interaction parameters for all strains when considering the exposure to pulsed lavage and the reincubation of the samples as factors (supplementary data tables III.1 and III.2). These significant interaction parameters indicate a synergy of pulsed lavage and antibiotic therapy on CFU counts.

Pulsed lavage significantly reduced the biomass in all strains of MRSA and MSSA by 81.7% to 98% (figures III.2.B and III.3.B). As was observed for CFU counts, the remaining bacteria restored the biofilms to control levels after a 24h reincubation in medium. The successive exposure to pulsed lavage

and vancomycin or flucloxacillin at either MIC or 20mg/L inhibited the restoration of the biofilms to control levels. No subsequent reduction in biomass following exposure to antibiotics was observed. Comparably to CFU counts, the two-way ANOVA analysis showed a highly significant ($p=0.005$ to $p<0.001$) interaction parameter for all strains when considering the exposure to pulsed lavage and the reincubation of the samples as factors (supplementary data tables III.3 and III.4). Likewise, these results point towards a synergy of pulsed lavage and antibiotic therapy on biomass.

Microscopy was used to evaluate pulsed lavage samples (figures III.2.C and III.3.C). Pulsed lavage removed most of the cells for both strains, leaving small clusters on the surface of the coupons. The remaining cells appeared to be mostly viable. As was observed for CFU counts and biomass measurements, the incubation of samples treated with pulsed lavage without antibiotics resulted in a complete restoration of the biofilms, with images similar to those of the controls (figures III.2.C & III.3.C). The incubation with vancomycin or flucloxacillin at MIC or 20mg/L did not alter the density of cell clusters of the samples. The proportion of dead cells seemed to increase when the samples were exposed to a therapeutic concentration of antibiotics when compared to controls.

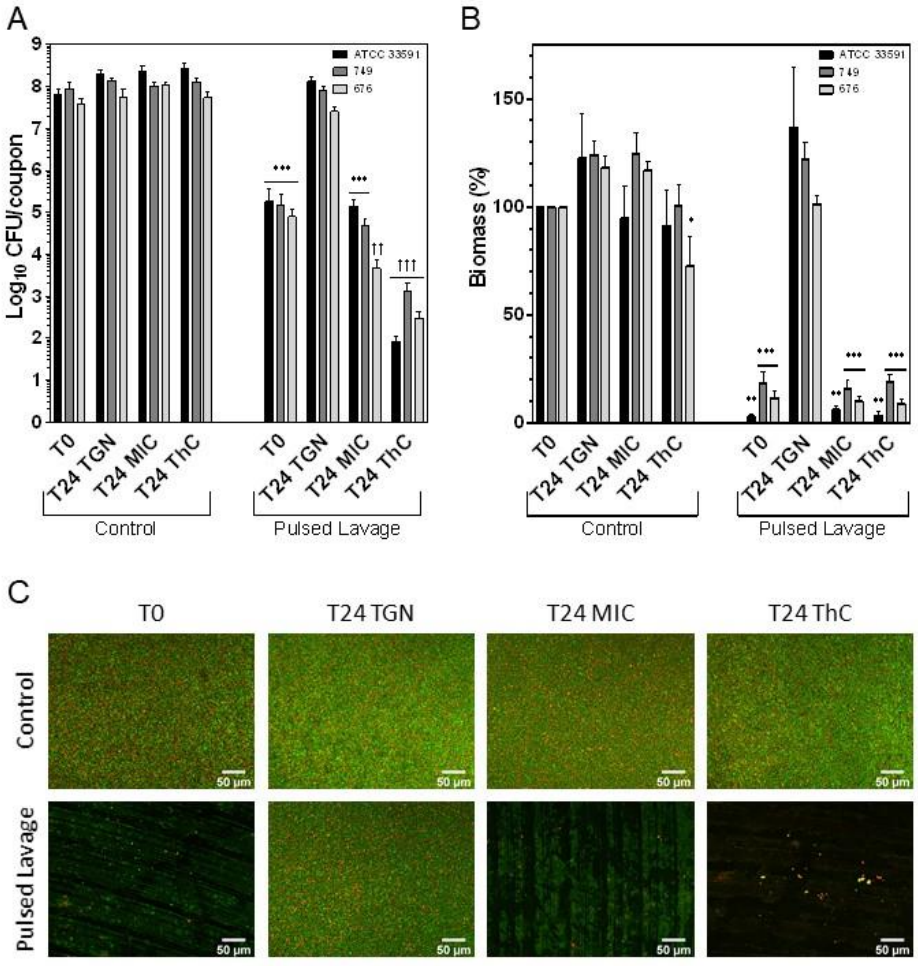

A
B
C
ATCC 33591
749
676
Log10 CFU/coupon
Biomass (%)
T0
T24 TGN
T24 MIC
T24 ThC
Control
Pulsed Lavage
50 µm

Figure III.2. Effects of irrigation and vancomycin on MRSA biofilms grown for 24h in TGN. A: CFU counts; B: biomass expressed in percentage of T0 controls; C: MIP of Z-stack acquired at 20x magnification following Live (green fluorescence, Syto 9) /Dead (red fluorescence, Propidium Iodide) staining. Scale bar: 50µm. Control: control groups; Pulsed Lavage; groups treated with pulsed lavage; T0: samples analyzed after 24 h of growth; T24 TGN: T0 samples analyzed after 24 h of reincubation in TGN; T24 MIC: samples analyzed after 24 h of reincubation in TGN with vancomycin at MIC; T24 ThC: samples analyzed after 24 h of reincubation in TGN with vancomycin at 20 mg/L (therapeutic concentration). Data expressed as means of experiments and SEM. N experiments ≥ 3. Statistical analysis: two-way ANOVA followed by Holm-Sidàk post-hoc test. Comparisons to T0 control samples: *: $p<0.05$; **: $p<0.01$; ***: $p<0.001$. Comparisons to T0 irrigation samples: †: $p<0.05$; ††: $p<0.01$; †††: $p<0.001$.

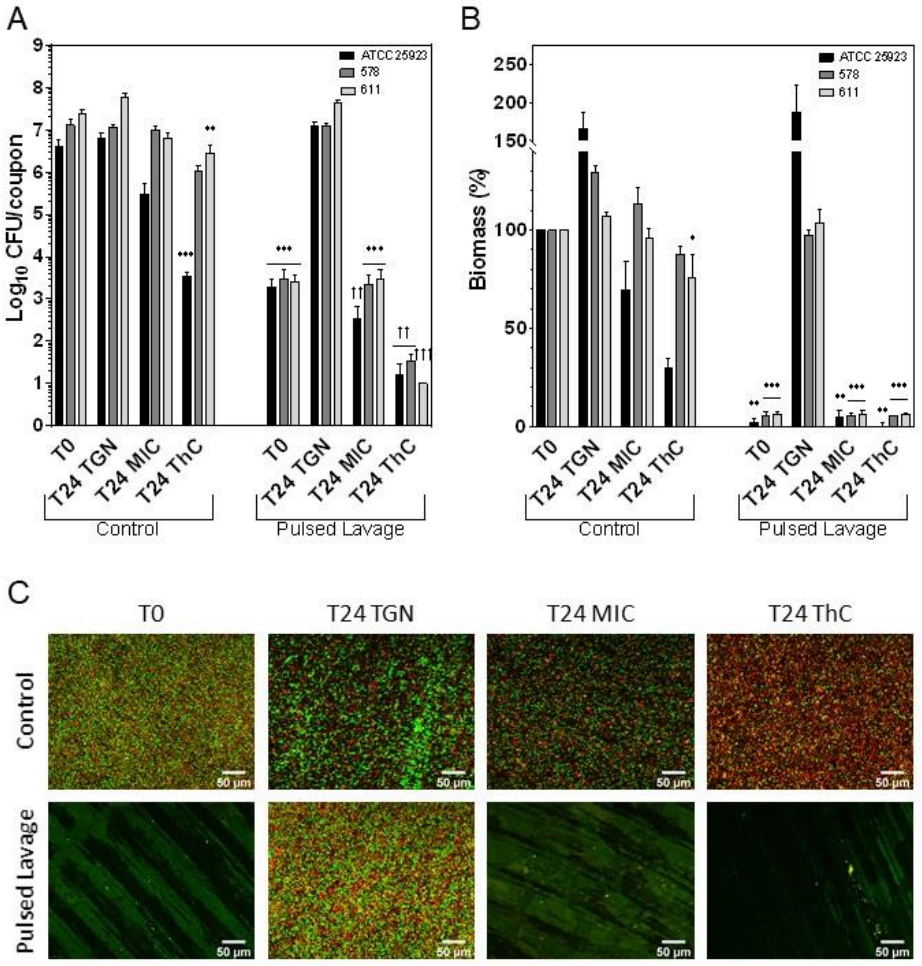

A
B
C
ATCC 25923
578
611
Log10 CFU/coupon
Biomass (%)
T0
T24 TGN
T24 MIC
T24 ThC
Control
Pulsed Lavage
50 µm

Figure III.3. Effects of irrigation and flucloxacillin on MSSA biofilms grown for 24h in TGN. A: CFU counts; B: biomass normalized as a percentage of T0 controls; C: MIP of Z-stack acquired at 20x magnification following Live (green fluorescence, Syto 9) /Dead (red fluorescence, Propidium Iodide) staining. Scale bar: 50µm. Control: control groups; Pulsed Lavage; groups treated with pulsed lavage; T0: samples analyzed after 24 h of growth; T24 TGN: T0 samples analyzed after 24 h of reincubation in TGN; T24 MIC: samples analyzed after 24 h of reincubation in TGN with flucloxacillin at MIC; T24 ThC: samples analyzed after 24 h of reincubation in TGN with flucloxacillin at 20 mg/L (therapeutic concentration). Data expressed as means of experiments and SEM. N experiments ≥ 3. Statistical analysis: two-way ANOVA followed by Holm-Sidàk post-hoc test. Comparisons to T0 control samples: *: $p<0.05$; **: $p<0.01$; ***: $p<0.001$. Comparisons to T0 irrigation samples: †: $p<0.05$; ††: $p<0.01$; †††: $p<0.001$.

4 Discussion

Our results show a synergistic effect of sequential pulsed-lavage and antimicrobial therapy with either vancomycin or flucloxacillin at clinically relevant concentrations against *Staphylococcus aureus* biofilms grown on titanium coupons. This combination of pulsed lavage with antibiotics at concentrations compatible with a parenteral administration to simulate PJI has not been previously reported. Knecht et al. published on the combination of pulsed lavage and incubation with tobramycin- and vancomycin-loaded calcium sulfate beads, showing a strong synergy (409). However, the antibiotic concentrations eluted in the culture medium were not determined, limiting the extrapolation of the results. Wolcott et al. (416) studied the combination of pulsed lavage and gentamicin against *S. aureus* biofilms in a chronic wound model. A synergy of the two treatments was observed, but the concentration of gentamicin was far above the human C_{max} after the administration of a conventional dose, limiting the extrapolation of the results to a clinical setting. Collectively, prior data and the data herein underline the importance of surgical irrigation of infected wound and implant surfaces prior to the administration of adequate antibiotic doses to observe a strong synergy and achieve maximal sustainable reduction in bacterial inoculum.

The independent use of pulsed lavage against *S. aureus* biofilms appeared to remove most of the biofilm cells and biomass in our experiments. This contrasts with previous studies that reported a 1 to 2 $\log_{10}$ reduction in cell numbers following pulsed lavage (244, 358, 409). This discrepancy between our results and previous studies may be due to differences in strains, material surfaces or culture conditions. However, the conditions used here likely closer

simulate clinical conditions, with a comparatively short distance between the nozzle and the coupons, and a volume of fluid to sample surface ratio of 40ml/cm². Moreover, we studied a larger variety of strains, limiting the confounding factor of strain-dependent effects.

Despite a substantial reduction in CFU counts, we noted that residual bacteria on the coupons after pulsed lavage were sufficient to restore a biofilm after a 24h incubation, consistent with what was previously shown by other authors.(244)

We observed that vancomycin at its recommended serum trough concentration had no effect on reducing MRSA bacterial inocula via CFU or biomass if the biofilms were not first disrupted by pulsed lavage, consistent with previous data that vancomycin activity within biofilms is poor. Several authors have described that vastly supratherapeutic concentrations of vancomycin were required to observe a significant reduction in CFU counts (234) or in the metabolic activity (412, 417) of MRSA biofilms. The low penetration of vancomycin in *S. aureus* biofilms may explain these observations (418).

In contrast, a limited strain-dependent effect of flucloxacillin was observed against MSSA biofilms in the absence of pulse lavage. Flucloxacillin is a narrow spectrum β-lactam antibiotic, directed against *Staphylococci* and *Streptococci*, which is recommended in combination with rifampicin for MSSA and methicillin-susceptible *S. epidermidis* prosthetic joint infections, alongside nafcillin and oxacillin (59, 419, 420). Only a few conflicting studies have been published about the in vitro effect of flucloxacillin against *S.*

aureus biofilms, pointing towards a variable, strain-dependent effect (421-424), analogous to our observations.

Our study presents several limitations. First, biofilms were grown only on Ti6Al4V as a substrate. This decision was based on the previous observation by Urish et al. (358) that the differences between metallic substrates are tenuous when considering the effect of pulsed lavage. Second, we limited the growth period of the biofilms before treatment to 24h. While the biofilms were mature from a microbiological perspective, it could be argued that older biofilms would develop a more complex structure that could change the effect of the treatments we used. Third, we used antibiotics at set concentrations. While vancomycin is often administered in a continuous infusion, flucloxacillin is usually administered on a 2g, 4 times per day regimen and important variations in serum concentrations are observed over time between 2 administrations. We decided to use, in addition to the MIC, a concentration equivalent to the one observed 3h after administration of a 2g dose in order to mitigate this limitation. However, as this concentration remained constantly above the MIC for 24h, the observed effects of flucloxacillin may be overestimated.

5 Conclusion

A synergy of pulsed lavage and vancomycin or flucloxacillin was observed against S. aureus biofilms grown on titanium alloy coupons. This effect was never reported when considering clinically relevant antibiotic concentrations. These results confirm the need for thorough irrigation of the metallic surfaces of implants during DAIR procedures to facilitate the subsequent action of antibiotics.

6 Author Contributions

HP, ARS, OC and FVB contributed to the conception and design of the study. GS and HRV provided clinical strains for the study. HP carried out experiments and analyzed data. HP and FVB wrote sections of the manuscript. All authors contributed to manuscript revision, read and approved the submitted version.

7 Funding

This work was supported by grants from the Fonds pour la Recherche dans l'Industrie et l'Agriculture (FRIA; Fonds de la Recherche Scientifique (FRS-FNRS) and the Orthenzy project (Win2Wal program of the Region Wallonne). H.P. received successive PhD fellowships from the Fondation Saint-Luc (Cliniques Universitaires Saint Luc, Université catholique de Louvain) and the FRIA. FVB is Research Director from the Belgian FRS-FNRS.

8 Conflict of Interest

The Interpulse pulse lavage devices were gifted by Stryker Co., Kalamazoo, MI, USA. The authors declare that the research was conducted in the absence of any other commercial or financial relationships that could be construed as a potential conflict of interest.

9 Acknowledgments

The authors thank Mrs Caroline Bouzin from the IREC imagery platform and Mr Alix Mangin from the Laboratoire de Pharmacologie Cellulaire et Moléculaire for their technical support.

10 Supplementary material

Table III.1. MRSA strains: Two-way ANOVA on CFU counts

Strains	Source	DF	SS	MS	F	P value
ATCC 33591	Reincubation	3	40.79	13.6	F (3, 24) = 52.64	P<0.001
	Pulsed-Lavage	1	84.16	84.16	F (1, 24) = 325.8	P<0.001
	Interaction	3	38.59	12.86	F (3, 24) = 49.81	P<0.001
	Residuals	24	6.199	0.2583		
	Total	31	169.7			
676	Reincubation	3	25.13	8.378	F (3, 24) = 54.87	P<0.001
	Pulsed-Lavage	1	79.84	79.84	F (1, 24) = 522.9	P<0.001
	Interaction	3	31.14	10.38	F (3, 24) = 67.98	P<0.001
	Residuals	24	3.664	0.1527		
	Total	31	139.8			
749	Reincubation	3	28.56	9.522	F (3, 24) = 43.72	P<0.001
	Pulsed-Lavage	1	74.2	74.2	F (1, 24) = 340.7	P<0.001
	Interaction	3	25.43	8.478	F (3, 24) = 38.92	P<0.001
	Residuals	24	5.227	0.2178		
	Total	31	133.4			

DF : degrees of freedom ; SS : sum of squares ; MS : mean square

Table III.2. MSSA strains: Two-way ANOVA on CFU counts

Strains	Source	DF	SS	MS	F	P value
ATCC 25923	Reincubation	3	104.7	34.91	F (3, 24) = 60.24	P<0.001
	Pulsed-Lavage	1	48.77	48.77	F (1, 24) = 84.15	P<0.001
	Interaction	3	24.46	8.155	F (3, 24) = 14.07	P<0.001
	Residuals	24	13.91	0.5796		
	Total	31	191.9			
578	Reincubation	3	49.93	16.64	F (3, 24) = 42.52	P<0.001
	Pulsed-Lavage	1	81.59	81.59	F (1, 24) = 208.5	P<0.001
	Interaction	3	28.24	9.413	F (3, 24) = 24.05	P<0.001
	Residuals	24	9.394	0.3914		
	Total	31	169.2			
611	Reincubation	3	73.75	24.58	F (3, 24) = 79.85	P<0.001
	Pulsed-Lavage	1	81.52	81.52	F (1, 24) = 264.8	P<0.001
	Interaction	3	26.47	8.825	F (3, 24) = 28.67	P<0.001
	Residuals	24	7.388	0.3079		
	Total	31	189.1			

DF : degrees of freedom ; SS : sum of squares ; MS : mean square

Table III.3. MRSA strains: Two-way ANOVA on biomass

Strains	Source	DF	SS	MS	F	P value
ATCC 33591	Reincubation	3	38282	12761	F (3, 24) = 14.85	P<0.001
	Pulsed-Lavage	1	33695	33695	F (1, 24) = 39.21	P<0.001
	Interaction	3	16838	5613	F (3, 24) = 6.532	P=0.002
	Residuals	24	20622	859.2		
	Total	31	109437			
676	Reincubation	3	21349	7116	F (3, 24) = 51.32	P<0.001
	Pulsed-Lavage	1	38133	38133	F (1, 24) = 275	P<0.001
	Interaction	3	9099	3033	F (3, 24) = 21.87	P<0.001
	Residuals	24	3328	138.7		
	Total	31	71909			
749	Reincubation	3	22114	7371	F (3, 24) = 41.31	P<0.001
	Pulsed-Lavage	1	37638	37638	F (1, 24) = 210.9	P<0.001
	Interaction	3	12613	4204	F (3, 24) = 23.56	P<0.001
	Residuals	24	4283	178.4		
	Total	31	76649			

DF : degrees of freedom ; SS : sum of squares ; MS : mean square

Table III.4. MSSA strains: Two-way ANOVA on biomass

Strains	Source	DF	SS	MS	F	P value
ATCC 25923	Reincubation	3	128267	42756	F (3, 24) = 44.43	P<0.001
	Pulsed-Lavage	1	14610	14610	F (1, 24) = 15.18	P<0.001
	Interaction	3	15854	5285	F (3, 24) = 5.492	P=0.005
	Residuals	24	23093	962.2		
	Total	31	181825			
578	Reincubation	3	22625	7542	F (3, 24) = 138.1	P<0.001
	Pulsed-Lavage	1	50168	50168	F (1, 24) = 918.5	P<0.001
	Interaction	3	6500	2167	F (3, 24) = 39.67	P<0.001
	Residuals	24	1311	54.62		
	Total	31	80603			
611	Reincubation	3	20168	6723	F (3, 24) = 60.51	P<0.001
	Pulsed-Lavage	1	32823	32823	F (1, 24) = 295.4	P<0.001
	Interaction	3	10358	3453	F (3, 24) = 31.08	P<0.001
	Residuals	24	2667	111.1		
	Total	31	66016			

DF : degrees of freedom ; SS : sum of squares ; MS : mean square

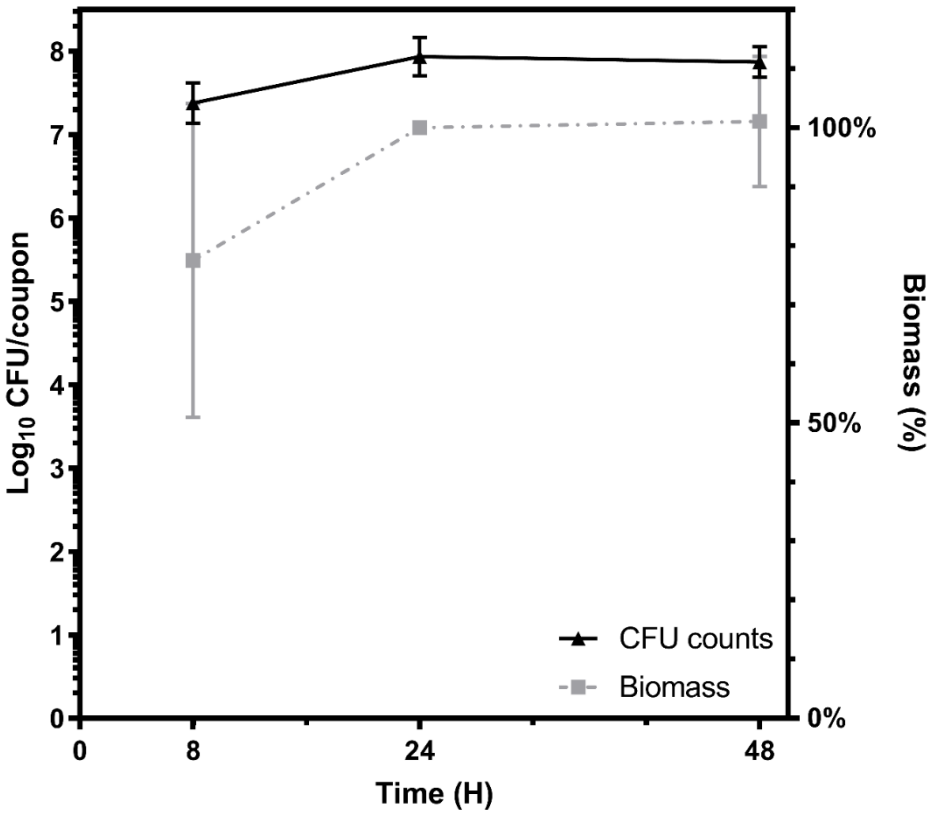


Figure III.1. Growth of ATCC 33591 biofilms on Ti6Al4V coupons over time. CFU counts (triangles, black) expressed in logarithm, biomass (squares, grey), expressed in percentage of 24h biofilms biomass. Data expressed as means of experiments and SEM. N experiments =3.

Chapter IV: *in-vitro* study of enzymatic debridement

In-vitro study of the synergistic effect of an enzyme cocktail and antibiotics against biofilms in a prosthetic joint infection model

Hervé Poilvache, M.D. [a, b, c], Albert Ruiz-Sorribas, M.Sc. [b], Olivier Cornu, M.D., Ph.D. [a, c], Françoise Van Bambeke, Pharm.D., Ph.D. [b *]

[a] Université catholique de Louvain, Institut de Recherche Expérimentale et Clinique, Neuromusculoskeletal Laboratory, Brussels, Belgium

[b] Université catholique de Louvain, Louvain Drug Research Institute, Pharmacologie cellulaire et moléculaire, Brussels, Belgium

[c] Cliniques Universitaires Saint-Luc, Orthopedic Surgery Department, Brussels, Belgium

Published in *Antimicrobial Agents and Chemotherapy*, January 2021, 65:e01699-20
DOI: https://doi.org/10.1128/AAC.01699-20

Abstract

Prosthetic Joint Infections (PJI) are frequent complications of arthroplasties. Their treatment is made complex by the rapid formation of bacterial biofilms, limiting the effectiveness of antibiotic therapy. In this study, we explore the effect of a tri-enzymatic cocktail (TEC) consisting of an endo-1,4-β-D-glucanase, a β-1,6-hexosaminidase, and an RNA/DNA non-specific endonuclease combined with antibiotics of different classes against biofilms of S. aureus, S. epidermidis, and E. coli grown on Ti6Al4V substrates. Biofilms were grown in TSB with 10g/L glucose and 20g/L NaCl (TGN). Mature biofilms were assigned to a control group or treated with the TEC for 30 minutes, then either analyzed or reincubated for 24h in TGN or TGN with antibiotics. The cytotoxicity of the TEC was assayed against MG-63 osteoblasts, primary murine fibroblasts, and J-774 macrophages using the LDH release test. The TEC dispersed 80.3 to 95.2% of the biofilms' biomass after 30 minutes. The reincubation of the treated biofilms with antibiotics resulted in a synergistic reduction of the total culturable bacterial count (CFU) compared to biofilms treated with antibiotics alone in the three tested species (additional reduction from 2 to more than 3 log10 CFU). No toxicity of the TEC was observed against the tested cell lines after a 24h incubation. The combination of pretreatment with TEC followed by a 24h incubation with antibiotics had a synergistic effect against biofilms of S. aureus, S. epidermidis, and E. coli. Further studies should assess the potential of the TEC as an adjuvant therapy in in-vivo models of PJI.

Keywords: ***Staphylococcus aureus*, *Staphylococcus epidermidis*, *Escherichia coli*, biofilms, dispersin B, endonuclease, cellulase, prosthetic joint infection**

1 Introduction

Prosthetic Joint Infections (PJI) are catastrophic complications of joint replacement surgeries. With a prevalence of 2.0% to 2.4% in patients following a total knee or total hip replacement (23), PJIs represent one of the leading failure causes of arthroplasties (21).

The most prevalent species encountered in PJIs are *Staphylococcus aureus*, coagulase-negative staphylococci, streptococci, and Gram-negative bacilli (81). These species are known to adhere to the surfaces of implants and to form complex communities embedded in an extracellular matrix called biofilms. In these structures, bacteria become tolerant to antibiotics up to concentrations 1000 times the MIC of planktonic cells (17, 19, 204).

Surgical Debridement, Implant Retention, and Antibiotic therapy (DAIR) is the preferred treatment strategy of acute (less than 3 weeks of symptoms) PJI (59), with better functional outcomes (41) and lower costs (20, 425) than alternative strategies. However, the observed failure rate is considerable (89, 426). These failures are partly explained by an insufficient biofilm removal during the debridement surgery, as was shown in-vitro by Urish *et al.* (358) and Poilvache *et al.* (427).

As a consequence, the need for new adjuvant treatments to facilitate the dispersal of biofilms has been recognized in the literature (150, 310, 364, 428, 429). Among mechanical and pharmaceutical approaches, the use of hydrolytic enzymes targeting specific components of the biofilm matrix has been suggested (364). The dispersal potential of single enzymes targeting individual matrix components, such as extracellular DNA,

exopolysaccharides, or extra-cellular proteins has been demonstrated by previous authors in in-vitro models (374, 384, 430, 431). Moreover, the synergy of the combination of these enzymes with antibiotics (377, 388) or antiseptics (378, 432) against biofilms has been reported in previous studies.

However, these previous studies did not address the variety in matrix composition amongst bacterial species as they focused on the effect of single enzymes on selected species. For this reason, a broad-spectrum tri-enzymatic cocktail (hereafter referred to as TEC for Tri-enzymatic cocktail), composed of an endo-1,4-β-D-glucanase, a β-1,6-hexosaminidase and a recombinant RNA/DNA non-specific endonuclease (see Materials and Methods), was tested, targeting the matrix of *Escherichia coli*, *Enterococcus faecalis*, *Klebsiella pneumoniae*, *Pseudomonas aeruginosa*, *Staphylococcus aureus*, and *Staphylococcus epidermidis* biofilms (patents n°WO2017/211737 A1 and n°BE2020/5726).

In this study, we investigated the dispersal effect of this tri-enzyme cocktail against *Staphylococcus aureus, Staphylococcus epidermidis*, and *Escherichia coli* mono microbial biofilms grown in vitro on titanium alloy surfaces similar to prosthetic implants and examined its synergy in combination with a broad selection of antibiotics belonging to different classes recommended for PJI treatment (59) at concentrations relevant to human use.

2 Materials and Methods

2.1 Bacterial strains, antibiotics, and enzymes

2.2 Strains

The methicillin-resistant *Staphylococcus aureus* ATCC 33591, methicillin-resistant *Staphylococcus epidermidis* ATCC 35984, and the *Escherichia coli* ATCC 47076 were used as representatives of the bacterial species usually encountered in PJI.

2.3 Antibiotics

The following antibiotics were used as laboratory standards: ciprofloxacin HCl (potency: 93.9%), and moxifloxacin HCl (potency: 90.9%) from Bayer AG, Leverkusen, Germany, colistin (potency: 79.6%) and doxycycline (potency: 90.2%), from Sigma-Aldrich, Saint-Louis, MO, USA, and linezolid (potency: 99.2%; RibX Pharmaceuticals, Morristown, NJ, USA). The following antibiotics were used as powders for injections in humans: ceftazidime (potency: 72.5%; Panpharma France, Luitré, France), daptomycin (potency: 100%; MSD, Puteaux, France), meropenem (potency: 92%; Hospira Benelux BVBA, Brussels, Belgium), rifampin (potency: 100%; Aventis, Schiltigheim, France), vancomycin (potency: 97.5%; Mylan, Hoeilaart, Belgium). The antibiotic concentrations were set on the basis of the PK/PD characteristics of the antibiotics studied and their pharmacokinetic parameters in humans described in the EUCAST rationales for clinical breakpoints or in the literature (Table IV.2).

2.4 Tri-enzymatic cocktail (TEC)

The tri-enzymatic cocktail (TEC; OrthenzyQure) used in this study was designed and provided by OneLife SA (Louvain-la-Neuve, Belgium). It consits in a sterile Tris-buffered (pH=7) aqueous solution containing 400 U/ml of aspecific DNA/RNA endonuclease from *Serratia marcescens* (c-lecta GMBH, Liepzig, Germany), 50U/ml of endo-1,4-β-D-glucanase from *Aspergillus niger* (Sigma) and 0.06 U/ml of β-*N*-acetylhexosminidase from *Actinobacillus pleuropneumoniae* (GIGA, Liège, Belgium) (composition described in patent publication numbers WO2017/211737 and BE2020/5726). The TEC was stored at 4 °C and was heated at 37°C for 30 minutes before use. The TEC is available upon request at OneLife SA for research purposes (under R&D reference OL-RD1000/OrthenzyQure).

In order to assay the biofilm dispersal effect of the individual enzymes, OneLife provided solutions of the individual enzymes at concentrations identical to those used in the TEC.

2.5 Susceptibility testing

MICs were determined by microdilution following the CLSI protocol (410) in MHB-ca and TGN (TSB + 2% NaCl + 1% glucose), i.e. the medium used for growing biofilms. MICs of daptomycin were tested in MHB-ca and TGN containing 50 mg/L of Ca^{2+}.

MBECs were assayed by growing biofilms in Calgary Biofilm Devices (CBD, Innovotech, Edmonton, Canada) in MHB-ca and TGN. Bacterial suspensions were prepared in PBS, starting from overnight cultures on TSA from frozen stocks. The suspensions were adjusted to a turbidity of 0.5

McFarland and diluted 1:10 in medium. 150µL were added per well of the CBDs. The CBDs were incubated for 24h at 37°C, under a continuous rotation of 50rpm to allow biofilm formation. Antibiotic dilutions in the two media – with 50mg/L of Ca^{2+} when assaying daptomycin - were prepared in new 96 wells plates at concentrations ranging from 1024mg/L to 0.5 mg/L (256 mg/L to 0.125 mg/L for meropenem). The lids of the CBDs were rinsed twice in PBS before being transferred to the plates containing the antibiotics. The plates were then incubated for 24h at 37°C with a continuous rotation of 50 rpm. At the end of the antibiotic challenge, the lids were rinsed twice in PBS before being transferred to new plates containing plain media. The plates were then sonicated for 10 minutes (Branson 5510 Ultrasonic bath, Emerson Electric, Saint-Louis, MO, USA). New steriles lids were placed and the plates were incubated for 24h at 37°C without agitation. At the end of the incubation period, the plates were examined for bacterial growth and optical density measures at 650nm were performed using a Spectramax M3 spectrophotometer (Molecular Devices, San Jose, CA, USA).

2.6 Biofilm culture

Bacterial suspensions were prepared in PBS, starting from overnight cultures on TSA from frozen stocks. The suspensions were adjusted to an OD_{620nm} of 0.5 (~8.5 $\log_{10}$ CFU/mL) using a CECIL 2021 spectrophotometer (Cecil Instruments Ltd, Milton, United-Kingdom). The suspension was then diluted 1:100 in TGN. The biofilms were grown on titanium alloy (Ti-6Al-4V) coupons (Biosurface, Bozeman, MN, USA) in 12 wells plates using 3mL of the final suspension per coupon. The plates were incubated for 24 h (ATCC 33591 and ATCC 35984) or 48 h (ATCC 47076) at 37°C, with a constant orbital shaking of 50 rpm. In the case of strain ATCC 47076 biofilms, the

medium was changed after 24 h. These culture times were selected as they allowed the biofilms to reach steady states over the study period and were determined in previous growth kinetic experiments for *S. aureus* (427). The culture duration period for *S. epidermidis* was derived from these results. Growth kinetic experiments were performed in this study for *E. coli* biofilms and showed that a steady state was reached after 48h of culture. Samples were analyzed for CFU counts and biomass every 24h for the growth kinetic experiments.

2.7 Biofilm treatments

2.7.1 Individual enzymes assay

The biofilms samples were rinsed twice with sterile PBS. They were then transferred to 24 wells plates filled with either 1mL of TEC or 1mL of one of the individual enzymes at 37°C. The plates were then incubated for 30 minutes at 37°C. At the end of the incubation period, the biofilm were rinsed twice in sterile PBS and assayed for total biomass (see below).

2.7.2 Combination of enzymatic cocktail and antibiotics

The biofilm samples were separated into a control group and an enzyme cocktail group. The coupons of both groups were rinsed twice in sterile PBS before being submitted to the treatments. The tri-enzyme cocktail group samples were transferred to a 24 wells plate, which wells were previously filled with 1mL of enzyme cocktail at 37°C. The plates were then incubated at 37°C with no agitation for either 15, 30, and 60 minutes (when studying the kinetics of activity) or 30 minutes (other experiments). After incubation, the samples were rinsed twice in sterile PBS before either immediate analysis

(see below for analysis techniques descriptions) or reincubation. Control group samples were directly rinsed in sterile PBS. All samples were then reincubated for 24 h at 37°C, under a constant orbital shaking of 50 rpm in TGN or TGN containing antibiotics at set concentrations (TGN + 50 mg/L of Ca^{2+} for samples exposed to daptomycin) (see Table 2) in 12 wells plates containing 3 mL of medium per well.

2.8 Biofilms analysis

The coupons were rinsed twice in sterile PBS and then analyzed using the following techniques:

2.8.1 CFU counts

Coupons were placed in 15 mL conical tubes (Greiner Bio-One International GmbH, Kremsmünster, Austria) filled with 2 mL of sterile PBS. In order to detach the biofilms and suspend the bacteria, the tubes were then vortexed for 30 s at maximum intensity (Vortex-Genie 2, Scientific Industries Inc., Bohemia, NY, USA), sonicated for 5 min (Branson 5510 Ultrasonic bath, Emerson Electric, Saint-Louis, MO, USA), and vortexed again for 30 s. The suspension was then sampled and serially diluted, before plating on TSA. The TSA plates were then incubated for 24 to 48 h at 37°C until the colonies reached an adequate size. CFU counts were then obtained using an automated method (image acquisition using Gel Doc XR+ and image processing using Quantity One (BioRad, Hercules, CA, USA).

2.8.2 Biomass assay

Coupons were dried overnight at 60°C. They were then stained with 1 mL of 1% crystal violet solution for 10 min (Sigma-Aldrich Corp.). The coupons

were then rinsed twice using deionized water to remove the excess dye. Afterward, they were placed for 1 h in 24 wells plates filled with 1 mL of 66% acetic acid solution (Merck KGaA, Darmstadt, Germany) to resolubilize the dye. The coupons were removed from the wells and the absorbance of the solution was read at 570 nm using a Spectramax M3 spectrophotometer (Molecular Devices, San Jose, CA, USA).

2.8.3 Fluorescence microscopy

Coupons were rinsed twice in sterile deionized water to avoid interference from phosphate ions. They were then stained using the Filmtracer LIVE/DEAD Biofilm Viability Kit (Thermo Fisher Scientific Inc., Waltham, MA, USA) according to the manufacturer's instructions. Coupons were then rinsed again twice in sterile deionized water before imaging using an AxioImager.Z1 microscope fitted with an ApoTome1 attachment (Zeiss, Oberkochen, Germany) at a 20x magnification. The images were post-processed using FIJI (413, 414), using the maximum intensity projection technique and by adjusting the brightness of the channels.

2.9 Cytotoxicity assays

2.9.1 Cell Culture

J774 murine macrophages (Sandoz Forschung Laboratories, Vienna, Austria) (433), MG-63 human osteoblasts (ATCC CRL-1427), and primary murine fibroblasts (434) were used for the cytotoxicity assays. The cells were grown in RPMI 1640 or Dulbecco's Modified Eagle Medium supplemented with 10% of fetal bovine serum (all products from Thermo Fisher Scientific Inc.,

Waltham, MA, USA) at 37°C in a 5% CO_2 atmosphere. The cells were used for the assays between passages 2 and 5.

The cells were cultured initially in 250 cm^3 cell culture flasks before being transferred to 96 wells plates, at a concentration of 10^4 cells per well. The plates were incubated for 24 h at 37°C with 5% CO_2 to allow cellular adhesion to the wells before testing.

2.9.2 Assay

Cytotoxicity was assessed by measuring the release of the cytoplasmic enzyme lactate dehydrogenase (LDH) in the culture medium, using the Cytotoxicity Detection Kit (Sigma-Aldrich). The wells were rinsed with sterile PBS before adding 100µL of medium with 1% decomplemented fetal bovine serum. 100µL of the following test substances were then added to the wells (final concentrations): TEC (concentration used against biofilms and half of this concentration), Triton X-100 solution (1%, positive control), medium with 1% decomplemented serum (negative control). Three empty wells per experiment were filled with 200µL of medium with 1% decomplemented serum to measure the background signal.

The plates were then incubated for 1 h or 24 h, at 37°C in a 5% CO_2 atmosphere. 100µL of the supernatant of each well was aspirated and transferred to a new 96 wells plate and added by 100 µL of the extemporaneously prepared LDH assay solution, as per the manufacturer's instructions. The plates were then incubated for 30 min at room temperature in the dark. The light absorbance was then measured at 490 nm and 650 nm using a Spectramax M3 spectrophotometer (Molecular Devices, San Jose, CA, USA).

2.10 Data transformation and statistical analysis

CFU counts were normalized using a base 10 logarithmic transformation before analysis. Absorbance values of the biomass assays were transformed into percentages of the T0 controls after subtracting the average value of negative controls. The absorbance values of the LDH assays were transformed in percentages using the following equation:

$$\boldsymbol{Cytotoxicity}\ (\%) = \frac{\boldsymbol{Abs.exp.value}_{420nm-650nm} - \boldsymbol{Abs.control}\ (-)_{420nm-650nm}}{\boldsymbol{Abs.control}\ (+)_{420nm-650nm} - \boldsymbol{Abs.control}\ (-)_{420nm-650nm}} \times \mathbf{100}$$

The statistical analysis was then performed using R (version 3.6.1) and the package car (version 3.0.6) or in GraphPad 8.4.3 (GraphPad Software, San Diego, CA). The TEC kinetics experiments data were analyzed using repeated measure ANOVA followed by paired t-tests with Holm correction. The data relating to the combined effect of TEC and antibiotics were analyzed using two-way ANOVA, after assessing the normality of residues with QQ plots and the equality of variances using the Levene test. The Tukey HSD test was used to perform pairwise comparisons. The synergy of treatments was defined as a statistically significant interaction parameter of the two-way ANOVAs (415). The threshold for alpha errors is of 0.05. The data reported in the text are the means with the 95% confidence interval.

3 Results

3.1 **Antibiotics susceptibility of planktonic bacteria and of biofilms**

The minimal inhibitory concentrations (MIC) and minimal biofilm eradication concentrations (MBEC) are shown in Table IV.1. The strains were susceptible to all tested antibiotics according to the CLSI breakpoints, except for the ATCC 33591 MRSA strain which was resistant to doxycycline. For this reason, doxycycline was not used against ATCC 33591 biofilms for the next experiments. The MIC in MHB-ca and TGN were within two dilutions of each other. Most of the MBECs exceeded the MICs by a hundred or thousand-fold factor, to the notable exception of daptomycin, linezolid and moxifloxacin against the strain ATCC 33591 in MHB-Ca. The MBECs could not be established in TGN for the strain ATCC 47076 as we observed inconsistent results across replicates. All MBECs were found to be higher than the concentrations chosen for the coupons assays (Table IV.2).

Table IV.1. Minimal Inhibitory Concentrations and Minimal Biofilm Eradication Concentrations (mg/L)

Antibiotic	Assay	ATCC 33591		ATCC 35984		ATCC 47076	
		MHB-Ca	TGN	MHB-Ca	TGN	MHB-Ca	TGN
Daptomycin	MIC	1	1	1	1	-	-
(DAP)	MBEC	4	>1024	>1024	>1024	-	-
Doxycycline	MIC	16	16	0.25	0.25	-	-
(DOX)	MBEC	-	-	128	512	-	-
Linezolid	MIC	2	1	2	1	-	-
(LZD)	MBEC	8	>1024	>1024	>1024	-	-
Moxifloxacin	MIC	0.125	0.125	0.06	0.125	-	-
(MXF)	MBEC	2	>1024	>1024	>1024	-	-
Rifampin	MIC	0.004	0.004	0.004	0.004	-	-
(RIF)	MBEC	8	2	128	4	-	-
Vancomycin	MIC	1	8	2	8	-	-
(VAN)	MBEC	>1024	>1024	>1024	>1024	-	-
Ceftazidime	MIC	-	-	-	-	0.25	0.125
(CEF)	MBEC	-	-	-	-	>1024	*
Ciprofloxacin	MIC	-	-	-	-	0.016	0.03
(CIP)	MBEC	-	-	-	-	128	*
Colistin	MIC	-	-	-	-	0.5	0.25
(CST)	MBEC	-	-	-	-	>1024	*
Meropenem	MIC	-	-	-	-	0.03	0.06
(MEM)	MBEC	-	-	-	-	>256	*

Values in bold indicate an MIC superior to the CLSI breakpoint values (410).

*: The MBEC assays results for the ATCC 47076 strain were unreliable and were not included.

Table IV.2. Antibiotics experimental concentrations and rationales.

Antibiotic	Concentration (mg/L)	Rationale
Daptomycin (DAP)	30	$\frac{AUC_{0-24h}}{24h}$
Doxycycline (DOX)	1.5	$\frac{AUC_{0-24h}}{24h}$
Linezolid (LZD)	5	C_{min}
Moxifloxacin (MXF)	1.5	$\frac{AUC_{0-24h}}{24h}$
Rifampin (RIF)	2.5	$\frac{AUC_{0-24h}}{24h}$
Vancomycin (VAN)	2	Target trough concentration (20 mg/L)
Ceftazidime (CEF)	3.8	C_{min}
Ciprofloxacin (CIP)	1.625	$\frac{AUC_{0-24h}}{24h}$
Colistin (CST)	2.5	$\frac{AUC_{0-24h}}{24h}$
Meropenem (MEM)	0.25	C_{min}

Note: Pharmacokinetic and PK/PD informations obtained from the EUCAST rationales for clinical breakpoints documents or from the literature (references in supplementary materials Table 1).

3.2 **Kinetics of TEC effect**

The effect of TEC on ATCC 33591 MRSA biofilms is illustrated in Figure IV.1 for CFU counts (a) and biomass (b and c). The CFU counts decreased modestly after 15 minutes of incubation (-0.68 $\log_{10}$ CFU, p = 0.0365 from time 0) and no statistically significant differences were observed between the subsequent incubation times. A sharp decrease in the total biomass was observed after a 15 minutes incubation (-72.0% from time 0, p = 3.3e-06) and appeared to be maximal after 30 minutes (-95.82% from time 0, p = 7.0e-07; -19.45% from 15 min, p = 0.014). These effects were corroborated by macroscopic observation of the crystal violet stained samples (fig. IV.1.c). Based on these results, an incubation time of 30 minutes with TEC was adopted for the next experiments.

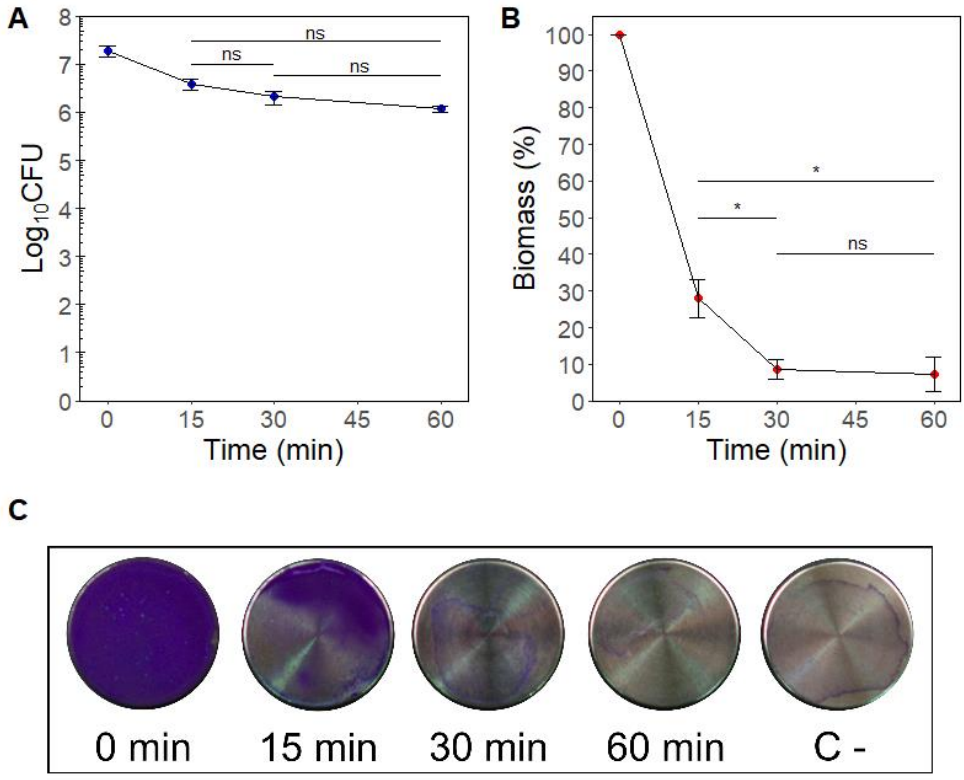


Figure IV.1. Kinetics of biofilm dispersal by TEC against MRSA *S. aureus* ATCC 33591 biofilms. A: Log_{10} CFU counts per coupon; B: Total biomass assay (expressed as the percentage of Time 0 control); C: Pictures of biofilm samples exposed to TEC for the indicated times (C-: negative control [coupon incubated in sterile culture medium]) stained with crystal violet). The values indicate the means of triplicate experiments (+/- standard error). Statistical analysis: repeated measure ANOVA, followed by paired t-tests with Holm correction. *: $p<0.05$.

3.3 **Effect of individual enzymes compared to the TEC**

In a preliminary experiment, the effect of the individual enzymes composing the TEC was tested against biofilms of each of the three species in comparison with the cocktail (Figure IV.2). The TEC was found to be at least equivalent to the most effective single enzyme against all three species. While we did not observe any significant biofilm dispersal when treating MRSE ATCC 35984 biofilms with the individual enzymes, exposure to the TEC resulted in a 93% reduction of the biomass ($p<0.0001$). The RNA/DNA endonuclease was found to be equivalent to the TEC against MRSA ATCC 33591 and the β-1,6-hexosaminidase was equivalent to the TEC against *E. coli* ATCC 47076.

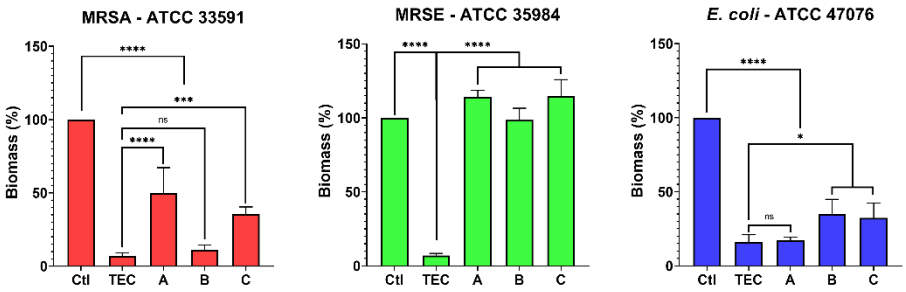


Figure IV.2. Effect of a 30 minutes treatment with the individual enzymes on the biomass of ATCC 33591, ATCC 35984, and ATCC 47076 biofilms and comparison to the TEC. Ctl: Control; TEC: Tri-Enzymatic Cocktail; A: β-*N*-acetylhexosaminidase; B: DNA/RNA endonuclease; C: endo-1,4-β-D-glucanase. Data expressed as percentage of the control. The values indicate the means of triplicate experiments (+/- standard error). Statistical analysis: two-way ANOVA followed by Holm-Sidàk post-hoc test. NS: no significant difference *: $p<0.05$; **: $p<0.01$; ***: $p<0.001$; ****: $p<0.0001$

3.4 **Effect of TEC and of antibiotics alone or in combination against biofilms**

Biofilms exposed to TEC for 30 minutes were washed and reincubated in medium supplemented or not with antibiotics at clinically relevant concentrations (Table IV.2). The results are illustrated in Figures IV.3 (MRSA ATCC 33591), IV.4 (MRSE ATCC 35984), and IV.5 (*E. coli* ATCC 47076) for CFU counts (panels A), biomass (panels B) and fluorescence microscopy (panels C). The details of the comparisons are shown in Tables IV.2 to IV.7 of the supplementary materials.

A 30 min exposure of the coupons to TEC significantly reduced the CFU counts and biomass of all strains. The CFU counts were reduced by 2.04 $\log_{10}$ in strain ATCC 33591, 2.54 $\log_{10}$ in strain ATCC 35984, and 1.24 $\log_{10}$ in strain ATCC 47076. Biomass was reduced by 95.2% in strain ATCC 33591, 88.6% in strain ATCC 35984, and 80.3% in strain ATCC 47076.

A 24h reincubation of control samples was not associated with significant changes in CFU counts. Their biomass remained stable in strains ATCC 35984 and ATCC 47076 but increased by 24.4% in strain ATCC 33591. Similarly, the CFU counts of the samples treated with the enzyme cocktail and then reincubated for 24 h in TGN were similar to those of non-treated samples for all three strains. The biomass was however significantly lower than for control group samples for ATCC 33591 (-19.1%) and ATCC 35984 (-34.7%) biofilms.

The effect of a 24h exposure to antibiotics on control biofilms was variable *vs*. CFU counts and generally weak or inexistent *vs.* the biomass when compared to initial controls (statistical analyses shown in supplemental materials Tables IV.2 to IV.7).

Against staphylococci, vancomycin (20 mg/L) caused a 1.84 log_{10} CFU increase in the CFU counts of MRSE ATCC 35984 biofilms but no changes MRSA ATCC 33591. Conversely, the biomass of MRSA samples increased by 22.3% but did not change significantly in MRSE samples. Rifampin (2.5 mg/L) caused a significant reduction of the CFU counts in both strains (ATCC 33591: -1.59 log_{10} CFU; ATCC 35984 -3.39 log_{10} CFU) but did not affect the biomass of either strain. Linezolid (5 mg/L) had a limited effect on the CFU counts of strain ATCC 33591 (-1.50 log_{10}) and did not affect the CFU counts of strain ATCC 35984, nor the biomass of both strains. Moxifloxacin (1.5 mg/L) impacted both strains differently despite similar MICs. In ATCC 33591 samples, the CFU counts did not change, and the biomass increased by 29.7%, while in ATCC 35984, a 2.52 log_{10} CFU decrease was observed and the biomass remained stable. Daptomycin (30 mg/L) had a strong effect on the CFU counts of both strains (ATCC 33591: -4.99 log_{10}; ATCC 35984: -3.50l og_{10}), as well as a moderate effect on the biomass of strain 33591 (-20.2%), while the biomass of strain ATCC 35984 remained unchanged. Doxycycline (1.5 mg/L) was used against MRSE ATCC 35984 only as MRSA ATCC 33591 was resistant. No significant effect was observed for either CFU counts or biomass. Against *E. coli* ATCC 47076 biofilms, ceftazidime (3.8 mg/L) and ciprofloxacin (1.625 mg/L) had a significant effect on CFU counts (ceftazidime: -2.06 log_{10}; ciprofloxacin: -3.21 log_{10})

and biomass (ceftazidime: -61.7%; ciprofloxacin: -48.33%), while colistin (2.5 mg/L) and meropenem (0.25 mg/L) did not.

Turning now to the results for biofilms of the three strains successively exposed to TEC and antibiotics at set concentrations, we observed significant reductions of CFU counts and biomass when compared to samples treated only with antibiotics, except for the CFU counts of MRSA ATCC 33591 samples treated with daptomycin (which were already markedly decreased by the antibiotic alone) and the biomass of *E. coli* ATCC 47076 treated with ceftazidime (for which the difference between samples preexposed or not to the TEC cocktail did not reach significance). The difference in CFU counts between the samples preexposed to the enzymes and the control group samples was always higher than 2 $\log_{10}$ and exceeded 3 $\log_{10}$ in MRSA ATCC 33591 samples treated with vancomycin (-4.22 $\log_{10}$, $p<0.0001$) or moxifloxacin (-3.87 $\log_{10}$, $p<0.0001$), in MRSE ATCC 35984 samples treated with vancomycin (-6.84 $\log_{10}$, $p<0.0001$), and in all *E. coli* ATCC 470476 samples exposed to any of the 4 tested antibiotics (ceftazidime: -5.23 $\log_{10}$, $p<0.0001$); ciprofloxacin: -3.98 $\log_{10}$, $p<0.0001$; colistin: -5.57 $\log_{10}$, $p<0.0001$; meropenem: -6.11 $\log_{10}$, $p<0.0001$). The difference in biomass between samples treated with antibiotics alone or with the combination of TEC and antibiotics exceeded 80% in most conditions, except for strain ATCC 33591 samples treated with daptomycin and strain ATCC 47076 samples treated with ciprofloxacin, and colistin. The two-way ANOVA analysis (supplementary materials Tables IV.8 to IV.13) showed significant interaction parameters in all cases when considering the exposure to the enzyme cocktail and the reincubation of the samples as factors. This suggests that the tri-enzyme cocktail and the antibiotics have a synergistic effect on

both CFU counts and biomass of all three strains. The analysis of biofilms using fluorescence microscopy after live/dead staining (figures IV.3, IV.4, IV.5, panels C) illustrates the observed CFU counts and biomass assays. The treatment of samples with the TEC dispersed an important proportion of the bacterial cells, which were enough to regrow a biofilm after 24h of reincubation in TGN. This recovery appeared to be inhibited by the reincubation with antibiotics. The aspect of control samples exposed during 24h to vancomycin, ciprofloxacin, and meropenem appeared unchanged from the samples incubated in TGN, keeping a majority of live cells (green), while the samples incubated with daptomycin exhibited a high proportion of dead cells (red).

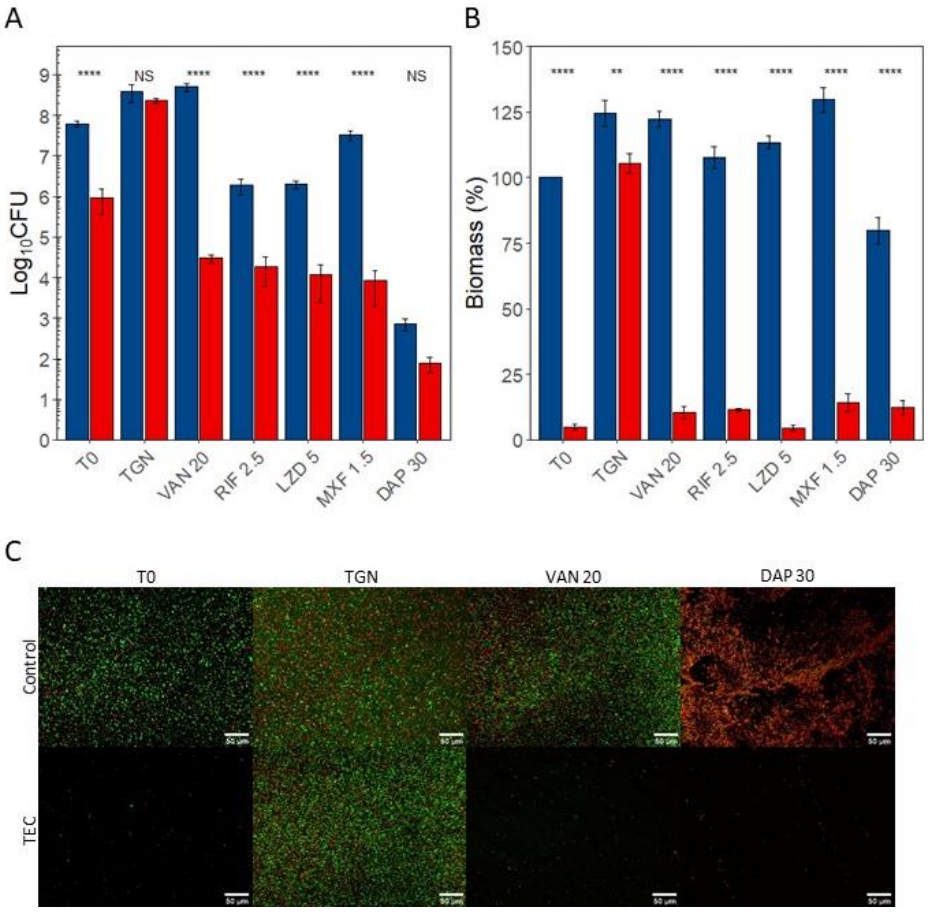


Figure IV.3. Effect of the combination of the TEC with antibiotics on MRSA ATCC 33591 biofilms. A: CFU counts; B: Biomass; C: Fluorescence microscopy. A & B: blue: controls, red: samples treated for 30 minutes with TEC. T0: no reincubation; TGN: 24h reincubation in TGN; Others: 24h reincubation in TGN with antibiotics at the indicated concentrations (see Table 1). CFU counts expressed in $\log_{10}$ CFU per coupon, biomass expressed in percentage of T0 controls. The values indicate the means of triplicate experiments (+/- standard error). Statistical analysis: two-way ANOVA followed by Tukey HSD comparing control samples to samples exposed to the enzymatic cocktail. NS: no significant difference *: $p<0.05$; **: $p<0.01$; ***: $p<0.001$; ****: $p<0.0001$. C: Green: living cells (SYTO 9); red: dead cells (Propidium Iodide). 20x magnification. Scale bars represent 50µm.

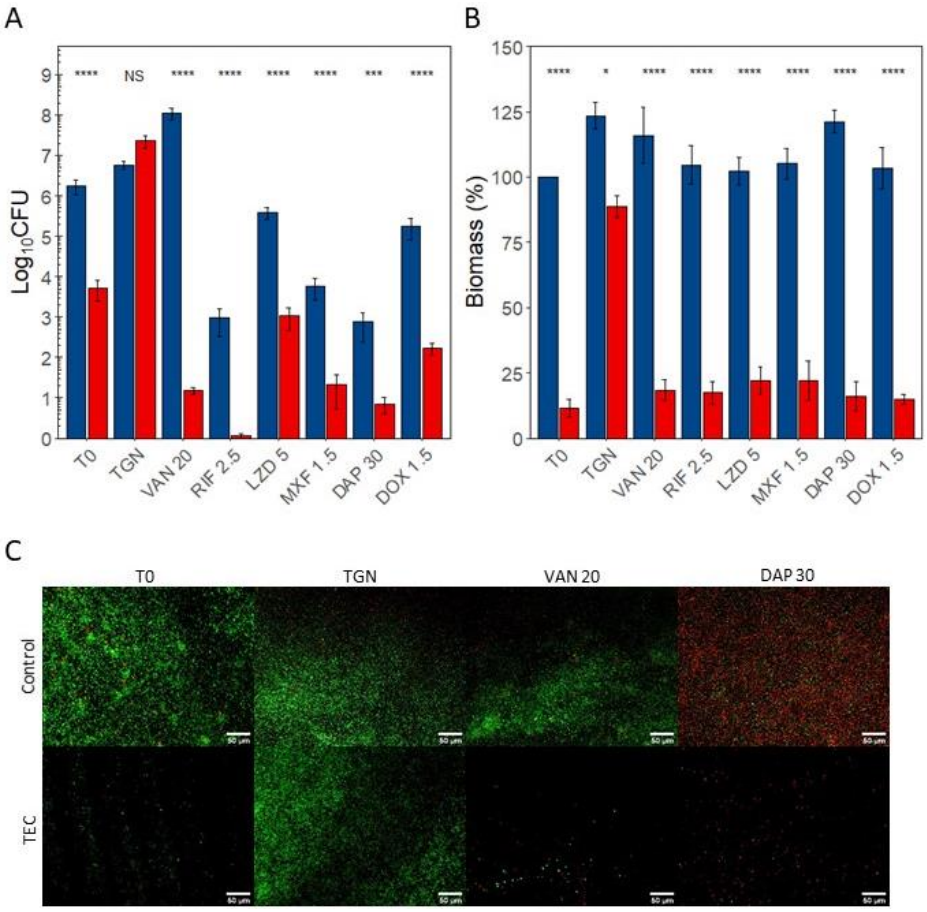


Figure IV.4. Effect of the combination of the TEC with antibiotics on MRSE ATCC biofilms. A: CFU counts; B: Biomass; C: Fluorescence microscopy.A & B: blue: controls, red: samples treated for 30 minutes with TEC. T0: no reincubation; TGN: 24h reincubation in TGN; Others: 24h reincubation in TGN with antibiotics at the indicated concentrations (see Table 1). CFU counts expressed in log_{10} CFU per coupon, biomass expressed in percentage of T0 controls. The values indicate the means of triplicate experiments (+/- standard error). Statistical analysis: two-way ANOVA followed by Tukey HSD comparing control samples to samples exposed to the enzymatic cocktail. NS: no significant difference *: $p<0.05$; **: $p<0.01$; ***: $p<0.001$; ****: $p<0.0001$. C: Green: living cells (SYTO 9); red: dead cells (Propidium Iodide). 20x magnification. Scale bars represent 50µm.

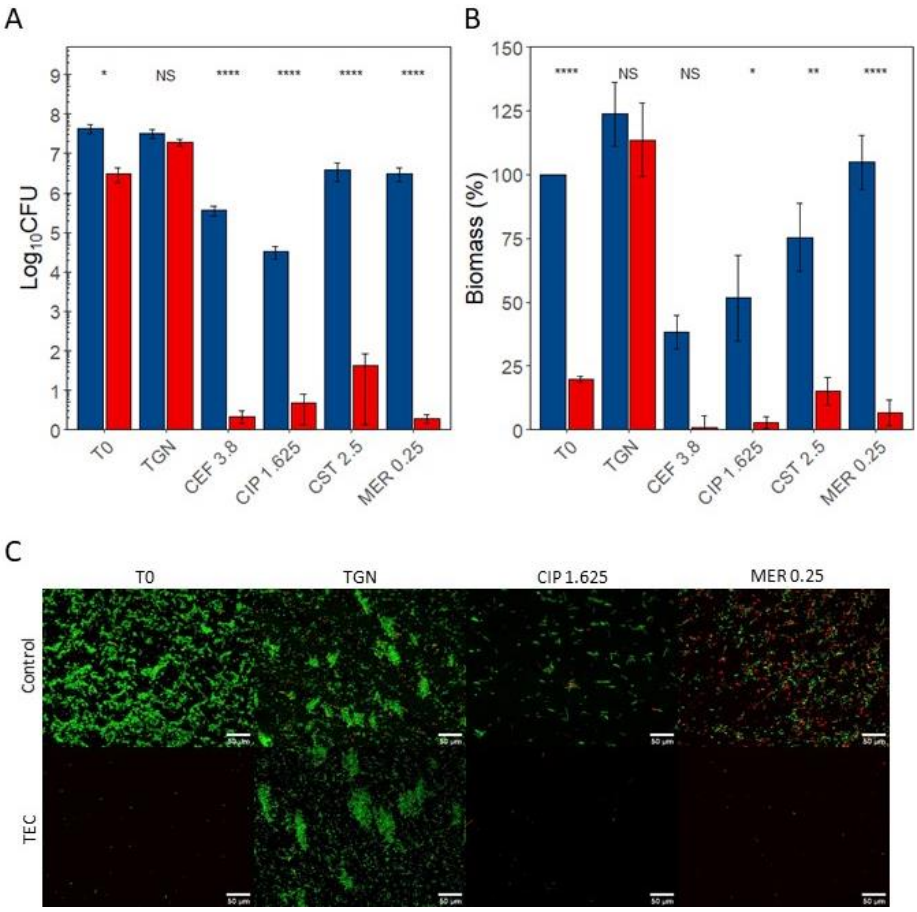


Figure IV.5. Effect of the combination of the TEC with antibiotics on *E. coli* ATCC 47076 biofilms. A: CFU counts; B: Biomass; C: Fluorescence microscopy. A & B: blue: controls, red: samples treated for 30 minutes with TEC. T0: no reincubation; TGN: 24h reincubation in TGN; Others: 24h reincubation in TGN with antibiotics at the indicated concentrations (see Table 1). CFU counts expressed in $\log_{10}$ CFU per coupon, biomass expressed in percentage of T0 controls. The values indicate the means of triplicate experiments (+/- standard error). Statistical analysis: two-way ANOVA followed by Tukey HSD comparing control samples to samples exposed to the enzymatic cocktail. NS: no significant difference *: $p<0.05$; **: $p<0.01$; ***: $p<0.001$; ****: $p<0.0001$. C: Green: living cells (SYTO 9); red: dead cells (Propidium Iodide). 20x magnification. Scale bars represent 50µm.

3.5 **Cytotoxicity tests**

The cytotoxicity of the tri-enzyme cocktail for different types of eukaryotic cells was then evaluated by measuring the release of the cytosolic enzyme LDH in the culture medium after 1 h and 24 h exposures to TEC at two concentrations (concentration used against biofilms and a 1:1 dilution). At 1 h, no significant toxicity was detected (values <5% in all cases). At 24 h, the release of the cytosolic enzyme lactate dehydrogenase (LDH) reached 3.0% (IC 95%: -1.1;7.0) for primary murine fibroblasts; -1.6% (IC 95%: -4.7%;1.4) for MG-63 human osteosarcoma cells and -3.2% (IC 95%: -17.0;10.7) for J774 murine macrophages.

4 Discussion

This study found that a tri-enzymatic cocktail containing two glycoside hydrolases (an endo-1,4-β-D-glucanase and a β-1,6-hexosaminidase) and a non-specific RNA/DNA endonuclease had a significant dispersal effect on mature biofilms of *S. aureus*, *S. epidermidis*, and *E. coli* reference strains grown on titanium alloy and that the successive treatment of these biofilms with this enzyme cocktail and antibiotics at concentrations relevant to the clinical setting was synergistic, resulting in significantly lower residual CFU counts than with either individual treatment.

While the potential of glycoside hydrolases and DNase I as biofilm dispersal agents has been previously described in the literature (364, 374), the originality of our work resides in the association of enzymes targeting biofilm matrix components found in biofilms of varied species (435), which is hypothesized to help sidestep the limited spectrum of individual enzymes caused by the significant variations in matrix contents observed among bacterial species and strains (170, 436). Indeed, the results of individual enzymes assays performed in this study underline the added value of combining enzymes as done in the TEC. The β-1,6-hexosaminidase used in this study is a Dispersin B homolog targeting the poly-β-1,6-*N*-acetylglucosamine (PNAG) component of the biofilm matrix (194, 375). PNAG is an important constituent of the matrix of multiple species' biofilms and is required for the formation of biofilm by *S. epidermidis* (170, 437, 438) and *S. aureus* strains expressing the *icaABCD* operon (170, 439) and of *E. coli* strains expressing the *pgaABCD* locus (169, 436). Dispersin B was shown to disperse the biofilms of PNAG-producing strains of multiple

species, including those included in our study (168, 376, 430). Cellulase is as endo-1,4-β-D-glucanase targeting cellulose, which is an important constituent of the biofilm matrix of *Enterobacter* spp. (178), including *E. coli* (440). It has been shown to disperse *E. coli* (432) and *Pseudomonas aeruginosa* (384) biofilms in-vitro. The recombinant non-specific endonuclease targets both DNA and RNA phosphodiester bonds (441). DNA is a common component of the biofilm matrix of most bacterial species, including *S. aureus*, *S. epidermidis*, and *E. coli* (442). While the biofilm dispersal properties of this enzyme had not been previously investigated, it has been favorably compared to the widely studied DNAse I (374) for the hydrolysis of DNA in sputum (443).

The dispersal of biofilms by enzymes similar to the ones constituting TEC was shown in previous publications to reduce the tolerance of bacterial biofilms to antibiotics (380, 384, 388) and antiseptics (432). However, limitations related to the use of single enzymes have been reported. Izano *et al.* observed that DNAse I did not disperse biofilms of *S. epidermidis* contrarily to *S. aureus* and that Dispersin B had an inverse effect by dispersing *S. epidermidis* biofilms and leaving *S. aureus* biofilms intact. Accordingly, they found that the dispersal of these biofilms by the appropriate enzyme (DNAse I for *S. aureus* of Dispersin B for *S. epidermidis*) improved the effect of the detergent cetylpyridinium chloride on CFU counts (168).

Our results illustrate the broad spectrum of the tri-enzymatic cocktail, which stems from the combination of enzymes with different activity spectrums (435). Furthermore, these results support the hypothesis of a synergy of enzymatic dispersal and a broad selection of antibiotics at concentrations

clinically relevant to the treatment of PJIs against biofilms. As could be expected from the observed MBEC values, the antibiotic concentrations used for the coupons assays had a minimal effect on control biofilms, but their combination with an enzymatic pre-treatment resulted in significant reductions of culturable cell numbers as well as total biomass in nearly all combinations of bacterial species and antibiotics.

The cytotoxicity of TEC to different cell lines relevant to the joint environment (macrophages, fibroblasts, osteoblasts) was found to be negligible after a 24h exposure. An explanation to this observation could be that the targets of these enzymes are either not produced by mammalian cells (cellulose), or irrelevant to their proliferation (eDNA and PNAG).

These results should however be interpreted with caution as our study presents some limitations. We limited ourselves to the study of biofilms of reference strains. While this facilitates the replication of our results by other teams in comparison to clinical strains, the loss of diversity in gene expression could mask the effect of the variability in matrix composition observed in some species (444). The antibiotic concentrations considered in our study did not take into account the serum protein binding. Among the drugs used in this study, doxycycline and daptomycin show a high serum protein binding, which could lead to an over-estimation of their effects in our experimental setting. However, the albumin concentration in synovial fluid is three to four times inferior to the serum concentration (445). This difference in albumin concentrations could lead to a higher free fraction of drugs in the synovial fluid than in serum. For this reason, the total serum concentration appeared to be a reasonable estimate that limited the risk of underestimating the effects

of antibiotics. The in-vitro nature of our experiments limits the extrapolation to the clinical setting as it does not represent the diversity of the situations encountered in a clinical setting, nor does the use of set concentrations of antibiotics reproduce the complex pharmacokinetics observed in the bone and joint environment (263).

However, these observations support our hypothesis that a treatment approach combining a local administration, such as an intra-articular injection, of a broad-spectrum enzymatic cocktail and antibiotics could prove to be beneficial in a PJI setting where the variety of pathological bacterial species encountered is important (81). Further studies in more refined models such as animal PJI models should therefore be undertaken to confirm our in-vitro results and determine an adequate strategy around this approach in complement to DAIR.

5 Authors Contributions

HP designed and performed the experiments and data analysis, the other authors provided helpful suggestions regarding experiments' design or performance.
All authors contributed to the writing of the manuscript.

6 Funding

The experiments presented in this manuscript were funded by the *Région Wallonne* through a Win²Wal grant (Orthenzy; grant number 1810122) and the F.R.S.-FNRS (*Fonds de la Recherche Scientifique – FNRS)* (grants T.0189.16 and J.0162.19).
HP is the beneficiary of a FRIA (*Fonds pour la formation à la Recherche dans l'Industrie et dans l'Agriculture*) grant of the FRS-FNRS. FVB is a Research Director of the FRS-FNRS.

7 Conflicts of Interest

The authors declare that they have no affiliations or involvement with any entity with financial interests related to the content of this manuscript.

8 Acknowledgments

The authors would like to thank Mr. Alix Mangin for his technical help and OneLife SA for providing the tri-enzymatic cocktail for academic research purposes, and its R&D team for their intellectual contribution to the project.

9 Supplementary material

Table IV.1. Antibiotics experimental concentrations and rationales.

Antibiotic	Concentration (mg/L)	Rationale	References
Daptomycin (DAP)	30	$\frac{AUC_{0-24h}}{24h}$	(446, 447)
Doxycycline (DOX)	1.5	$\frac{AUC_{0-24h}}{24h}$	(448)
Linezolid (LZD)	5	C_{min}	(449)
Moxifloxacin (MXF)	1.5	$\frac{AUC_{0-24h}}{24h}$	(450)
Rifampin (RIF)	2.5	$\frac{AUC_{0-24h}}{24h}$	(451)
Vancomycin (VAN)	20	Target trough concentration (20 mg/L)	(59, 452)
Ceftazidime (CEF)	3.8	C_{min}	(453, 454)
Ciprofloxacin (CIP)	1.625	$\frac{AUC_{0-24h}}{24h}$	(455)
Colistin (CST)	2.5	$\frac{AUC_{0-24h}}{24h}$	(456)
Meropenem (MEM)	0.25	C_{min}	(457)

Table IV.2. ATCC 33591 (MRSA). Log_{10} CFU counts. Tukey HSD results.

Comparisons	Differences	95% confidence intervals		Adjusted p values	
		Lower	Upper		
CDD:T0-Control:T0	-2.04	-3.25	-0.83	0.00004	****
Control:TGN-Control:T0	0.67	-0.54	1.88	0.78924	NS
CDD:TGN-Control:T0	0.56	-0.65	1.77	0.93022	NS
Control:VAN 20-Control:T0	0.90	-0.40	2.21	0.46604	NS
CDD:VAN 20-Control:T0	-3.32	-4.63	-2.02	0.00000	****
Control:RIF 2.5-Control:T0	-1.59	-2.89	-0.28	0.00620	**
CDD:RIF 2.5-Control:T0	-3.42	-4.73	-2.12	0.00000	****
Control:LIN 5-Control:T0	-1.50	-2.81	-0.20	0.01196	*
CDD:LIN 5-Control:T0	-4.02	-5.32	-2.71	0.00000	****
Control:MXF 1.5-Control:T0	-0.31	-1.62	0.99	0.99992	NS
CDD:MXF 1.5-Control:T0	-4.18	-5.48	-2.87	0.00000	****
Control:DAP 30-Control:T0	-4.99	-6.30	-3.69	0.00000	****
CDD:DAP 30-Control:T0	-6.05	-7.36	-4.75	0.00000	****
CDD:TGN-Control:TGN	-0.11	-1.32	1.10	1.00000	NS
CDD:VAN 20-Control:VAN 20	-4.22	-5.62	-2.83	0.00000	****
CDD:RIF 2.5-Control:RIF 2.5	-1.83	-3.23	-0.44	0.00223	**
CDD:LIN 5-Control:LIN 5	-2.51	-3.91	-1.12	0.00001	****
CDD:MXF 1.5-Control:MXF 1.5	-3.87	-5.26	-2.47	0.00000	****
CDD:DAP 30-Control:DAP 30	-1.06	-2.45	0.34	0.31803	NS

Table IV.3. ATCC 33591 (MRSA). Biomass assay (% of T0 control). Tukey HSD results

Comparisons	Differences	95% Confidence Intervals		Adjusted p values	
		Lower	Upper		
CDD:T0-Control:T0	-95.2	-113.7	-76.6	0	****
Control:TGN-Control:T0	24.4	5.9	43.0	0.00213	***
CDD:TGN-Control:T0	5.3	-13.3	23.9	0.99933	NS
Control:VAN 20-Control:T0	22.2	2.2	42.3	0.01804	*
CDD:VAN 20-Control:T0	-89.6	-109.7	-69.5	0	****
Control:RIF 2.5-Control:T0	7.8	-12.3	27.8	0.98545	NS
CDD:RIF 2.5-Control:T0	-88.6	-108.6	-68.5	0.00000	****
Control:LIN 5-Control:T0	13.3	-6.8	33.4	0.53801	NS
CDD:LIN 5-Control:T0	-95.4	-115.5	-75.4	0.00000	****
Control:MXF 1.5-Control:T0	21.8	1.7	41.8	0.02281	*
CDD:MXF 1.5-Control:T0	-85.8	-105.9	-65.7	0.00000	****
Control:DAP 30-Control:T0	-20.2	-38.8	-1.6	0.02187	*
CDD:DAP 30-Control:T0	-87.7	-106.3	-69.1	0.00000	****
CDD:TGN-Control:TGN	-19.1	-37.7	-0.5	0.03864	*
CDD:VAN 20-Control:VAN 20	-111.8	-133.3	-90.4	0	****
CDD:RIF 2.5-Control:RIF 2.5	-96.3	-117.8	-74.9	0	****
CDD:LIN 5-Control:LIN 5	-108.8	-130.2	-87.3	0	****
CDD:MXF 1.5-Control:MXF 1.5	-107.5	-129.0	-86.1	0	****
CDD:DAP 30-Control:DAP 30	-67.5	-86.0	-48.9	0	****

Table IV.4. ATCC 35984 (MRSE). Log_{10} CFU counts. Tukey HSD results.

Comparisons	Differences	95% confidence intervals		Adjusted p values	
		Lower	Upper		
CDD:T0-Control:T0	-2.54	-3.85	-1.24	0.00000	****
Control:TGN-Control:T0	0.59	-0.72	1.89	0.95620	NS
CDD:TGN-Control:T0	1.16	-0.15	2.46	0.13330	NS
Control:VAN 20-Control:T0	1.84	0.54	3.15	0.00071	***
CDD:VAN 20-Control:T0	-5.00	-6.30	-3.69	0.00000	****
Control:RIF 2.5-Control:T0	-3.39	-4.69	-2.08	0.00000	****
CDD:RIF 2.5-Control:T0	-6.10	-7.41	-4.80	0.00000	****
Control:LIN 5-Control:T0	-0.62	-1.92	0.69	0.93571	NS
CDD:LIN 5-Control:T0	-3.39	-4.69	-2.08	0.00000	****
Control:MXF 1.5-Control:T0	-2.52	-3.83	-1.22	0.00000	****
CDD:MXF 1.5-Control:T0	-5.09	-6.40	-3.79	0.00000	****
Control:DAP 30-Control:T0	-3.50	-4.80	-2.19	0.00000	****
CDD:DAP 30-Control:T0	-5.45	-6.75	-4.15	0.00000	****
Control:DOX 1.5-Control:T0	-1.06	-2.37	0.24	0.22905	NS
CDD:DOX 1.5-Control:T0	-4.00	-5.30	-2.69	0.00000	****
CDD:TGN-Control:TGN	0.57	-0.74	1.87	0.96787	NS
CDD:VAN 20-Control:VAN 20	-6.84	-8.14	-5.53	0.00000	****
CDD:RIF 2.5-Control:RIF 2.5	-2.72	-4.02	-1.41	0.00000	****
CDD:LIN 5-Control:LIN 5	-2.77	-4.07	-1.46	0.00000	****
CDD:MXF 1.5-Control:MXF 1.5	-2.57	-3.87	-1.26	0.00000	****
CDD:DAP 30-Control:DAP 30	-1.95	-3.26	-0.65	0.00028	***
CDD:DOX 1.5-Control:DOX 1.5	-2.93	-4.24	-1.63	0.00000	****

Table IV.5. ATCC 35984 (MRSE). Biomass assay (% of T0 control). Tukey HSD results.

Comparisons	Differences	95% confidence intervals		Adjusted p values	
		Lower	Upper		
CDD:T0-Control:T0	-88.5	-118.3	-58.8	0.00000	****
Control:TGN-Control:T0	23.4	-6.3	53.1	0.27459	NS
CDD:TGN-Control:T0	-11.3	-41.0	18.4	0.99056	NS
Control:VAN 20-Control:T0	15.9	-13.8	45.6	0.84551	NS
CDD:VAN 20-Control:T0	-81.6	-111.3	-51.9	0.00000	****
Control:RIF 2.5-Control:T0	4.7	-25.0	34.4	1.00000	NS
CDD:RIF 2.5-Control:T0	-82.7	-112.4	-52.9	0.00000	****
Control:LIN 5-Control:T0	2.3	-27.4	32.0	1.00000	NS
CDD:LIN 5-Control:T0	-77.9	-107.6	-48.2	0.00000	****
Control:MXF 1.5-Control:T0	5.2	-24.5	34.9	1.00000	NS
CDD:MXF 1.5-Control:T0	-78.1	-107.8	-48.4	0.00000	****
Control:DAP 30-Control:T0	21.2	-8.5	50.9	0.42780	NS
CDD:DAP 30-Control:T0	-84.0	-113.7	-54.3	0.00000	****
Control:DOX 1.5-Control:T0	3.3	-26.4	33.0	1.00000	NS
CDD:DOX 1.5-Control:T0	-85.2	-114.9	-55.5	0.00000	****
CDD:TGN-Control:TGN	-34.7	-64.4	-5.0	0.00965	**
CDD:VAN 20-Control:VAN 20	-97.5	-127.2	-67.8	0.00000	****
CDD:RIF 2.5-Control:RIF 2.5	-87.3	-117.0	-57.6	0.00000	****
CDD:LIN 5-Control:LIN 5	-80.3	-110.0	-50.6	0.00000	****
CDD:MXF 1.5-Control:MXF 1.5	-83.2	-112.9	-53.5	0.00000	****
CDD:DAP 30-Control:DAP 30	-105.2	-134.9	-75.5	0.00000	****
CDD:DOX 1.5-Control:DOX 1.5	-88.6	-118.3	-58.9	0.00000	****

Table IV.6. ATCC 47076 (E. coli). Log_{10} CFU counts. Tukey HSD results.

Comparisons	Differences	95% confidence intervals		Adjusted p values	
		Lower	Upper		
CDD:T0-Control:T0	-1.24	-2.40	-0.08	0.02515	*
Control:TGN-Control:T0	-0.10	-1.26	1.06	1.00000	NS
CDD:TGN-Control:T0	-0.33	-1.49	0.83	0.99942	NS
Control:CEF 3.8-Control:T0	-2.06	-3.31	-0.81	0.00004	****
CDD:CEF 3.8-Control:T0	-7.29	-8.54	-6.04	0.00000	****
Control:CEF 42-Control:T0	-7.05	-8.21	-5.89	0.00000	****
CDD:CEF 42-Control:T0	-7.29	-8.45	-6.14	0.00000	****
Control:CIP 1.625-Control:T0	-3.21	-4.36	-2.05	0.00000	****
CDD:CIP 1.625-Control:T0	-7.19	-8.35	-6.03	0.00000	****
Control:CST 2.5-Control:T0	-1.23	-2.48	0.02	0.05593	NS
CDD:CST 2.5-Control:T0	-6.80	-8.05	-5.55	0.00000	****
Control:MER 0.25-Control:T0	-1.21	-2.46	0.03	0.06433	NS
CDD:MER 0.25-Control:T0	-7.33	-8.58	-6.08	0.00000	****
Control:MER 6.25-Control:T0	-6.81	-7.97	-5.65	0.00000	****
CDD:MER 6.25-Control:T0	-7.27	-8.43	-6.11	0.00000	****
CDD:TGN-Control:TGN	-0.23	-1.39	0.93	0.99999	NS
CDD:CEF 3.8-Control:CEF 3.8	-5.23	-6.56	-3.89	0.00000	****
CDD:CEF 42-Control:CEF 42	-0.24	-1.40	0.92	0.99999	NS
CDD:CIP 1.625-Control:CIP 1.625	-3.98	-5.14	-2.83	0.00000	****
CDD:CST 2.5-Control:CST 2.5	-5.57	-6.90	-4.23	0.00000	****
CDD:MER 0.25-Control:MER 0.25	-6.11	-7.45	-4.78	0.00000	****
CDD:MER 6.25-Control:MER 6.25	-0.46	-1.62	0.70	0.98238	NS

Table IV.7. ATCC 47076 (E. coli). Biomass assay (% of T0 control). Tukey HSD results.

Comparisons	Differences	95% confidence intervals		Adjusted p values	
		Lower	Upper		
CDD:T0-Control:T0	-80.3	-126.2	-34.3	0.00001	****
Control:TGN-Control:T0	16.1	-29.8	62.0	0.99498	NS
CDD:TGN-Control:T0	13.5	-32.4	59.4	0.99924	NS
Control:CEF 3.8-Control:T0	-61.7	-111.3	-12.1	0.00415	**
CDD:CEF 3.8-Control:T0	-99.1	-148.7	-49.5	0.00000	****
Control:CEF 42-Control:T0	-86.0	-131.9	-40.1	0.00000	****
CDD:CEF 42-Control:T0	-92.5	-138.5	-46.6	0.00000	****
Control:CIP 1.625-Control:T0	-48.3	-94.3	-2.4	0.03043	*
CDD:CIP 1.625-Control:T0	-97.3	-143.2	-51.4	0.00000	****
Control:CST 2.5-Control:T0	-24.6	-70.5	21.4	0.84212	NS
CDD:CST 2.5-Control:T0	-84.9	-130.8	-38.9	0.00000	****
Control:MER 0.25-Control:T0	4.8	-44.8	54.4	1.00000	NS
CDD:MER 0.25-Control:T0	-93.4	-143.0	-43.8	0.00000	****
Control:MER 6.25-Control:T0	-82.9	-128.9	-37.0	0.00001	****
CDD:MER 6.25-Control:T0	-93.8	-139.7	-47.8	0.00000	****
CDD:TGN-Control:TGN	-2.6	-48.5	43.3	1.00000	NS
CDD:CEF 3.8-Control:CEF 3.8	-37.4	-90.4	15.7	0.45113	NS
CDD:CEF 42-Control:CEF 42	-6.6	-52.5	39.4	1.00000	NS
CDD:CIP 1.625-Control:CIP 1.625	-49.0	-94.9	-3.0	0.02665	*
CDD:CST 2.5-Control:CST 2.5	-60.3	-106.2	-14.4	0.00194	**
CDD:MER 0.25-Control:MER 0.25	-98.2	-151.2	-45.2	0.00000	****
CDD:MER 6.25-Control:MER 6.25	-10.8	-56.7	35.1	0.99995	NS

Table IV.8. ATCC 33591 (MRSA). Two-way ANOVA results using the log_{10} CFU counts as the criterion

Predictor	Sum of Squares	df	Mean Square	F	p	partial η^2	partial η^2 90% CI [LL, UL]
(Intercept)	1449.57	1	1449.57	8707.75	.000		
CDD exposure	59.28	1	59.28	356.11	.000	.92	[.86, .94]
Antibiotics exposure	147.16	6	24.53	147.34	.000	.97	[.93, .97]
CDD exposure x Antibiotics exposure	21.22	6	3.54	21.25	.000	.80	[.63, .83]
Error	5.33	32	0.17				

Note. LL and UL represent the lower-limit and upper-limit of the partial η^2 confidence interval, respectively.

Table IV.9. ATCC 33591 (MRSA). Two-way ANOVA results using the biomass (% of T0 control) as the criterion

Predictor	Sum of Squares	df	Mean Square	F	p	partial η^2	partial η^2 90% CI [LL, UL]
(Intercept)	212225.00	1	212225.00	5587.20	.000		
CDD exposure	90525.70	1	90525.70	2383.25	.000	.99	[.98, .99]
Antibiotics exposure	24406.45	6	4067.74	107.09	.000	.95	[.91, .96]
CDD exposure x Antibiotics exposure	13014.65	6	2169.11	57.11	.000	.91	[.83, .92]
Error	1291.46	34	37.98				

Note. LL and UL represent the lower-limit and upper-limit of the partial η^2 confidence interval, respectively.

Table IV.10. ATCC 35984 (MRSE). Two-way ANOVA results using the log_{10} CFU counts as the criterion

Predictor	Sum of Squares	df	Mean Square	F	p	partial η^2	partial η^2 90% CI [LL, UL]
(Intercept)	661.86	1	661.86	3992.47	.000		
CDD exposure	88.73	1	88.73	535.24	.000	.94	[.91, .96]
Antibiotics exposure	147.56	7	21.08	127.16	.000	.97	[.93, .97]
CDD exposure x Antibiotics exposure	42.68	7	6.10	36.78	.000	.89	[.78, .90]
Error	5.30	32	0.17				

Note. LL and UL represent the lower-limit and upper-limit of the partial η^2 confidence interval, respectively.

Table IV.11. ATCC 35984 (MRSE). Two-way ANOVA results using the biomass (% of T0 control) as the criterion

Predictor	Sum of Squares	df	Mean Square	F	p	partial η^2	partial η^2 90% CI [LL, UL]
(Intercept)	221395.68	1	221395.68	2275.06	.000		
CDD exposure	83023.52	1	83023.52	853.15	.000	.96	[.94, .97]
Antibiotics exposure	10680.41	7	1525.77	15.68	.000	.77	[.57, .81]
CDD exposure x Antibiotics exposure	4683.78	7	669.11	6.88	.000	.60	[.30, .65]
Error	3114.06	32	97.31				

Note. LL and UL represent the lower-limit and upper-limit of the partial η^2 confidence interval, respectively.

Table IV.12. ATCC 47076 (E. coli). Two-way ANOVA results using the log_{10} CFU counts as the criterion

Predictor	Sum of Squares	df	Mean Square	F	p	partial η^2	partial η^2 90% CI [LL, UL]
(Intercept)	801.94	1	801.94	3518.29	.000		
CDD exposure	142.93	1	142.93	627.07	.000	.95	[.92, .97]
Antibiotics exposure	178.80	5	35.76	156.89	.000	.96	[.93, .97]
CDD exposure x Antibiotics exposure	53.17	5	10.63	46.65	.000	.89	[.78, .91]
Error	6.84	30	0.23				

Note. LL and UL represent the lower-limit and upper-limit of the partial η^2 confidence interval, respectively.

Table IV.13. ATCC 47076 (E. coli). Two-way ANOVA results using the biomass (% of T0 control) as the criterion

Predictor	Sum of Squares	df	Mean Square	F	p	partial η^2	partial η^2 90% CI [LL, UL]
(Intercept)	127753.01	1	127753.01	355.84	.000		
CDD exposure	33719.94	1	33719.94	93.92	.000	.75	[.59, .81]
Antibiotics exposure	47008.62	5	9401.72	26.19	.000	.80	[.64, .84]
CDD exposure x Antibiotics exposure	8678.67	5	1735.73	4.83	.002	.43	[.12, .52]
Error	11488.71	32	359.02				

Note. LL and UL represent the lower-limit and upper-limit of the partial η^2 confidence interval, respectively.

Chapter V: *in-vivo* study of the association of DAIR and enzymes

Innovative in-vivo model of PJI treated with DAIR and application to a pilot study of an enzymatic adjuvant treatment.

Authors: Hervé Poilvache, MD [a, b, c]; Françoise Van Bambeke, PharmD, PhD [b]; Olivier Cornu, MD, PhD [a, b]

Affiliations :

[a] Université catholique de Louvain, Institut de Recherche Expérimentale et Clinique, Neuromusculoskeletal Laboratory, Brussels, Belgium

[b] Université catholique de Louvain, Louvain Drug Research Institute, Pharmacologie cellulaire et moléculaire, Brussels, Belgium

[c] Cliniques Universitaires Saint-Luc, Orthopedic Surgery Department, Brussels, Belgium

In preparation.

Abstract:

Introduction: Periprosthetic joint infections (PJI) are catastrophic complications of joint replacement. Debridement, implant retention, and antibiotic therapy (DAIR) is the usual strategy in acute infections but fails in 45% of MRSA infections. We describe a model of infected arthroplasty in rabbits, treated with debridement and a clinically-relevant course of vancomycin, and apply it to the study of a promising enzymatic adjuvant treatment (TEC).

Methods: 20 rabbits were assigned to groups: vancomycin pharmacokinetics (A), infection (B), DAIR (C), DAIR with TEC (D). All groups received a tibial arthroplasty using a Ti-6Al-4V implant. Groups B, C, and D were infected per-operatively with a 5.5 $\log_{10}$ MRSA inoculum. After one week, groups C and D knees were debrided, and group D received 3ml of TEC intra-articularly. Groups A, C, and D received one week of vancomycin. Pharmacokinetic profiles were obtained in group A following 1st and 5th injections. Animals were euthanized two weeks after the arthroplasty. Implants and tissue samples were processed for bacterial counts and histology.

Results: Average vancomycin $AUC_{0\text{-}12}$ were 213.0mg*h/L (1st injection) and 207.8mg*h/L (5th injection), reaching clinical targets. All inoculated animals were infected. CFUs were reproducible in groups B. A sharp decrease was observed in groups C and D. Serum markers, and leukocyte counts increased significantly in infected groups. TEC did not significantly reduce the CFU counts.

Conclusion: We developed a reproducible model of PJI treated with DAIR, using vancomycin at clinically-relevant concentrations. TEC did not prove to be effective in this model, and its formulation requires improvements.

Keywords: Prosthetic Joint Infection, *in-vivo*, *Staphylococcus aureus*, DAIR, vancomycin, pharmacokinetics, enzymes

1 Introduction

Prosthetic Joint Infections (PJIs) are a catastrophic complication of joint replacement surgery (13) and are one of the leading causes of failure following hip and knee replacement (458, 459). PJIs and their treatments generate significant morbidity (11) and mortality (12) in affected patients and represent a substantial burden to healthcare systems (20, 22, 23).

PJIs are caused by a variety of pathogens. *Staphylococcus aureus* is the most frequently isolated species (87, 403). Among these, Methicillin-Resistant *S. aureus* (MRSA) strains represent 12.8% to 48.1% of isolates, with important variations between countries (81). MRSA strains are of particular concern in the setting of PJIs as these strains are highly prevalent in acute infections (64) and are a significant risk factor for treatment failure following debridement surgery, implant retention, and antibiotic therapy (DAIR) (93). DAIR is usually favored in acute infection cases – occurring less than four weeks after the index surgery – as it is a less invasive procedure with superior functional outcomes compared to staged implant replacement (41, 460). However, patients suffering from an MRSA PJI suffered from a 45% failure rate in a large multi-centric study (93).

This high failure rate is multifactorial but is in part due to the propensity of *S. aureus* to attach to surfaces or aggregate and form biofilms (461). Biofilms are bacterial communities embedded in a complex self-produced extracellular matrix that isolates them from their environment (15). Bacteria in biofilms tolerate antibiotic concentrations up to 1000-fold higher than planktonic bacteria (19) and can evade the host's immune system (94), leading to chronic infections.

Consequently, the development of biofilm targeting therapies with a potential application in orthopedics is of particular interest (310). Multiple strategies and therapeutic agents have been described, including quorum sensing inhibitors (462), antibacterial peptides (353), physical disruption of biofilm (360), and enzymatic digestion of the extracellular matrix (463). We recently reported promising *in-vitro* results using a broad-spectrum tri-enzymatic cocktail (TEC) in combination with multiple classes of antibiotics against MRSA, MRSE, and *E. coli* biofilms (464), leading us to design a clinically relevant PJI *in-vivo* model adequate for testing innovative therapeutic strategies in the setting of DAIR strategies.

Multiple *in-vivo* models have been proposed in the literature to study PJI and its treatment. These vary in complexity but, for the most part, poorly reproduce the periprosthetic environment, limiting their clinical relevancy ((265) for review).

The objective of this study is the development of a clinically relevant model of knee arthroplasty in New-Zealand White (NZW) rabbits, using Ti-6Al-4V 3D printed unicompartmental tibial implants infected with an MRSA reference strain. The development of this model integrates the study of vancomycin pharmacokinetics in NZW rabbits to reproduce the clinical targets used in the treatment of *S. aureus* infections. The impact of DAIR on the bacterial load of the implant and relevant tissues, inflammatory markers, and histological appearance of joint tissues were compared to control animals and animals treated with DAIR and an adjuvant local injection of TEC.

2 Methods

2.1 **Study design**

In-vivo experiments were performed following the approval of the protocols by the local ethics committee [2019/UCL/MD/041]. 20 female New-Zealand White (NZW) rabbits were assigned to 4 groups in a non-blinded way: group A: vancomycin pharmacokinetics, group B: infection, group C: DAIR treatment, group D: TEC treatment (figure V.1). All animals benefitted from a minimum of 7 days of acclimatization period during which no treatment was performed. After the acclimatization period, a uni-compartmental tibial arthroplasty was performed in all groups with a custom-designed Ti-6Al-4V implant. The joints of the animals from groups B, C, and D were inoculated with 6 $\log_{10}$ CFU of MRSA strain ATCC 33591. After 7 days, the infected joints of the animals of groups C and D were surgically debrided and the animals from group D received an intra-articular injection of the TEC enzyme cocktail at the end of the procedure. Animals of groups A, C, and D received IV injections of 50mg/kg of vancomycin twice a day 7 days after the initial surgery (group A) or immediately after the debridement procedure (groups C and D). In group A animals, pharmacokinetic profiles of serum vancomycin were performed following the 1^{st} and 5^{th} injections. Blood samples were obtained every two days for total leucocyte counts, differential leukocyte counts, serum CRP and procalcitonin concentrations measurements, and serum vancomycin monitoring (groups C and D). All animals were sacrificed 14 days after the initial surgery. The implants and samples from the joint tissues were processed for microbiological assessment and histology.

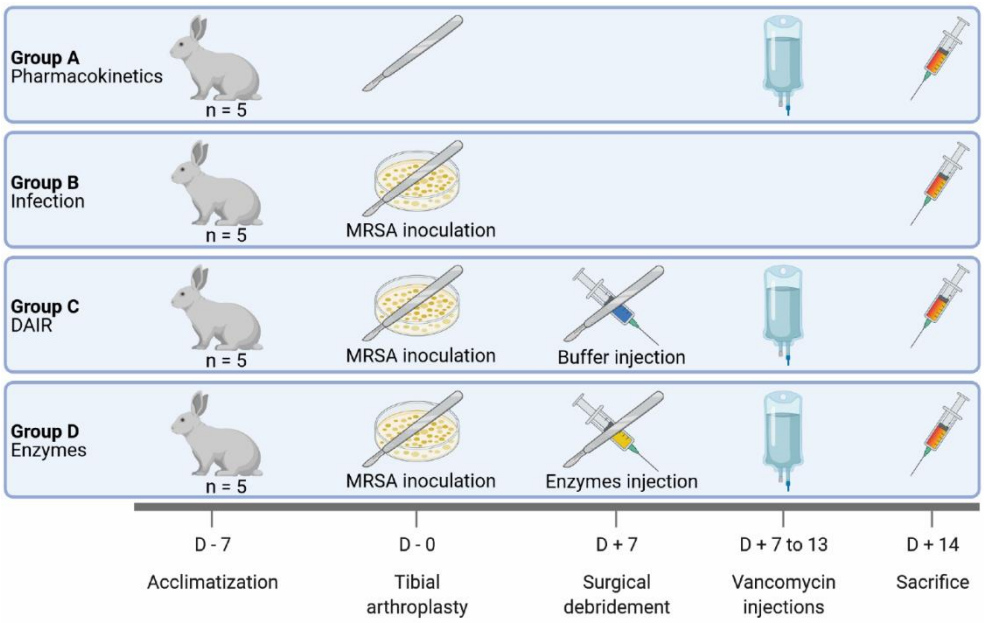


Figure V.1. Experimental design. The animals were assigned to four groups of 5 animals each. Group A animals were used to confirm the validity of the implants designs and to assay the pharmacokinetics of vancomycin; Group B animals were used to validate the bacterial inoculum; Group C animals were infected and treated with a surgical debridement followed by the intra-articular injection of Tris-HCl buffer and a one week course of IV vancomycin; Group D animals were infected and treated with a surgical debridement followed by the intra-articular injection of the TEC enzymatic cocktail and a one week course of IV vancomycin.

2.2 **Animals**

20 specific pathogens-free female NZW rabbits weighing 3.0 to 3.5 kg were obtained from CER Groupe (Marloie, Belgium). The animals were held in a level 2 biosafety room, with controlled temperature and hygrometry and

automated lightning set to a 12h/12h regimen. The animals were kept in cages with a ground surface of 6625cm² and a height of 51cm, equipped with a raised platform and a shelter, alone or in pairs. The cages' floors were covered with wood chippings and cleaned daily. The animals were watered *ad libitum* with fresh water and were fed *ad libitum* with hay and rabbit-specific pellets. The environment was further enriched with wooden toys. All animals acclimated for a minimum of 7 days before the experiments.

2.3 **Bacteria**

The Methicillin-Resistant *Staphylococcus aureus* strain ATCC 33591 was used. The MIC (1 µg/ml) and MBEC (>1024 µg/ml) for vancomycin were determined previously (464). Bacteria were grown overnight on tryptic soy agar (TSA) plates from frozen stock. Some colonies were then suspended in sterile PBS, adjusted to an OD_{620nm} of 0.5 (~8 $\log_{10}$ CFU), and diluted 1:10 in PBS. The bacterial suspension was stored at 4°C until inoculation (1.5-2h). Serial dilutions of the bacterial inoculum were plated on TSA to confirm the bacterial inoculum.

2.4 **Antibiotics and enzyme cocktail**

Vancomycin powder for injection (Mylan bvba, Hoeilaart, Belgium) was reconstituted with 0.9% saline (Baxter SA, Lessines, Belgium) at a 50 mg/ml concentration. The TEC enzymatic cocktail (patents WO2017/211737 and BE2020/5726) was provided as a sterile aqueous solution by OneLife SA (Louvain-la-Neuve, Belgium) containing 400 U/ml of an aspecific DNA/RNA endonuclease from *Serratia marcescens* (c-Lecta, Leipzig, Germany), 50 U/ml of an endo-1,4-β-D-glucanase from *Aspergillus niger* (Sigma-Aldrich, Saint Louis, MO, USA) and 2.6 U/ml of a β-*N*-

acetylhexosaminidase from *Actinobacillus pleuropneumoniae* (Novozymes, Bagsværd, Denmark) suspended in a pH 7.0 20 mM Tris-HCl solution.

2.5 **Implant Design**

Uni-compartmental tibial implants were designed using Fusion 360 (Autodesk, Ca, USA) following the dissection of the knees 4 NZW rabbits carcasses provided by CER Groupe (Marloie, Belgium). The final implant design and specific instruments were 3D printed in Ti-6Al-4V by Materialise NV (Leuven, Belgium) (figure V.2).

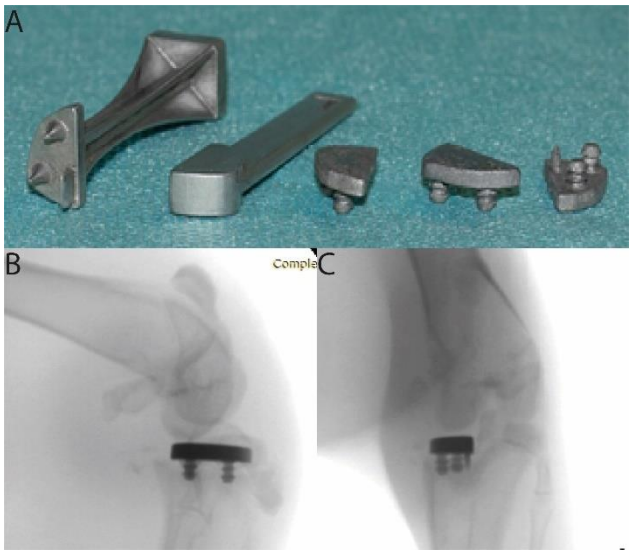


Figure V.2. Panel A: Ti-6Al-4V implants (right) and instruments (left). Panels B and C: Post-mortem radiographs showing the position of the implant in AP (B) and lateral (C) views.

2.6 **Surgical procedure**

2.6.1 **Anesthesia and analgesia**

General anesthesia was obtained by the intramuscular injection of 35 mg/kg of ketamine (Nimatek, Dechra Pharmaceuticals PLC, Northwich, United Kingdom), 5mg/kg of xylazine (Rompun, Bayer AG, Leverkusen, Germany), and 0.1 mg/kg of butorphanol (Dolorex, MSD Animal Health, Kenilworth, NJ, USA). Anesthesia was confirmed by the loss of muscle tone and the absence of corneal reflex. The cornea was protected by the application of an ocular gel (Ocugel, URSAPHARM GmbH, Saarbrücken, Germany). The rabbits received an IV perfusion of 800mg of paracetamol (Fresenius Kabi, Bad Homburg vor der Höhe, Germany) during the surgery. 12.5µg/h transdermal fentanyl patches (Durogesic, Janssen-Cilag NV, Beerse, Belgium) were applied immediately after the surgery for postoperative analgesic treatment.

2.6.2 **Arthroplasty**

The hairs of the operated leg were trimmed on the eve of the surgery. Following general anesthesia, the animals were installed in a Class II biosafety cabinet. The operated leg was disinfected twice with 2% chlorhexidine gluconate alcohol solution (Qualiphar, Bornem, Belgium) and the leg was draped. The joint was approached through a medial parapatellar incision. The medial meniscus was resected and 5mm of the medial tibial plateau was removed using a high-speed burr. The cut height was confirmed using a spacer block. The bone surface was then further prepared using a custom tibial punch. After irrigation of the joint space with sterile saline, the final implants were impacted. The joint was then further irrigated with sterile

saline. The joint capsule, subcutaneous tissues, and skin were closed separately with running sutures using a 3/0 polyester thread. The joints of groups B, C, and D animals were inoculated by intra-articular injection of 100 µl of a $10^{6.5}$ CFU/ml MRSA suspension after the closure of the subcutaneous tissues. The wounds were then covered using an antiseptic spray and dressed.

2.6.3 **Debridement**

Animals of groups C and D were operated on one week after the initial surgery. Following anesthesia, the operated leg was disinfected twice with 2 % chlorhexidine gluconate alcohol solution and the leg was draped. The initial approach was re-used. Pus samples were collected immediately after the capsule was breached and stored on ice until analyzed. The joint was then thoroughly debrided, a synovectomy was performed and the joint space was irrigated with 200ml of sterile saline using a 50ml syringe. The wound closure was performed in a similar way to the first surgery. Following skin closure, 3ml of either 20mM pH 7.0 Tris-HCl buffer (identical to the TEC buffer) or TEC cocktail was injected in the joint space, and a dressing similar to the first surgery was applied.

2.6.4 **Post-operative follow-up (incl. blood sampling & weight)**

The pain level of the animals was monitored daily using the rabbit grimace scale (465). To further assess the wellbeing of the animals, the rabbits were weighed twice a week.

Blood samples were obtained every two days by venipuncture of the marginal ear veins to assess the evolution of the total leucocyte count, differential leukocyte count, c-reactive protein (CRP) serum levels, procalcitonin serum

levels, and serum vancomycin levels if applicable. Samples were collected in either K3 EDTA tubes or gel and clot activator tubes (Vacutest Kima s.r.l., Arzergrande, Italy). Samples collected in K3 EDTA tubes were stored at 4°C before analysis. Samples collected in gel and clot activator tubes were kept at room temperature until complete coagulation and were then centrifuged at 2000g for 10 minutes at 20°C. The serum was then collected and stored at -80°C before analysis.

2.6.5 **Vancomycin treatment and pharmacokinetics**

Vancomycin injections were initiated one week after surgery in group A, and immediately after the debridement procedure in groups C and D. The animals of these three groups received 50 mg/kg of vancomycin by intra-venous injections through a catheter every 12h for 7 days. This dosage was chosen following a literature review and its adequacy to attain therapeutic concentrations. Blood samples were obtained in group A animals before injection, and 1h, 2h, 4h, 6h, 10h, and 12h after the 1^{st} and 5^{th} doses to study the vancomycin serum concentration kinetics and confirm the adequacy of this regimen. Based on these results, the vancomycin serum concentrations in groups C and D were monitored every two days 6h after injection.

2.6.6 **Euthanasia**

All animals were euthanized two weeks after the initial surgery by an intravenous injection of 100mg/kg of sodium pentobarbital (Dolethal, Vetoquinol, Magny-Vernois, France). The death of the animals was confirmed by cardiac auscultation. Following the euthanasia, the animals were installed in a Class II biosafety cabinet, the skin of the operated leg was disinfected twice with 2% chlorhexidine digluconate alcohol solution and the

limb was draped. The knee was dissected in aseptic conditions. Pus, articular capsule, tibial bone, and the implant were sampled for microbiological analysis using clean instruments, rinsed in sterile PBS (except pus), fragmented with clean instruments (bone and capsule), transferred to sterile tared tubes containing five 5 mm steel beads (bone and capsule), and kept on ice before analysis. The anterior half of the tibial epiphysis and metaphysis were cut and were fixated in 4% buffered formaldehyde (VWR Chemicals, Radnor, PA, USA) for histological analysis.

2.7 **Colony-Forming Units counts**

Bone and capsule samples were weighted, 3ml of sterile PBS was added to the tubes and then homogenized by shaking for 15 minutes using a TissueLyser II device (Qiagen, Hilden, Germany). The tubes containing the implants were filled with 2ml of sterile PBS, vortexed for 30 seconds, sonicated for 5 minutes (Branson 5510 Ultrasonic bath, Emerson Electric, Saint-Louis, MO, USA), and vortexed for 30 seconds. The pus samples were weighted, then 3ml of sterile PBS was added to the tubes and the samples were vortexed for 1 minute. The recovered liquids from all samples were then serially diluted in sterile PBS and plated on TSA plates. The plates were incubated at 37°C for 7 days. Initial CFU counts were done after 48h. The plates were examined after 7 days to identify possible contaminations.

2.8 **Serum antibiotic dosing**

Vancomycin serum concentrations were quantified using the Roche VANC3 assay using a COBAS 8000 automated analyzer (Roche Diagnostics GmbH, Mannheim, Germany) on serum samples.

2.9 **Serum markers**

CRP serum concentrations were assayed using the ABCAM rabbit CRP ELISA kit (ab157726; ABCAM, Cambridge, United Kingdom) on serum samples diluted 2.000 to 4.000 times in the supplied dilution solution, following the manufacturer's instructions. Procalcitonin serum concentrations were assayed using the MyBioSource rabbit procalcitonin ELISA kit (MBS7606572; MyBioSource Inc., San Diego, CA, USA) on serum samples diluted 4 times in the supplied dilution solution, following the manufacturer's instructions. Creatinine serum concentrations were measured in group A animals using a Fuji Dri-Chem analyzer (Fujifilm Corporation, Tokyo, Japan) with CRE-PIII slides, as per the manufacturer's instructions.

2.10 **Blood cells count**

Manual counting methods were used for the leucocytes and differential counts. For leukocyte counts, blood samples collected in K3-EDTA tubes were diluted 20 times in Türk's solution (3% acetic acid, 0.01% crystal violet, in mQ water). After 5 minutes, 10 µl of the diluted samples were placed in an improved Neubauer cell count chamber (Paul Marienfeld GmbH & Co. KG, Lauda-Königshofen, Germany). The cells in 4 large squares were counted and averaged. Three separate counts were performed for each sample. For differential counts, blood films were done from K3-EDTA blood samples. After fixation in methanol, the blood films were stained using the May-Grünwald-Giemsa technique (466). White blood cells were counted at 100x magnification to determine the differential counts.

2.11 **Histology**

The tibial and femur samples were fixated in 4% buffered formaldehyde for one week. The samples were then decalcified in hydrochloric acid (DC3 decalcifier, VWR Chemicals) for one week and included in paraffin. 5µm sections were cut in a coronal plane using a Microm HM340 E microtome (Microm International GmbH, Walldorf, Germany) and mounted on SuperFrost Plus slides (Thermo Scientific, Waltham, MA, UA). Samples were stained with Masson's trichrome blue stain. The slides were then scanned at a 200x magnification using SCN400 (Leica Biosystems GmbH, Wetzlar, Germany) scanner and examined for the qualitative assessment of inflammatory infiltration, and cartilage alterations.

2.12 **Data transformation and statistical analysis**

CFU counts were transformed to base 10 logarithms and divided by the weight of the sample. The neutrophils over lymphocytes ratio was used to describe the differential counts. Hyperbolic interpolation was used to transform the raw ELISA results of serum CRP and procalcitonin assays. Vancomycin serum AUCs were computed using the trapezoid rule. The values reported in the text are the mean and the 95% CI (in brackets) or the median and the 95% CI obtained by bootstrapping (in brackets). The statistical analyses were done using GraphPad 8.0.1 (GraphPad Software Inc, San Diego, CA, USA) or R 3.6.2 (R Core Team, 2019).

3 Results

3.1 **Post-operative outcomes**

All animals survived until the end of the experiments without reaching the predefined humane endpoints. Pain levels remained acceptable following the surgery. No wound discharge or opening was observed. Progressive weight loss was observed in animals of all groups and was more severe in groups B, C, and D (supplementary material, figure V.1). No implant loosening was observed during either debridement procedures or dissections.

3.2 **Vancomycin pharmacokinetics and therapeutic monitoring**

The median $AUC_{0\text{-}12h}$ following the first vancomycin injection was 206.7 mg*h/L (figure V.3.A) [175.7; 212.9]. Following the fifth injection, the median $AUC_{0\text{-}12h}$ was 210.8 mg*h/L (figure V.3.B) [176.9; 260.4]. The comparison of the two $AUC_{0\text{-}12h}$ using the Wilcoxon signed-rank test showed no statistically significant difference (p= 0.81, figure V.3.C).

Serum creatinine concentrations in group A animals were found to be stable throughout the experiment, with no influence of either the surgery or the administration of vancomycin (supplementary material, figure V.2).

As the vancomycin serum concentrations approached 0 µg/mL 12h after the injections, therapeutic monitoring of group C and D animals was done 6h after the injections. The comparison of the 6h vancomycin serum concentrations of groups A, C, and D using the Kruskal-Wallis test showed no statistically significant differences (p=0.55, figure V.3.D).

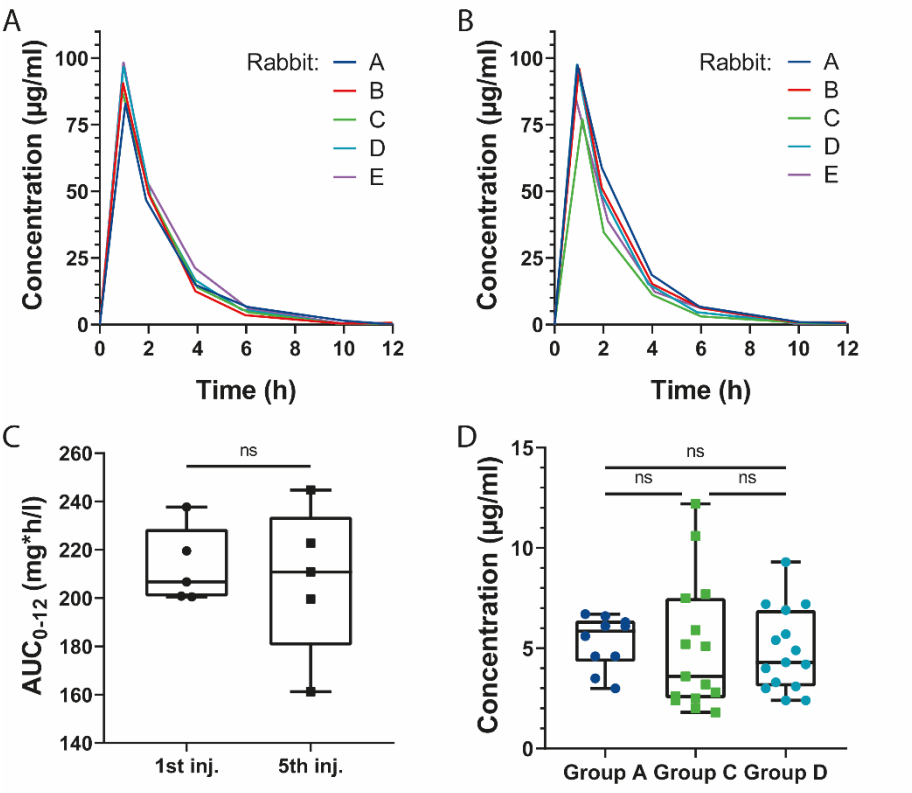


Figure V.3. Panels A and B: Serum concentration (mg/L) of vancomycin evolution following the first (A) and fifth (B) injections in group A rabbits. Panel C: Box plots of the $AUC_{0\text{-}12}$ after the first (left) and fifth (right) injections. $AUC_{0\text{-}12h}$ were computed using the trapezoidal method. $AUC_{0\text{-}12h}$ were compared with the Wilcoxon test. N = 5. Panel D: Box plots of the serum concentrations of vancomycin 6h after injection in groups A, C, and D. Concentrations were compared with the Kruskal-Wallis test followed by the Dunn test. N= 10 (group A), 15 (groups C and D).

3.3 **Microbiology**

CFU counts for all conditions are illustrated in figure V.4. No bacterial contamination of group A samples was observed, confirming the asepsis of the surgical procedures. The bacterial inoculums were similar in all groups. At the time of debridement, the CFU counts in the pus of groups C and D were identical. After euthanasia, we observed reproducible CFU counts in all samples of group B animals. Significant reductions in CFU counts were observed in bone, pus, and implant samples of group C compared to group B, albeit with more variability. No statistically significant reduction was observed in capsule samples despite a reduced average. A comparable reduction in CFU counts was observed in group D when compared to group B. The comparison of groups C and D does not reveal statistically significant differences or a clear trend favoring either treatment.

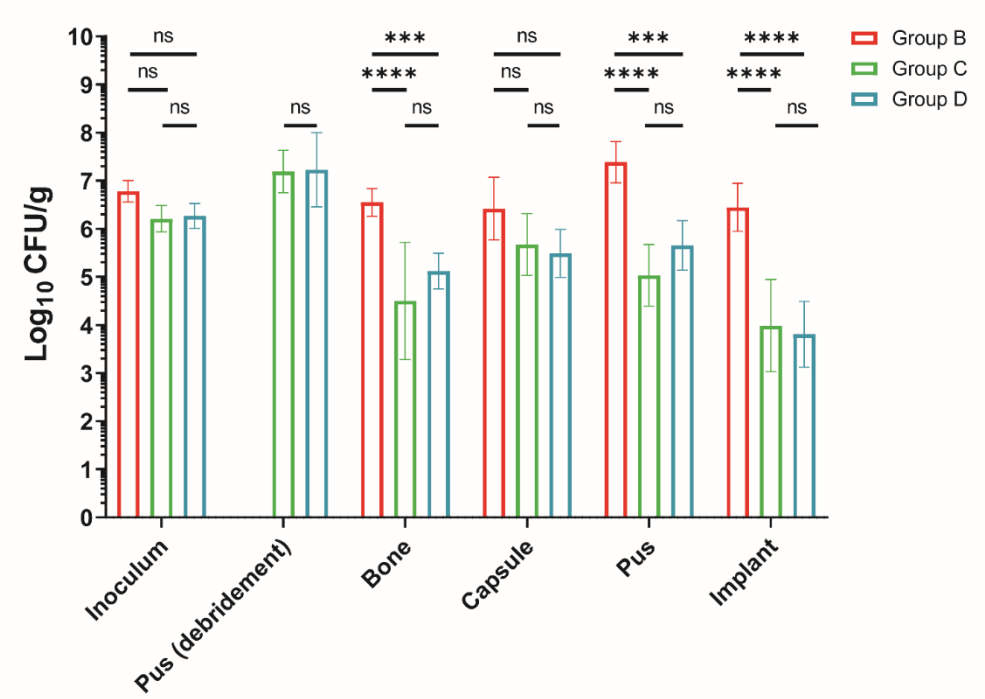


Figure V.4. Bacterial loads in the different samples for rabbits of groups B (blue), C (red), and D (green) and multiple comparisons. Statistical analysis: two-way ANOVA and Tukey HSD. ns: $p>0.05$; *: $p<0.05$; **: $p<0.01$; ***: $p<0.001$; ****: $p<0.0001$. N = 5.

3.4 Serum markers

CRP serum concentrations are illustrated in figure V.5 panel A (group A and B) and panel B (group C and D). Baseline CRP serum concentrations were found to be similar across the four groups. The CRP levels increased rapidly in infected animals and a statistically significant difference with group A animals was observed from day 2 (group B) or day 4 (groups C and D). The evolution of serum CRP concentrations of groups B, C, and D was similar until day 6 (group C) or 8 (group D). The CRP concentrations of group C and

D animals steadily decreased following the debridement surgery and were no longer found to be statistically different from group A animals after day 8 (group C) or day 10 (group D). No statistically significant differences were found between group C and D animals during the experiments.

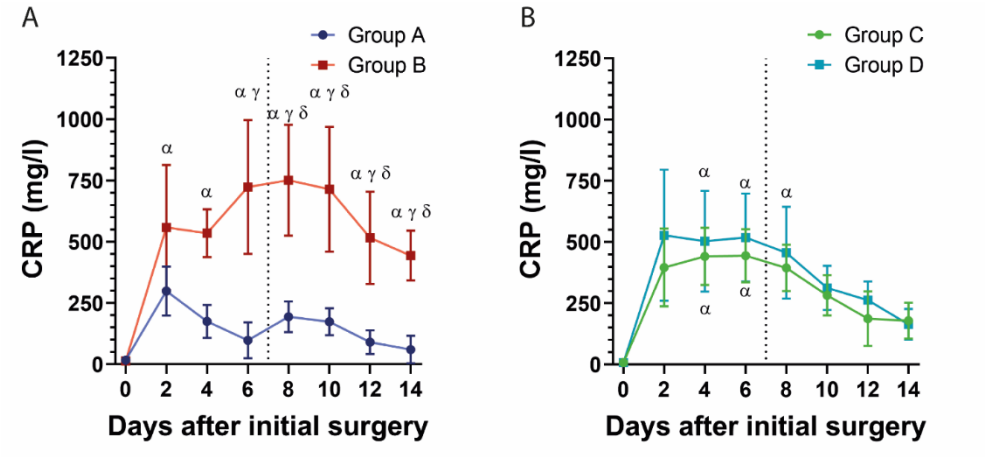


Figure V.5. Post-operative evolution of the serum C-reactive protein (mg/l) in groups A & B (panel A) and groups C & D (panel B). Vertical dashed lines indicate the day of debridement surgery. Statistical analysis: two-way repeated-measures ANOVA and Tukey HSD post-hoc test. Symbols indicate a statistically ($p<0.05$) significant difference for the following comparisons: α indicate differences with group A, γ indicate differences with group C, and δ indicate differences with group D. N = 5.

Procalcitonin serum concentrations were found to fluctuate throughout the experiment, with no influence of the groups (supplementary material, figure V.3).

3.5 **Leukocytes counts**

Leukocyte counts were shown in figure V.6, panels A (groups A and B) and B (groups C and D). The baseline leukocyte counts were similar across the four groups, and a uniform increase was observed following the initial surgery. A return to pre-operative levels was observed in group A animals 6 days after the initial surgery, while a sustained increase was observed in the other three groups, with significant differences with group A observed at day 6 (group B) and day 8 (group D). The peak in leukocyte counts in group C and D was observed at day 8 and were significantly higher in group D animals (difference of 6260 leukocytes/mm³ [1527;10992], p=0.001). No further differences were observed between the four groups after day 8.

Neutrophils over lymphocytes ratios are shown in figure V.6, panels C (groups A and B) and B (groups C and D). No significant differences were observed at baseline. A sharp increase in the ratios was observed in infected groups following the initial surgery, diverging clearly from group A animals at day 2, and was sustained during most of the experiment. Group D animals had a significantly higher ratio than group B animals at day 8. The ratio in group C animals peaked at day 8 but was not statistically different from other groups. The ratios of groups C and D animals decreased progressively after day 8 and were no longer statistically significant from non-infected animals.

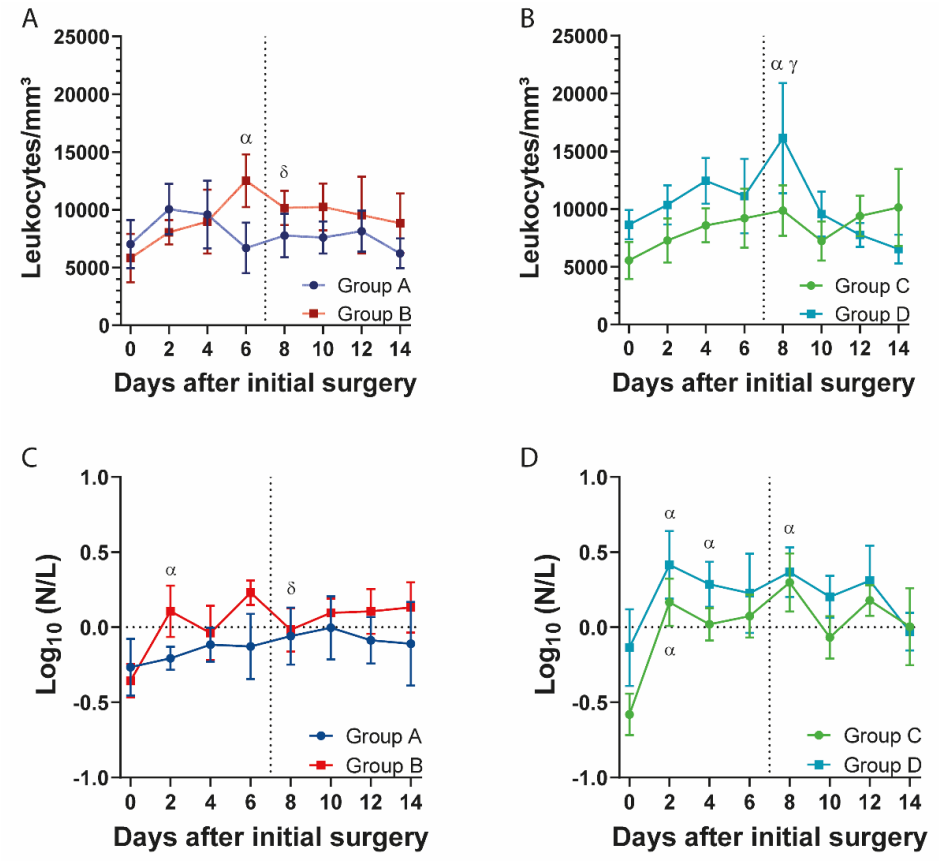


Figure V.6. Post-operative evolution of the total leukocytes counts (panels A & B) and neutrophils over lymphocytes ratio expressed in base 10 logarithms (panels C & D). Vertical dashed lines indicate the day of debridement surgery. Horizontal dashed lines indicate an N/L ratio of 1. Statistical analysis: two-way repeated-measures ANOVA and Tukey HSD post-hoc test. ns: $p>0.05$; *: $p<0.05$; **: $p<0.01$; ***: $p<0.001$; ****: $p<0.0001$. N = 5.

3.6 **Histology**

The histological examination of the samples colored with Masson's blue trichrome (Figure V.7) showed that the bone trabeculae in direct contact with the implant were abundantly infiltrated with granulomatous materials in group B animals. Aggregated granulomatous materials were also observed on the surface of the cartilage and in the articular recesses. These infiltrates were absent in group A animals and were markedly reduced in groups C and D animals. The articular cartilage surfaces appeared healthy in all four groups. Minimal ulcerations were observed in limited cases and did not appear to be associated with a particular group.

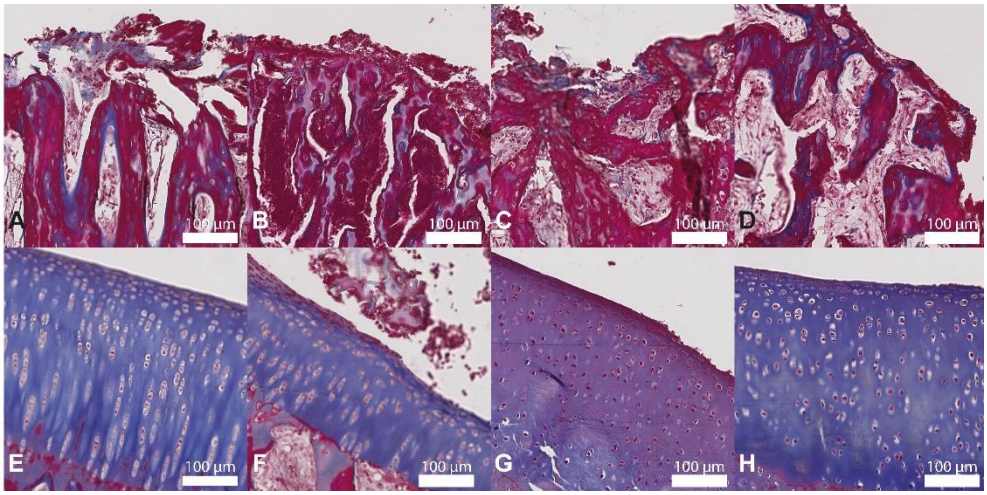


Figure V.7. Histological images of the bone-implant interface and articular cartilage stained with Masson's blue trichrome of groups A (panels A and E respectively), B (B and F), C (C and G), and D (D and H). 200x magnification, scale bar: 100 µm.

4 Discussion

Our study describes the development of a novel *in-vivo* model of acute PJI using custom-designed 3D printed Ti-6Al-4V unicompartmental tibial implants, infected per-operatively with a reference MRSA strain and treated with DAIR. This model allowed to reproducibly reach the usual therapeutic targets for the selected antibiotic (vancomycin) and to monitor the effect of the treatment in infected animals treated with DAIR alone or combined with an experimental enzymatic cocktail.

This model presents significant advantages and improvements over others previously described, making it especially suited for the study of PJI treated with DAIR. The choice of a unicompartmental tibial implant 3D printed in Ti-6Al-4V implanted in a weight-bearing position, exposed to friction, and accessible to a mechanical debridement increases the clinical relevancy over earlier models. Indeed, most models use non clinically relevant implants, using either k-wires implanted in small rodents femurs – thus not exposed to the joint space or to the mechanical constraints usually applied to arthroplasty implants and inaccessible to a surgical debridement - (270, 467-470), screws implanted in the lateral femoral condyles of rabbits – thus not exposed to mechanical stresses - (271, 471, 472), or the use of silicone elastomer implants replacing the proximal part of the tibia in rabbits but made of a material of no clinical relevance to PJI (473). The exposure of the implants to mechanical stresses and the choice of clinically relevant materials are crucial considerations for the design of models used to study infections where biofilm formation is expected. Mechanical stresses such as shear stress and pressure are known factors driving the production of extracellular polymeric substance

in *S. aureus* biofilms and inducing water flux within the biofilms (163, 474). Also, the adhesion of bacteria and the development of biofilm have long been known to be strongly influenced by the composition (154, 475) and the surface properties of their substratum (476, 477). The use of other materials has been noted by previous authors as limiting clinical relevancy (265, 271).

Over the last decade, a trend towards the development of clinically relevant implants was observed, facilitated in part by the advances in additive manufacturing (277, 278, 281). These models are characterized by the use of load-bearing knee replacement implants manufactured using clinically relevant materials such as stainless steel, titanium alloy, and polyethylene. However, most of these models present limitations in their experimental and clinical relevance for the study of DAIR inherent to the choice of animal species.

In a rat model of total knee arthroplasty infected with different *S. aureus* inoculums the authors observed a normalization of the inflammation parameters after 2 weeks in the absence of treatment. This spontaneous healing was attributed to a robust immune response of the rats and was considered by the authors to be a substantial limitation to the use of the model for the study of PJI treatments (277). A. Carli et al reported the first use of 3D printed implants in a PJI model in 2016 (265). The authors designed a Ti-6Al-4V tibial replacement implant adapted to mice knees and infected by the intra-articular injection of *S. aureus* (278). This model was recently used to study the application of an adjuvant treatment using bacteriophage lysins after a surgical debridement followed by a vancomycin treatment (279). While this model reproduces PJI in a clinically relevant manner, the use of mice presents intrinsic limitations. The modest size of mice knees limits the possibilities of

sampling for analysis, requiring the use of multiple animals to study the bacterial load and the histological alterations of the bone. Moreover, the poor venous access and limited blood volume of mice hiders the reproduction of clinically relevant antibiotics pharmacokinetics and their monitoring as well as the longitudinal study of the hemogram and of inflammatory markers.

The choice of larger animals such as NZW rabbits allowed us to multiply the number of samples available from each specimen, facilitating the comparison of microbiological and histological samples, and the longitudinal monitoring of CRP, PCT, and leukocyte counts, while also enabling the administration of vancomycin by intravenous injections and its monitoring, reproducing a clinically relevant regimen.

Similar sampling considerations lead Lopez et al. to develop a comparable model of rabbit tibial arthroplasty using 3D printed implants infected by an intra-articular inoculation with *S. aureus* (280, 281). However, to our knowledge, this model has not been used yet to study therapeutic interventions following infection.

We used a 5.5 $\log_{10}$ CFU bacterial inoculum similar to what is usually reported in the literature (278, 281), inducing an infection in all animals with no fatal sepsis observed. This infection resulted in reproducible *S. aureus* counts in all samples at one- and two-weeks post-surgery. The observed CFU counts are however difficult to compare to those of previous studies because of important variability in protocols and the reporting of values. Debridement surgery, followed by the intravenous administration of vancomycin, significantly reduced the bacterial counts in all samples, to the exception of the joint capsule, despite a careful synovectomy. The histological

examination of bone samples was consistent with the CFU counts, revealing a stark reduction in inflammatory infiltrates after treatment. Following DAIR, the reductions in CFUs in bone samples and on the implants appeared to be proportionately more pronounced than what Sosa et al. reported (279). The increased impact of DAIR on CFU counts in our model may result from multiple factors, including a more thorough debridement procedure and a better controlled vancomycin regimen.

Indeed, we observed that the intravenous injection of 50mg/kg of vancomycin twice a day consistently achieved the commonly accepted therapeutic target for the treatment of *S. aureus* infections of an $AUC_{0\text{-}24h}$ over MIC ratio over 350 (452). No renal toxicity was observed using this dosing regimen. We were able to monitor the vancomycin serum concentrations in infected animals and observed no significant discrepancy with the control group. Previously published studies investigating the pharmacokinetics of vancomycin in NZW rabbits found that similar dosing regimens were required to reach this target (478, 479). In contrast to these studies, we observed higher peak concentrations and lower trough concentrations, suggesting a higher clearance in our model. These lower through concentrations drove us to monitor the vancomycin serum concentrations of the infected animals 6h after the injection instead of the usual through concentration monitoring.

Our model was then used to perform a pilot study of the in-vivo activity of a previously described tri-enzymatic cocktail (TEC) targeting the biofilm matrix (464) as an adjuvant therapy to DAIR. Although we previously reported a strong synergy of TEC with vancomycin in-vitro, we did not

observe any significant differences in CFU counts or other infection markers with a standard DAIR treatment. We attribute this lack of differences to a decrease in volume of the enzymatic solution in the knee due to wound leakage and resorption. Modifications in the formulation of the enzymatic solution, such as the use of hydrogels, are considered to prolong its presence in the joint and improve its effects on the biofilms. The association with locally delivered antibiotics is also considered in order to fully benefit from the degradation of biofilms following the application of enzymes (416).

Our model presents some limitations. The most significant is the limited tolerance of rabbits to some antibiotics, including rifampin. Gatin et al. reported a 23% fatality rate in a rabbit PJI model when the treatments included rifampin (480). Rifampin, in association with other antibiotics, is known to be effective against staphylococcal biofilms *in-vitro* and *in-vivo* (481), and its use in combination with another antibiotic in the treatment of patients suffering from staphylococcal PJI is recommended by the IDSA (59). Still, as our model was designed to evaluate adjuvant treatments to DAIR, we believe that the use of a suboptimal antibiotic therapy may be justified to emphasize the effect of the tested agent. Infected animals gradually lost weight throughout the experiment, approaching the predefined humane endpoints two weeks after inoculation. This limits the utilization of our model to short treatment periods. The use of lower inoculum could be considered but carries the risk of not inducing an infection in all animals (277). While no implant loosening was observed, the absence of bone cement means that the bone cut may have been incompletely covered by the implant. However, as radiolucent lines are common following joint replacement (482), we believe this does not impact the relevancy of our model. Moreover, this could prove advantageous

to show the impact of injectable treatments of biofilms by allowing the formation of biofilm inaccessible to mechanical debridement. Lastly, we limited our study to the use of a single reference MRSA strain. While common in the literature for *in-vivo* models, the use of clinical strains may have given greater relevancy to our study. Nevertheless, this limitation presents the advantage of facilitating the replication of our results.

Despite these limitations, the clinical relevancy and the reproducibility of this model make it a prime choice to study DAIR and adjuvant therapies applied in this context. Further refinements could be brought by studying the use of clinical strains or of other bacterial species found in PJI, as well as by investigating the pharmacokinetics and tolerance of other antibiotic agents.

5 Conclusion

This study describes the development of a novel clinically relevant *in-vivo* model of acute MRSA prosthetic joint infection in New-Zealand White rabbits treated with a surgical debridement and an intra-venous vancomycin treatment and its application to the pilot study of an adjuvant therapy using an enzymatic cocktail. We showed that this model allowed for the development of a reproducible infection in all subjects. Vancomycin was administered intravenously twice a day, using a dosing regimen that attained the clinical targets for *S. aureus* infections and, combined with a thorough debridement procedure, reduced significantly the bacterial load in most samples. The enzymatic cocktail did not display any significant added effect over standard debridement, despite promising *in-vitro* results. Further research should concentrate on the development of new formulations such as hydrogels to increase its effects in this *in-vivo* model.

6 Data Availability Statement

The data for the experiments reported in this publication is available upon request to the corresponding author.

7 Authors Contributions

HP designed and performed the experiments, analyzed the data, and drafted the manuscript. AM contributed to the realization of the experiments. All authors contributed to the revision and improvement of the manuscript.

8 Funding

The experiments presented in this manuscript were funded by the Région Wallonne through a Win2Wal grant (Orthenzy; grant number 1810122) and the F.R.S.-FNRS (Fonds de la Recherche Scientifique – FNRS) (grants T.0189.16 and J.0162.19). H.P. is the beneficiary of a FRIA (Fonds pour la formation à la Recherche dans l'Industrie et dans l'Agriculture) grant of the FRS-FNRS. F.V.B. is a research director of the FRS-FNRS.

9 Conflicts of Interest

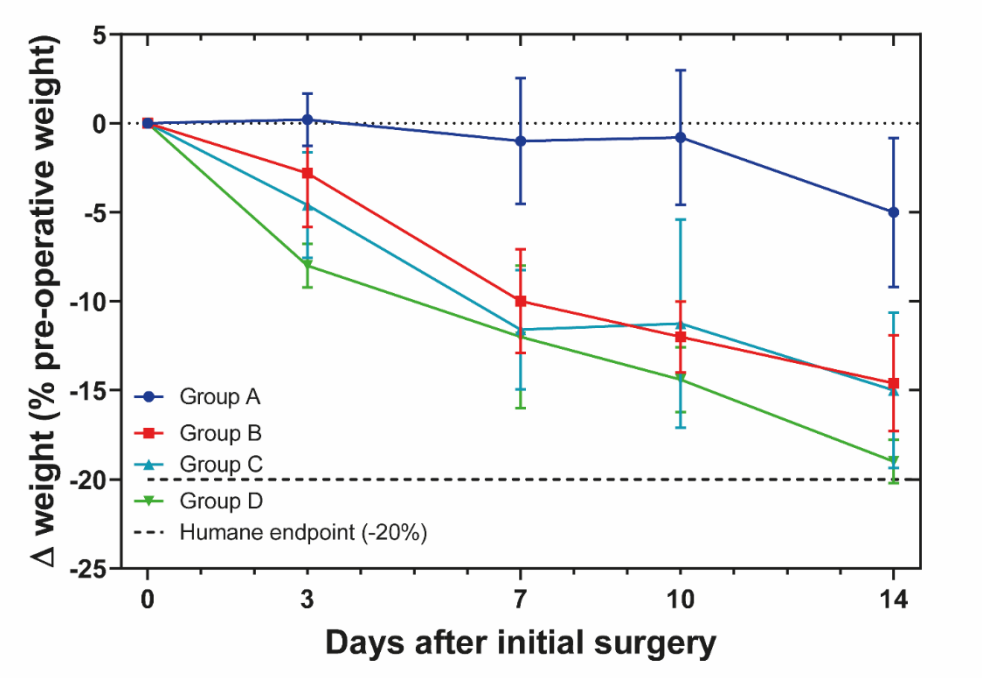
The authors have no affiliations or involvement with any entity with interests related to this manuscript.

10 Acknowledgments

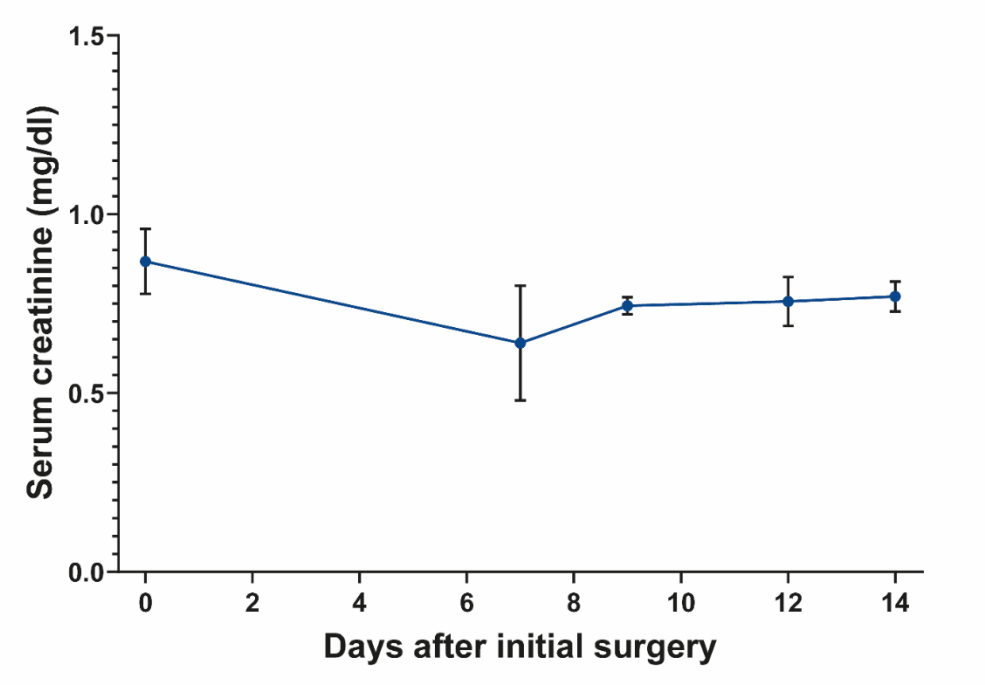
The authors would like to thank Alix Mangin for his invaluable help and dedication to the project, Caroline Bouzin, Ph.D., Marc de Bournonville, and

Michèle De Beukelaer from the 2IP platform for their advice and help in the preparation of histological samples, Sébastien Druart from the NEFR laboratory for his help in the dosing of creatinine, Professor Jean-Paul Dehoux from the faculty animal facilities for his advice over the anesthesia of rabbits, Professor Hector Rodriguez-Villalobos from the microbiology department of the Cliniques Universitaires Saint-Luc for the use of the TissueLyser, and Professor Pierre Wallemacq from the clinical biology department of the Cliniques Universitaires Saint-Luc for allowing us to perform vancomycin dosing. Figure 1 was created with Biorender.

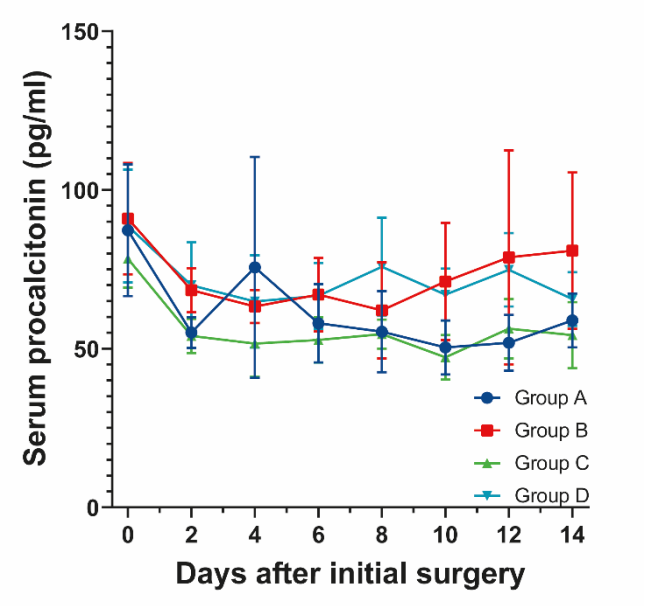
11 Supplementary material



Supplementary figure V.1. Post-operative evolution of the animals' weight, expressed as a percentage of the pre-operative weight. Points: means; error bars: standard errors.



Supplementary figure V.2. Post-operative evolution of group A animals' serum creatinine concentration. Points: means; error bars: standard errors.



Supplementary figure V.3. Post-operative evolution of the serum procalcitonin concentrations (pg/ml). Points: means; error bars: standard errors.

Chapter VI: General discussion

1 Main achievements of the thesis

Biofilm formation is associated with a reduced susceptibility of bacteria to antibiotics and is thought to represent a significant factor in failures following the treatment of PJI with DAIR. Multiple strategies have been suggested in the literature to address this issue. Biofilm dispersal, using mechanical or pharmaceutical approaches, has been shown to restore the susceptibility of bacteria to antibiotics and appears promising as an adjunct to DAIR.

In this work, we describe the effects of biofilm dispersal using either a standard technique – pulsed-lavage – or a novel tri-enzymatic cocktail targeting three constituents of the biofilm matrix combined with an antibiotic therapy in *in-vitro* and *in-vivo* models relevant to PJI. The main achievements of this work are summarized below.

1.1 **The tri-enzymatic cocktail is safe and effective against the biofilms of species relevant to PJI**

The results of our second study confirm the potency of the tri-enzymatic cocktail developed with our industrial partner to disperse the biofilms of three bacterial species relevant to PJI, making up over 75% of the species involved in acute PJI (64), in an *in-vitro* model, and show the superiority of this approach compared to the use of single enzymes. To our knowledge, our article was the first to report on the use of a broad-spectrum enzymatic combination and to demonstrate its effects on multiple species relevant to the orthopedic field. Interestingly, we showed that the dispersal of biofilm

induced by the enzymatic cocktail occurred in a comparatively short time frame, with an exposure to the enzymes for 30 min dispersing most of the biofilms. Conversely, in most of the previously published studies, the biofilms were exposed to enzymes for longer periods ranging from 1h to 24h (377, 383, 483), complicating their potential use in a clinical setting.

Our results also underline the safety of this approach. We did not observe any significant *in-vitro* cytotoxicity of the enzymatic solution against cell lines representative of the joint environment. Its use *in-vivo*, combined with a surgical debridement and a systemic antibiotic therapy, was not associated with any significant adverse reactions that could have suggested a significant bacteremia. This is particularly significant considering a previous report of lethal bacteremia following the dispersal of *P. aeruginosa* biofilms using glycoside hydrolases in a mouse model of chronic wound (356).

1.2 Biofilm dispersal is an effective method to restore the susceptibility of bacteria to antibiotics *in-vitro*

The results of the experiments presented in the first two studies illustrate the tolerance of biofilms exposed to clinically relevant concentrations of most antibiotics recommended for the treatment of PJI. Indeed, we observed only minimal reductions in CFU counts from biofilms samples exposed to most antibiotics, at clinically relevant concentrations. Only daptomycin, against *S. aureus* and *S. epidermidis*, and rifampin, against *S. epidermidis*, appeared to cause microbiologically significant reductions in CFU counts.

Dispersal of the biofilms, either using pulsed-lavage or our enzymatic cocktail, not only reduced the CFU counts of all the biofilms but also improved the effect of antibiotics on the remaining bacteria in a synergistic

fashion. These observations are consistent with the literature. A similar synergy of pulsed-lavage and antiseptics was shown in a model of *S. aureus* biofilms that inspired the development of our model (244, 357). The synergy of pulsed-lavage and antibiotics applied locally using calcium sulfate beads was also published as our project was underway (409). However, to our knowledge, our study was the first to show that this synergy was present with antibiotics used at concentrations similar to serum concentrations in patients. The sensitizing effect of the enzymatic dispersal of biofilms to antibiotics is well known. Again, our work distinguishes itself by showing the consistency of this effect across a variety of species and antibiotics.

1.3 **Development and application of an innovative *in-vivo* model of PJI**

The encouraging results of the *in-vitro* experiments assaying the effect of the combination of the enzymatic cocktail and antibiotics on biofilms led us to develop an *in-vivo* model of PJI to further our investigations. We designed our model to reproduce as closely as possible a PJI using a Ti-6Al-4V tibial plateau replacement placed in a load-bearing position, acutely infected with a per-operative intra-articular injection of *S. aureus*. Our choice of rabbits as model animals stemmed from our intent to administer systemic antibiotics, control their pharmacokinetics, and measure inflammatory blood markers, which required an accessible venous network, and to perform a surgical debridement procedure in some groups which was facilitated by the larger size of rabbits.

Our results, presented in the third article, show that we were able to reproducibly induce an infection in our rabbits, with bacteria found in important numbers on the implant and the surrounding tissues. This infection

caused a significant increase in the serum CRP in all infected animals. We demonstrated that vancomycin could be administered intravenously for 7 days, that we could reach relevant clinical serum concentration targets, and that the serum concentrations could be monitored over the treatment period. We further showed that a reproducible and well-tolerated DAIR procedure was possible in animals one week after the infection, resulting in significant reductions of serum CRP and CFU counts in most samples. While our results do not indicate a benefit of enzymatic cocktail injection following DAIR, we nonetheless demonstrated its innocuity for the animals. To our knowledge, our model is the first clinically relevant PJI model in rabbits where a DAIR was attempted. Indeed, while a similar PJI model was recently described by López-Torres et al. (281), no publications have described its use for the assessment of a therapeutic intervention.

2 Limitations of this work

The studies performed for this work present limitations that are inherent to their models and design. Limitations common to the different studies, as well as the most important ones specific to the *in-vitro* model, are acknowledged below. Specific limitations of each study are exposed in the respective articles.

2.1 **Common limitations**

2.1.1 **Focus on a limited number of bacterial strains**

Besides our first *in-vitro* study, we limited our investigation to biofilms of reference strains for our second *in-vitro* study and to a single reference MRSA strain for our *in-vivo* study. This lack of diversity is probably one of the most

important limitations of this work. Indeed, it is well described in the literature that the strains encountered in a clinical setting present significant genetic differences leading to variations in antibiotic susceptibility (484) and biofilm matrix composition (438, 444) that our studies do not completely account for. The concerns over the lack of variety of matrixes composition are somewhat alleviated by our study of the dispersal of biofilms by single enzymes that revealed significant differences between species. However, it is clear to us that further studies should include clinical isolates of the most common species encountered in PJIs to generalize our results.

2.1.2 **Focus on a single substratum**

We limited our studies to biofilms grown on a Ti-6Al-4V substratum. While titanium alloys are extremely common in orthopedics, other materials such as CoCr alloys, 316L stainless steel, UHMWPE, or ceramics are also frequently used. These materials present different surface chemistries, roughness, and hydrophilic characteristics that may impact biofilm formation and production on their surfaces and limit the generalization of our results (161, 239, 477). However, the real impact of this factor on our results is disputable. A previous study by Lauderdale et al. investigated the impact of substratum materials on the dispersal of biofilms grown in drip flow reactors and did not conclude to any significant differences related to the substratum (485). Further studies should investigate the influence of different clinically relevant materials on biofilm dispersal.

2.1.3 **Single species biofilms**

While the vast majority of PJIs are monomicrobial, polymicrobial infections make up to 27.4% of early acute infections for which a treatment with DAIR

would be attempted. Some associations of species in biofilms are known to be more tolerant to antibiotics than their single-species counterparts and may prove more challenging to treat (486, 487). Although we limited our studies to single-species biofilm models, investigations over this important aspect of the pathology, including enzymatic dispersal, are currently performed by another member of our laboratory, Mr. Albert Ruiz-Sorribas.

2.1.4 **Absence of rifampin-based antibiotic combinations**

The importance of using rifampin accompanied by a second antibiotic in the treatment of staphylococcal PJIs is well established in the literature. In our studies, we chose to focus on the combination of biofilm dispersal with single antibiotics. This choice is the result of distinct considerations for *in-vitro* and *in-vivo* experiments. *In-vitro*, we considered that focusing on single antibiotics would allow us to confirm that the observed synergies were indeed attributable to each antibiotic tested and did not result from the combination to rifampin. This consideration arose from initial experiments that tested the combination of vancomycin and rifampin against

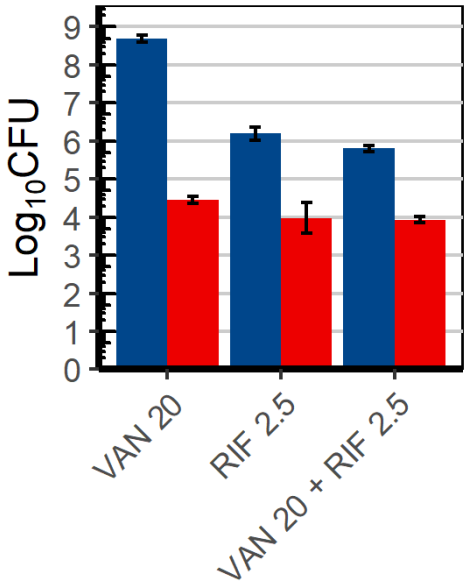


Figure VI.1:. Effect of vancomycin and rifampin alone or combined on ATCC 33591 biofilms CFU counts. Blue: controls; Red: treated with TEC. $N_{experiments}=3$. (unpublished)

MRSA biofilms alone or combined with our enzymatic cocktail, where we observed results identical to those of rifampin alone (Figure VI.1).

In animal studies, we decided to abstain from using rifampin because of concerns for toxicity to the microbiota of rabbits. Microbiota balance is crucial in rabbits and is an important concern when antibiotics are prescribed in veterinary practice (488), and rifampin use has been shown to induce major long-lasting alterations to the microbiota in experimental models (489). The risk of administrating rifampin to rabbits is thus significant, as a report of Gatin et al. illustrates. In their series of PJI models in rabbits, rifampin use was associated with a 23% mortality rate because of diarrhea (480).

The absence of rifampin-based combinations results in a significant divergence from clinical recommendations and should be considered for the interpretation of our results. Further experiments should strive to either include these combinations or study pathogens or situations for which such combinations are not usually recommended.

2.1.5 **Focus on a single enzymatic formulation**

Our studies, both *in-vitro* and *in-vivo*, focused on the application of the tri-enzymatic cocktail developed in collaboration with our industrial partner. Even though our experiments showed the superiority of this approach over the use of single enzymes for the dispersal of the biofilms of the species we studied, other enzyme combinations or protocols of administration could have been considered. For example, the sequential use of proteinase K and cellulase has been shown to be promising to disperse *E. coli* biofilms and to restore their susceptibility to sodium hypochlorite (432). While we did not explore these possibilities in this work, the study of other enzyme

combinations is currently the focus of researches led by one other member of our laboratory.

2.2 Limitations specific to the *in-vitro* experiments

2.2.1 Low throughput of the model

The use of coupons as substratum for biofilm culture presents some significant advantages over other *in-vitro* models such as microtiter plates biofilm assays. Using coupons facilitates the handling of the samples, allowing for the study of the mechanical dispersal of the biofilms, reproducible rinsing and bacterial cells recuperation steps, and the realization of microscopy images, while the use of clinically relevant materials promotes the development of biofilms attached to the substratum in more relevant ways. However, this model requires handling each sample individually, which strongly hinders the experiments' throughput compared to microtiter plate assays. This important characteristic of the model is the main reason for the relatively limited number of conditions assayed in this work.

2.2.2 Limited clinical relevancy of the model

Through the use of a clinically relevant substratum and the application of shear-stress to the biofilms, we attempted to increase the relevancy of our growth conditions. It can be argued that this clinical relevancy is still limited.

We used a general-purpose medium (TSB) with added glucose and sodium chloride for their positive influence on biofilm formation (490). This medium has a composition that differs from that of synovial fluid in terms of proteins, nutrients, and salts content as well as viscosity and may have influenced our results (233, 234, 491). It should however be noted that there exists no

artificial synovial fluid for microbiological studies and that the volumes required for our experiments were incompatible with the use of synovial fluid from patients or animals. The development of an artificial synovial fluid adapted to bacterial culture could lead to a significant improvement of our models and should be considered.

The shear stress used in our study was determined empirically by comparing the production of biofilm and its reproducibility when the samples were rotated at different speeds (unpublished results). However, to our knowledge, there is no available data concerning the shear stresses to which different sections of the implants are exposed in THA and TKA and our approach appears reasonable in this context.

Finally, because of its closed design, this model does not allow for the reproduction of the pharmacokinetic profiles of the antibiotics used. Our biofilms were exposed to constant concentrations, which may have led to an overestimation of the effects of some antibiotics. This issue may have been further exacerbated by the lack of proteins in the medium, exposing the biofilms to unbound antibiotics.

3 Perspectives

The results of this work and the methods developed to achieve these open up several new research questions. Besides some of the points evoked while stating the limitations of our work, we believe that the following subjects are especially promising for future researches.

3.1 **Modified dosage form for the delivery of the enzymatic cocktail**

Despite promising *in-vitro* results, the *in-vivo* effects of the TEC were disappointing. We have formulated the hypothesis that this dismal effect may result from the seeping of the enzymatic solution through the surgical wound, escaping the joint prematurely, limiting the biofilms exposure period to the enzymes. Therefore, we postulate that a drug form allowing the immobilization of the enzymes in the joint and a controlled release could improve our results. An interesting option to achieve this goal would be the development of a hydrogel formulation. As described in this introduction, the use of hydrogels as carriers for antimicrobial agents has already been described in the literature (332), comforting the validity of this approach. Proof-of-concept experiments are currently underway using two gelling agents: sodium alginate and poloxamer 407. These two molecules are known for their biocompatibility and, concerning poloxamer 407, a potential to inhibit biofilm formation (492-494). Preliminary results using sodium alginate showed a rapid release of proteins from the gels, with over 80% of the release occurring over the first 8 hours and a sustained activity of the enzymes following their release. These promising results inspire us to pursue our experiments and attempt to fine-tune the enzymes' release.

3.2 **Combinations of the enzymatic cocktail with other antimicrobial agents**

As we have shown in our experiments, the bacteria remaining on surfaces following debridement can reform a biofilm in a relatively short time frame, corresponding to what other authors have described as a therapeutic window (416). In order to benefit the most from the biofilm disruption caused by the

surgical debridement and the exposure to our enzymatic cocktail, we postulate that the addition of an antimicrobial agent to the cocktail could be beneficial. We currently envision using a broad-spectrum antibiotic, such as vancomycin or gentamicin, already commonly used in orthopedics as locally applied antibiotics using PMMA, calcium sulfate, or the DAC hydrogel as carriers (329, 330, 495), applied with the enzymatic cocktail using a hydrogel carrier. Another option we envision is the addition of bacteriophages to the enzymatic cocktail. Another researcher from our laboratory, Mr. Steven De Soir, is currently developing cocktails of bacteriophages adapted to the most common pathogens found in PJIs. Data in the literature show that bacteriophage penetration in biofilms is facilitated by matrix degradation (496). It is then conceivable that the combination of enzymatic and bacteriophage cocktails could prove synergistic.

3.3 **Preventive use of the enzymatic cocktail**

PNAG and eDNA, two of the EPS constituents targeted by our enzymatic cocktail, are crucial to the initial steps of biofilm formation (17). Their degradation, by respectively dispersin B and DNAse I, has been shown to inhibit partially the formation of *S. aureus* and *S. epidermidis* biofilms in an *in-vitro* model (168). It is thus conceivable that the enzymatic cocktail tested in this work, combined with antimicrobials, and applied as a hydrogel on the implants, could prove beneficial to the prevention of PJI.

3.4 **Modifications to the *in-vivo* model**

We developed our *in-vivo* PJI model with the specific intent of testing our enzymatic cocktail in conjunction with DAIR in the setting of an acute infection caused by *S. aureus*. While this model leads to a reproducible

infection that resembles PJI in humans, it suffers from limitations such as the rapid weight loss of our animals and the digestive sensitivity of rabbits to rifampin. Some adaptions to the model could probably help avoid these limitations while maintaining its clinical relevancy. For example, instead of a staphylococcus, the infection could be induced by a Gram-negative bacillus such as *E. coli*, allowing us to use a single antibiotic such as a second-generation cephalosporin or ciprofloxacin (59), while the severity of the infection could be reduced by decreasing the initial inoculum as disease severity appears to be influenced by this parameter (277).

4 Conclusion

Our work shows the impact of biofilm disruption by pulsed-lavage and enzymatic digestion of the extra-cellular matrix on the antibiotic susceptibility of bacteria in an *in-vitro* model relevant to PJI and has led to the development of a novel *in-vivo* acute PJI model. While we could not demonstrate an added effect of the application of enzymes on the evolution of the infection, we remain convinced of the potential of this adjunctive treatment and believe that this work and the methods developed therefor will support the elaboration of new preventive and therapeutic interventions for PJI.

References

1. Flemming H-C, Wingender J. The biofilm matrix. Nature Reviews Microbiology. 2010;8(9):623-33.
2. Pechkova E, Tripathi S, Ravelli RBG, McSweeney S, Nicolini C. Radiation stability of proteinase K crystals grown by LB nanotemplate method. Journal of Structural Biology. 2009;168(3):409-18.
3. Ramasubbu N, Thomas LM, Ragunath C, Kaplan JB. Structural Analysis of Dispersin B, a Biofilm-releasing Glycoside Hydrolase from the Periodontopathogen Actinobacillus actinomycetemcomitans. Journal of Molecular Biology. 2005;349(3):475-86.
4. Lahm A, Suck D. DNase I-induced DNA conformation: 2 Å Structure of a DNase I-octamer complex. Journal of Molecular Biology. 1991;222(3):645-67.
5. Tande AJ, Patel R. Prosthetic joint infection. Clin Microbiol Rev. 2014;27(2):302-45.
6. OCDE. Hip and knee replacement2019.
7. Hartzler MA, Li K, Geary MB, Odum SM, Springer BD. Complications in the treatment of prosthetic joint infection. Bone Joint J. 2020;102-b(6_Supple_A):145-50.
8. Aboltins C, Dowsey MM, Peel T, Lim WK, Parikh S, Stanley P, et al. Early prosthetic hip joint infection treated with debridement, prosthesis retention and biofilm-active antibiotics: functional outcomes, quality of life and complications. Internal medicine journal. 2013;43(7):810-5.
9. Tsaras G, Osmon DR, Mabry T, Lahr B, St Sauveur J, Yawn B, et al. Incidence, secular trends, and outcomes of prosthetic joint infection: a population-based study, olmsted county, Minnesota, 1969-2007. Infect Control Hosp Epidemiol. 2012;33(12):1207-12.
10. Mur I, Jordán M, Rivera A, Pomar V, González JC, López-Contreras J, et al. Do Prosthetic Joint Infections Worsen the Functional Ambulatory Outcome of Patients with Joint Replacements? A Retrospective Matched Cohort Study. Antibiotics (Basel). 2020;9(12).
11. Lueck E, Schlaepfer TE, Schildberg FA, Randau TM, Hischebeth GTR, Jaenisch M, et al. The psychological burden of a two-stage exchange of infected total hip and knee arthroplasties. Journal of Health Psychology. 2020:1359105320948583.
12. Berend KR, Lombardi AV, Jr., Morris MJ, Bergeson AG, Adams JB, Sneller MA. Two-stage treatment of hip periprosthetic joint infection is

associated with a high rate of infection control but high mortality. Clin Orthop Relat Res. 2013;471(2):510-8.
13. Zimmerli W, Trampuz A, Ochsner PE. Prosthetic-joint infections. N Engl J Med. 2004;351(16):1645-54.
14. Stoodley P, Nistico L, Johnson S, Lasko LA, Baratz M, Gahlot V, et al. Direct demonstration of viable Staphylococcus aureus biofilms in an infected total joint arthroplasty. A case report. J Bone Joint Surg Am. 2008;90(8):1751-8.
15. Costerton JW, Stewart PS, Greenberg EP. Bacterial biofilms: a common cause of persistent infections. Science. 1999;284(5418):1318-22.
16. Romano CL, Trentinaglia MT, De Vecchi E, Logoluso N, George DA, Morelli I, et al. Cost-benefit analysis of antibiofilm microbiological techniques for peri-prosthetic joint infection diagnosis. BMC infectious diseases. 2018;18(1):154.
17. Arciola CR, Campoccia D, Montanaro L. Implant infections: adhesion, biofilm formation and immune evasion. Nat Rev Microbiol. 2018;16(7):397-409.
18. de Vor L, Rooijakkers SHM, van Strijp JAG. Staphylococci evade the innate immune response by disarming neutrophils and forming biofilms. FEBS Letters. 2020;594(16):2556-69.
19. Stewart PS. Antimicrobial Tolerance in Biofilms. Microbiol Spectr. 2015;3(3).
20. Klouche S, Sariali E, Mamoudy P. Total hip arthroplasty revision due to infection: A cost analysis approach. Orthopaedics & Traumatology: Surgery & Research. 2010;96(2):124-32.
21. Bozic KJ, Kamath AF, Ong K, Lau E, Kurtz S, Chan V, et al. Comparative Epidemiology of Revision Arthroplasty: Failed THA Poses Greater Clinical and Economic Burdens Than Failed TKA. Clin Orthop Relat Res. 2015;473(6):2131-8.
22. Klug A, Gramlich Y, Rudert M, Drees P, Hoffmann R, Weißenberger M, et al. The projected volume of primary and revision total knee arthroplasty will place an immense burden on future health care systems over the next 30 years. Knee surgery, sports traumatology, arthroscopy : official journal of the ESSKA. 2020:1-12.
23. Kurtz SM, Lau E, Watson H, Schmier JK, Parvizi J. Economic burden of periprosthetic joint infection in the United States. J Arthroplasty. 2012;27(8 Suppl):61-5 e1.
24. Dimitriou D, Antoniadis A, Flury A, Liebhauser M, Helmy N. Total Hip Arthroplasty Improves the Quality-Adjusted Life Years in Patients Who

Exceeded the Estimated Life Expectancy. J Arthroplasty. 2018;33(11):3484-9.
25. Shan L, Shan B, Suzuki A, Nouh F, Saxena A. Intermediate and long-term quality of life after total knee replacement: a systematic review and meta-analysis. J Bone Joint Surg Am. 2015;97(2):156-68.
26. Karachalios T, Komnos G, Koutalos A. Total hip arthroplasty: Survival and modes of failure. EFORT Open Rev. 2018;3(5):232-9.
27. Howell SM, Shelton TJ, Hull ML. Implant Survival and Function Ten Years After Kinematically Aligned Total Knee Arthroplasty. The Journal of Arthroplasty. 2018;33(12):3678-84.
28. Bozic KJ, Kurtz SM, Lau E, Ong K, Chiu V, Vail TP, et al. The Epidemiology of Revision Total Knee Arthroplasty in the United States. Clinical Orthopaedics and Related Research®. 2010;468(1):45-51.
29. Bozic KJ, Kurtz SM, Lau E, Ong K, Vail TP, Berry DJ. The Epidemiology of Revision Total Hip Arthroplasty in the United States. JBJS. 2009;91(1).
30. BVOT, SORBCOT. Orthopride: Belgian Hip and Knee Arthroplasty Registry Annual Report 2018. RIZIV/INAMI; 2019.
31. Quinlan ND, Werner BC, Brown TE, Browne JA. Risk of Prosthetic Joint Infection Increases Following Early Aseptic Revision Surgery of Total Hip and Knee Arthroplasty. The Journal of Arthroplasty. 2020;35(12):3661-7.
32. Lenguerrand E, Whitehouse MR, Beswick AD, Kunutsor SK, Burston B, Porter M, et al. Risk factors associated with revision for prosthetic joint infection after hip replacement: a prospective observational cohort study. Lancet Infect Dis. 2018;18(9):1004-14.
33. Jafari SM, Coyle C, Mortazavi SMJ, Sharkey PF, Parvizi J. Revision hip arthroplasty: infection is the most common cause of failure. Clinical orthopaedics and related research. 2010;468(8):2046-51.
34. Lenguerrand E, Whitehouse MR, Beswick AD, Kunutsor SK, Foguet P, Porter M, et al. Risk factors associated with revision for prosthetic joint infection following knee replacement: an observational cohort study from England and Wales. The Lancet Infectious diseases. 2019;19(6):589-600.
35. Suarez J, Griffin W, Springer B, Fehring T, Mason JB, Odum S. Why Do Revision Knee Arthroplasties Fail? The Journal of Arthroplasty. 2008;23(6, Supplement):99-103.
36. Hadley CJ, Sodhi N, Anis H, Ricchetti E, Mont MA, Erickson BJ, et al. Nationwide trends of surgical site infections rates after primary shoulder arthroplasty. Seminars in Arthroplasty: JSES. 2020.

37. Johansson L, Hailer NP, Rahme H. High incidence of periprosthetic joint infection with propionibacterium acnes after the use of a stemless shoulder prosthesis with metaphyseal screw fixation - a retrospective cohort study of 241 patients propionibacter infections after eclipse TSA. BMC Musculoskeletal Disorders. 2017;18(1):203.
38. Patton D, Kiewiet N, Brage M. Infected Total Ankle Arthroplasty: Risk Factors and Treatment Options. Foot & Ankle International. 2015;36(6):626-34.
39. Myerson MS, Shariff R, Zonno AJ. The Management of Infection Following Total Ankle Replacement: Demographics and Treatment. Foot & Ankle International. 2014;35(9):855-62.
40. Wildeman P, Rolfson O, Söderquist B, Wretenberg P, Lindgren V. What Are the Long-term Outcomes of Mortality, Quality of Life, and Hip Function after Prosthetic Joint Infection of the Hip? A 10-year Follow-up from Sweden. Clin Orthop Relat Res. 2021.
41. Grammatopoulos G, Bolduc ME, Atkins BL, Kendrick BJL, McLardy-Smith P, Murray DW, et al. Functional outcome of debridement, antibiotics and implant retention in periprosthetic joint infection involving the hip: a case-control study. Bone Joint J. 2017;99-B(5):614-22.
42. Zmistowski B, Karam JA, Durinka JB, Casper DS, Parvizi J. Periprosthetic Joint Infection Increases the Risk of One-Year Mortality. JBJS. 2013;95(24).
43. Lum ZC, Natsuhara KM, Shelton TJ, Giordani M, Pereira GC, Meehan JP. Mortality During Total Knee Periprosthetic Joint Infection. The Journal of Arthroplasty. 2018;33(12):3783-8.
44. Bozic KJ, Ries MD. The impact of infection after total hip arthroplasty on hospital and surgeon resource utilization. J Bone Joint Surg Am. 2005;87(8):1746-51.
45. Garfield K, Noble S, Lenguerrand E, Whitehouse MR, Sayers A, Reed MR, et al. What are the inpatient and day case costs following primary total hip replacement of patients treated for prosthetic joint infection: a matched cohort study using linked data from the National Joint Registry and Hospital Episode Statistics. BMC medicine. 2020;18(1):335.
46. Singh JA, Yu S, Chen L, Cleveland JD. Rates of Total Joint Replacement in the United States: Future Projections to 2020–2040 Using the National Inpatient Sample. The Journal of Rheumatology. 2019;46(9):1134.
47. Ackerman IN, Bohensky MA, Zomer E, Tacey M, Gorelik A, Brand CA, et al. The projected burden of primary total knee and hip replacement for

osteoarthritis in Australia to the year 2030. BMC musculoskeletal disorders. 2019;20(1):90-.
48. Erivan R, Villatte G, Dartus J, Reina N, Descamps S, Boisgard S. Progression and projection for hip surgery in France, 2008-2070: Epidemiologic study with trend and projection analysis. Orthop Traumatol Surg Res. 2019;105(7):1227-35.
49. Rupp M, Lau E, Kurtz SM, Alt V. Projections of Primary TKA and THA in Germany From 2016 Through 2040. Clin Orthop Relat Res. 2020;478(7):1622-33.
50. Patel A, Pavlou G, Mújica-Mota RE, Toms AD. The epidemiology of revision total knee and hip arthroplasty in England and Wales. The Bone & Joint Journal. 2015;97-B(8):1076-81.
51. Hunter DJ, Bierma-Zeinstra S. Osteoarthritis. The Lancet. 2019;393(10182):1745-59.
52. OCDE. Demographic trends2017.
53. Zhang Y, Jordan JM. Epidemiology of osteoarthritis. Rheumatic diseases clinics of North America. 2008;34(3):515-29.
54. Sassi F, Devaux M, Cecchini M, Rusticelli E. Obésité : Analyses des tendances dans les pays de l'OCDE. 2009.
55. Haase CL, Eriksen KT, Lopes S, Satylganova A, Schnecke V, McEwan P. Body mass index and risk of obesity-related conditions in a cohort of 2.9 million people: Evidence from a UK primary care database. Obes Sci Pract. 2020;7(2):137-47.
56. Premkumar A, Kolin DA, Farley KX, Wilson JM, McLawhorn AS, Cross MB, et al. Projected Economic Burden of Periprosthetic Joint Infection of the Hip and Knee in the United States. The Journal of Arthroplasty. 2021;36(5):1484-9.e3.
57. Parvizi J, Gehrke T. Definition of Periprosthetic Joint Infection. The Journal of Arthroplasty. 2014;29(7):1331.
58. Corvec S, Portillo ME, Pasticci BM, Borens O, Trampuz A. Epidemiology and New Developments in the Diagnosis of Prosthetic Joint Infection. The International Journal of Artificial Organs. 2012;35(10):923-34.
59. Osmon DR, Berbari EF, Berendt AR, Lew D, Zimmerli W, Steckelberg JM, et al. Diagnosis and management of prosthetic joint infection: clinical practice guidelines by the Infectious Diseases Society of America. Clin Infect Dis. 2013;56(1):e1-e25.
60. Parvizi J, Tan TL, Goswami K, Higuera C, Della Valle C, Chen AF, et al. The 2018 Definition of Periprosthetic Hip and Knee Infection: An

Evidence-Based and Validated Criteria. The Journal of Arthroplasty. 2018;33(5):1309-14.e2.
61. McNally M, Sousa R, Wouthuyzen-Bakker M, Chen AF, Soriano A, Vogely HC, et al. The EBJIS definition of periprosthetic joint infection. The Bone & Joint Journal. 2020;103-B(1):18-25.
62. Renz N, Yermak K, Perka C, Trampuz A. Alpha Defensin Lateral Flow Test for Diagnosis of Periprosthetic Joint Infection: Not a Screening but a Confirmatory Test. JBJS. 2018;100(9):742-50.
63. Tsukayama DT, Estrada R, Gustilo RB. Infection after Total Hip Arthroplasty. A Study of the Treatment of One Hundred and Six Infections*. JBJS. 1996;78(4):512-23.
64. Benito N, Mur I, Ribera A, Soriano A, Rodríguez-Pardo D, Sorlí L, et al. The Different Microbial Etiology of Prosthetic Joint Infections according to Route of Acquisition and Time after Prosthesis Implantation, Including the Role of Multidrug-Resistant Organisms. J Clin Med. 2019;8(5):673.
65. de Vries L, van der Weegen W, Neve WC, Das H, Ridwan BU, Steens J. The Effectiveness of Debridement, Antibiotics and Irrigation for Periprosthetic Joint Infections after Primary Hip and Knee Arthroplasty. A 15 Years Retrospective Study in Two Community Hospitals in the Netherlands. J Bone Jt Infect. 2016;1:20-4.
66. McPherson EJ, Tontz W, Jr., Patzakis M, Woodsome C, Holtom P, Norris L, et al. Outcome of infected total knee utilizing a staging system for prosthetic joint infection. Am J Orthop (Belle Mead NJ). 1999;28(3):161-5.
67. McPherson EJ, Woodson C, Holtom P, Roidis N, Shufelt C, Patzakis M. Periprosthetic total hip infection: outcomes using a staging system. Clin Orthop Relat Res. 2002(403):8-15.
68. Wolf M, Clar H, Friesenbichler J, Schwantzer G, Bernhardt G, Gruber G, et al. Prosthetic joint infection following total hip replacement: results of one-stage versus two-stage exchange. Int Orthop. 2014;38(7):1363-8.
69. Petis SM, Perry KI, Mabry TM, Hanssen AD, Berry DJ, Abdel MP. Two-Stage Exchange Protocol for Periprosthetic Joint Infection Following Total Knee Arthroplasty in 245 Knees without Prior Treatment for Infection. J Bone Joint Surg Am. 2019;101(3):239-49.
70. Huang Z, Wu Q, Fang X, Li W, Zhang C, Zeng H, et al. Comparison of culture and broad-range polymerase chain reaction methods for diagnosing periprosthetic joint infection: analysis of joint fluid, periprosthetic tissue, and sonicated fluid. International Orthopaedics. 2018;42(9):2035-40.
71. Kalbian I, Park JW, Goswami K, Lee Y-K, Parvizi J, Koo K-H. Culture-negative periprosthetic joint infection: prevalence, aetiology,

evaluation, recommendations, and treatment. International Orthopaedics. 2020;44(7):1255-61.
72. Trampuz A, Piper KE, Jacobson MJ, Hanssen AD, Unni KK, Osmon DR, et al. Sonication of removed hip and knee prostheses for diagnosis of infection. N Engl J Med. 2007;357(7):654-63.
73. Rak M, KavcIc M, Trebse R, Co RA. Detection of bacteria with molecular methods in prosthetic joint infection: sonication fluid better than periprosthetic tissue. Acta Orthop. 2016;87(4):339-45.
74. Drago L, Signori V, De Vecchi E, Vassena C, Palazzi E, Cappelletti L, et al. Use of dithiothreitol to improve the diagnosis of prosthetic joint infections. Journal of orthopaedic research : official publication of the Orthopaedic Research Society. 2013;31(11):1694-9.
75. Sambri A, Cadossi M, Giannini S, Pignatti G, Marcacci M, Neri MP, et al. Is Treatment With Dithiothreitol More Effective Than Sonication for the Diagnosis of Prosthetic Joint Infection? Clin Orthop Relat Res. 2018;476(1):137-45.
76. Karbysheva S, Di Luca M, Butini ME, Winkler T, Schütz M, Trampuz A. Comparison of sonication with chemical biofilm dislodgement methods using chelating and reducing agents: Implications for the microbiological diagnosis of implant associated infection. PloS one. 2020;15(4):e0231389-e.
77. Bellova P, Knop-Hammad V, Königshausen M, Mempel E, Frieler S, Gessmann J, et al. Sonication of retrieved implants improves sensitivity in the diagnosis of periprosthetic joint infection. BMC Musculoskelet Disord. 2019;20(1):623.
78. Portillo ME, Salvado M, Sorli L, Alier A, Martinez S, Trampuz A. Multiplex PCR of sonication fluid accurately differentiates between prosthetic joint infection and aseptic failure. J Infect. 2012;65(6):541.
79. Gomez E, Cazanave C, Cunningham SA, Greenwood-Quaintance KE, Steckelberg JM, Uhl JR, et al. Prosthetic joint infection diagnosis using broad-range PCR of biofilms dislodged from knee and hip arthroplasty surfaces using sonication. J Clin Microbiol. 2012;50(11):3501-8.
80. Ivy MI, Thoendel MJ, Jeraldo PR, Greenwood-Quaintance KE, Hanssen AD, Abdel MP, et al. Direct Detection and Identification of Prosthetic Joint Infection Pathogens in Synovial Fluid by Metagenomic Shotgun Sequencing. Journal of clinical microbiology. 2018;56(9):e00402-18.
81. Aggarwal VK, Bakhshi H, Ecker NU, Parvizi J, Gehrke T, Kendoff D. Organism profile in periprosthetic joint infection: pathogens differ at two

arthroplasty infection referral centers in Europe and in the United States. The journal of knee surgery. 2014;27(5):399-406.
82. Götz F, Bannerman T, Schleifer K-H. The Genera Staphylococcus and Macrococcus. In: Dworkin M, Falkow S, Rosenberg E, Schleifer K-H, Stackebrandt E, editors. The Prokaryotes: Volume 4: Bacteria: Firmicutes, Cyanobacteria. New York, NY: Springer US; 2006. p. 5-75.
83. Wertheim HFL, Melles DC, Vos MC, van Leeuwen W, van Belkum A, Verbrugh HA, et al. The role of nasal carriage in Staphylococcus aureus infections. The Lancet Infectious Diseases. 2005;5(12):751-62.
84. Magill SS, Edwards JR, Bamberg W, Beldavs ZG, Dumyati G, Kainer MA, et al. Multistate point-prevalence survey of health care-associated infections. N Engl J Med. 2014;370(13):1198-208.
85. Monaco M, Pimentel de Araujo F, Cruciani M, Coccia EM, Pantosti A. Worldwide Epidemiology and Antibiotic Resistance of Staphylococcus aureus. In: Bagnoli F, Rappuoli R, Grandi G, editors. Staphylococcus aureus: Microbiology, Pathology, Immunology, Therapy and Prophylaxis. Cham: Springer International Publishing; 2017. p. 21-56.
86. Lee AS, de Lencastre H, Garau J, Kluytmans J, Malhotra-Kumar S, Peschel A, et al. Methicillin-resistant Staphylococcus aureus. Nature Reviews Disease Primers. 2018;4(1):18033.
87. Zeller V, Kerroumi Y, Meyssonnier V, Heym B, Metten M-A, Desplaces N, et al. Analysis of postoperative and hematogenous prosthetic joint-infection microbiological patterns in a large cohort. Journal of Infection. 2018;76(4):328-34.
88. Sendi P, Banderet F, Graber P, Zimmerli W. Periprosthetic joint infection following Staphylococcus aureus bacteremia. Journal of Infection. 2011;63(1):17-22.
89. Urish KL, Bullock AG, Kreger AM, Shah NB, Jeong K, Rothenberger SD, et al. A Multicenter Study of Irrigation and Debridement in Total Knee Arthroplasty Periprosthetic Joint Infection: Treatment Failure Is High. J Arthroplasty. 2018;33(4):1154-9.
90. Zhu MF, Kim K, Cavadino A, Coleman B, Munro JT, Young SW. Success Rates of Debridement, Antibiotics, and Implant Retention in 230 Infected Total Knee Arthroplasties: Implications for Classification of Periprosthetic Joint Infection. The Journal of Arthroplasty. 2020.
91. Shohat N, Goswami K, Tan TL, Yayac M, Soriano A, Sousa R, et al. 2020 Frank Stinchfield Award: Identifying who will fail following irrigation and debridement for prosthetic joint infection. The Bone & Joint Journal. 2020;102-B(7_Supple_B):11-9.

92. Bradbury T, Fehring TK, Taunton M, Hanssen A, Azzam K, Parvizi J, et al. The fate of acute methicillin-resistant Staphylococcus aureus periprosthetic knee infections treated by open debridement and retention of components. J Arthroplasty. 2009;24(6 Suppl):101-4.
93. Lora-Tamayo J, Murillo O, Iribarren JA, Soriano A, Sanchez-Somolinos M, Baraia-Etxaburu JM, et al. A large multicenter study of methicillin-susceptible and methicillin-resistant Staphylococcus aureus prosthetic joint infections managed with implant retention. Clin Infect Dis. 2013;56(2):182-94.
94. Ricciardi BF, Muthukrishnan G, Masters E, Ninomiya M, Lee CC, Schwarz EM. Staphylococcus aureus Evasion of Host Immunity in the Setting of Prosthetic Joint Infection: Biofilm and Beyond. Curr Rev Musculoskelet Med. 2018;11(3):389-400.
95. de Mesy Bentley KL, Trombetta R, Nishitani K, Bello-Irizarry SN, Ninomiya M, Zhang L, et al. Evidence of Staphylococcus Aureus Deformation, Proliferation, and Migration in Canaliculi of Live Cortical Bone in Murine Models of Osteomyelitis. Journal of bone and mineral research : the official journal of the American Society for Bone and Mineral Research. 2017;32(5):985-90.
96. Stracquadanio S, Musso N, Costantino A, Lazzaro LM, Stefani S, Bongiorno D. Staphylococcus aureus Internalization in Osteoblast Cells: Mechanisms, Interactions and Biochemical Processes. What Did We Learn from Experimental Models? Pathogens (Basel, Switzerland). 2021;10(2):239.
97. Gómez-Junyent J, Lora-Tamayo J, Baraia-Etxaburu J, Sánchez-Somolinos M, Iribarren JA, Rodriguez-Pardo D, et al. Implant Removal in the Management of Prosthetic Joint Infection by Staphylococcus aureus: Outcome and Predictors of Failure in a Large Retrospective Multicenter Study. Antibiotics (Basel, Switzerland). 2021;10(2):118.
98. Byrd AL, Belkaid Y, Segre JA. The human skin microbiome. Nat Rev Microbiol. 2018;16(3):143-55.
99. Michels R, Last K, Becker SL, Papan C. Update on Coagulase-Negative Staphylococci—What the Clinician Should Know. Microorganisms. 2021;9(4):830.
100. Becker K, Heilmann C, Peters G. Coagulase-negative staphylococci. Clinical microbiology reviews. 2014;27(4):870-926.
101. Campoccia D, Testoni F, Ravaioli S, Cangini I, Maso A, Speziale P, et al. Orthopedic implant infections: Incompetence of Staphylococcus epidermidis, Staphylococcus lugdunensis, and Enterococcus faecalis to invade osteoblasts. J Biomed Mater Res A. 2016;104(3):788-801.

102. Zmistowski B, Fedorka CJ, Sheehan E, Deirmengian G, Austin MS, Parvizi J. Prosthetic Joint Infection Caused by Gram-Negative Organisms. The Journal of Arthroplasty. 2011;26(6, Supplement):104-8.
103. Doi Y, Bonomo RA, Hooper DC, Kaye KS, Johnson JR, Clancy CJ, et al. Gram-Negative Bacterial Infections: Research Priorities, Accomplishments, and Future Directions of the Antibacterial Resistance Leadership Group. Clinical infectious diseases : an official publication of the Infectious Diseases Society of America. 2017;64(suppl_1):S30-S5.
104. Lory S. The Family Streptococcaceae. In: Rosenberg E, DeLong EF, Lory S, Stackebrandt E, Thompson F, editors. The Prokaryotes: Firmicutes and Tenericutes. Berlin, Heidelberg: Springer Berlin Heidelberg; 2014. p. 367-70.
105. Lora-Tamayo J, Senneville É, Ribera A, Bernard L, Dupon M, Zeller V, et al. The Not-So-Good Prognosis of Streptococcal Periprosthetic Joint Infection Managed by Implant Retention: The Results of a Large Multicenter Study. Clinical Infectious Diseases. 2017;64(12):1742-52.
106. Yadav P, Verma S, Bauer R, Kumari M, Dua M, Johri AK, et al. Deciphering Streptococcal Biofilms. Microorganisms. 2020;8(11):1835.
107. García-Solache M, Rice LB. The Enterococcus: a Model of Adaptability to Its Environment. Clinical Microbiology Reviews. 2019;32(2):e00058-18.
108. Thompson O, Rasmussen M, Stefánsdóttir A, Christensson B, Åkesson P. A population-based study on the treatment and outcome of enterococcal prosthetic joint infections. A consecutive series of 55 cases. J Bone Joint Infect. 2019;4(6):285-91.
109. Renz N, Trebse R, Akgün D, Perka C, Trampuz A. Enterococcal periprosthetic joint infection: clinical and microbiological findings from an 8-year retrospective cohort study. BMC infectious diseases. 2019;19(1):1083.
110. Achermann Y, Goldstein EJ, Coenye T, Shirtliff ME. Propionibacterium acnes: from commensal to opportunistic biofilm-associated implant pathogen. Clin Microbiol Rev. 2014;27(3):419-40.
111. Pottinger P, Butler-Wu S, Neradilek MB, Merritt A, Bertelsen A, Jette JL, et al. Prognostic Factors for Bacterial Cultures Positive for Propionibacterium acnes and Other Organisms in a Large Series of Revision Shoulder Arthroplasties Performed for Stiffness, Pain, or Loosening. JBJS. 2012;94(22):2075-83.
112. Zeller V, Ghorbani A, Strady C, Leonard P, Mamoudy P, Desplaces N. Propionibacterium acnes: An agent of prosthetic joint infection and colonization. Journal of Infection. 2007;55(2):119-24.

113. Jacobs AME, Van Hooff ML, Meis JF, Vos F, Goosen JHM. Treatment of prosthetic joint infections due to Propionibacterium. Acta Orthopaedica. 2016;87(1):60-6.
114. Vilchez HH, Escudero-Sanchez R, Fernandez-Sampedro M, Murillo O, Auñón Á, Rodríguez-Pardo D, et al. Prosthetic Shoulder Joint Infection by Cutibacterium acnes: Does Rifampin Improve Prognosis? A Retrospective, Multicenter, Observational Study. Antibiotics. 2021;10(5):475.
115. Flurin L, Greenwood-Quaintance KE, Patel R. Microbiology of polymicrobial prosthetic joint infection. Diagnostic Microbiology and Infectious Disease. 2019;94(3):255-9.
116. Tan TL, Kheir MM, Tan DD, Parvizi J. Polymicrobial Periprosthetic Joint Infections: Outcome of Treatment and Identification of Risk Factors. JBJS. 2016;98(24):2082-8.
117. Tyner H, Patel R. Propionibacterium acnes biofilm – A sanctuary for Staphylococcus aureus? Anaerobe. 2016;40:63-7.
118. Vandecandelaere I, Van Nieuwerburgh F, Deforce D, Coenye T. Metabolic activity, urease production, antibiotic resistance and virulence in dual species biofilms of Staphylococcus epidermidis and Staphylococcus aureus. PloS one. 2017;12(3):e0172700-e.
119. Escudero-Sanchez R, Senneville E, Digumber M, Soriano A, Del Toro MD, Bahamonde A, et al. Suppressive antibiotic therapy in prosthetic joint infections: a multicentre cohort study. Clin Microbiol Infect. 2020;26(4):499-505.
120. Haasper C, Buttaro M, Hozack W, Aboltins CA, Borens O, Callaghan JJ, et al. Irrigation and Debridement. The Journal of Arthroplasty. 2014;29(2, Supplement):100-3.
121. Argenson JN, Arndt M, Babis G, Battenberg A, Budhiparama N, Catani F, et al. Hip and Knee Section, Treatment, Debridement and Retention of Implant: Proceedings of International Consensus on Orthopedic Infections. J Arthroplasty. 2019;34(2S):S399-S419.
122. Garrido-Gomez J, Arrabal-Polo MA, Giron-Prieto MS, Cabello-Salas J, Torres-Barroso J, Parra-Ruiz J. Descriptive analysis of the economic costs of periprosthetic joint infection of the knee for the public health system of Andalusia. J Arthroplasty. 2013;28(7):1057-60.
123. Brimmo O, Ramanathan D, Schiltz NK, Pillai AL, Klika AK, Barsoum WK. Irrigation and Debridement Before a 2-Stage Revision Total Knee Arthroplasty Does Not Increase Risk of Failure. J Arthroplasty. 2016;31(2):461-4.

124. Wouthuyzen-Bakker M, Sebillotte M, Lomas J, Taylor A, Palomares EB, Murillo O, et al. Clinical outcome and risk factors for failure in late acute prosthetic joint infections treated with debridement and implant retention. J Infect. 2019;78(1):40-7.
125. Duque AF, Post ZD, Lutz RW, Orozco FR, Pulido SH, Ong AC. Is There Still a Role for Irrigation and Debridement With Liner Exchange in Acute Periprosthetic Total Knee Infection? J Arthroplasty. 2017;32(4):1280-4.
126. Bialecki J, Bucsi L, Fernando N, Foguet P, Guo S, Haddad F, et al. Hip and Knee Section, Treatment, One Stage Exchange: Proceedings of International Consensus on Orthopedic Infections. The Journal of Arthroplasty. 2019;34(2, Supplement):S421-S6.
127. Aalirezaie A, Abolghasemian M, Busato T, Dennis D, Ghazavi M, Holst DC, et al. Hip and Knee Section, Treatment, Two-Stage Exchange: Proceedings of International Consensus on Orthopedic Infections. The Journal of Arthroplasty. 2019;34(2, Supplement):S439-S43.
128. Klouche S, Leonard P, Zeller V, Lhotellier L, Graff W, Leclerc P, et al. Infected total hip arthroplasty revision: One- or two-stage procedure? Orthopaedics & Traumatology: Surgery & Research. 2012;98(2):144-50.
129. Choi H-R, Kwon Y-M, Freiberg AA, Malchau H. Comparison of One-Stage Revision With Antibiotic Cement Versus Two-Stage Revision Results for Infected Total Hip Arthroplasty. The Journal of Arthroplasty. 2013;28(8, Supplement):66-70.
130. Boettner F, Cross MB, Nam D, Kluthe T, Schulte M, Goetze C. Functional and Emotional Results Differ After Aseptic vs Septic Revision Hip Arthroplasty. HSS J. 2011;7(3):235-8.
131. Kurtz SM, Lau EC, Son M-S, Chang ET, Zimmerli W, Parvizi J. Are We Winning or Losing the Battle With Periprosthetic Joint Infection: Trends in Periprosthetic Joint Infection and Mortality Risk for the Medicare Population. The Journal of Arthroplasty. 2018;33(10):3238-45.
132. Kheir MM, Tan TL, Gomez MM, Chen AF, Parvizi J. Patients With Failed Prior Two-Stage Exchange Have Poor Outcomes After Further Surgical Intervention. The Journal of Arthroplasty. 2017;32(4):1262-5.
133. Kalra KP, Lin KK, Bozic KJ, Ries MD. Repeat 2-Stage Revision for Recurrent Infection of Total Hip Arthroplasty. The Journal of Arthroplasty. 2010;25(6):880-4.
134. Ghazavi M, Mortazavi J, Patzakis M, Sheehan E, Tan TL, Yazdi H. Hip and Knee Section, Treatment, Salvage: Proceedings of International

Consensus on Orthopedic Infections. The Journal of Arthroplasty. 2019;34(2, Supplement):S459-S62.
135. Orfanos AV, Michael RJ, Keeney BJ, Moschetti WE. Patient-reported outcomes after above-knee amputation for prosthetic joint infection. Knee. 2020;27(3):1101-5.
136. Vincenten CM, Den Oudsten BL, Bos PK, Bolder SBT, Gosens T. Quality of life and health status after Girdlestone resection arthroplasty in patients with an infected total hip prosthesis. Journal of bone and joint infection. 2019;4(1):10-5.
137. Chalmers BP, Matrka AK, Sems SA, Abdel MP, Sierra RJ, Hanssen AD, et al. Two-stage arthrodesis for complex, failed, infected total knee arthroplasty. Bone Joint J. 2020;102-b(6_Supple_A):170-5.
138. Pradier M, Robineau O, Boucher A, Titecat M, Blondiaux N, Valette M, et al. Suppressive antibiotic therapy with oral tetracyclines for prosthetic joint infections: a retrospective study of 78 patients. Infection. 2018;46(1):39-47.
139. American Academy of Orthopaedic Surgeons. Diagnosis and Prevention of Periprosthetic Joint Infections Evidence-Based Clinical Practice Guideline. 2019 [updated March 11, 2019. Available from: https://www.aaos.org/globalassets/quality-and-practice-resources/pji/pji-clinical-practice-guideline-final-9-18-19-.pdf
140. Bernard L, Arvieux C, Brunschweiler B, Touchais S, Ansart S, Bru J-P, et al. Antibiotic Therapy for 6 or 12 Weeks for Prosthetic Joint Infection. New England Journal of Medicine. 2021;384(21):1991-2001.
141. Wouthuyzen-Bakker M, Tornero E, Morata L, Nannan Panday PV, Jutte PC, Bori G, et al. Moxifloxacin plus rifampin as an alternative for levofloxacin plus rifampin in the treatment of a prosthetic joint infection with Staphylococcus aureus. International Journal of Antimicrobial Agents. 2018;51(1):38-42.
142. Donlan RM, Costerton JW. Biofilms: survival mechanisms of clinically relevant microorganisms. Clinical microbiology reviews. 2002;15(2):167-93.
143. Leeuwenhoek AV. IV. An extract of a letter from Mr. Anth. Van Leuwenhoek, concerning animalcules found on the teeth; of the scaleyness of the skin, &c. Philosophical Transactions of the Royal Society of London. 1693;17(197):646-9.
144. Christensen GD, Simpson WA, Bisno AL, Beachey EH. Adherence of slime-producing strains of Staphylococcus epidermidis to smooth surfaces. Infect Immun. 1982;37(1):318-26.

145. Marrie TJ, Nelligan J, Costerton JW. A scanning and transmission electron microscopic study of an infected endocardial pacemaker lead. Circulation. 1982;66(6):1339-41.
146. Tunney MM, Patrick S, Gorman SP, Nixon JR, Anderson N, Davis RI, et al. Improved detection of infection in hip replacements. A currently underestimated problem. J Bone Joint Surg Br. 1998;80(4):568-72.
147. Neut D, van Horn JR, van Kooten TG, van der Mei HC, Busscher HJ. Detection of biomaterial-associated infections in orthopaedic joint implants. Clin Orthop Relat Res. 2003(413):261-8.
148. Stoodley P, Conti SF, DeMeo PJ, Nistico L, Melton-Kreft R, Johnson S, et al. Characterization of a mixed MRSA/MRSE biofilm in an explanted total ankle arthroplasty. FEMS Immunol Med Microbiol. 2011;62(1):66-74.
149. Zimmerli W, Sendi P. Orthopaedic biofilm infections. APMIS : acta pathologica, microbiologica, et immunologica Scandinavica. 2017;125(4):353-64.
150. Arciola CR, Campoccia D, Speziale P, Montanaro L, Costerton JW. Biofilm formation in Staphylococcus implant infections. A review of molecular mechanisms and implications for biofilm-resistant materials. Biomaterials. 2012;33(26):5967-82.
151. Heilmann C, Hussain M, Peters G, Götz F. Evidence for autolysin-mediated primary attachment of Staphylococcus epidermidis to a polystyrene surface. Mol Microbiol. 1997;24(5):1013-24.
152. Alam F, Balani K. Adhesion force of staphylococcus aureus on various biomaterial surfaces. J Mech Behav Biomed Mater. 2017;65:872-80.
153. Ivanova EP, Truong VK, Webb HK, Baulin VA, Wang JY, Mohammodi N, et al. Differential attraction and repulsion of Staphylococcus aureus and Pseudomonas aeruginosa on molecularly smooth titanium films. Sci Rep. 2011;1:165-.
154. Schildhauer TA, Robie B, Muhr G, Koller M. Bacterial adherence to tantalum versus commonly used orthopedic metallic implant materials. J Orthop Trauma. 2006;20(7):476-84.
155. Koseki H, Yonekura A, Shida T, Yoda I, Horiuchi H, Morinaga Y, et al. Early Staphylococcal Biofilm Formation on Solid Orthopaedic Implant Materials: In Vitro Study. PLOS ONE. 2014;9(10):e107588.
156. Naylor PT, Myrvik QN, Gristina A. Antibiotic Resistance of Biomaterial-Adherent Coagulase-Negative and Coagulase-Positive Staphylococci. Clinical Orthopaedics and Related Research®. 1990;261:126-33.

157. Baier RE, Meyer AE, Natiella JR, Natiella RR, Carter JM. Surface properties determine bioadhesive outcomes: Methods and results. Journal of Biomedical Materials Research. 1984;18(4):337-55.
158. Paharik AE, Horswill AR. The Staphylococcal Biofilm: Adhesins, Regulation, and Host Response. Microbiol Spectr. 2016;4(2):10.1128/microbiolspec.VMBF-0022-2015.
159. Clarke SR, Foster SJ. Surface Adhesins of Staphylococcus aureus. In: Poole RK, editor. Advances in microbial physiology. 51: Academic Press; 2006. p. 187-224.
160. Chahales P, Thanassi DG. Structure, Function, and Assembly of Adhesive Organelles by Uropathogenic Bacteria. Microbiology spectrum. 2015;3(5):10.1128/microbiolspec.UTI-0018-2013.
161. Harapanahalli AK, Chen Y, Li J, Busscher HJ, van der Mei HC. Influence of Adhesion Force on icaA and cidA Gene Expression and Production of Matrix Components in Staphylococcus aureus Biofilms. Applied and environmental microbiology. 2015;81(10):3369-78.
162. Ranieri MR, Whitchurch CB, Burrows LL. Mechanisms of biofilm stimulation by subinhibitory concentrations of antimicrobials. Current opinion in microbiology. 2018;45:164-9.
163. Hou J, Veeregowda DH, van de Belt-Gritter B, Busscher HJ, van der Mei HC. Extracellular Polymeric Matrix Production and Relaxation under Fluid Shear and Mechanical Pressure in Staphylococcus aureus Biofilms. Applied and environmental microbiology. 2018;84(1):e01516-17.
164. Thoendel M, Kavanaugh JS, Flack CE, Horswill AR. Peptide signaling in the staphylococci. Chem Rev. 2011;111(1):117-51.
165. Boles BR, Horswill AR. Agr-mediated dispersal of Staphylococcus aureus biofilms. PLoS pathogens. 2008;4(4):e1000052-e.
166. Sloan TJ, Murray E, Yokoyama M, Massey RC, Chan WC, Bonev BB, et al. Timing Is Everything: Impact of Naturally Occurring Staphylococcus aureus AgrC Cytoplasmic Domain Adaptive Mutations on Autoinduction. Journal of bacteriology. 2019;201(20):e00409-19.
167. Flemming HC, Wingender J, Szewzyk U, Steinberg P, Rice SA, Kjelleberg S. Biofilms: an emergent form of bacterial life. Nat Rev Microbiol. 2016;14(9):563-75.
168. Izano EA, Amarante MA, Kher WB, Kaplan JB. Differential roles of poly-N-acetylglucosamine surface polysaccharide and extracellular DNA in Staphylococcus aureus and Staphylococcus epidermidis biofilms. Applied and environmental microbiology. 2008;74(2):470-6.

169. Wang X, Preston JF, 3rd, Romeo T. The pgaABCD locus of Escherichia coli promotes the synthesis of a polysaccharide adhesin required for biofilm formation. J Bacteriol. 2004;186(9):2724-34.
170. Rohde H, Burandt EC, Siemssen N, Frommelt L, Burdelski C, Wurster S, et al. Polysaccharide intercellular adhesin or protein factors in biofilm accumulation of Staphylococcus epidermidis and Staphylococcus aureus isolated from prosthetic hip and knee joint infections. Biomaterials. 2007;28(9):1711-20.
171. Sabate Bresco M, Harris LG, Thompson K, Stanic B, Morgenstern M, O'Mahony L, et al. Pathogenic Mechanisms and Host Interactions in Staphylococcus epidermidis Device-Related Infection. Front Microbiol. 2017;8:1401.
172. Schilcher K, Horswill AR. Staphylococcal Biofilm Development: Structure, Regulation, and Treatment Strategies. Microbiology and Molecular Biology Reviews. 2020;84(3):e00026-19.
173. Ulrich M, Bastian M, Cramton SE, Ziegler K, Pragman AA, Bragonzi A, et al. The staphylococcal respiratory response regulator SrrAB induces ica gene transcription and polysaccharide intercellular adhesin expression, protecting Staphylococcus aureus from neutrophil killing under anaerobic growth conditions. Mol Microbiol. 2007;65(5):1276-87.
174. Knobloch JK-M, Bartscht K, Sabottke A, Rohde H, Feucht H-H, Mack D. Biofilm Formation by Staphylococcus epidermidis Depends on Functional RsbU, an Activator of the sigB Operon: Differential Activation Mechanisms Due to Ethanol and Salt Stress. Journal of Bacteriology. 2001;183(8):2624-33.
175. Rode TM, Langsrud S, Holck A, Møretrø T. Different patterns of biofilm formation in Staphylococcus aureus under food-related stress conditions. Int J Food Microbiol. 2007;116(3):372-83.
176. Rachid S, Ohlsen K, Witte W, Hacker J, Ziebuhr W. Effect of subinhibitory antibiotic concentrations on polysaccharide intercellular adhesin expression in biofilm-forming Staphylococcus epidermidis. Antimicrob Agents Chemother. 2000;44(12):3357-63.
177. Cerca N, Jefferson KK. Effect of growth conditions on poly-N-acetylglucosamine expression and biofilm formation in Escherichia coli. FEMS Microbiology Letters. 2008;283(1):36-41.
178. Zogaj X, Bokranz W, Nimtz M, Römling U. Production of cellulose and curli fimbriae by members of the family Enterobacteriaceae isolated from the human gastrointestinal tract. Infection and immunity. 2003;71(7):4151-8.

179. Solano C, García B, Valle J, Berasain C, Ghigo JM, Gamazo C, et al. Genetic analysis of Salmonella enteritidis biofilm formation: critical role of cellulose. Mol Microbiol. 2002;43(3):793-808.
180. Høiby N, Ciofu O, Bjarnsholt T. Pseudomonas aeruginosa biofilms in cystic fibrosis. Future microbiology. 2010;5(11):1663-74.
181. Whitchurch CB, Tolker-Nielsen T, Ragas PC, Mattick JS. Extracellular DNA required for bacterial biofilm formation. Science. 2002;295(5559):1487.
182. Das T, Sharma PK, Busscher HJ, van der Mei HC, Krom BP. Role of Extracellular DNA in Initial Bacterial Adhesion and Surface Aggregation. Applied and environmental microbiology. 2010;76(10):3405-8.
183. Das T, Sehar S, Manefield M. The roles of extracellular DNA in the structural integrity of extracellular polymeric substance and bacterial biofilm development. Environ Microbiol Rep. 2013;5(6):778-86.
184. Ibáñez de Aldecoa AL, Zafra O, González-Pastor JE. Mechanisms and Regulation of Extracellular DNA Release and Its Biological Roles in Microbial Communities. Frontiers in Microbiology. 2017;8(1390).
185. Hamilton HL, Domínguez NM, Schwartz KJ, Hackett KT, Dillard JP. Neisseria gonorrhoeae secretes chromosomal DNA via a novel type IV secretion system. Mol Microbiol. 2005;55(6):1704-21.
186. Thomas VC, Hiromasa Y, Harms N, Thurlow L, Tomich J, Hancock LE. A fratricidal mechanism is responsible for eDNA release and contributes to biofilm development of Enterococcus faecalis. Mol Microbiol. 2009;72(4):1022-36.
187. Alhede M, Alhede M, Qvortrup K, Kragh KN, Jensen PØ, Stewart PS, et al. The origin of extracellular DNA in bacterial biofilm infections in vivo. Pathogens and Disease. 2020;78(2).
188. Speziale P, Pietrocola G, Foster TJ, Geoghegan JA. Protein-based biofilm matrices in Staphylococci. Front Cell Infect Microbiol. 2014;4:171.
189. Tielen P, Kuhn H, Rosenau F, Jaeger K-E, Flemming H-C, Wingender J. Interaction between extracellular lipase LipA and the polysaccharide alginate of Pseudomonas aeruginosa. BMC microbiology. 2013;13:159-.
190. Zhang W, Sun J, Ding W, Lin J, Tian R, Lu L, et al. Extracellular matrix-associated proteins form an integral and dynamic system during Pseudomonas aeruginosa biofilm development. Frontiers in cellular and infection microbiology. 2015;5:40-.
191. König B, Jaeger KE, Sage AE, Vasil ML, König W. Role of Pseudomonas aeruginosa lipase in inflammatory mediator release from

human inflammatory effector cells (platelets, granulocytes, and monocytes. Infection and Immunity. 1996;64(8):3252-8.
192. Amanatidou E, Matthews AC, Kuhlicke U, Neu TR, McEvoy JP, Raymond B. Biofilms facilitate cheating and social exploitation of β-lactam resistance in Escherichia coli. npj Biofilms and Microbiomes. 2019;5(1):36.
193. Le KY, Villaruz AE, Zheng Y, He L, Fisher EL, Nguyen TH, et al. Role of Phenol-Soluble Modulins in Staphylococcus epidermidis Biofilm Formation and Infection of Indwelling Medical Devices. Journal of Molecular Biology. 2019;431(16):3015-27.
194. Kaplan JB, Velliyagounder K, Ragunath C, Rohde H, Mack D, Knobloch JKM, et al. Genes involved in the synthesis and degradation of matrix polysaccharide in Actinobacillus actinomycetemcomitans and Actinobacillus pleuropneumoniae biofilms. Journal of bacteriology. 2004;186(24):8213-20.
195. Kogan G, Sadovskaya I, Chaignon P, Chokr A, Jabbouri S. Biofilms of clinical strains of Staphylococcus that do not contain polysaccharide intercellular adhesin. FEMS Microbiology Letters. 2006;255(1):11-6.
196. O'Neill E, Pozzi C, Houston P, Humphreys H, Robinson DA, Loughman A, et al. A novel Staphylococcus aureus biofilm phenotype mediated by the fibronectin-binding proteins, FnBPA and FnBPB. J Bacteriol. 2008;190(11):3835-50.
197. Abraham NM, Jefferson KK. Staphylococcus aureus clumping factor B mediates biofilm formation in the absence of calcium. Microbiology (Reading). 2012;158(Pt 6):1504-12.
198. Barbu EM, Mackenzie C, Foster TJ, Höök M. SdrC induces staphylococcal biofilm formation through a homophilic interaction. Mol Microbiol. 2014;94(1):172-85.
199. Schroeder K, Jularic M, Horsburgh SM, Hirschhausen N, Neumann C, Bertling A, et al. Molecular characterization of a novel Staphylococcus aureus surface protein (SasC) involved in cell aggregation and biofilm accumulation. PLoS One. 2009;4(10):e7567.
200. Geoghegan JA, Corrigan RM, Gruszka DT, Speziale P, O'Gara JP, Potts JR, et al. Role of surface protein SasG in biofilm formation by Staphylococcus aureus. J Bacteriol. 2010;192(21):5663-73.
201. Merino N, Toledo-Arana A, Vergara-Irigaray M, Valle J, Solano C, Calvo E, et al. Protein A-mediated multicellular behavior in Staphylococcus aureus. J Bacteriol. 2009;191(3):832-43.

202. Schwartz K, Syed AK, Stephenson RE, Rickard AH, Boles BR. Functional amyloids composed of phenol soluble modulins stabilize Staphylococcus aureus biofilms. PLoS Pathog. 2012;8(6):e1002744.
203. Brauner A, Fridman O, Gefen O, Balaban NQ. Distinguishing between resistance, tolerance and persistence to antibiotic treatment. Nat Rev Microbiol. 2016;14(5):320-30.
204. Ceri H, Olson ME, Stremick C, Read RR, Morck D, Buret A. The Calgary Biofilm Device: new technology for rapid determination of antibiotic susceptibilities of bacterial biofilms. J Clin Microbiol. 1999;37(6):1771-6.
205. Mah TF, O'Toole GA. Mechanisms of biofilm resistance to antimicrobial agents. Trends Microbiol. 2001;9(1):34-9.
206. Hoyle BD, Alcantara J, Costerton JW. Pseudomonas aeruginosa biofilm as a diffusion barrier to piperacillin. Antimicrobial Agents and Chemotherapy. 1992;36(9):2054-6.
207. Suci PA, Mittelman MW, Yu FP, Geesey GG. Investigation of ciprofloxacin penetration into Pseudomonas aeruginosa biofilms. Antimicrobial Agents and Chemotherapy. 1994;38(9):2125-33.
208. De Beer D, Srinivasan R, Stewart PS. Direct measurement of chlorine penetration into biofilms during disinfection. Applied and environmental microbiology. 1994;60(12):4339-44.
209. Shigeta M, Tanaka G, Komatsuzawa H, Sugai M, Suginaka H, Usui T. Permeation of Antimicrobial Agents through Pseudomonas aeruginosa Biofilms: A Simple Method. Chemotherapy. 1997;43(5):340-5.
210. Zheng Z, Stewart PS. Penetration of Rifampin through Staphylococcus epidermidis Biofilms. Antimicrobial Agents and Chemotherapy. 2002;46(3):900-3.
211. Huang CT, Xu KD, McFeters GA, Stewart PS. Spatial patterns of alkaline phosphatase expression within bacterial colonies and biofilms in response to phosphate starvation. Applied and environmental microbiology. 1998;64(4):1526-31.
212. Sternberg C, Christensen BB, Johansen T, Toftgaard Nielsen A, Andersen JB, Givskov M, et al. Distribution of bacterial growth activity in flow-chamber biofilms. Applied and environmental microbiology. 1999;65(9):4108-17.
213. Tanaka G, Shigeta M, Komatsuzawa H, Sugai M, Suginaka H, Usui T. Effect of the growth rate of Pseudomonas aeruginosa biofilms on the susceptibility to antimicrobial agents: beta-lactams and fluoroquinolones. Chemotherapy. 1999;45(1):28-36.

214. Walters MC, 3rd, Roe F, Bugnicourt A, Franklin MJ, Stewart PS. Contributions of antibiotic penetration, oxygen limitation, and low metabolic activity to tolerance of Pseudomonas aeruginosa biofilms to ciprofloxacin and tobramycin. Antimicrob Agents Chemother. 2003;47(1):317-23.
215. Liao J, Sauer K. The MerR-like transcriptional regulator BrlR contributes to Pseudomonas aeruginosa biofilm tolerance. Journal of bacteriology. 2012;194(18):4823-36.
216. Liao J, Schurr MJ, Sauer K. The MerR-like regulator BrlR confers biofilm tolerance by activating multidrug efflux pumps in Pseudomonas aeruginosa biofilms. Journal of bacteriology. 2013;195(15):3352-63.
217. Kvist M, Hancock V, Klemm P. Inactivation of efflux pumps abolishes bacterial biofilm formation. Applied and environmental microbiology. 2008;74(23):7376-82.
218. Lewis K. Multidrug tolerance of biofilms and persister cells. Curr Top Microbiol Immunol. 2008;322:107-31.
219. Molin S, Tolker-Nielsen T. Gene transfer occurs with enhanced efficiency in biofilms and induces enhanced stabilisation of the biofilm structure. Current Opinion in Biotechnology. 2003;14(3):255-61.
220. Reisner A, Höller BM, Molin S, Zechner EL. Synergistic Effects in Mixed Escherichia coli Biofilms: Conjugative Plasmid Transfer Drives Biofilm Expansion. Journal of Bacteriology. 2006;188(10):3582-8.
221. Águila-Arcos S, Álvarez-Rodríguez I, Garaiyurrebaso O, Garbisu C, Grohmann E, Alkorta I. Biofilm-Forming Clinical Staphylococcus Isolates Harbor Horizontal Transfer and Antibiotic Resistance Genes. Frontiers in Microbiology. 2017;8(2018).
222. Hughes D, Andersson DI. Selection of resistance at lethal and non-lethal antibiotic concentrations. Current opinion in microbiology. 2012;15(5):555-60.
223. Lebeaux D, Ghigo JM, Beloin C. Biofilm-related infections: bridging the gap between clinical management and fundamental aspects of recalcitrance toward antibiotics. Microbiol Mol Biol Rev. 2014;78(3):510-43.
224. Roilides E, Simitsopoulou M, Katragkou A, Walsh TJ. How Biofilms Evade Host Defenses. Microbiol Spectr. 2015;3(3):287-300.
225. Günther F, Wabnitz GH, Stroh P, Prior B, Obst U, Samstag Y, et al. Host defence against Staphylococcus aureus biofilms infection: phagocytosis of biofilms by polymorphonuclear neutrophils (PMN). Mol Immunol. 2009;46(8-9):1805-13.

226. Thurlow LR, Hanke ML, Fritz T, Angle A, Aldrich A, Williams SH, et al. Staphylococcus aureus biofilms prevent macrophage phagocytosis and attenuate inflammation in vivo. J Immunol. 2011;186(11):6585-96.
227. Kristian SA, Birkenstock TA, Sauder U, Mack D, Götz F, Landmann R. Biofilm Formation Induces C3a Release and Protects Staphylococcus epidermidis from IgG and Complement Deposition and from Neutrophil-Dependent Killing. The Journal of Infectious Diseases. 2008;197(7):1028-35.
228. Hanke ML, Angle A, Kielian T. MyD88-dependent signaling influences fibrosis and alternative macrophage activation during Staphylococcus aureus biofilm infection. PLoS One. 2012;7(8):e42476.
229. Thurlow LR, Hanke ML, Fritz T, Angle A, Aldrich A, Williams SH, et al. Staphylococcus aureus Biofilms Prevent Macrophage Phagocytosis and Attenuate Inflammation In Vivo. The Journal of Immunology. 2011;186(11):6585-96.
230. Scherr TD, Hanke ML, Huang O, James DB, Horswill AR, Bayles KW, et al. Staphylococcus aureus Biofilms Induce Macrophage Dysfunction Through Leukocidin AB and Alpha-Toxin. mBio. 2015;6(4).
231. Peschel A, Otto M. Phenol-soluble modulins and staphylococcal infection. Nat Rev Microbiol. 2013;11(10):667-73.
232. Lebeaux D, Chauhan A, Rendueles O, Beloin C. From in vitro to in vivo Models of Bacterial Biofilm-Related Infections. Pathogens. 2013;2(2):288-356.
233. Diaz Iglesias Y, Van Bambeke F. Activity of Antibiotics against Pseudomonas aeruginosa in an In Vitro Model of Biofilms in the Context of Cystic Fibrosis: Influence of the Culture Medium. Antimicrob Agents Chemother. 2020;64(4).
234. Diaz Iglesias Y, Wilms T, Vanbever R, Van Bambeke F. Activity of Antibiotics against Staphylococcus aureus in an In Vitro Model of Biofilms in the Context of Cystic Fibrosis: Influence of the Culture Medium. Antimicrob Agents Chemother. 2019;63(7):AAC.00602-19.
235. ASTM E2799-17, Standard Test Method for Testing Disinfectant Efficacy against Pseudomonas aeruginosa Biofilm using the MBEC Assay. West Conshohocken, PA, USA: ASTM International; 2017.
236. Harrison JJ, Ceri H, Yerly J, Stremick CA, Hu Y, Martinuzzi R, et al. The use of microscopy and three-dimensional visualization to evaluate the structure of microbial biofilms cultivated in the Calgary Biofilm Device. Biol Proced Online. 2006;8:194-215.
237. Salek MM, Jones SM, Martinuzzi RJ, editors. Methicillin resistant Staphylococcus aureus biofilm susceptibility in response to increased level of

shear stresses and flow agitation. 2009 IEEE 35th Annual Northeast Bioengineering Conference; 2009 3-5 April 2009.
238. Tomlin KL, Malott RJ, Ramage G, Storey DG, Sokol PA, Ceri H. Quorum-Sensing Mutations Affect Attachment and Stability of Burkholderia cenocepacia Biofilms. Applied and environmental microbiology. 2005;71(9):5208.
239. Patel SS, Aruni W, Inceoglu S, Akpolat YT, Botimer GD, Cheng WK, et al. A comparison of Staphylococcus aureus biofilm formation on cobalt-chrome and titanium-alloy spinal implants. J Clin Neurosci. 2016;31:219-23.
240. Kaur S, Harjai K, Chhibber S. In Vivo Assessment of Phage and Linezolid Based Implant Coatings for Treatment of Methicillin Resistant S. aureus (MRSA) Mediated Orthopaedic Device Related Infections. PloS one. 2016;11(6):e0157626-e.
241. Jennings JA, Carpenter DP, Troxel KS, Beenken KE, Smeltzer MS, Courtney HS, et al. Novel Antibiotic-loaded Point-of-care Implant Coating Inhibits Biofilm. Clin Orthop Relat Res. 2015;473(7):2270-82.
242. Drago L, Romano CL, Mattina R, Signori V, De Vecchi E. Does dithiothreitol improve bacterial detection from infected prostheses? A pilot study. Clin Orthop Relat Res. 2012;470(10):2915-25.
243. Belfield K, Bayston R, Hajduk N, Levell G, Birchall JP, Daniel M. Evaluation of combinations of putative anti-biofilm agents and antibiotics to eradicate biofilms of Staphylococcus aureus and Pseudomonas aeruginosa. J Antimicrob Chemother. 2017;72(9):2531-8.
244. Schwechter EM, Folk D, Varshney AK, Fries BC, Kim SJ, Hirsh DM. Optimal irrigation and debridement of infected joint implants: an in vitro methicillin-resistant Staphylococcus aureus biofilm model. J Arthroplasty. 2011;26(6 Suppl):109-13.
245. Coenye T, Nelis HJ. In vitro and in vivo model systems to study microbial biofilm formation. J Microbiol Methods. 2010;83(2):89-105.
246. Honraet K, Goetghebeur E, Nelis HJ. Comparison of three assays for the quantification of Candida biomass in suspension and CDC reactor grown biofilms. Journal of Microbiological Methods. 2005;63(3):287-95.
247. Goeres DM, Loetterle LR, Hamilton MA, Murga R, Kirby DW, Donlan RM. Statistical assessment of a laboratory method for growing biofilms. Microbiology. 2005;151(3):757-62.
248. Microbiology Laboratory MB-19-05: Preparing a Pseudomonas aeruginosa or Staphylococcus aureus Biofilm using the CDC Biofilm Reactor. Ft. Meade, MD: Office of Pesticide Programs,; 2020.

249. ASTM E2562-17, Standard Test Method for Quantification of Pseudomonas aeruginosa Biofilm Grown with High Shear and Continuous Flow using CDC Biofilm Reactor. West Conshohocken, PA, USA: ASTM International; 2017.
250. Ashton NN, Allyn G, Porter ST, Haussener TJ, Sebahar PR, Looper RE, et al. In vitro testing of a first-in-class tri-alkylnorspermidine-biaryl antibiotic in an anti-biofilm silicone coating. Acta Biomaterialia. 2019;93:25-35.
251. Kang J, Dietz MJ, Li B. Antimicrobial peptide LL-37 is bactericidal against Staphylococcus aureus biofilms. PloS one. 2019;14(6):e0216676-e.
252. Siala W, Rodriguez-Villalobos H, Fernandes P, Tulkens PM, Van Bambeke F. Activities of Combinations of Antistaphylococcal Antibiotics with Fusidic Acid against Staphylococcal Biofilms in In Vitro Static and Dynamic Models. Antimicrob Agents Chemother. 2018;62(7).
253. El Haj C, Murillo O, Ribera A, Lloberas N, Gómez-Junyent J, Tubau F, et al. Evaluation of linezolid or trimethoprim/sulfamethoxazole in combination with rifampicin as alternative oral treatments based on an in vitro pharmacodynamic model of staphylococcal biofilm. Int J Antimicrob Agents. 2018;51(6):854-61.
254. ASTM E2647-20, Standard Test Method for Quantification of Pseudomonas aeruginosa Biofilm Grown Using Drip Flow Biofilm Reactor with Low Shear and Continuous Flow. West Conshohocken, PA, USA: ASTM International; 2020.
255. Leonetti S, Tuvo B, Campanella B, Legnaioli S, Onor M, Bramanti E, et al. Evaluation of Microbial Adhesion and Biofilm Formation on Nano-Structured and Nano-Coated Ortho-Prosthetic Materials by a Dynamic Model. Int J Environ Res Public Health. 2020;17(3):1013.
256. O'Donnell JA, Wu M, Cochrane NH, Belay E, Myntti MF, James GA, et al. Efficacy of common antiseptic solutions against clinically relevant microorganisms in biofilm. The Bone & Joint Journal. 2021;103-B(5):908-15.
257. Gupta TT, Gupta NK, Pestrak MJ, Dusane DH, Harro JM, Horswill AR, et al. Staphylococcus aureus Aggregates on Orthopedic Materials under Varying Levels of Shear Stress. Applied and environmental microbiology. 2020;86(19):e01234-20.
258. Zimmerli W, Waldvogel FA, Vaudaux P, Nydegger UE. Pathogenesis of foreign body infection: description and characteristics of an animal model. J Infect Dis. 1982;146(4):487-97.

259. Murillo O, Doménech A, Garcia A, Tubau F, Cabellos C, Gudiol F, et al. Efficacy of high doses of levofloxacin in experimental foreign-body infection by methicillin-susceptible Staphylococcus aureus. Antimicrobial agents and chemotherapy. 2006;50(12):4011-7.
260. Schwank S, Rajacic Z, Zimmerli W, Blaser J. Impact of bacterial biofilm formation on in vitro and in vivo activities of antibiotics. Antimicrobial agents and chemotherapy. 1998;42(4):895-8.
261. Goerke C, Fluckiger U, Steinhuber A, Zimmerli W, Wolz C. Impact of the regulatory loci agr, sarA and sae of Staphylococcus aureus on the induction of α-toxin during device-related infection resolved by direct quantitative transcript analysis. Mol Microbiol. 2001;40(6):1439-47.
262. Renz N, Trampuz A, Zimmerli W. Controversy about the Role of Rifampin in Biofilm Infections: Is It Justified? Antibiotics. 2021;10(2):165.
263. Landersdorfer CB, Bulitta JB, Kinzig M, Holzgrabe U, Sorgel F. Penetration of antibacterials into bone: pharmacokinetic, pharmacodynamic and bioanalytical considerations. Clinical pharmacokinetics. 2009;48(2):89-124.
264. Roy ME, Peppers MP, Whiteside LA, Lazear RM. Vancomycin concentration in synovial fluid: direct injection into the knee vs. intravenous infusion. J Arthroplasty. 2014;29(3):564-8.
265. Carli AV, Ross FP, Bhimani SJ, Nodzo SR, Bostrom MP. Developing a Clinically Representative Model of Periprosthetic Joint Infection. J Bone Joint Surg Am. 2016;98(19):1666-76.
266. Li D, Gromov K, Soballe K, Puzas JE, O'Keefe RJ, Awad H, et al. Quantitative mouse model of implant-associated osteomyelitis and the kinetics of microbial growth, osteolysis, and humoral immunity. Journal of orthopaedic research : official publication of the Orthopaedic Research Society. 2008;26(1):96-105.
267. Nishitani K, Sutipornpalangkul W, de Mesy Bentley KL, Varrone JJ, Bello-Irizarry SN, Ito H, et al. Quantifying the natural history of biofilm formation in vivo during the establishment of chronic implant-associated Staphylococcus aureus osteomyelitis in mice to identify critical pathogen and host factors. Journal of orthopaedic research : official publication of the Orthopaedic Research Society. 2015;33(9):1311-9.
268. Niska JA, Shahbazian JH, Ramos RI, Francis KP, Bernthal NM, Miller LS. Vancomycin-Rifampin Combination Therapy Has Enhanced Efficacy against an Experimental Staphylococcus aureus Prosthetic Joint Infection. Antimicrobial Agents and Chemotherapy. 2013;57(10):5080.

269. Bernthal NM, Stavrakis AI, Billi F, Cho JS, Kremen TJ, Simon SI, et al. A Mouse Model of Post-Arthroplasty Staphylococcus aureus Joint Infection to Evaluate In Vivo the Efficacy of Antimicrobial Implant Coatings. PLOS ONE. 2010;5(9):e12580.
270. Brunotte M, Rupp M, Stotzel S, Sommer U, Mohammed W, Thormann U, et al. A new small animal model for simulating a two-stage-revision procedure in implant-related methicillin-resistant Staphylococcus aureus bone infection. Injury. 2019;50(11):1921-8.
271. Craig MR, Poelstra KA, Sherrell JC, Kwon MS, Belzile EL, Brown TE. A novel total knee arthroplasty infection model in rabbits. Journal of orthopaedic research : official publication of the Orthopaedic Research Society. 2005;23(5):1100-4.
272. Zhai H, Pan J, Pang E, Bai B. Lavage with allicin in combination with vancomycin inhibits biofilm formation by Staphylococcus epidermidis in a rabbit model of prosthetic joint infection. PLoS One. 2014;9(7):e102760.
273. Cremieux AC, Mghir AS, Bleton R, Manteau M, Belmatoug N, Massias L, et al. Efficacy of sparfloxacin and autoradiographic diffusion pattern of [14C]Sparfloxacin in experimental Staphylococcus aureus joint prosthesis infection. Antimicrob Agents Chemother. 1996;40(9):2111-6.
274. Sipehia R. X-ray Photoelectron Spectroscopy Studies, Surface Tension Measurements, Immobilization of Human Serum Albumin, Human Fibrinogen and Human Fibronectin onto Ammonia Plasma Treated Surfaces of Biomaterials Useful for Cardiovascular Implants and Artificial Cornea Implants. Biomaterials, Artificial Cells and Immobilization Biotechnology. 1993;21(5):647-58.
275. Salehi A, Tsai S, Pawar V, Sprague J, Hunter G, Varma SK, et al. Wettability Analysis of Orthopaedic Materials Using Optical Contact Angle Methods. Key Engineering Materials. 2006;309-311:1199-202.
276. Ni YX, Feng B, Wang J, Lu X, Qu S, Weng J. Decyl bis phosphonate–protein surface modification of Ti–6Al–4V via a layer-by-layer technique. Journal of Materials Science. 2009;44(15):4031-9.
277. Soe NH, Jensen NV, Nurnberg BM, Jensen AL, Koch J, Poulsen SS, et al. A novel knee prosthesis model of implant-related osteomyelitis in rats. Acta Orthop. 2013;84(1):92-7.
278. Carli AV, Bhimani S, Yang X, Shirley MB, de Mesy Bentley KL, Ross FP, et al. Quantification of Peri-Implant Bacterial Load and in Vivo Biofilm Formation in an Innovative, Clinically Representative Mouse Model of Periprosthetic Joint Infection. J Bone Joint Surg Am. 2017;99(6):e25.

279. Sosa BR, Niu Y, Turajane K, Staats K, Suhardi V, Carli A, et al. 2020 John Charnley Award: The antimicrobial potential of bacteriophage-derived lysin in a murine debridement, antibiotics, and implant retention model of prosthetic joint infection. The Bone & Joint Journal. 2020;102-B(7_Supple_B):3-10.
280. López T, II, Sanz-Ruíz P, León-Román VE, Navarro-García F, Priego-Sánchez R, Vaquero-Martín J. 3D printing in experimental orthopaedic surgery: do it yourself. Eur J Orthop Surg Traumatol. 2019;29(5):967-73.
281. López T, II, Sanz-Ruíz P, Navarro-García F, León-Román VE, Vaquero-Martín J. Experimental reproduction of periprosthetic joint infection: Developing a representative animal model. Knee. 2020;27(3):1106-12.
282. Mannala GK, Rupp M, Alagboso F, Kerschbaum M, Pfeifer C, Sommer U, et al. Galleria mellonella as an alternative in vivo model to study bacterial biofilms on stainless steel and titanium implants. Altex. 2021;38(2):245-52.
283. Koch R. Zur Untersuchung von pathogenen Organismen (1881). Robert Koch : Zentrale Texte. Berlin, Heidelberg: Springer Berlin Heidelberg; 2018. p. 45-111.
284. Sutton S. Accuracy of plate counts. Journal of Validation Technology. 2011 2011 Summer:42+.
285. Pasquaroli S, Zandri G, Vignaroli C, Vuotto C, Donelli G, Biavasco F. Antibiotic pressure can induce the viable but non-culturable state in Staphylococcus aureus growing in biofilms. J Antimicrob Chemother. 2013;68(8):1812-7.
286. Mandakhalikar KD, Rahmat JN, Chiong E, Neoh KG, Shen L, Tambyah PA. Extraction and quantification of biofilm bacteria: Method optimized for urinary catheters. Sci Rep. 2018;8(1):8069.
287. Bogachev MI, Volkov VY, Markelov OA, Trizna EY, Baydamshina DR, Melnikov V, et al. Fast and simple tool for the quantification of biofilm-embedded cells sub-populations from fluorescent microscopic images. PloS one. 2018;13(5):e0193267-e.
288. Cerca F, Trigo G, Correia A, Cerca N, Azeredo J, Vilanova M. SYBR green as a fluorescent probe to evaluate the biofilm physiological state of Staphylococcus epidermidis, using flow cytometry. Can J Microbiol. 2011;57(10):850-6.
289. Mountcastle SE, Vyas N, Villapun VM, Cox SC, Jabbari S, Sammons RL, et al. Biofilm viability checker: An open-source tool for automated

biofilm viability analysis from confocal microscopy images. npj Biofilms and Microbiomes. 2021;7(1):44.
290. Trafny EA, Lewandowski R, Zawistowska-Marciniak I, Stępińska M. Use of MTT assay for determination of the biofilm formation capacity of microorganisms in metalworking fluids. World J Microbiol Biotechnol. 2013;29(9):1635-43.
291. O'Brien J, Wilson I, Orton T, Pognan F. Investigation of the Alamar Blue (resazurin) fluorescent dye for the assessment of mammalian cell cytotoxicity. European journal of biochemistry. 2000;267(17):5421-6.
292. Pettit RK, Weber CA, Kean MJ, Hoffmann H, Pettit GR, Tan R, et al. Microplate Alamar blue assay for Staphylococcus epidermidis biofilm susceptibility testing. Antimicrobial Agents and Chemotherapy. 2005;49(7):2612-7.
293. Peeters E, Nelis HJ, Coenye T. Comparison of multiple methods for quantification of microbial biofilms grown in microtiter plates. J Microbiol Methods. 2008;72(2):157-65.
294. Butini ME, Gonzalez Moreno M, Czuban M, Koliszak A, Tkhilaishvili T, Trampuz A, et al. Real-Time Antimicrobial Susceptibility Assay of Planktonic and Biofilm Bacteria by Isothermal Microcalorimetry. In: Donelli G, editor. Advances in Microbiology, Infectious Diseases and Public Health: Volume 13. Cham: Springer International Publishing; 2019. p. 61-77.
295. Braissant O, Bachmann A, Bonkat G. Microcalorimetric assays for measuring cell growth and metabolic activity: Methodology and applications. Methods. 2015;76:27-34.
296. Lewis K. Persister cells. Annu Rev Microbiol. 2010;64:357-72.
297. Stepanovic S, Vukovic D, Hola V, Di Bonaventura G, Djukic S, Cirkovic I, et al. Quantification of biofilm in microtiter plates: overview of testing conditions and practical recommendations for assessment of biofilm production by staphylococci. APMIS : acta pathologica, microbiologica, et immunologica Scandinavica. 2007;115(8):891-9.
298. Pitts B, Hamilton MA, Zelver N, Stewart PS. A microtiter-plate screening method for biofilm disinfection and removal. Journal of Microbiological Methods. 2003;54(2):269-76.
299. Ommen P, Zobek N, Meyer RL. Quantification of biofilm biomass by staining: Non-toxic safranin can replace the popular crystal violet. J Microbiol Methods. 2017;141:87-9.

300. Azeredo J, Azevedo NF, Briandet R, Cerca N, Coenye T, Costa AR, et al. Critical review on biofilm methods. Crit Rev Microbiol. 2017;43(3):313-51.
301. Ruiz-Sorribas A, Poilvache H, Kamarudin N, Braem A, Van Bambeke F. In vitro polymicrobial inter-kingdom three-species biofilm model: influence of hyphae on biofilm formation and bacterial physiology. Biofouling. 2021:In press.
302. Little B, Wagner P, Ray R, Pope R, Scheetz R. Biofilms: An ESEM evaluation of artifacts introduced during SEM preparation. Journal of Industrial Microbiology. 1991;8(4):213-21.
303. Romanò CL, Scarponi S, Gallazzi E, Romanò D, Drago L. Antibacterial coating of implants in orthopaedics and trauma: a classification proposal in an evolving panorama. Journal of orthopaedic surgery and research. 2015;10:157-.
304. Singh AV, Vyas V, Patil R, Sharma V, Scopelliti PE, Bongiorno G, et al. Quantitative characterization of the influence of the nanoscale morphology of nanostructured surfaces on bacterial adhesion and biofilm formation. PloS one. 2011;6(9):e25029-e.
305. Gallardo-Moreno AM, Pacha-Olivenza MA, Saldaña L, Pérez-Giraldo C, Bruque JM, Vilaboa N, et al. In vitro biocompatibility and bacterial adhesion of physico-chemically modified Ti6Al4V surface by means of UV irradiation. Acta Biomater. 2009;5(1):181-92.
306. Rivardo F, Turner RJ, Allegrone G, Ceri H, Martinotti MG. Anti-adhesion activity of two biosurfactants produced by Bacillus spp. prevents biofilm formation of human bacterial pathogens. Applied Microbiology and Biotechnology. 2009;83(3):541-53.
307. Yin IX, Zhang J, Zhao IS, Mei ML, Li Q, Chu CH. The Antibacterial Mechanism of Silver Nanoparticles and Its Application in Dentistry. International journal of nanomedicine. 2020;15:2555-62.
308. Gosheger G, Hardes J, Ahrens H, Streitburger A, Buerger H, Erren M, et al. Silver-coated megaendoprostheses in a rabbit model--an analysis of the infection rate and toxicological side effects. Biomaterials. 2004;25(24):5547-56.
309. Wafa H, Grimer RJ, Reddy K, Jeys L, Abudu A, Carter SR, et al. Retrospective evaluation of the incidence of early periprosthetic infection with silver-treated endoprostheses in high-risk patients. The Bone & Joint Journal. 2015;97-B(2):252-7.
310. Moriarty TF, Kuehl R, Coenye T, Metsemakers WJ, Morgenstern M, Schwarz EM, et al. Orthopaedic device-related infection: current and future

interventions for improved prevention and treatment. EFORT Open Rev. 2016;1(4):89-99.
311. Antoci V, Jr., King SB, Jose B, Parvizi J, Zeiger AR, Wickstrom E, et al. Vancomycin covalently bonded to titanium alloy prevents bacterial colonization. Journal of orthopaedic research : official publication of the Orthopaedic Research Society. 2007;25(7):858-66.
312. Lucke M, Schmidmaier G, Sadoni S, Wildemann B, Schiller R, Haas NP, et al. Gentamicin coating of metallic implants reduces implant-related osteomyelitis in rats. Bone. 2003;32(5):521-31.
313. Metsemakers WJ, Emanuel N, Cohen O, Reichart M, Potapova I, Schmid T, et al. A doxycycline-loaded polymer-lipid encapsulation matrix coating for the prevention of implant-related osteomyelitis due to doxycycline-resistant methicillin-resistant Staphylococcus aureus. Journal of controlled release : official journal of the Controlled Release Society. 2015;209:47-56.
314. Fuchs T, Stange R, Schmidmaier G, Raschke MJ. The use of gentamicin-coated nails in the tibia: preliminary results of a prospective study. Archives of orthopaedic and trauma surgery. 2011;131(10):1419-25.
315. Metsemakers W, Reul M, Nijs S. The use of gentamicin-coated nails in complex open tibia fracture and revision cases: a retrospective analysis of a single centre case series and review of the literature. Injury. 2015;46(12):2433-7.
316. Schmidmaier G, Kerstan M, Schwabe P, Südkamp N, Raschke M. Clinical experiences in the use of a gentamicin-coated titanium nail in tibia fractures. Injury. 2017;48(10):2235-41.
317. Wang G, Li X, Wang Z. APD3: the antimicrobial peptide database as a tool for research and education. Nucleic Acids Res. 2016;44(D1):D1087-93.
318. Pasupuleti M, Schmidtchen A, Malmsten M. Antimicrobial peptides: key components of the innate immune system. Critical Reviews in Biotechnology. 2012;32(2):143-71.
319. Kazemzadeh-Narbat M, Cheng H, Chabok R, Alvarez MM, de la Fuente-Nunez C, Phillips KS, et al. Strategies for antimicrobial peptide coatings on medical devices: a review and regulatory science perspective. Critical Reviews in Biotechnology. 2021;41(1):94-120.
320. Chen R, Willcox MDP, Ho KKK, Smyth D, Kumar N. Antimicrobial peptide melimine coating for titanium and its in vivo antibacterial activity in rodent subcutaneous infection models. Biomaterials. 2016;85:142-51.

321. Chen X, Hirt H, Li Y, Gorr S-U, Aparicio C. Antimicrobial GL13K Peptide Coatings Killed and Ruptured the Wall of Streptococcus gordonii and Prevented Formation and Growth of Biofilms. PLOS ONE. 2014;9(11):e111579.
322. Zhang S, Zhou X, Liu T, Huang Y, Li J. The effects of Peptide Mel4-coated titanium plates on infection rabbits after internal fixation of open fractures. Archives of orthopaedic and trauma surgery. 2021.
323. Balaure PC, Grumezescu AM. Recent Advances in Surface Nanoengineering for Biofilm Prevention and Control. Part II: Active, Combined Active and Passive, and Smart Bacteria-Responsive Antibiofilm Nanocoatings. Nanomaterials (Basel). 2020;10(8):1527.
324. Li X, Wu B, Chen H, Nan K, Jin Y, Sun L, et al. Recent developments in smart antibacterial surfaces to inhibit biofilm formation and bacterial infections. Journal of Materials Chemistry B. 2018;6(26):4274-92.
325. Sebastian S, Liu Y, Christensen R, Raina DB, Tägil M, Lidgren L. Antibiotic containing bone cement in prevention of hip and knee prosthetic joint infections: A systematic review and meta-analysis. J Orthop Translat. 2020;23:53-60.
326. Anagnostakos K. Therapeutic Use of Antibiotic-loaded Bone Cement in the Treatment of Hip and Knee Joint Infections. J Bone Joint Infect. 2017;2(1):29-37.
327. Kuechle DK, Landon GC, Musher DM, Noble PC. Elution of Vancomycin, Daptomycin, and Amikacin From Acrylic Bone Cement. Clinical Orthopaedics and Related Research®. 1991;264:302-8.
328. van de Belt H, Neut D, Schenk W, van Horn JR, van der Mei HC, Busscher HJ. Staphylococcus aureus biofilm formation on different gentamicin-loaded polymethylmethacrylate bone cements. Biomaterials. 2001;22(12):1607-11.
329. Anagnostakos K, Meyer C. Antibiotic Elution from Hip and Knee Acrylic Bone Cement Spacers: A Systematic Review. BioMed research international. 2017;2017:4657874-.
330. Drago L, Boot W, Dimas K, Malizos K, Hänsch GM, Stuyck J, et al. Does implant coating with antibacterial-loaded hydrogel reduce bacterial colonization and biofilm formation in vitro? Clinical orthopaedics and related research. 2014;472(11):3311-23.
331. Boot W, Gawlitta D, Nikkels PGJ, Pouran B, van Rijen MHP, Dhert WJA, et al. Hyaluronic Acid-Based Hydrogel Coating Does Not Affect Bone Apposition at the Implant Surface in a Rabbit Model. Clinical orthopaedics and related research. 2017;475(7):1911-9.

332. De Meo D, Calogero V, Are L, Cavallo AU, Persiani P, Villani C. Antibiotic-Loaded Hydrogel Coating to Reduce Early Postsurgical Infections in Aseptic Hip Revision Surgery: A Retrospective, Matched Case-Control Study. Microorganisms. 2020;8(4):571.
333. Stavrakis AI, Zhu S, Hegde V, Loftin AH, Ashbaugh AG, Niska JA, et al. In Vivo Efficacy of a "Smart" Antimicrobial Implant Coating. The Journal of bone and joint surgery American volume. 2016;98(14):1183-9.
334. Chan BK, Abedon ST. Bacteriophages and their enzymes in biofilm control. Curr Pharm Des. 2015;21(1):85-99.
335. Eaton MD, Bayne-Jones S. Bacteriophage therapy: Review of the principles and results of the use of bacteriophage in the treatment of infections. Journal of the American Medical Association. 1934;103(23):1769-76.
336. Sulakvelidze A, Alavidze Z, Morris JG. Bacteriophage Therapy. Antimicrobial Agents and Chemotherapy. 2001;45(3):649-59.
337. Lu TK, Koeris MS. The next generation of bacteriophage therapy. Current opinion in microbiology. 2011;14(5):524-31.
338. Rose T, Verbeken G, Vos DD, Merabishvili M, Vaneechoutte M, Lavigne R, et al. Experimental phage therapy of burn wound infection: difficult first steps. Int J Burns Trauma. 2014;4(2):66-73.
339. Lu TK, Collins JJ. Dispersing biofilms with engineered enzymatic bacteriophage. Proceedings of the National Academy of Sciences. 2007;104(27):11197-202.
340. Pearl S, Gabay C, Kishony R, Oppenheim A, Balaban NQ. Nongenetic individuality in the host-phage interaction. PLoS Biol. 2008;6(5):e120.
341. Morris JL, Letson HL, Elliott L, Grant AL, Wilkinson M, Hazratwala K, et al. Evaluation of bacteriophage as an adjunct therapy for treatment of peri-prosthetic joint infection caused by Staphylococcus aureus. PloS one. 2019;14(12):e0226574-e.
342. Doub JB, Ng VY, Johnson AJ, Slomka M, Fackler J, Horne B, et al. Salvage Bacteriophage Therapy for a Chronic MRSA Prosthetic Joint Infection. Antibiotics (Basel). 2020;9(5).
343. Cano EJ, Caflisch KM, Bollyky PL, Van Belleghem JD, Patel R, Fackler J, et al. Phage Therapy for Limb-threatening Prosthetic Knee Klebsiella pneumoniae Infection: Case Report and In Vitro Characterization of Anti-biofilm Activity. Clin Infect Dis. 2020.
344. Ferry T, Leboucher G, Fevre C, Herry Y, Conrad A, Josse J, et al. Salvage Debridement, Antibiotics and Implant Retention ("DAIR") With

Local Injection of a Selected Cocktail of Bacteriophages: Is It an Option for an Elderly Patient With Relapsing Staphylococcus aureus Prosthetic-Joint Infection? Open Forum Infect Dis. 2018;5(11):ofy269-ofy.
345. Ferry T, Kolenda C, Batailler C, Gustave CA, Lustig S, Malatray M, et al. Phage Therapy as Adjuvant to Conservative Surgery and Antibiotics to Salvage Patients With Relapsing S. aureus Prosthetic Knee Infection. Front Med (Lausanne). 2020;7:570572.
346. Doub JB, Ng VY, Wilson E, Corsini L, Chan BK. Successful Treatment of a Recalcitrant Staphylococcus epidermidis Prosthetic Knee Infection with Intraoperative Bacteriophage Therapy. Pharmaceuticals (Basel). 2021;14(3):231.
347. Ferry T, Batailler C, Petitjean C, Chateau J, Fevre C, Forestier E, et al. The Potential Innovative Use of Bacteriophages Within the DAC(®) Hydrogel to Treat Patients With Knee Megaprosthesis Infection Requiring "Debridement Antibiotics and Implant Retention" and Soft Tissue Coverage as Salvage Therapy. Front Med (Lausanne). 2020;7:342.
348. Naureen Z, Malacarne D, Anpilogov K, Dautaj A, Camilleri G, Cecchin S, et al. Comparison between American and European legislation in the therapeutical and alimentary bacteriophage usage. Acta Biomed. 2020;91(13-S):e2020023-e.
349. Kim BO, Kim ES, Yoo YJ, Bae HW, Chung IY, Cho YH. Phage-Derived Antibacterials: Harnessing the Simplicity, Plasticity, and Diversity of Phages. Viruses. 2019;11(3).
350. Pastagia M, Schuch R, Fischetti VA, Huang DB. Lysins: the arrival of pathogen-directed anti-infectives. Journal of Medical Microbiology. 2013;62(10):1506-16.
351. Schuch R, Khan BK, Raz A, Rotolo JA, Wittekind M. Bacteriophage Lysin CF-301, a Potent Antistaphylococcal Biofilm Agent. Antimicrobial Agents and Chemotherapy. 2017;61(7):e02666-16.
352. Fowler VG, Jr., Das AF, Lipka-Diamond J, Schuch R, Pomerantz R, Jáuregui-Peredo L, et al. Exebacase for patients with Staphylococcus aureus bloodstream infection and endocarditis. The Journal of clinical investigation. 2020;130(7):3750-60.
353. Scheper H, Wubbolts JM, Verhagen JAM, de Visser AW, van der Wal RJP, Visser LG, et al. SAAP-148 Eradicates MRSA Persisters Within Mature Biofilm Models Simulating Prosthetic Joint Infection. Frontiers in microbiology. 2021;12:625952-.
354. De Brucker K, Delattin N, Robijns S, Steenackers H, Verstraeten N, Landuyt B, et al. Derivatives of the mouse cathelicidin-related antimicrobial

peptide (CRAMP) inhibit fungal and bacterial biofilm formation. Antimicrob Agents Chemother. 2014;58(9):5395-404.
355. Yan C-Y, Liu Y-Z, Xu Z-H, Yang H-Y, Li J. Comparison of Antibacterial Effect of Cationic Peptide LL-37 and Cefalexin on Clinical Staphylococcus aureus-induced Infection after Femur Fracture Fixation. Orthop Surg. 2020;12(4):1313-8.
356. Fleming D, Rumbaugh K. The Consequences of Biofilm Dispersal on the Host. Sci Rep. 2018;8(1):10738-.
357. Smith DC, Maiman R, Schwechter EM, Kim SJ, Hirsh DM. Optimal Irrigation and Debridement of Infected Total Joint Implants with Chlorhexidine Gluconate. J Arthroplasty. 2015;30(10):1820-2.
358. Urish KL, DeMuth PW, Craft DW, Haider H, Davis CM, 3rd. Pulse lavage is inadequate at removal of biofilm from the surface of total knee arthroplasty materials. J Arthroplasty. 2014;29(6):1128-32.
359. Pijls BG, Sanders I, Kuijper EJ, Nelissen R. Synergy between induction heating, antibiotics, and N-acetylcysteine eradicates Staphylococcus aureus from biofilm. Int J Hyperthermia. 2020;37(1):130-6.
360. Pijls BG, Sanders I, Kujiper EJ, Nelissen R. Induction heating for eradicating Staphylococcus epidermidis from biofilm. Bone Joint Res. 2020;9(4):192-9.
361. Briggs T, Blunn G, Hislop S, Ramalhete R, Bagley C, McKenna D, et al. Antimicrobial photodynamic therapy-a promising treatment for prosthetic joint infections. Lasers Med Sci. 2018;33(3):523-32.
362. Dong Y, Chen S, Wang Z, Peng N, Yu J. Synergy of ultrasound microbubbles and vancomycin against Staphylococcus epidermidis biofilm. J Antimicrob Chemother. 2013;68(4):816-26.
363. Guo H, Wang Z, Du Q, Li P, Wang Z, Wang A. Stimulated phase-shift acoustic nanodroplets enhance vancomycin efficacy against methicillin-resistant Staphylococcus aureus biofilms. International journal of nanomedicine. 2017;12:4679-90.
364. Vuotto C, Donelli G. Novel Treatment Strategies for Biofilm-Based Infections. Drugs. 2019;79(15):1635-55.
365. Brackman G, Coenye T. Quorum sensing inhibitors as anti-biofilm agents. Curr Pharm Des. 2015;21(1):5-11.
366. Gov Y, Bitler A, Dell'Acqua G, Torres JV, Balaban N. RNAIII inhibiting peptide (RIP), a global inhibitor of Staphylococcus aureus pathogenesis: structure and function analysis. Peptides. 2001;22(10):1609-20.

367. Simonetti O, Cirioni O, Ghiselli R, Goteri G, Scalise A, Orlando F, et al. RNAIII-Inhibiting Peptide Enhances Healing of Wounds Infected with Methicillin-Resistant Staphylococcus aureus. Antimicrobial Agents and Chemotherapy. 2008;52(6):2205-11.
368. Anguita-Alonso P, Giacometti A, Cirioni O, Ghiselli R, Orlando F, Saba V, et al. RNAIII-inhibiting-peptide-loaded polymethylmethacrylate prevents in vivo Staphylococcus aureus biofilm formation. Antimicrobial agents and chemotherapy. 2007;51(7):2594-6.
369. Garrigós C, Murillo O, Lora-Tamayo J, Vivas M, Tubau F, Cabellos C, et al. RNAIII inhibiting peptide against foreign-body infection by methicillin-resistant Staphylococcus aureus. Journal of Infection. 2012;65(6):586-8.
370. Barraud N, Storey MV, Moore ZP, Webb JS, Rice SA, Kjelleberg S. Nitric oxide-mediated dispersal in single- and multi-species biofilms of clinically and industrially relevant microorganisms. Microb Biotechnol. 2009;2(3):370-8.
371. Barraud N, Schleheck D, Klebensberger J, Webb JS, Hassett DJ, Rice SA, et al. Nitric oxide signaling in Pseudomonas aeruginosa biofilms mediates phosphodiesterase activity, decreased cyclic di-GMP levels, and enhanced dispersal. J Bacteriol. 2009;191(23):7333-42.
372. Cherny KE, Sauer K. Pseudomonas aeruginosa Requires the DNA-Specific Endonuclease EndA To Degrade Extracellular Genomic DNA To Disperse from the Biofilm. Journal of bacteriology. 2019;201(18):e00059-19.
373. Howlin RP, Cathie K, Hall-Stoodley L, Cornelius V, Duignan C, Allan RN, et al. Low-Dose Nitric Oxide as Targeted Anti-biofilm Adjunctive Therapy to Treat Chronic Pseudomonas aeruginosa Infection in Cystic Fibrosis. Mol Ther. 2017;25(9):2104-16.
374. Fleming D, Rumbaugh KP. Approaches to Dispersing Medical Biofilms. Microorganisms. 2017;5(2).
375. Kaplan JB, Ragunath C, Ramasubbu N, Fine DH. Detachment of Actinobacillus actinomycetemcomitans biofilm cells by an endogenous beta-hexosaminidase activity. Journal of bacteriology. 2003;185(16):4693-8.
376. Itoh Y, Wang X, Hinnebusch BJ, Preston JF, 3rd, Romeo T. Depolymerization of beta-1,6-N-acetyl-D-glucosamine disrupts the integrity of diverse bacterial biofilms. J Bacteriol. 2005;187(1):382-7.
377. Hogan S, Zapotoczna M, Stevens NT, Humphreys H, O'Gara JP, O'Neill E. Potential use of targeted enzymatic agents in the treatment of Staphylococcus aureus biofilm-related infections. J Hosp Infect. 2017;96(2):177-82.

378. Darouiche RO, Mansouri MD, Gawande PV, Madhyastha S. Antimicrobial and antibiofilm efficacy of triclosan and DispersinB combination. J Antimicrob Chemother. 2009;64(1):88-93.
379. Donelli G, Francolini I, Romoli D, Guaglianone E, Piozzi A, Ragunath C, et al. Synergistic activity of dispersin B and cefamandole nafate in inhibition of staphylococcal biofilm growth on polyurethanes. Antimicrob Agents Chemother. 2007;51(8):2733-40.
380. Waryah CB, Wells K, Ulluwishewa D, Chen-Tan N, Gogoi-Tiwari J, Ravensdale J, et al. In Vitro Antimicrobial Efficacy of Tobramycin Against Staphylococcus aureus Biofilms in Combination With or Without DNase I and/or Dispersin B: A Preliminary Investigation. Microbial Drug Resistance. 2016;23(3):384-90.
381. Venketaraman V, Lin AK, Le A, Kachlany SC, Connell ND, Kaplan JB. Both leukotoxin and poly-N-acetylglucosamine surface polysaccharide protect Aggregatibacter actinomycetemcomitans cells from macrophage killing. Microb Pathog. 2008;45(3):173-80.
382. Kalpana BJ, Aarthy S, Pandian SK. Antibiofilm Activity of α-Amylase from Bacillus subtilis S8-18 Against Biofilm Forming Human Bacterial Pathogens. Applied Biochemistry and Biotechnology. 2012;167(6):1778-94.
383. Lim ES, Koo OK, Kim M-J, Kim J-S. Bio-enzymes for inhibition and elimination of Escherichia coli O157:H7 biofilm and their synergistic effect with sodium hypochlorite. Sci Rep. 2019;9(1):9920-.
384. Fleming D, Chahin L, Rumbaugh K. Glycoside Hydrolases Degrade Polymicrobial Bacterial Biofilms in Wounds. Antimicrob Agents Chemother. 2017;61(2):e01998-16.
385. Shak S, Capon DJ, Hellmiss R, Marsters SA, Baker CL. Recombinant human DNase I reduces the viscosity of cystic fibrosis sputum. Proc Natl Acad Sci U S A. 1990;87(23):9188-92.
386. Tetz GV, Artemenko NK, Tetz VV. Effect of DNase and antibiotics on biofilm characteristics. Antimicrobial agents and chemotherapy. 2009;53(3):1204-9.
387. Thomas VC, Thurlow LR, Boyle D, Hancock LE. Regulation of autolysis-dependent extracellular DNA release by Enterococcus faecalis extracellular proteases influences biofilm development. J Bacteriol. 2008;190(16):5690-8.
388. Kaplan JB, LoVetri K, Cardona ST, Madhyastha S, Sadovskaya I, Jabbouri S, et al. Recombinant human DNase I decreases biofilm and

increases antimicrobial susceptibility in staphylococci. The Journal of antibiotics. 2012;65(2):73-7.
389. Nijland R, Hall MJ, Burgess JG. Dispersal of biofilms by secreted, matrix degrading, bacterial DNase. PLoS One. 2010;5(12):e15668.
390. Nair A, Perry A, Perry JD, Gould FK, Samuel J. In vitro effects of combined iron chelation, antibiotics and matrix disruption on clinical isolates of Pseudomonas aeruginosa. Journal of Antimicrobial Chemotherapy. 2019;75(3):586-92.
391. Ebeling W, Hennrich N, Klockow M, Metz H, Orth HD, Lang H. Proteinase K from Tritirachium album Limber. Eur J Biochem. 1974;47(1):91-7.
392. Kumar Shukla S, Rao TS. Dispersal of Bap-mediated Staphylococcus aureus biofilm by proteinase K. The Journal of antibiotics. 2013;66(2):55-60.
393. Shukla SK, Rao TS. Staphylococcus aureus biofilm removal by targeting biofilm-associated extracellular proteins. Indian J Med Res. 2017;146(Supplement):S1-S8.
394. Cui H, Ma C, Lin L. Co-loaded proteinase K/thyme oil liposomes for inactivation of Escherichia coli O157:H7 biofilms on cucumber. Food Funct. 2016;7(9):4030-40.
395. Gonzalez Moreno M, Trampuz A, Di Luca M. Synergistic antibiotic activity against planktonic and biofilm-embedded Streptococcus agalactiae, Streptococcus pyogenes and Streptococcus oralis. J Antimicrob Chemother. 2017;72(11):3085-92.
396. Fredheim EG, Klingenberg C, Rohde H, Frankenberger S, Gaustad P, Flaegstad T, et al. Biofilm formation by Staphylococcus haemolyticus. J Clin Microbiol. 2009;47(4):1172-80.
397. Chaignon P, Sadovskaya I, Ragunah C, Ramasubbu N, Kaplan JB, Jabbouri S. Susceptibility of staphylococcal biofilms to enzymatic treatments depends on their chemical composition. Appl Microbiol Biotechnol. 2007;75(1):125-32.
398. Brady AJ, Laverty G, Gilpin DF, Kearney P, Tunney M. Antibiotic susceptibility of planktonic- and biofilm-grown staphylococci isolated from implant-associated infections: should MBEC and nature of biofilm formation replace MIC? J Med Microbiol. 2017;66(4):461-9.
399. Kim MJ, Lim ES, Kim JS. Enzymatic Inactivation of Pathogenic and Nonpathogenic Bacteria in Biofilms in Combination with Chlorine. J Food Prot. 2019;82(4):605-14.

400. Farrell RE. Chapter 2 - Creating a Ribonuclease-Free Environment. In: Farrell RE, editor. RNA Methodologies (Fifth Edition): Academic Press; 2017. p. 55-74.
401. Zimmerli W. Clinical presentation and treatment of orthopaedic implant-associated infection. J Intern Med. 2014;276(2):111-9.
402. Siqueira MB, Klika AK, Higuera CA, Barsoum WK. Modes of failure of total knee arthroplasty: registries and realities. The journal of knee surgery. 2015;28(2):127-38.
403. Peel TN, Cheng AC, Buising KL, Choong PF. Microbiological aetiology, epidemiology, and clinical profile of prosthetic joint infections: are current antibiotic prophylaxis guidelines effective? Antimicrob Agents Chemother. 2012;56(5):2386-91.
404. Pulido L, Ghanem E, Joshi A, Purtill JJ, Parvizi J. Periprosthetic joint infection: the incidence, timing, and predisposing factors. Clin Orthop Relat Res. 2008;466(7):1710-5.
405. Mottola C, Matias CS, Mendes JJ, Melo-Cristino J, Tavares L, Cavaco-Silva P, et al. Susceptibility patterns of Staphylococcus aureus biofilms in diabetic foot infections. BMC Microbiol. 2016;16(1):119.
406. Qasim SN, Swann A, Ashford R. The DAIR (debridement, antibiotics and implant retention) procedure for infected total knee replacement - a literature review. SICOT J. 2017;3:2-.
407. Morgan J, Holder G, Desoutter G. The measurement and comparison of jet characteristics of surgical pulse lavage devices. J Arthroplasty. 2003;18(1):45-50.
408. Deirmengian C, Greenbaum J, Lotke PA, Booth RE, Jr., Lonner JH. Limited success with open debridement and retention of components in the treatment of acute Staphylococcus aureus infections after total knee arthroplasty. J Arthroplasty. 2003;18(7 Suppl 1):22-6.
409. Knecht CS, Moley JP, McGrath MS, Granger JF, Stoodley P, Dusane DH. Antibiotic loaded calcium sulfate bead and pulse lavage eradicates biofilms on metal implant materials in vitro. Journal of orthopaedic research : official publication of the Orthopaedic Research Society. 2018;36(9):2349-54.
410. Clinical and Laboratory Standards Institute (CLSI). Performance Standards for Antimicrobial Susceptibility Testing. 28th ed. Wayne, Pennsylvania, USA: Clinical and Laboratory Standards Institute; 2018.
411. Federal Agency for Medicines and Health Products (FAMHP). Floxapen. 2017(Rev.nr.1711 – EMA/PRAC/610988/2017 + BE517777):Rev.nr.1711 – EMA/PRAC/610988/2017 + BE517777.

412. Liu C, Bayer A, Cosgrove SE, Daum RS, Fridkin SK, Gorwitz RJ, et al. Clinical practice guidelines by the infectious diseases society of america for the treatment of methicillin-resistant Staphylococcus aureus infections in adults and children. Clin Infect Dis. 2011;52(3):e18-55.
413. Rueden CT, Schindelin J, Hiner MC, DeZonia BE, Walter AE, Arena ET, et al. ImageJ2: ImageJ for the next generation of scientific image data. BMC Bioinformatics. 2017;18(1):529.
414. Schindelin J, Arganda-Carreras I, Frise E, Kaynig V, Longair M, Pietzsch T, et al. Fiji: an open-source platform for biological-image analysis. Nat Methods. 2012;9(7):676-82.
415. Slinker BK. The statistics of synergism. J Mol Cell Cardiol. 1998;30(4):723-31.
416. Wolcott RD, Rumbaugh KP, James G, Schultz G, Phillips P, Yang Q, et al. Biofilm maturity studies indicate sharp debridement opens a time-dependent therapeutic window. J Wound Care. 2010;19(8):320-8.
417. Bauer J, Siala W, Tulkens PM, Van Bambeke F. A combined pharmacodynamic quantitative and qualitative model reveals the potent activity of daptomycin and delafloxacin against Staphylococcus aureus biofilms. Antimicrob Agents Chemother. 2013;57(6):2726-37.
418. Siala W, Mingeot-Leclercq MP, Tulkens PM, Hallin M, Denis O, Van Bambeke F. Comparison of the antibiotic activities of Daptomycin, Vancomycin, and the investigational Fluoroquinolone Delafloxacin against biofilms from Staphylococcus aureus clinical isolates. Antimicrob Agents Chemother. 2014;58(11):6385-97.
419. Trampuz A, Widmer AF. Infections associated with orthopedic implants. Curr Opin Infect Dis. 2006;19(4):349-56.
420. Boyle KK, Kuo FC, Horcajada JP, Hughes H, Cavagnaro L, Marculescu C, et al. General Assembly, Treatment, Antimicrobials: Proceedings of International Consensus on Orthopedic Infections. J Arthroplasty. 2019;34(2S):S225-S37.
421. Gander S, Finch R. The effects of exposure at constant (1 h) or exponentially decreasing concentrations of quinupristin/dalfopristin on biofilms of Gram-positive bacteria. J Antimicrob Chemother. 2000;46(1):61-7.
422. Townsend EM, Sherry L, Kean R, Hansom D, Mackay WG, Williams C, et al. Implications of Antimicrobial Combinations in Complex Wound Biofilms Containing Fungi. Antimicrob Agents Chemother. 2017;61(9):e00672-17.

423. Van den Driessche F, Brackman G, Swimberghe R, Rigole P, Coenye T. Screening a repurposing library for potentiators of antibiotics against Staphylococcus aureus biofilms. Int J Antimicrob Agents. 2017;49(3):315-20.
424. Ravn C, Furustrand Tafin U, Betrisey B, Overgaard S, Trampuz A. Reduced ability to detect surface-related biofilm bacteria after antibiotic exposure under in vitro conditions. Acta Orthop. 2016;87(6):644-50.
425. Peel TN, Dowsey MM, Buising KL, Liew D, Choong PFM. Cost analysis of debridement and retention for management of prosthetic joint infection. Clinical Microbiology and Infection. 2013;19(2):181-6.
426. Kunutsor SK, Beswick AD, Whitehouse MR, Wylde V, Blom AW. Debridement, antibiotics and implant retention for periprosthetic joint infections: A systematic review and meta-analysis of treatment outcomes. J Infect. 2018;77(6):479-88.
427. Poilvache H, Ruiz-Sorribas A, Sakoulas G, Rodriguez-Villalobos H, Cornu O, Van Bambeke F. Synergistic Effects of Pulsed Lavage and Antimicrobial Therapy Against Staphylococcus aureus Biofilms in an in-vitro Model. Front Med (Lausanne). 2020;7(527):527.
428. Stoodley P, Ehrlich GD, Sedghizadeh PP, Hall-Stoodley L, Baratz ME, Altman DT, et al. Orthopaedic biofilm infections. Curr Orthop Pract. 2011;22(6):558-63.
429. Romano CL, Toscano M, Romano D, Drago L. Antibiofilm agents and implant-related infections in orthopaedics: where are we? J Chemother. 2013;25(2):67-80.
430. Kaplan JB, Ragunath C, Velliyagounder K, Fine DH, Ramasubbu N. Enzymatic detachment of Staphylococcus epidermidis biofilms. Antimicrob Agents Chemother. 2004;48(7):2633-6.
431. Tetz GV, Artemenko NK, Tetz VV. Effect of DNase and antibiotics on biofilm characteristics. Antimicrob Agents Chemother. 2009;53(3):1204-9.
432. Lim ES, Koo OK, Kim MJ, Kim JS. Bio-enzymes for inhibition and elimination of Escherichia coli O157:H7 biofilm and their synergistic effect with sodium hypochlorite. Sci Rep. 2019;9(1):9920.
433. Snyderman R, Pike MC, Fischer DG, Koren HS. Biologic and biochemical activities of continuous macrophage cell lines P388D1 and J774.1. J Immunol. 1977;119(6):2060-6.
434. Tulkens P, Beaufay H, Trouet A. Analytical fractionation of homogenates from cultured rat embryo fibroblasts. J Cell Biol. 1974;63(2 Pt 1):383-401.

435. Siala W, Hoche A, Van Bambeke F, Vanzieleghem T. Activity of combinations of an enzymatic cocktail (CDD) with antibiotics against biofilms of clinical isolates of ESKAPE pathogens. ECCMID 2018 - 28th European Congress of Clinical Microbiology and Infectious Diseases; 21-24 april 2018; Madrid2018.
436. Horvat M, Pannuri A, Romeo T, Dogsa I, Stopar D. Viscoelastic response of Escherichia coli biofilms to genetically altered expression of extracellular matrix components. Soft Matter. 2019;15(25):5042-51.
437. Mack D, Fischer W, Krokotsch A, Leopold K, Hartmann R, Egge H, et al. The intercellular adhesin involved in biofilm accumulation of Staphylococcus epidermidis is a linear beta-1,6-linked glucosaminoglycan: purification and structural analysis. Journal of Bacteriology. 1996;178(1):175-83.
438. Post V, Harris LG, Morgenstern M, Mageiros L, Hitchings MD, Meric G, et al. Comparative Genomics Study of Staphylococcus epidermidis Isolates from Orthopedic-Device-Related Infections Correlated with Patient Outcome. J Clin Microbiol. 2017;55(10):3089-103.
439. Gowrishankar S, Kamaladevi A, Balamurugan K, Pandian SK. In Vitro and In Vivo Biofilm Characterization of Methicillin-Resistant Staphylococcus aureus from Patients Associated with Pharyngitis Infection. Biomed Res Int. 2016;2016:1289157.
440. Zogaj X, Nimtz M, Rohde M, Bokranz W, Romling U. The multicellular morphotypes of Salmonella typhimurium and Escherichia coli produce cellulose as the second component of the extracellular matrix. Mol Microbiol. 2001;39(6):1452-63.
441. Nestle M, Roberts WK. An extracellular nuclease from Serratia marcescens. I. Purification and some properties of the enzyme. J Biol Chem. 1969;244(19):5213-8.
442. Jakubovics NS, Shields RC, Rajarajan N, Burgess JG. Life after death: the critical role of extracellular DNA in microbial biofilms. Letters in applied microbiology. 2013;57(6):467-75.
443. Vafina G, Zainutdinova E, Bulatov E, Filimonova MN. Endonuclease from Gram-Negative Bacteria Serratia marcescens Is as Effective as Pulmozyme in the Hydrolysis of DNA in Sputum. Front Pharmacol. 2018;9:114-.
444. O'Gara JP. ica and beyond: biofilm mechanisms and regulation in Staphylococcus epidermidis and Staphylococcus aureus. FEMS Microbiol Lett. 2007;270(2):179-88.

445. Levick JR. Permeability of rheumatoid and normal human synovium to specific plasma proteins. Arthritis Rheum. 1981;24(12):1550-60.
446. European Committee on Antimicrobial Susceptibility Testing. Daptomycin: Rationale for the EUCAST clinical breakpoints, version 1.0. http://www.eucast.org; 2005.
447. Dvorchik BH, Brazier D, DeBruin MF, Arbeit RD. Daptomycin pharmacokinetics and safety following administration of escalating doses once daily to healthy subjects. Antimicrob Agents Chemother. 2003;47(4):1318-23.
448. European Committee on Antimicrobial Susceptibility Testing. Doxycycline: Rationale for the EUCAST clinical breakpoints, version 1.0. http://www.eucast.org; 2009.
449. European Committee on Antimicrobial Susceptibility Testing. Linezolid: Rationale for the EUCAST clinical breakpoints, version 1.0. http://www.eucast.org; 2005.
450. European Committee on Antimicrobial Susceptibility Testing. Moxifloxacin: Rationale for the EUCAST clinical breakpoints, version 2.3. http://www.eucast.org; 2007.
451. European Committee on Antimicrobial Susceptibility Testing. Rifampicin: Rationale for the EUCAST clinical breakpoints, version 1.0. http://www.eucast.org; 2010.
452. European Committee on Antimicrobial Susceptibility Testing. Vancomycin: Rationale for the EUCAST clinical breakpoints, version 2.1. http://www.eucast.org.; 2010.
453. European Committee on Antimicrobial Susceptibility Testing. Ceftazidime: Rationale for the EUCAST clinical breakpoints, version 1.0. http://www.eucast.org; 2010.
454. Luthy R, Blaser J, Bonetti A, Simmen H, Wise R, Siegenthaler W. Comparative multiple-dose pharmacokinetics of cefotaxime, moxalactam, and ceftazidime. Antimicrob Agents Chemother. 1981;20(5):567-75.
455. European Committee on Antimicrobial Susceptibility Testing. Ciprofloxacin: Rationale for the EUCAST clinical breakpoints, version 1.9. http://www.eucast.org; 2007.
456. European Committee on Antimicrobial Susceptibility Testing. Colistin: Rationale for the EUCAST clinical breakpoints, version 1.0. http://www.eucast.org; 2010.
457. European Committee on Antimicrobial Susceptibility Testing. Meropenem: Rationale for the EUCAST clinical breakpoints, version 1.5. http://www.eucast.org; 2009.

458. Jonas K, Nils W, Alexander D, Stefan B, Henning W, Thilo F. The etiology of revision total hip arthroplasty: current trends in a retrospective survey of 3450 cases. Archives of orthopaedic and trauma surgery. 2020;140(9):1265-73.
459. Delanois RE, Mistry JB, Gwam CU, Mohamed NS, Choksi US, Mont MA. Current Epidemiology of Revision Total Knee Arthroplasty in the United States. The Journal of Arthroplasty. 2017;32(9):2663-8.
460. Dzaja I, Howard J, Somerville L, Lanting B. Functional outcomes of acutely infected knee arthroplasty: a comparison of different surgical treatment options. Can J Surg. 2015;58(6):402-7.
461. Archer NK, Mazaitis MJ, Costerton JW, Leid JG, Powers ME, Shirtliff ME. Staphylococcus aureus biofilms: properties, regulation, and roles in human disease. Virulence. 2011;2(5):445-59.
462. Anguita-Alonso P, Giacometti A, Cirioni O, Ghiselli R, Orlando F, Saba V, et al. RNAIII-Inhibiting-Peptide-Loaded Polymethylmethacrylate Prevents In Vivo Staphylococcus aureus Biofilm Formation. Antimicrobial Agents and Chemotherapy. 2007;51(7):2594.
463. Kaplan JB. Therapeutic potential of biofilm-dispersing enzymes. Int J Artif Organs. 2009;32(9):545-54.
464. Poilvache H, Ruiz-Sorribas A, Cornu O, Van Bambeke F. In Vitro Study of the Synergistic Effect of an Enzyme Cocktail and Antibiotics against Biofilms in a Prosthetic Joint Infection Model. Antimicrob Agents Chemother. 2021;65(4).
465. Hampshire V, Robertson S. Using the facial grimace scale to evaluate rabbit wellness in post-procedural monitoring. Lab Anim (NY). 2015;44(7):259-60.
466. Piaton E, Fabre M, Goubin-Versini I, Bretz-Grenier M-F, Courtade-Saïdi M, Vincent S, et al. Recommandations techniques et règles de bonne pratique pour la coloration de May-Grünwald-Giemsa : revue de la littérature et apport de l'assurance qualité. Annales de Pathologie. 2015;35(4):294-305.
467. Aguilera-Correa JJ, Garcia-Casas A, Mediero A, Romera D, Mulero F, Cuevas-López I, et al. A New Antibiotic-Loaded Sol-Gel Can Prevent Bacterial Prosthetic Joint Infection: From in vitro Studies to an in vivo Model. Frontiers in Microbiology. 2020;10(2935).
468. Thompson JM, Miller RJ, Ashbaugh AG, Dillen CA, Pickett JE, Wang Y, et al. Mouse model of Gram-negative prosthetic joint infection reveals therapeutic targets. JCI Insight. 2018;3(17):e121737.
469. Kaur S, Harjai K, Chhibber S. In Vivo Assessment of Phage and Linezolid Based Implant Coatings for Treatment of Methicillin Resistant S.

aureus (MRSA) Mediated Orthopaedic Device Related Infections. PLoS One. 2016;11(6):e0157626.
470. Folsch C, Federmann M, Lakemeier S, Kuehn KD, Kittinger C, Kerwat M, et al. Systemic antibiotic therapy does not significantly improve outcome in a rat model of implant-associated osteomyelitis induced by Methicillin susceptible Staphylococcus aureus. Archives of orthopaedic and trauma surgery. 2016;136(4):585-92.
471. Gilotra M, Nguyen T, Jaffe D, Sterling R. Dilute betadine lavage reduces implant-related bacterial burden in a rabbit knee prosthetic infection model. Am J Orthop (Belle Mead NJ). 2015;44(2):E38-41.
472. Yagi H, Kihara S, Mittwede PN, Maher PL, Rothenberg AC, Falcione A, et al. Development of a large animal rabbit model for chronic periprosthetic joint infection. Bone Joint Res. 2021;10(3):156-65.
473. Belmatoug N, Crémieux AC, Bleton R, Volk A, Saleh-Mghir A, Grossin M, et al. A new model of experimental prosthetic joint infection due to methicillin-resistant Staphylococcus aureus: a microbiologic, histopathologic, and magnetic resonance imaging characterization. The Journal of Infectious Diseases. 1996;174(2):414-7.
474. Stoodley P, Jacobsen A, Dunsmore BC, Gage L, Wilson S, Lappin-Scott H, et al. The influence of fluid shear and AICI3 on the material properties of Pseudomonas aeruginosa PAO1 and Desulfovibrio sp. EX265 biofilms2001. 113-20 p.
475. Peltonen LI, Kinnari TJ, Aarnisalo AA, Kuusela P, Jero J. Comparison of bacterial adherence to polylactides, silicone, and titanium. Acta Oto-Laryngologica. 2007;127(6):587-93.
476. Cordero J, Munuera L, Folgueira MD. The influence of the chemical composition and surface of the implant on infection. Injury. 1996;27:S/C34-S/C7.
477. Teughels W, Van Assche N, Sliepen I, Quirynen M. Effect of material characteristics and/or surface topography on biofilm development. Clinical Oral Implants Research. 2006;17(S2):68-81.
478. Ramos-Martin V, Johnson A, Livermore J, McEntee L, Goodwin J, Whalley S, et al. Pharmacodynamics of vancomycin for CoNS infection: experimental basis for optimal use of vancomycin in neonates. J Antimicrob Chemother. 2016;71(4):992-1002.
479. Tattevin P, Saleh-Mghir A, Davido B, Ghout I, Massias L, Garcia de la Maria C, et al. Comparison of six generic vancomycin products for treatment of methicillin-resistant Staphylococcus aureus experimental endocarditis in rabbits. Antimicrob Agents Chemother. 2013;57(3):1157-62.

480. Gatin L, Saleh-Mghir A, Massin P, Crémieux AC. Critical analysis of experimental models of periprosthetic joint infection. Orthop Traumatol Surg Res. 2015;101(7):851-5.
481. Zimmerli W, Sendi P. Role of Rifampin against Staphylococcal Biofilm Infections In Vitro, in Animal Models, and in Orthopedic-Device-Related Infections. Antimicrobial agents and chemotherapy. 2019;63(2):e01746-18.
482. Hoskins W, Gorup P, Claireaux H, Stokes C, Bingham R. High incidence of radiolucent lines at the implant-cement interface of a new total knee replacement. ANZ J Surg. 2020;90(7-8):1299-302.
483. Hogan S, O'Gara JP, O'Neill E. Novel Treatment of Staphylococcus aureus Device-Related Infections Using Fibrinolytic Agents. Antimicrob Agents Chemother. 2018;62(2).
484. Mandell JB, Orr S, Koch J, Nourie B, Ma D, Bonar DD, et al. Large variations in clinical antibiotic activity against Staphylococcus aureus biofilms of periprosthetic joint infection isolates. Journal of orthopaedic research : official publication of the Orthopaedic Research Society. 2019;37(7):1604-9.
485. Lauderdale KJ, Malone CL, Boles BR, Morcuende J, Horswill AR. Biofilm dispersal of community-associated methicillin-resistant Staphylococcus aureus on orthopedic implant material. Journal of orthopaedic research : official publication of the Orthopaedic Research Society. 2010;28(1):55-61.
486. Marculescu CE, Cantey JR. Polymicrobial prosthetic joint infections: risk factors and outcome. Clinical orthopaedics and related research. 2008;466(6):1397-404.
487. Kong EF, Tsui C, Kucharíková S, Andes D, Van Dijck P, Jabra-Rizk MA. Commensal Protection of Staphylococcus aureus against Antimicrobials by Candida albicans Biofilm Matrix. mBio. 2016;7(5).
488. Varga M. Chapter 1 - Rabbit Basic Science. In: Varga M, editor. Textbook of Rabbit Medicine (Second Edition): Butterworth-Heinemann; 2014. p. 3-108.
489. Namasivayam S, Maiga M, Yuan W, Thovarai V, Costa DL, Mittereder LR, et al. Longitudinal profiling reveals a persistent intestinal dysbiosis triggered by conventional anti-tuberculosis therapy. Microbiome. 2017;5(1):71-.
490. Lim Y, Jana M, Luong TT, Lee CY. Control of glucose- and NaCl-induced biofilm formation by rbf in Staphylococcus aureus. J Bacteriol. 2004;186(3):722-9.

491. Ropes MW, Rossmeisl EC, Bauer W. The origin and nature of normal human synovial fluid. The Journal of Clinical Investigation. 1940;19(6):795-9.
492. Growney Kalaf EA, Flores R, Bledsoe JG, Sell SA. Characterization of slow-gelling alginate hydrogels for intervertebral disc tissue-engineering applications. Materials Science and Engineering: C. 2016;63:198-210.
493. Zölß C, Cech JD. Efficacy of a new multifunctional surfactant-based biomaterial dressing with 1% silver sulphadiazine in chronic wounds. International Wound Journal. 2016;13(5):738-43.
494. Treter J, Bonatto F, Krug C, Soares GV, Baumvol IJR, Macedo AJ. Washing-resistant surfactant coated surface is able to inhibit pathogenic bacteria adhesion. Applied Surface Science. 2014;303:147-54.
495. Flierl MA, Culp BM, Okroj KT, Springer BD, Levine BR, Della Valle CJ. Poor Outcomes of Irrigation and Debridement in Acute Periprosthetic Joint Infection With Antibiotic-Impregnated Calcium Sulfate Beads. J Arthroplasty. 2017;32(8):2505-7.
496. Hanlon GW, Denyer SP, Olliff CJ, Ibrahim LJ. Reduction in exopolysaccharide viscosity as an aid to bacteriophage penetration through Pseudomonas aeruginosa biofilms. Applied and environmental microbiology. 2001;67(6):2746-53.